NUREG/CR-6902
LA-UR-05-7631

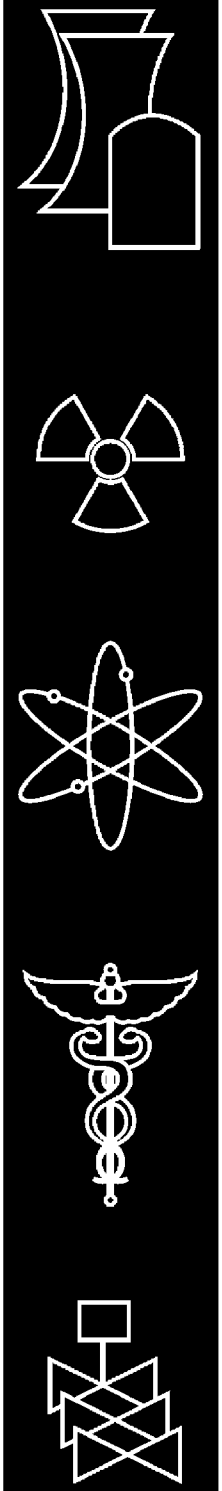

Effects of Insulation Debris on Throttle-Valve Flow Performance

A Subtask of GSI-191

Los Alamos National Laboratory

U.S. Nuclear Regulatory Commission
Office of Nuclear Regulatory Research
Washington, DC 20555-0001

NUREG/CR-6902
LA-UR-05-7631

Effects of Insulation Debris on Throttle-Valve Flow Performance

A Subtask of GSI-191

Manuscript Completed: March 2006
Date Published: March 2006

Principal Investigators:
C.B. Dale[1], P. Sadasivan[1], B.C. Letellier[1]

Prepared by:
P. Sadasivan[1], C.B. Dale[1], A.K. Maji[2], K. Howe[2],
F. Carles[2], C.E. Anderson[2], B.C. Letellier[1]

[1]Los Alamos National Laboratory
Los Alamos, NM 87545

Subcontractors:
[2]University of New Mexico
Department of Civil Engineering
Albuquerque, NM 87110

E. Geiger, NRC Project Manager

Prepared for
Division of Fuel, Engineering and Radiological Research
Office of Nuclear Regulatory Research
U.S. Nuclear Regulatory Commission
Washington, DC 20555-0001
NRC Job Code Y6871

This page intentionally left blank.

ABSTRACT

This document describes a series of tests conducted to assess the potential for loss-of-coolant-accident (LOCA)–generated debris to be trapped in the throttle valve downstream of the sump screen. Trapping of debris in the valve has important consequences for emergency-core-cooling-system (ECCS) operation because it may result in unacceptably high pressure losses in the system and consequent degradation of ECCS performance. Tests have been performed using a range of loadings and compositions of insulation introduced either as a single batch or as a set of successive batches. The tests used a surrogate throttle valve designed to simulate a range of representative valve configurations in use within United States pressurized-water reactors. This test program was the second in a series of Nuclear-Regulatory-Commission-sponsored tests that were conducted to address the effects downstream of the ECCS sump screens.

The first test program in this series addressed the potential for LOCA-generated debris materials to penetrate the sump screen. The current tests addressed the downstream effects of the debris that was able to penetrate the sump screen in these earlier tests. The test data provided information on the potential blockage of the high-pressure safety-injection throttle valves caused by single slugs of unmixed debris, as well as the potential for enhanced blockage caused by single or multiple batches of combinations of debris types. The insulation debris that was tested included calcium silicate (CalSil) insulation, NUKON™ fiberglass insulation, and reflective metallic insulation (RMI); however, many other types of insulation exist in plants. The range of debris sizes was based on the results of the screen penetration tests.

Debris blockage in the valve was gauged using the valve-loss-coefficient K, which was calculated using measured data for the pressure drop across the valve, the flow rate through the valve, and the temperature of the water. As the effective flow area of the valve decreased because of blockage, the loss coefficient increased. The overall approach was first to establish baseline loss coefficients for each valve configuration of interest and then to compare loss coefficients for various debris flow conditions with the data to get an indication of the extent of blockage caused by the debris. In addition, baseline loss coefficients were determined for selected known blockages (blockage-area fractions simulated using shims) to determine the relationship between K and the blocked-area fraction, as well as the blockage detection threshold of the system (~5%–8%). Loss coefficients for debris flow conditions then were compared with those for shim blockage data to obtain estimates of the blockage-area fractions.

Data from tests with single batches of unmixed debris showed that, in general, higher debris loadings and larger debris sizes (relative to the throttle-valve opening) resulted in higher observed increases in K. The K increases were higher for RMI than for NUKON for equivalent mass loadings. However, NUKON is judged to be more likely than RMI or CalSil to cause throttle valve blockage because of the propensity for NUKON to transport and penetrate the sump screen.

Tests using CalSil-RMI mixtures were the only two-component combinations that exhibited clear increases in K when compared with results from analogous single-debris CalSil and RMI tests. The results of tests performed using NUKON-RMI or CalSil-NUKON mixtures did not differ significantly from results for analogous separate tests, with one possible exception. One mixture test performed using unsieved CalSil with NUKON showed an appreciable increase in

valve blockage compared with single-debris NUKON tests. However, it is unclear if this result is attributed to clumping within the unsieved CalSil or to retention by NUKON fibers within the valve.

The three-component mixture tests were divided into two types of tests: (1) homogeneous mixtures of RMI, CalSil, and NUKON; and (2) sequential additions of each debris type using different ordering. Tests using homogeneous mixtures of RMI, CalSil, and NUKON showed an increase in valve blockage when compared with analogous single-debris RMI tests. However, no particular debris introduction sequence resulted in increases in valve blockage compared with results for homogeneous mixtures. Further, in the tests where NUKON was introduced first in the debris sequence, the blockage was much less than for homogeneous mixtures.

Three accumulation tests were performed to investigate the potential for a cumulative increase in valve clogging as a result of a stream of debris batches reaching the valve. In these tests, multiple batches of debris were introduced at ~15-min intervals over a period of 3 h. Three debris types and loadings were tested. The tests with 25 g each of successive additions of NUKON-CalSil showed a sustained increase in K over time as more and more debris reached the valve. However, consistent with the variability observed in other tests, the increase in K was not observed following all additions of debris. Some debris additions did not result in any increase in K, suggesting that no net increase in valve blockage occurred at that step. Accumulation tests with periodic additions of CalSil alone (after early introduction of NUKON) also showed that some CalSil additions triggered increases in K, whereas others did not. Relative to single-debris CalSil tests, larger K increases were observed after some CalSil additions, which suggests that the potential exists for CalSil to be trapped by NUKON or RMI that may be present in the valve.

The results for replicated single-debris, multiple-debris, and accumulation tests exhibited significant test-to-test variability. This variability is consistent with the inherent randomness involved in the process; the propensity for trapping of debris in the valve gap is a function of the random orientation of the individual pieces as they enter the valve gap. Further, the bending or thrashing of the debris pieces inside the valve also is a random process. This variability makes it difficult to quantify trends in these results because only a limited number of replicate tests were performed for any single condition.

FOREWORD

On September 13, 2004, the U.S. Nuclear Regulatory Commission (NRC) issued Generic Letter (GL) 2004-02, "Potential Impact of Blockage on Emergency Recirculation During Design-Basis Accidents at Pressurized-Water Reactors (PWRs)," to request that all PWR licensees perform an evaluation and ensure acceptable performance of the emergency core cooling and containment spray systems during sump recirculation following a loss-of-coolant accident (LOCA). This GL addresses technical issues associated with Generic Safety Issue (GSI) 191, "Assessment of Debris Accumulation on PWR Sump Performance." As part of the evaluation, the GL requested that licensees consider the effect of debris that is ingested through the sump screen on the performance of equipment downstream of the screen (i.e., downstream effects), such as the high-pressure safety injection (HPSI) throttle valves, pumps, piping, heat exchangers, and reactor vessel internals.

This report documents the second phase of NRC-sponsored research, conducted at the University of New Mexico under the supervision of Los Alamos National Laboratory, to address downstream effects. The first research phase (documented in NUREG/CR-6885, "Screen Penetration Test Report," dated October 2005) addressed the potential for debris materials to penetrate the sump screen. The primary objective of this second research phase was to parametrically assess the potential for ingested debris to be trapped in HPSI throttle valves. These tests used a surrogate throttle valve designed to simulate a range of representative valve configurations. The debris types that were tested included calcium silicate (CalSil) insulation, NUKON™ fiberglass insulation, and reflective metallic insulation (RMI). The test program evaluated blockages within the valve caused by (1) single slugs of individual debris types, (2) single slugs of various mixed-debris combinations, and (3) repeated loadings (multiple slugs) of various mixed-debris combinations to simulate debris accumulation over time.

Data from tests with single slugs of individual debris types showed that, in general, greater debris mass and larger debris sizes (relative to the throttle valve opening) resulted in the greatest amount of valve blockage. For equivalent mass loadings, valve blockage was greater for RMI than for NUKON debris. However, NUKON is considered more likely to lead to throttle valve blockage because it can more easily penetrate the sump screen. Mixtures of larger NUKON and RMI debris with smaller CalSil debris appeared to enhance valve blockage compared to analogous single-debris tests, presumably because the larger debris more effectively traps the smaller debris. Also, repeated loadings of mixed-debris combinations demonstrated that valve blockage can increase, albeit nonuniformly, with successive loadings. The implication is that blockage accumulation over time is possible. All test results were subject to significant test-to-test variability, which is expected given the inherent randomness in the accumulation of debris within a flow-restricting valve.

Consistent with the primary objective of this study, this report provides test data to support performance assessments of HPSI and other components downstream of the sump strainer screen to determine if they are affected by ingested debris following a postulated LOCA. Specifically, NRC staff can use knowledge gained from this study to evaluate licensees' responses to GL 2004-02.

Carl J. Paperiello, Director
Office of Nuclear Regulatory Research
U.S. Nuclear Regulatory Commission

This page intentionally left blank.

CONTENTS

Page

FIGURES

TABLES

Page

This page intentionally left blank.

EXECUTIVE SUMMARY

A series of scoping tests has been performed to investigate potential effects of debris streams composed of reflective metallic insulation (RMI), NUKON™ fiberglass insulation, and calcium silicate (CalSil) insulation on the throttle valves used in the high-pressure safety-injection (HPSI) systems of pressurized water reactors (PWRs). The tests were performed under the direction of Los Alamos National Laboratory in test facilities located at the University of New Mexico Civil Engineering Laboratory. This test program was the second in a series, following a previous test program (summarized in NUREG/CR-6885) that studied the propensity for debris to penetrate the sump screen. The current tests addressed the downstream effects of the debris that was able to penetrate the sump screen in these earlier tests. The test data provided information on the potential blockage of the throttle valves caused by single slugs of unmixed debris, as well as the potential for enhanced blockage caused by single or multiple batches of combinations of debris types.

The test program employed representative debris compositions and sizes. The debris types that were tested included CalSil, NUKON, and RMI. These insulation materials commonly are used in United States (U.S.) PWRs. The size range of each debris type tested was based on the results of the screen penetration tests. A surrogate valve capable of multiple configurations, rather than a specific plant valve, was used so that parametric studies readily could be performed. The surrogate valve was designed to be reasonably representative of the types of valve configurations used in U.S. PWRs.

The main geometric features of the valve that influenced the potential for clogging by debris were the perpendicular distance between the plug and seat and the angular orientation and length of the mating surfaces of the seat and plug. A range of gaps between 0.13 cm (0.05 in.) and 0.63 cm (0.25 in.) that spans typical PWR plant configurations was used in the tests. Stem angles of 5º and 45º were used in the tests. For the 5º stem angle, two stems of different diameters were used. The stem angles, angular orientation, and length of mating surfaces of the surrogate valve were determined through an informal survey of U.S. PWR plants and qualified vendors.

The goal for the selection of the pump (and subsequently the flow rate) for this testing was to obtain a pump of similar design to the HPSI pumps typically used in U.S. PWRs. The total HPSI flow required for the small-break loss-of-coolant accident of interest is on the order of 12.62–18.93 l/s (200–300 gpm). For HPSI systems having four injection paths, each path has an anticipated flow rate of 3.15–4.73 l/s (50–75 gpm) over a pressure drop (ΔP) of ~1.38 MPa (200 psi). The pump for this test program was chosen to achieve this performance and had a rated flow rate of 6.31 l/s (100 gpm). Because the pump was operated at 4.73 l/s (75 gpm) during testing, additional head was available to possibly purge debris from the valve in the event of clogging.

Debris blockage in the valve was gauged using the valve-loss-coefficient K, which was calculated using measured data for the pressure drop across the valve, the flow rate through the valve, and the temperature of the water. As the effective flow area of the valve decreased because of blockage, the loss coefficient increased. The overall approach first was to establish baseline loss coefficients for each valve configuration of interest and then compare loss

coefficients for various debris flow conditions with the baseline data to get an indication of the extent of blockage caused by the debris. In addition, loss coefficients were determined for selected known blockage areas (blockage-area fractions simulated using shims) to determine the relationship between *K* and the blocked-area fraction, as well as the blockage detection threshold of the system (~5%–8%). Loss coefficients for debris flow conditions then were compared with those for shim blockage data to obtain estimates of the blockage-area fractions.

Data from tests with single batches of unmixed debris showed that, in general, higher debris loadings and larger debris sizes (relative to the throttle-valve opening) resulted in higher increases in *K*. In single-debris tests with RMI, the highest observed increase in *K* was ~50%. Based on the results of the screen penetration tests performed previously, <20% of the RMI pieces of a given size penetrated the screen with the same opening size. When the RMI debris pieces had dimensions smaller than the screen size, a larger fraction of the pieces penetrated the screen; however, the current results show that these pieces were also able to clear the throttle valve—at least for the range of valve openings tested. The screen penetration tests showed that a significant fraction of CalSil passed through the screen, regardless of the screen-opening size. The current results show that the same result occurred in the valve, as well—practically all of the CalSil passed through the valve without causing appreciable blockage. The screen penetration tests showed that as much as 80% of the blender-processed NUKON debris penetrated the screen. The current results show that *K* increased by as much as 220% when the valve encountered a stream of blender-processed NUKON. This result translated to 45% blockage in the valve-opening flow area. Based on these results, NUKON is judged to be more likely than RMI or CalSil to cause throttle valve blockage. A large fraction of blender-processed NUKON was able to penetrate the test screen; much of it, in turn, could get trapped in the valve, thus resulting in significant increases in valve pressure loss.

Tests using CalSil-RMI mixtures were the only two-component combination that exhibited clear increases in *K* when compared with results from analogous single-debris CalSil and RMI tests. The results of tests performed using NUKON-RMI or CalSil-NUKON mixtures did not differ significantly from results for analogous separate tests for each debris component, with one possible exception. One mixture test performed using unsieved CalSil with NUKON showed an appreciable increase in valve blockage compared with single-debris NUKON tests. However, it is unclear if this result is attributed to clumping within the unsieved CalSil or to retention by NUKON fibers within the valve.

The three-component mixture tests were divided into two types of tests: (1) homogeneous mixtures of RMI, CalSil, and NUKON; and (2) sequential additions of each debris type using different ordering. Tests using homogeneous mixtures of RMI, CalSil, and NUKON showed an increase in valve blockage when compared with analogous single-debris RMI tests. However, no particular debris introduction sequence resulted in increases in valve blockage compared with results for homogeneous mixtures. Further, in the tests where NUKON was introduced first in the debris sequence, the blockage was much less than for homogeneous mixtures.

Three accumulation tests were performed to investigate the potential for a cumulative increase in valve clogging as a result of a sustained stream of debris batches reaching the valve. In these tests, multiple batches of debris were introduced at ~15-min intervals over a period of 3 h. Two of these tests were continued for an additional hour following the last debris addition to examine

the potential for erosion of debris trapped in the valve. Three debris types and loadings were tested. The tests with 25 g each of successive additions of NUKON-CalSil showed a sustained increase in *K* over time as more and more debris reached the valve. However, consistent with the variability observed in other tests, the increase in *K* was not observed following all additions of debris. Some debris additions did not result in any increase in *K*, suggesting that no net increase in valve blockage occurred at that step. When the loading at each step was reduced to 13 g each, the net increase in *K* over time was substantially less. This observation was consistent with single-debris results, which indicated relatively small blockage effects for lower debris loadings.

Accumulation tests with periodic additions of CalSil alone (after early introduction of NUKON) also showed that some debris addition events triggered increases in *K*, whereas others did not. Relative to single-debris CalSil tests, larger *K* increases were observed for some debris addition events, suggesting some potential for CalSil to be trapped in the valve by NUKON or RMI that may already have existed there. When one test was continued for 1 h following the final addition of debris, the valve-loss coefficient decreased precipitously at one point, suggesting erosion of the previously trapped debris.

The results for replicated single-debris, multiple-debris, and accumulation tests exhibited significant test-to-test variability. This variability is consistent with the inherent randomness involved in the process; the propensity for trapping of debris in the valve gap is a function of the random orientation of the individual pieces as they enter the valve gap. Further, the bending or thrashing of the debris pieces inside the valve also is a random process. This variability makes it difficult to quantify trends in these results because only a limited number of replicate tests were performed for any single condition.

This page intentionally left blank.

ABBREVIATIONS

ASTM	American Society for Testing and Materials
CalSil	Calcium Silicate
ECCS	Emergency-Core-Cooling System
GSI	Generic Safety Issue
HPSI	High-Pressure Safety Injection
LANL	Los Alamos National Laboratory
LOCA	Loss-of-Coolant Accident
NRC	Nuclear Regulatory Commission
PVC	Polyvinyl Chloride
PWR	Pressurized-Water Reactor
RMI	Reflective Metallic Insulation
U.S.	United States
UNM	University of New Mexico

This page intentionally left blank.

1 INTRODUCTION

The purpose of the Generic Safety Issue (GSI-191) research program was to determine if the transport and accumulation of debris in a containment following a loss-of-coolant accident (LOCA) would impede the operation of the emergency-core-cooling system (ECCS) in pressurized-water reactors (PWRs). In the event of a LOCA within a PWR containment, thermal insulation and other materials (e.g., coatings and concrete) in the vicinity of the break would be damaged and dislodged. A fraction of this material would be transported to the recirculation (or emergency) sump. The subject of debris transport fraction has been studied previously, as documented in Refs. 1 and 2. Part of the debris reaching the sump screen will accumulate on it, whereas the remainder will pass through the screen. The debris that accumulates on the screen can form a bed that acts as a filter, thus increasing the head loss across the screen. Excessive head loss may prevent or impede the flow of water to the ECCS or the containment-spray system, potentially degrading system performance or causing pump damage. The subject of debris penetration through the sump screen has been addressed in Ref. 3. Debris that passes through the screen first encounters the high-pressure safety-injection (HPSI) pumps, followed by the HPSI throttle valves. This study addresses the potential clogging of the throttle valves due to debris that can penetrate the screen.

1.1 Background

The HPSI throttle valves control the injection flow rates, balance the flow among multiple injection paths, and prevent pump runout conditions. The potential for clogging of the throttle valves has major implications on the operability of the HPSI system. As debris accumulates in a valve, flow resistance increases, resulting in an increased pressure drop across the valve. The increase in the system head could cause a flow reduction in the affected line and total flow as well; continued buildup of debris could completely shut off the flow in one or more lines. Therefore, it is important to gain an understanding of the conditions under which debris can clog the throttle valve; this understanding is the focus of the current testing program.

United States (U.S.) PWRs employ a variety of types of insulation and modes of encapsulation, ranging from nonencapsulated fiberglass to fully encapsulated stainless-steel reflective metallic insulation (RMI). Many PWRs have fiberglass and calcium silicate (CalSil) insulations in the containment, either on primary piping or on supporting systems. The types of fibrous insulation vary significantly, but much of it is found in the form of common low-density fiberglass (NUKON™[*]) and mineral wool. Some plants may have installed "high-performance" fiberglass on their primary systems for the higher insulation value, whereas other plants may have installed RMI for the low transportability. In general, the smaller pipes and steam generators are more likely to be insulated with fiberglass and CalSil than the reactor pressure vessel or the hot and cold leg piping.

The characteristics of the debris stream that reaches the throttle valve depend on the size distribution and composition of debris generated as a result of the LOCA, as well as the fraction of the debris that penetrates the sump screen. The composition of the debris stream reaching the throttle valve depends on the PWR in question. Some plants use fibrous insulation for essentially

[*] NUKON™ is a trademark of Owens Corning.

all of the piping, whereas others may use a combination of CalSil and fibrous insulation such as NUKON. As discussed in Ref. 2, the composition of the debris stream is also highly dependent on the location of the initiating LOCA. Preferential application of fiber insulation to smaller pipes and auxiliary pipes is more common, whereas RMI is used primarily on large components such as the reactor vessel and steam generators. This spatial dependency of the insulation application means that the debris source term will depend on the break location. This inherent lack of homogeneity in the debris stream implies that investigation of throttle valve clogging must consider the separate effects of different types of debris, as well as the effects of combinations of debris. The test matrix for the test program was developed accordingly.

Screen penetration testing (Ref. 3) provided data on the size of debris that would be likely to reach the throttle valve. For any given debris composition, the fraction of debris that penetrated the screen depended on the debris size relative to the screen-opening size, the flow velocity at the screen, and whether the debris reached the screen along the floor or in the flow.

The amount of CalSil passing through the screen was found to depend largely on how much of the CalSil was present in the form of clumps and how much of it was broken up by the momentum of the initiating LOCA jet or by the momentum of the recirculating flow. A significant amount of fine CalSil insulation could pass through screens of any mesh size. The fraction of NUKON that penetrated the screen also depended on the nature of aggregation. NUKON processed in a blender almost resulted in a suspension, and a significant fraction of it passed through screens of any mesh size, whereas NUKON processed in a leaf shredder resulted in agglomerated clumps that were almost entirely blocked by the screen.

The amount of RMI passing through the screen was found to depend on the size of the pieces relative to the mesh size of the screen and, to a lesser extent, on the flow velocity. In the screen penetration tests, when the size of the RMI pieces was approximately the same as the screen mesh, only a small fraction passed through the screen, regardless of the flow velocity. When the size of the RMI pieces was somewhat smaller than the screen mesh, a significant fraction (up to 75%) passed through the screen. The foregoing results of the screen penetration tests were used to guide the development of the test matrix for the throttle valve testing program.

1.2 Overall Approach

Debris blockage in the valve was gauged using the valve-loss-coefficient K, calculated using measured data for pressure drop across the valve, flow rate through the valve, and temperature of the water. As the flow area through the valve decreased as a result of blockage, the loss coefficient increased. The overall approach was first to establish baseline loss coefficients for each valve configuration of interest and then compare loss coefficients for various debris flow conditions with the baseline data to get an indication of the extent of blockage caused by the debris. In addition, loss coefficients were determined for selected known blockage conditions (blockage-area fractions simulated using shims). Loss coefficients for debris flow conditions then were compared with those for shim blockage data to obtain estimates of the blockage-area fractions.

The test program employed representative compositions and sizes for the debris stream. The valve configurations used in the tests were designed to span typical U.S. PWR plant

configurations. A surrogate valve capable of multiple configurations, rather than actual valves used in plants, was used so that parametric studies could be readily performed for multiple valve configurations. Types of debris, representative of insulation used in PWRs, were used in the tests, either singly or in combination. The debris types that were tested included CalSil, NUKON, and RMI. The range of sizes of the debris forms tested was based on the results of the screen penetration tests.

As discussed in the previous section, more RMI debris penetrated the screen when the characteristic dimensions were less than the screen size. Penetration behavior of CalSil and NUKON was determined more by the nature of aggregation of the debris rather than characteristic size. The screen mesh size varies considerably in U.S. PWR plants. However, a majority of the plants currently have screen mesh sizes between 0.317 cm (0.125 in.) and 0.63 cm (0.25 in.) (Ref. 2), although these mesh sizes may change as a result of planned sump screen modifications.

The quantity of debris that could reach the throttle valves post-LOCA could vary greatly, depending on the location and size of the break. Therefore, the amount of debris was examined parametrically in this test program and was not necessarily representative of what actual plant debris loading may be. In the case of RMI, the debris loading has been specified either as a number of pieces or as a mass in grams. For NUKON and CalSil, the debris loading has been specified as a mass in grams.

For traditional throttle valve designs, the gap between the plug and valve seat is the primary location that is susceptible to debris-related blockage. The main geometric features of this location that influence the potential for clogging by debris are the perpendicular distance between the plug and seat and the angular orientation and length of the mating surfaces of the seat and plug. To cover the range of gap sizes in throttle valves used in PWR plants, a range of gaps between 0.13 cm (0.05 in.) and 0.63 cm (0.25 in.) were used in the tests. Stem angles of 5º and 45º were used in the tests. For the 5º stem angle, two stems of different diameters were used. The stem angles, angular orientation, and length of mating surfaces of the surrogate valve were based on an informal survey of U.S. PWR plants and qualified vendors.

1.3 Objectives of Test Program

The overall objective of the test program was to assess the potential for debris to clog a HPSI throttle valve. This assessment required gathering the following types of data:

1. Baseline: valve characteristics for normal operating conditions. Data obtained from these tests were used to compare with data obtained from debris flow tests (#2–5) to estimate the increase in the loss coefficient resulting from debris blockage.
2. Shim blockage: valve characteristics for known blockage conditions. Loss-coefficient results determined from data obtained from these tests were used to gauge the detection threshold for the test system and as a basis for comparison with corresponding data obtained from debris flow tests listed in items 3–5 to estimate the extent of debris blockage.
3. Single-debris blockage: the extent of valve blockage that resulted when the valve was exposed to a single batch of any one type of debris.

4. Debris combination blockage: the valve blockage that resulted when the valve was exposed to a single batch of mixtures of debris, either as a homogeneous mixture or added successively.
5. Debris accumulation blockage: the cumulative effect of multiple batches of debris added sequentially to examine the potential for progressive buildup of debris in the valve.

1.3.1 Baseline

This element of the test program generated baseline data on the valve configurations of interest. Baseline tests included a determination of the valve-loss-coefficient *K* for different valve-stem/ring combinations for normal flow conditions with a range of valve openings. Baseline data for normal conditions was taken after each set of debris tests described in Sections 1.3.3–1.3.5 to keep track of potential changes in the baseline that occurred during testing.

1.3.2 Shim Blockage

Shim blockage tests also included a determination of the loss coefficient for selected valve stem/ring combinations for known blockage conditions. Blockage was simulated using shims of known areas, to establish the relationship between *K* and the percent area blockage as well as the detection threshold for blockage in the valve. The variation in loss coefficient as a function of blockage area also was determined.

1.3.3 Single-Debris Blockage

This component of the test program, designated as Test Series 1, addressed the issue of valve blockage caused by the retention of a single type of debris when the debris was added in a single batch. The specific objectives of the first phase of the test program were to generate data on clogging of the surrogate throttle valve configurations by single-debris types for a range of valve throat gaps and angles. The debris types included

1. RMI debris with characteristic dimensions between 0.317 cm (0.125 in.) and 0.63 cm (0.25 in.). This debris included square pieces with sides 0.317 cm (0.125 in.) and 0.63 cm (0.25 in.) or rectangular pieces with sides 0.317 cm (0.125 in.) and 1.27 cm (0.5 in.) (4:1 aspect ratio).
2. NUKON debris mixed in water.
3. CalSil debris.

1.3.4 Debris Combination Blockage

This part of the test program, designated as Test Series 2, addressed the issue of valve blockage caused by combinations of debris types. Each test involved the introduction of two or more types of debris. Specific combinations of debris composition, size, and/or mass were used. The debris combination was added in a single step. This series of tests addressed the potential for one type of debris to act as a nucleation source for retention of other debris types. The debris types used included

1. NUKON combined with RMI of different sizes;
2. CalSil combined with RMI of different sizes;
3. homogeneous mixtures of CalSil, NUKON, and RMI; and
4. combinations of CalSil, NUKON, and RMI introduced separately in a sequence.

1.3.5 Debris Accumulation Blockage

This component of the test program, designated as Test Series 3, examined the progressive clogging of the valve due to a slow buildup of debris. Multiple batches of debris were introduced at specified intervals for a period of several hours to determine the increase in blockage over time as a result of accumulation of debris in the valve.

1.4 Outline of Report

Section 2 provides a detailed description of the technical approach used for the test program. This approach included the methodology used in the experiments, the test facility used, the test matrix for the different series of tests, the test procedure used, and the data analysis methodology.

Section 3 provides the results of the baseline tests. Section 4 presents the single debris test results. The results of combinations of multiple debris types are summarized in Section 5, whereas Section 6 provides the debris accumulation results. In these sections, test results are typically presented in the form of valve-loss-coefficient K. Additional details of the data are provided in appendices. The conclusions drawn from the results of the test program are discussed in Section 7.

This page intentionally left blank.

2 TECHNICAL APPROACH

2.1 General Approach

The overall approach was to simulate appropriate PWR debris flow conditions through a throttle valve using a flow loop. The test apparatus had the flexibility to control local flow conditions, as well as debris quantity and debris types, consistent with the objectives in Section 1. The facility also was able to take applicable measurements and visual observations to characterize the debris blockage in the valve. A surrogate valve was used in all of the testing described in this report. This surrogate valve permitted the simulation of multiple valve configurations by using interchangeable valve plugs with the same valve body. Also, the surrogate valve was designed to facilitate easy assembly and disassembly, thus enabling inspection of the debris in the valve after each test.

2.2 Test Facility

The testing was conducted in the open channel hydraulics laboratory in the Ferris Engineering Building at the University of New Mexico (UNM). The tests used existing equipment in the laboratory and new equipment provided specifically for the throttle valve tests. The throttle valve was tested by using a constant speed pump to convey water or water mixed with debris through the valve. Water was supplied by an upstream flume, pumped through the throttle valve, and discharged back to the flume. Debris was added through a manifold located downstream of the pump and upstream of the throttle valve. The performance of the throttle valve was monitored with pressure transducers, flow meters, and thermocouples installed upstream and downstream of the throttle valve. The overall layout of the test loop is shown schematically in Figure 2-1, and a photograph of the flow loop excluding the flume is shown in Figure 2-2. The hydraulic system for the throttle valve test from the upstream flume, through the throttle valve is more thoroughly described in the following sections.

2.2.1 Flume

Water was provided to the suction side of the pump through the "linear hydraulic flume." The flume consisted of an open box 5.94 m (19.5 ft) long, 0.91 m (3 ft) wide, and 1.22 m (4 ft) high, with Plexiglas® side panels (Figure 2-3). A schematic of the flume is shown in Figure 2-4. Water was added to the flume using a variable-speed centrifugal pump capable of supplying water at 18.93-138.80 l/s (300-2200 gpm). Water was pumped from an underground reservoir through overhead piping that allowed the flume to be filled to the desired level. The water entered the flume through a 30.48-cm (12-in.)-diameter pipe at the upstream end of the flume. Water exited the flume through a 30.48-cm (12-in.)-diameter drain pipe located in the floor at the downstream end of the flume. During the throttle valve tests, water normally was maintained in the flume at a depth of 55.88-60.96 cm (22-24 in.). Water was added to the flume before testing, and except for tests lasting several hours, water was not added during the testing period. A U.S. Standard #100 screen was used at the downstream end of the 0.3-m (1-ft)-wide confined flow area to reduce the potential for damage to the flow meter and the pump.

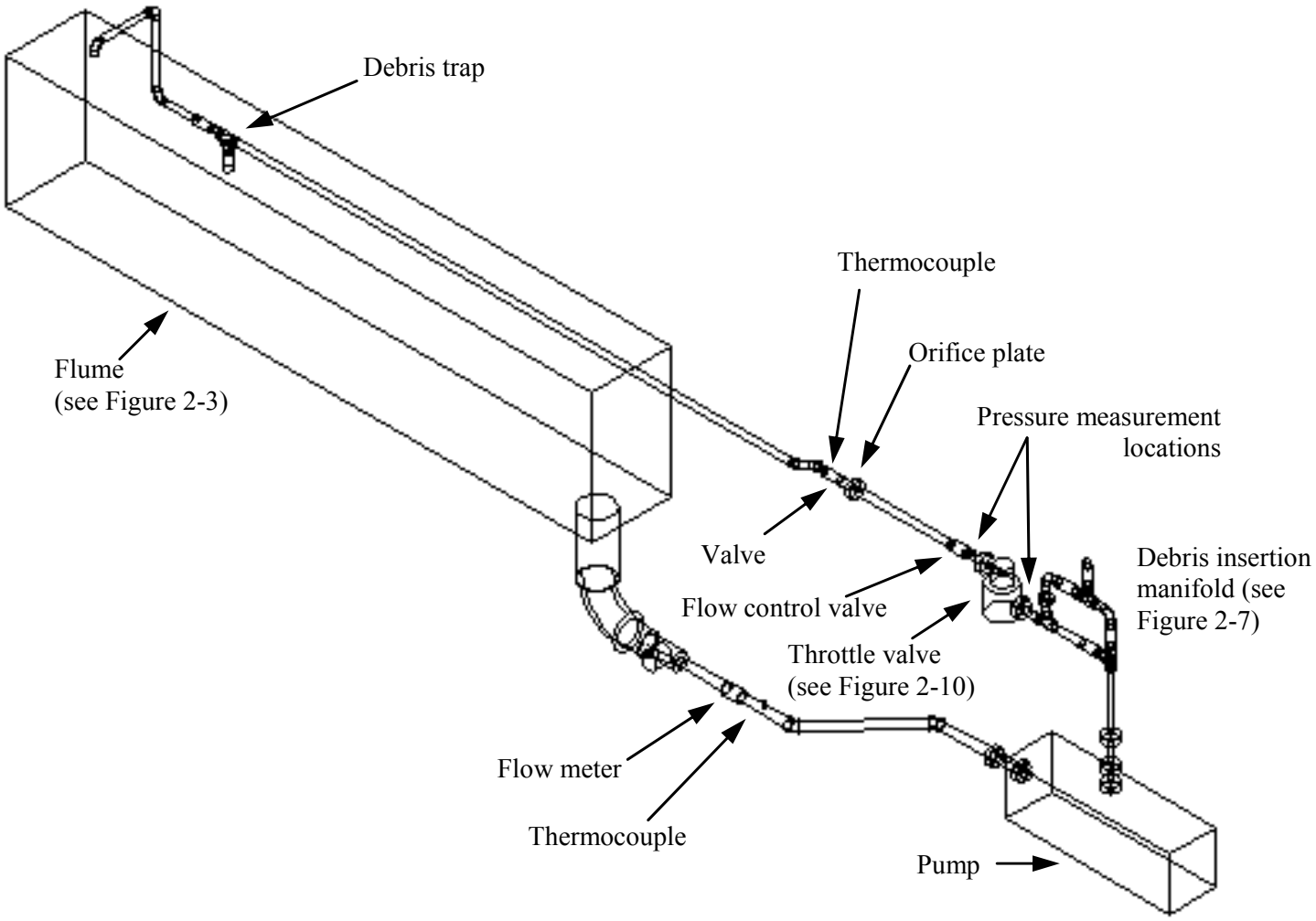

Figure 2-1. Schematic of the Throttle Valve Test Loop

Figure 2-2. Photograph of the Test Loop (Excluding the Flume)

2.2.2 Flume to Pump

Downstream of the flume drain pipe was a 30.48-cm (12-in.) butterfly valve, a 90º elbow, reducing sections to a 15.24-cm (6-in.)-diameter Schedule-40 poly-vinyl chloride (PVC) pipe, and a 15.24-com (6-in. × 6-in.) tee. Figure 2-5 shows the detail of this area. The 90º leg of the tee section was controlled by a sliding gate valve, which allowed water to be conveyed out of the throttle valve system to a water storage sump or to a surface drain. Except for tests lasting several hours, the sliding gate valve was closed during throttle valve testing.

The upstream flow meter was located 0.91 m (3 ft) downstream of the 15.24-cm × 15.24-cm (6-in. × 6-in.) tee. A fine-mesh screen was installed upstream of the flow meter to protect the flow meter from damage due to debris ingestion. Between the tee and the flow meter, a reducer fitting created a transition to a 7.62-cm (3-in.)-diameter Schedule-40 PVC pipe. The upstream turbine-

Figure 2-3. Linear Hydraulic Flume

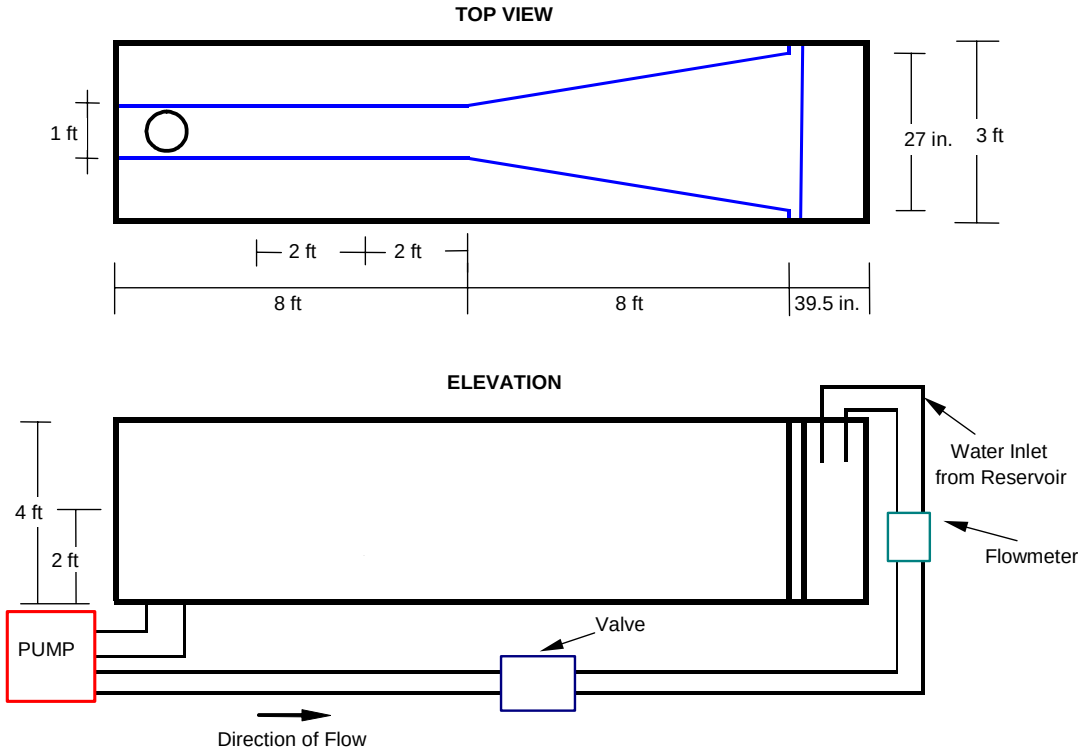

Figure 2-4. Schematic of Linear Hydraulic Flume (Not to Scale)

type flow meter used a meter-mounted display (Great Plains Industries Model A200) with 5.08-cm (2-in.)-diameter fittings. PVC fittings were used to transition between the 7.62-cm (3-in.)-diameter connecting pipe and the 5.08-cm (2-in.) fittings. A remotely mounted transmitter (Great Plains Industries Remote 4–20mA) allowed flow rate information to be transmitted to a datalogger as a 4-20-mA current signal or as a 0-5-V signal. The equipment was wired to provide a 0-5-V signal for the throttle valve tests. The remotely mounted transmitter had a response time of 0.7 s. The flow meter had a measurement range of 1.26-12.62 (20-200 gpm), with a relative accuracy of 1% of the reading. The maximum rated system pressure of the flow meter was 2.07 MPa (300 psi). The flow meter and transmitter were obtained as a prepackaged assembly from Cole-Palmer (Part number EW-05608-37).

Located 2.13 m (7 ft) downstream of the flow meter was an eight-stage constant speed pump [Flowserve Model WDE8, 3550 rpm, with a 14.50-cm (5.71-in.)-diameter open impeller and a rated flow capacity of 0-7.57 l/s (0-120 gpm)]. The pump was driven by a 30-kw (40-hp), three-phase, 208-230/460-V continuous-duty motor. At a flow rate of 6.31 l/s (100 gpm), the pump had a rated head of 246.28 m (808 ft); at a flow of 3.22 l/s (51 gpm), the pump had a design head of 328.27 m (1077 ft). The pump case had a 7.62-cm (3-in.)-diameter horizontal inlet fitting and a 0.61-cm (2-in.)-diameter vertical outlet fitting. Flexible vibration fittings were installed at the pump inlet and outlet to isolate the pump mechanically from the other portions of the apparatus.

The goal for the selection of the pump for this testing was to obtain a pump of similar design to the HPSI pumps commonly used in U.S. PWRs. The total HPSI flow required for the small-break LOCA of interest is on the order of 12.62–18.93 l/s (200–300 gpm). For HPSI systems having four injection paths, each path has an anticipated flow rate of 3.15–4.73 l/s (50–75 gpm) over a ΔP of ~~1.38 MPa (200 psi). The pump for this test program was chosen to achieve this performance and had a rated flow rate of 6.31 l/s (100 gpm). Because the pump was operated at 4.73 l/s (75 gpm) during testing, additional head was available to possibly purge debris from the valve in the event of clogging. Actual HPSI pumps would push up to the rated system pressure [15.5 MPa (2250 psi)] in an attempt to overcome actual valve blockage. Some tests were also performed at 6.12 l/s (97 gpm), near the rated flow of the pump, to provide a wider range of testing for parametric studies.

2.2.3 Pump Discharge to Throttle Valve

The section of the test loop from the discharge of the pump to the throttle valve is shown in Figure 2-6. The debris insertion manifold shown enlarged in Figure 2-7 was located 0.91 m (3 ft) downstream of the pump discharge. Use of the debris insertion manifold allowed debris to be inserted into the flow stream without disrupting the flow of water through the throttle valve. The debris insertion manifold used 5.08-cm (2-in.)-diameter galvanized steel piping. Two flow paths were provided by the debris insertion manifold: (1) a straight path with no debris and (2) a debris injection path that was connected to a 5.08-cm (2-in.)-diameter debris insertion port. It was also possible to have water simultaneously flowing through both the straight path and the debris injection path. Flow in the debris insertion manifold was controlled by four 5.08-cm (2-in.) ball valves (Hammond Model 8901 GLP 02-06). The piping diameter, 5.08 cm (2 in.), was chosen because it was the most common HPSI injection line size based on informal plant and vendor surveys.

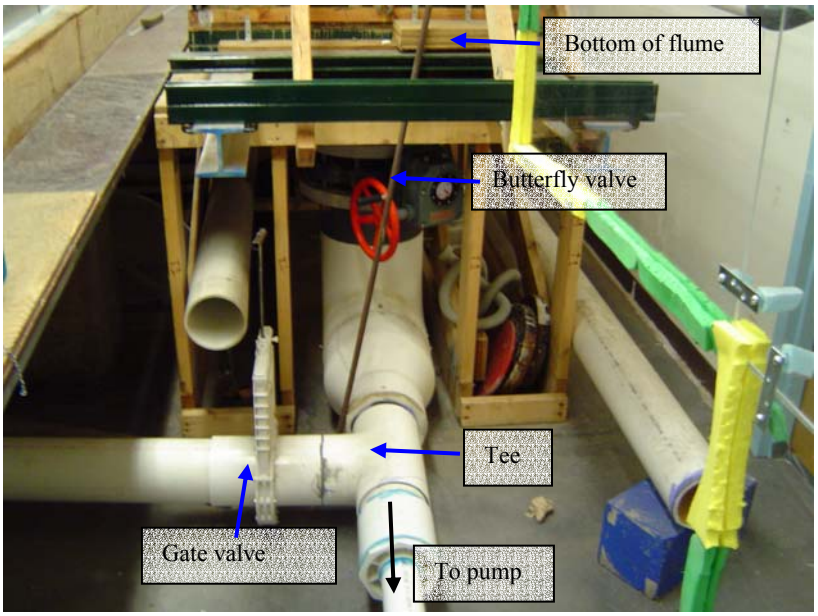

Figure 2-5. Discharge from Flume

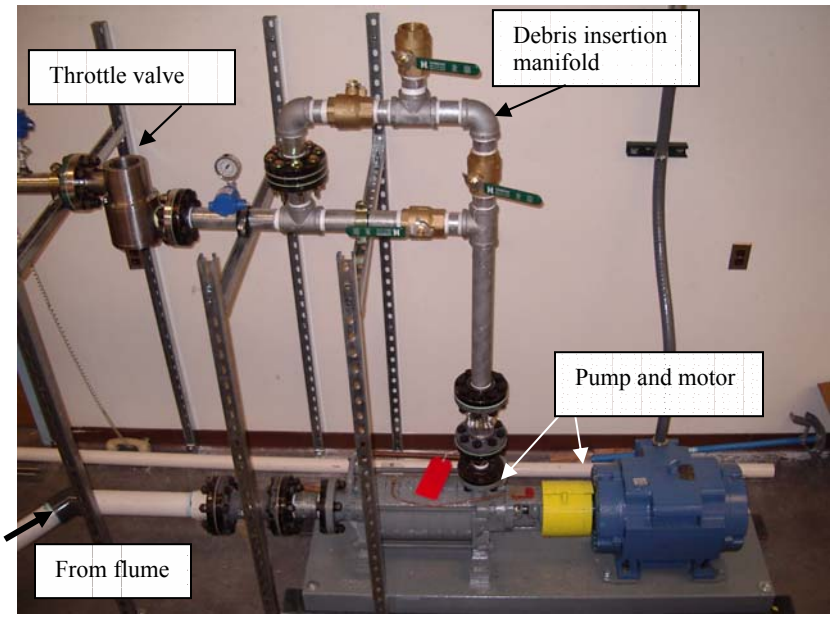

Figure 2-6. Detail of Test Loop from Pump to Throttle Valve

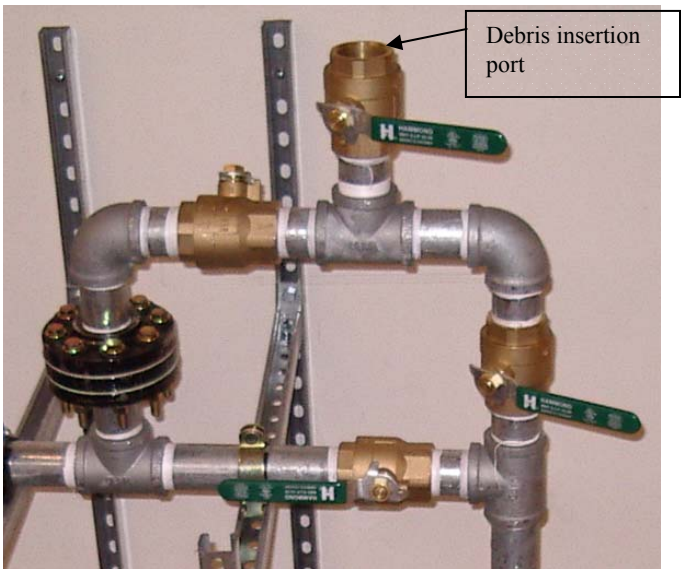

Figure 2-7. Debris Insertion Manifold

The upstream pressure transducer and pressure gauge were located 15.24 cm (6 in.) downstream of the debris insertion manifold (see Figure 2-8). The pressure transducer used was a Cole-Palmer Model 68070-08 [0-3.45 MPa (0-500 psi), output 4-20 mA]. Installation information included with the pressure transducer indicated that it was identical to a Sentra Systems, Inc., Model 256. The transducer could send only current signals (in milliamperes) to a datalogger. The transducer had an accuracy of ±0.13% of full scale [4.48 kPa at 3.45 MPa (0.65 psi at 500 psi) full scale] and a response time of 1-5 ms. A dial pressure gauge having a scale from 0-4.14 MPa (0-600 psi) also was placed at the location of the pressure transducer.

Figure 2-8. Detail Showing Location of Upstream Pressure Transducer

2.2.4 Throttle Valve

The surrogate throttle valve was located 15.24 cm (6 in.) downstream of the upstream pressure transducer (Figure 2-8). This valve was the primary focus of the test program described in this report, and all of the other equipment in the test facility was used to determine the flow conditions through the throttle valve. The valve used was a surrogate for throttle valves that are found in PWRs. Because a comprehensive database for U.S. PWR HPSI system parameters was lacking, informal surveys of plants and vendors were used to establish HPSI throttle valve parameters in the industry. Although a wide range of valve brands and types are used as HPSI throttle valves, anecdotal information from qualified valve vendors indicated that the most common valve used for this application is a globe valve The sizes employed are relatively small, typically in the range of 2.54-10.16 cm (1-4 in.) in diameter. The most common size is thought to be ~5.08 cm (2 in.).

Figure 2-9 illustrates the key features of globe valves. The basic plug-type globe valve has a stem-actuated plug that moves parallel to the bulk flow stream passing through the valve port opening. The plug position can be adjusted to either restrict or allow flow. Figure 2-9 shows two different types of globe valve plug and seat arrangements.

Because of the wide variety of HPSI throttle valves, no attempt was made to replicate or endorse a particular throttle valve design for the current study. The primary goal for the surrogate valve design was to be reasonably representative of the actual throttle valves in service by maintaining the flow complexity exhibited in common globe valve designs. With that in mind, ranges of appropriate valve clearances, angular orientations, inlet and exit diameters, and constriction lengths were determined from a qualified vendor supply catalog.

To maximize debris clogging, the valve gaps should be near the lower end of the service range and the angle and length of the flow path should be near the upper end of the service range. The surrogate valve was designed based on this conservative configuration and should maximize the blockage observed in these tests.

The surrogate valve was designed by ARES Corporation under contract to Los Alamos National Laboratory (LANL). A cross-section drawing of the valve is shown in Figure 2-10.The valve was constructed of stainless steel and had 5.08-cm (2-in.)-diameter inlet and outlet flanges. The valve was constructed so that the top or the bottom of the valve easily could be opened and inspected. The valve had a threaded valve stem that allowed precise adjustment of the space or gap between the seat plug and the seat ring. The gap, as measured perpendicular to the face of the seat plug, is the valve-opening distance that is referenced throughout this document. The valve stem movement was perpendicular to the plane of the seat ring. The seat plug was a truncated perpendicular cone such that the valve opening was always symmetrical. The top of the valve had a caliper block located near the threaded stem to enable the measurement of the vertical distance between the top of the caliper block and the top of the threaded valve stem. This distance changed as the valve was opened or closed. To obtain a specific valve opening, the manufacturer of the valve provided a table that showed the relationship between the caliper block measurements and valve seal gap. The procedure to set a specified valve opening was provided by the valve designer. The valve construction and gap setting procedure are described in Ref. 4.

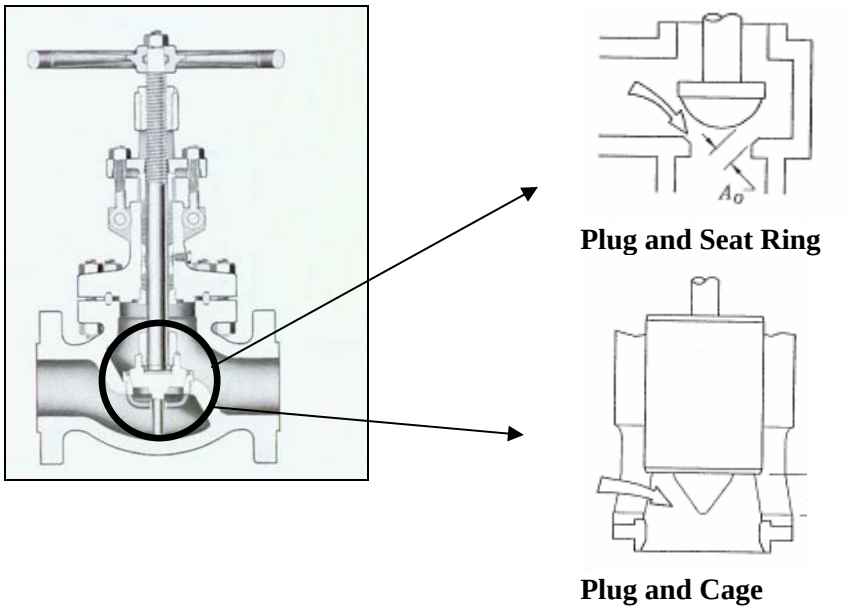

Figure 2-9. Basic Globe Valve Design with Possible Types of Valve Throat Configurations

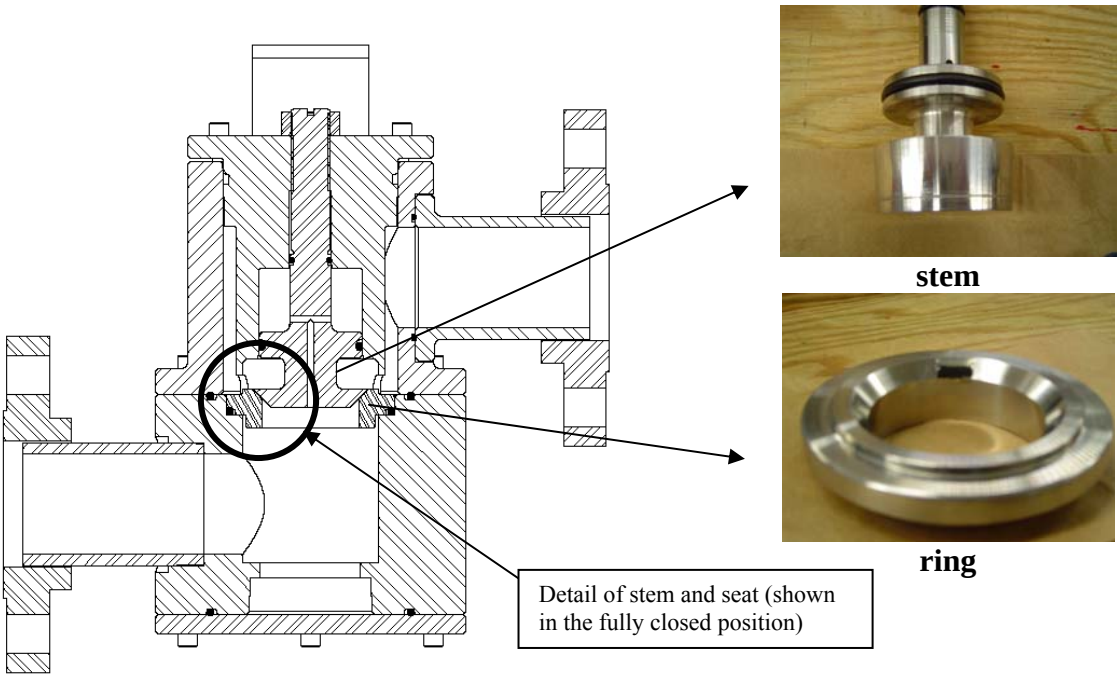

Figure 2-10. Detail of Surrogate Valve Stem and Ring

The valve was supplied with three interchangeable valve stem-seat plug and seat ring assemblies. The details of the assemblies are shown in Figure 2-11 through Figure 2-14. The external view of the throttle valve body is shown in Figure 2-15 and a photograph of the 5S and 5L stems is shown in Figure 2-16. The details are described as follows:

1. 5S: The seat plug was tapered at an angle of 5º from the axis of the valve stem so that the convergence angle of the seat plug sides was 10º (A in Figure 2-12). The maximum valve opening with this valve stem-seat plug was 0.2766 cm (0.1089 in.).

2. 5L: The seat plug was tapered at an angle of 5º from the axis of the valve stem so that the convergence angle of the seat plug sides was 10º. The maximum valve opening with this valve stem-seat plug was 0.127 cm (0.0501 in.).

3. 45L: The seat plug was tapered at an angle of 45º from the axis of the valve stem so that the convergence angle of the seat plug sides was 90º. The maximum valve opening with this valve stem-seat plug was 0.1033 cm (0.4066 in.).

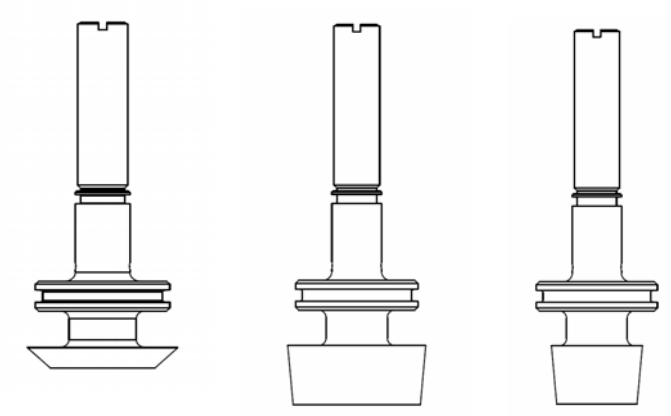

(a) Stem 45L (b) Stem 5L (c) Stem 5S

Figure 2-11. Valve Stems Used in the Tests

2.2.5 Downstream of Valve

The details of the test loop downstream of the valve are shown in Figure 2-17.

The downstream pressure transducer and pressure gauge were located 15.24 cm (6 in.) downstream of the throttle valve discharge flange. A Cole Palmer applications engineer indicated that turbulence had no impact on the accuracy of the pressure transducer reading as long as the pipe was filled; therefore, there was no straight run requirement for locating the pressure transducers. The pressure transducer and dial gauge were identical to the upstream pressure transducer and gauge. By measuring the pressures at each of the gauge locations, it was possible

to determine the pressure differential across the throttle valve. Pressure differential was one of the primary measurements used to establish performance of the throttle valve.

The flow control valve was located 15.24 cm (6 in.) downstream of the downstream pressure transducer. This 5.08-cm (2-in.)-diameter forged-steel globe valve had a pressure rating of 13.10 MPa (1900 psi) and provided the primary mechanism by which flow through the throttle valve was adjusted. Although the flow control valve could be opened fully to allow maximum system flow, the flow control valve was closed partially for most tests so that a specified flow rate [i.e., 4.73 l/s (75 gpm)] could be maintained. For each throttle valve test, the flow control valve was adjusted to an initial setting that was not changed until the test was completed.

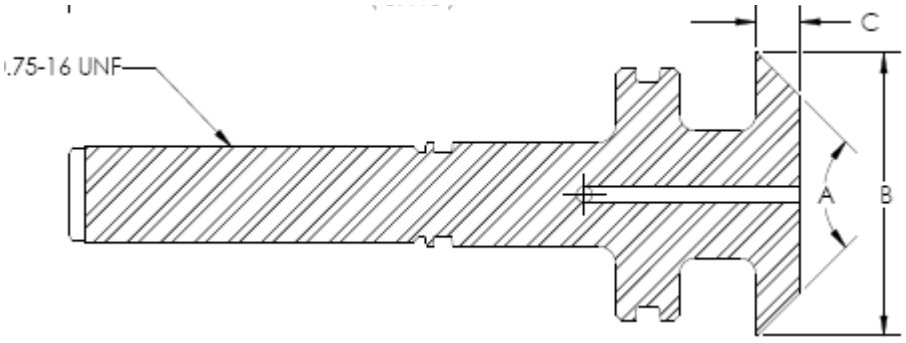

Stem Designation	Full-Angle A (deg)	Dimension B [cm (in.)]	Dimension C [cm (in.)]
45L	90	5.71 (2.25)	0.89 (0.35)
5L	10	5.71 (2.25)	2.54 (1.00)
5S	10	3.81 (1.50)	2.54 (1.00)

Figure 2-12. Key Dimensions of the Valve Stems

(a) Ring 45L (b) Ring 5L (c) Ring 5S

Figure 2-13. Valve Seat Rings Used in the Tests

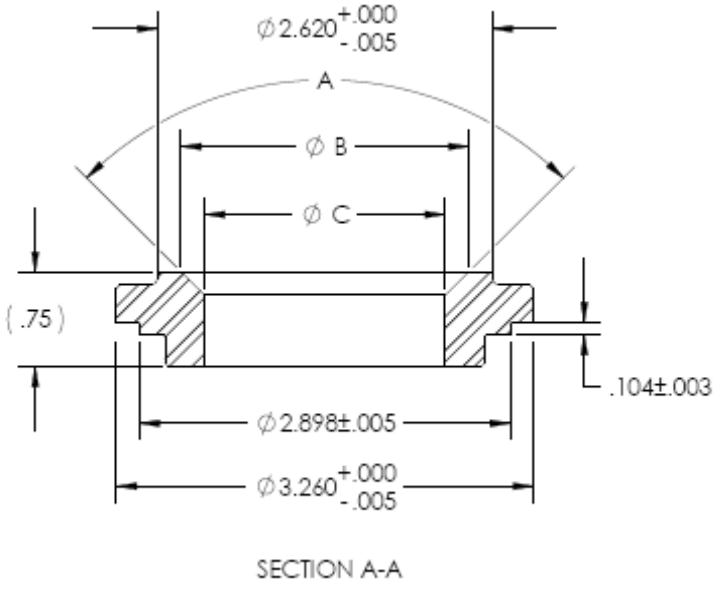

Stem Designation	Full-Angle A (deg)	Dimension B [cm (in.)]	Dimension C [cm (in.)]
45L	90	5.71 (2.25)	4.762 (1.875)
5L	10	5.71 (2.25)	n/a
5S	10	3.81 (1.50)	n/a

Figure 2-14. Key Dimensions of Valve Rings

Figure 2-15. Surrogate Throttle Valve

Figure 2-16. 5L and 5S Valve Stem-Seat Plugs and Seat Rings

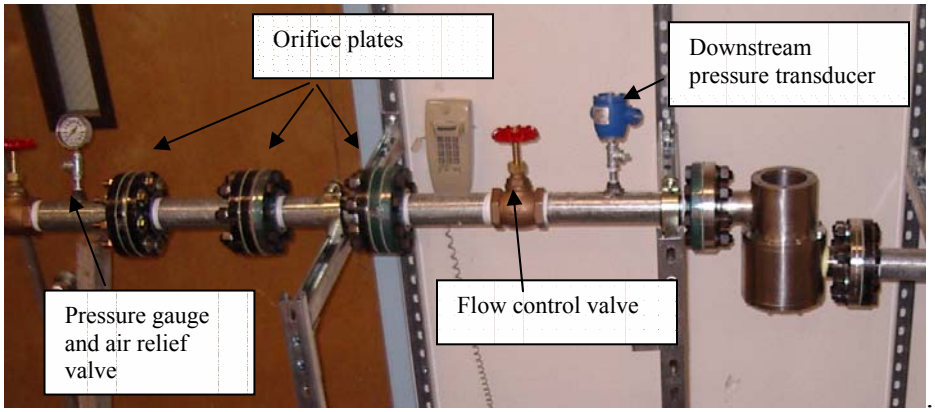

Figure 2-17. Part of the Test Loop Downstream of the Valve

Three orifice plates were initially located downstream of the flow control valve. The orifice plates were located 20.32 cm (8 in.) apart and the first orifice plate was located 15.24 cm (6 in.) downstream of the flow control valve. The orifice plates were placed to reduce the high pressure in the throttle valve to an acceptable pressure for discharge to the flume through PVC Schedule-40 pipe. The orifice plates also provided flow control when other valves were fully open. The orifice plates were 1.90-cm (0.75-in.) flat steel plates placed between flanged fittings with a 1.587-cm (0.625-in.)-diameter hole drilled in the center of the plate. The orifice plates restricted the flow on the adjoining 5.08-cm (2-in.)-diameter pipe.

The three orifice plates were used for Test Series 1 (Test series designations were defined in Sections 1.3.3–1.3.5. At the end of those tests, it was determined that a single orifice plate likely would serve the desired function and reduce the potential for debris trapping. Two of the orifice

plates were replaced with plates with 5.08-cm (2-in.)-diameter holes so that only one plate had a 1.587-cm (0.625-in.)-diameter flow restriction. The maximum system flow rate increased slightly with this modification, but the downstream pressure remained at an acceptable level. Test Series 2 and 3 were performed using a single orifice plate.

A dial pressure gauge and a manual air-bleed fitting were located 10.16 cm (4 in.) downstream of the downstream orifice plate. The gauge served to verify that the pressure below the orifice plate was sufficiently small that flows could be conveyed in Schedule-40 PVC pipe. The manual air-bleed valve was used to remove any air that might be trapped downstream of the orifice plates.

A low-pressure globe valve was placed 15.24 cm (6 in.) downstream of the dial pressure gauge. This valve was open during throttle valve testing but was closed to prevent backflow when the throttle valve was opened for inspection. Upstream of the low-pressure gate valve, galvanized steel pipe is used. Downstream of the valve, Schedule-40 PVC pipe was used.

The downstream flow meter was located 4.57 m (15 ft) downstream of the low-pressure gate valve. This flow meter was identical in model to the upstream flow meter. The downstream flow meter was in place during initial system testing and during throttle valve testing that used only RMI debris. Because this was a turbine-type gauge, it was found that RMI would become trapped in the gauge mechanism and that the downstream flow measurements would become erratic. Frequent removal of the meter for cleaning was required, and the downstream flow meter could not reliably measure flow when debris was added. The flow-meter manufacturer did not recommend this device for flow with debris. A concern was raised that use of fibrous debris such as NUKON would produce additional measurement problems; therefore, the flow meter was removed from the test apparatus for all subsequent tests.

Downstream of the downstream flow meter, 4.57 m (15 ft) of Schedule-40 PVC pipe was used to convey the flow back to the upstream end of the linear hydraulic flume. Within this length, a 1.22-m (4-ft) section of vertical pipe allowed the water to be conveyed above the high-water level in the flume, as shown in Figure 2-18a and b.

Immediately upstream of the vertical pipe section, two 5.08-cm (2-in.) ball valves (Hammond Model 8901 GLP 02-06) and a 5.08-cm × 5.08-cm (2-in. × 2-in.) PVC tee were used to create a vertical drain. This section of piping is shown schematically in Figure 2-19. During pumping, the drain valve could be opened and the main pipe valve closed to flush the discharge line of debris. The vertical pipe section also could be back-flushed to the open drain.

The discharge pipe to the linear hydraulic flume had a short section of vertical pipe that directed discharge water vertically downward to the water surface in the flume (Figure 2-18b). At this location, a screen collector was placed to capture larger debris particles before they entered the flume. Several screen collectors were manufactured from 5-gal. plastic buckets. The bottoms of the buckets were removed and replaced with 40- or 100-mesh stainless-steel screens. During testing with debris, the buckets were in place to capture debris. A screen collector also was used to collect debris that was flushed through the vertical drain valve. The detail of the debris recovery bucket is shown in Figure 2-20; this photograph was taken after a test using a NUKON-RMI mixture. Both types of debris are visible. The debris recovered from the bucket was dried in

an oven and then weighed to determine the mass of debris recovered (see definition of parameter W2 in Section 2.5).

This section describes the valves, pumps, gauges, transducers, and fittings used in the hydraulic system for testing the throttle valve. The other essential element was the data acquisition system, which is described in Section 2.3.1.

(a) downstream of orifice plates (b) return to flume

Figure 2-18. Details of the Fluid Return Section of the Test Loop

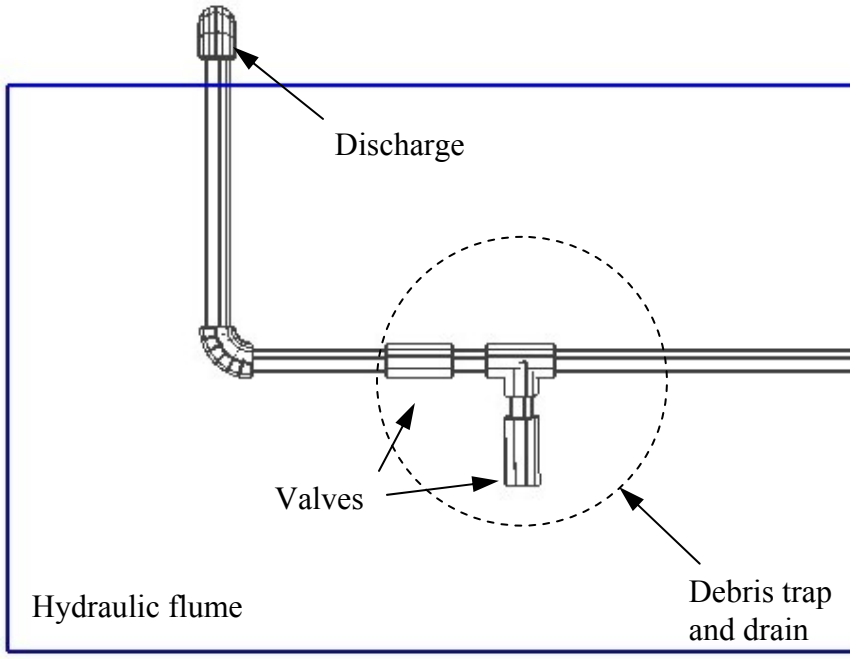

Figure 2-19. Detailed Schematic of the Fluid Return Line (Side Elevation)

Figure 2-20. Debris Recovery Bucket after a Test Involving a Mixture of RMI and NUKON

2.3 Data

2.3.1 Data Acquisition

Data from flow meters and pressure transducers were sent to a National Instruments Field Point Network Module (Model FP-1601) and a National Instruments Field Point Analog Input Module (Model FP-AI-100). The network module communicated with a computer used to store measured data, and the Analog Input Module communicated with instruments that measured electrical voltage or current. The network module was connected to the analog input module so that analog signals from the instrumentation were sent as digital signals to a data collection computer. The collection and processing of analog data was controlled by the National Instruments Lab View computer program. For the throttle valve tests, Lab View, Version 7.1 was used with a computer running Microsoft Windows XP. The Lab View program contained modules that defined the kind of analog signal (range of voltage or current) that the analog input module could receive and the frequency and type of data that would be stored on the data collection computer. The National Instruments Field Point Network Module and Analog Input Module were powered by a 24-V power supply that was included with the Field Point equipment.

When electrical power was supplied to the upstream and downstream pressure transducers, the transducers produced an electrical current signal (in milliamperes) that varied with the magnitude of the pressure measurement. This signal was processed through the Field Point equipment by the Lab View program to obtain measured pressure data. Similarly, when electrical power was supplied to the upstream and downstream flow meters, the remotely mounted transmitters produced a voltage signal (0-5 V) that varied with the magnitude of the flow. Both the current and the voltage signals had to be calibrated to the instrument measurements so that the measured

reading at the pressure transducer or flow meter was in agreement with the value recorded by the computer. A calibration equation within the Lab View program performed this task.

Power (24 V) had to be supplied to the pressure transducer and the flow-meter transmitter for the instruments to function. During initial throttle valve testing, four separate power supplies were used to supply power to each of the four monitoring devices (two pressure transducers and two flow meters). Subsequent review of recommended wiring diagrams for the analog input module indicated that a single power supply could be used to supply power to the analog input module and that this single power source could be used to provide power to all four monitoring devices. It was found that this single power source slightly reduced measurement variability and improved the quality of the recorded data. A further discussion of measurement variability is found in Sections 4, 5, and 6.

The choice of a data collection computer was found to impact the precision of the data that could be collected. Initial data collection used a collection interval of 100 ms, and a laptop computer with a 1.0-GHz or faster processor could collect data at this frequency. Because the testing of the throttle valve was measuring flow rate and pressure fluctuations that often lasted <1 s, it was desirable to reduce the data collection interval. A 2.0-GHz computer was used to collect data at an interval of 6 ms. To obtain this frequency, the Lab View program needed to be revised to minimize the graphical display of collected data and the computer had to be temporarily set up to minimize parallel processes, such as battery monitors and virus protection. A 1.0-GHz computer could not be used with a 6-ms data collection interval.

During the process of reprogramming Lab View for the 6-ms data collection interval, it was noted that the existing programming was not directly recording the measured data but was recording the average of the measurement plus the four previous measurements. This programming apparently derived from previous use of the program code in an application that did not have rapid changes in data values. For the throttle valve tests, the five-point averaging was not desirable and all subsequent testing was conducted with single-point data collection. These tests included the last two Cv baseline tests for the 45L and 5L stems; the June blockage tests; and throttle valve tests N-1 to N-9, D-1 to D-19, and A-1 to A-3. In general, the single-point sampling used data collection intervals of 0.006 s, but some long-term testing used intervals of 0.1 s. The use of single-point measurements in place of five-point averaging created an increase in the data measurement variability; however, the concurrent improvements in the electrical wiring more than compensated for this effect.

After completion of some of the early tests, it was observed that the recorded pressure readings had fluctuations that were considerably larger than could be attributed to the inherent measurement uncertainty of the pressure transducers. The measurements were fluctuating at ±13.79 kPa (±2 psi) from a general trend line. The recorded flow rates varied by ±0.0126 l/s (±0.2 gpm) from the general trend line at a flow rate of 4.73 l/s (75 gpm). A concern was raised that the level of data fluctuation could obscure important physical conditions that needed to be measured with the throttle valve tests. Many diagnostic studies were done to address this issue. Of the various diagnostics that were done, grounding of the various instruments and the data cable conduits produced the most improvement in data quality. The details are included in Appendix C.

2.3.2 Temperature Control

One other important property that affects throttle valve performance is the temperature of the water and the resulting changes in viscosity and density. Because the temperature of the water was not expected to have a large change during any single throttle valve test, it was not deemed necessary to have continuous temperature recording. Instead, manual collection of water temperature was used for the throttle valve tests. In general, the water temperature was measured at one time for tests lasting <10 min. Multiple measurements were used for longer-duration tests. Type-K thermocouples were installed in the PVC pipe sections upstream and downstream of the pump and throttle valve. One thermocouple was installed 0.61 m (2 ft) downstream of the upstream flow meter. The second thermocouple was installed 0.91 m (3 ft) downstream of the downstream orifice plate. In both the upstream and down stream locations, the thermocouples were reading fluid centerline temperature. Temperature measurements were obtained using a handheld meter (Omegaette HH308) designed to read type-K thermocouples.

When temperature data were obtained during throttle valve tests, it quickly was found that the temperature measurements of the upstream and the downstream thermocouples were not the same and that the downstream thermocouple consistently had a higher temperature than the upstream thermocouple. It was found that the temperature difference was related inversely to the pumping flow rate. At a flow of 4.73 l/s (75 gpm) [nominally 2.90 MPa (420 psi) at the upstream pressure tap], the temperature difference was ~1.28°C (2.3°F). This temperature change primarily was attributed to the energy supplied to the water by the pump. For short-duration tests, the volume of water in the flume was sufficient to limit the amount of temperature gain; however, for longer-duration tests, the heating of the water caused the system temperature to increase significantly.

2.4 Material Preparation

As noted earlier, the debris used in the tests consisted of RMI, NUKON, and CalSil. The debris types chosen for these tests were not intended to include everything that could be ingested in an ECCS (see Ref. 5 for a more comprehensive list of insulation and coating materials). The quantities of RMI, NUKON, and CalSil that were used in this study were based on the quantity needed to cause measurable blockage rather than being specifically linked to anticipated plant debris loadings. Specifications of the material used and the methods used to prepare them for the tests are discussed in this section.

2.4.1 RMI

The RMI debris was made of type-304 stainless-steel foils having a thickness of 0.005 cm (0.002 in.). The material was purchased in 0.61-m × 1.22-m (2-ft × 4-ft) sheets from Transco Products Inc. (Chicago, Illinois) and was prototypical of the foil that Transco uses to fabricate RMI cassettes. These sheets were cut by hand to the required dimensions. Three sizes of RMI debris were cut: 0.63-cm × 0.63-cm (1/4-in. × 1/4-in.) squares, 0.32-cm × 0.32-cm (1/8-in. × 1/8-in.) squares, and 0.32-cm × 1.27-cm (1/8-in. × 1/2-in.) rectangles. The sizes for the debris were determined by measuring with an ordinary graduated ruler and marking the RMI with a pencil. The debris then was cut to size with hand scissors and a paper cutter. For tests conducted after February 1, 2005, the RMI came from material that had been used previously in the tests

described in Ref. 1. The RMI material from that test had been cut into 5.08-cm × 5.08-cm (2-in. × 2-in.) (approximate) squares and crumpled by hand before testing. For the throttle valve tests, these RMI pieces were first flattened using the end of a flat wooden ruler; then the RMI was marked with a pencil and cut to size. With this process, some wrinkles remained on the flattened squares. Severely crumpled RMI squares were discarded. Figure 2-21 shows photographs of three sizes of RMI samples used in the experiments. Each photograph includes pieces before the tests, as well as pieces recovered after the tests, which show the bending and twisting that may occur as the RMI pieces pass through the test system.

Based on measurements of 25 cut debris pieces, the 0.63-cm × 0.63-cm (1/4-in. × 1/4-in.) debris had a mean weight of 0.0169 g, with a standard deviation of 0.0013 g; the 0.32-cm × 0.32-cm (1/8-in. × 1/8-in.) debris had a mean weight of 0.0038 g, with a standard deviation of 0.0007 g. Based on measurements of 10 cut debris particles, the 0.63-cm × 0.63-cm (1/4-in. × 1/4-in.) RMI samples had a mean dimension of 0.6642 cm (0.2615 in.), with a standard deviation of 0.315 cm (0.0124 in.); the 0.32-cm × 0.32-cm (1/8-in. × 1/8-in.) samples had a mean dimension of 0.3172 cm (0.1249 in.), with a standard deviation of 0.03 cm (0.010 in.).

The RMI was added to the tests in measured batches. The measurements were obtained by placing the debris in a small plastic container, with the material weighed using a 0.01-g balance. Except when combined with other debris types, the RMI was added to the debris insertion manifold in dry form. In all cases, the manifold was filled with water before debris was introduced to eliminate air pockets.

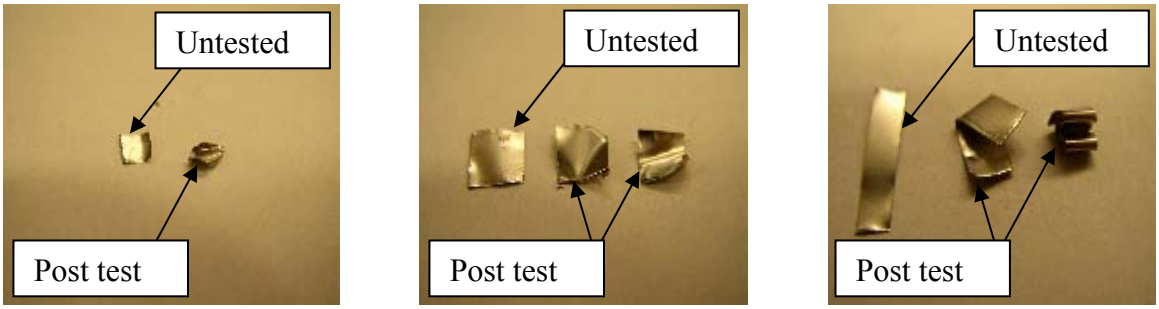

(a) 0.32 cm × 0.32 cm (1/8 in. × 1/8 in.)

(b) 0.63 cm × 0.63 cm (1/4 in. × 1/4 in.)

(c) 0.32 cm × 1.27 cm (1/8 in. × 1/2 in.)

Figure 2-21. Examples of RMI Samples

2.4.2 NUKON

NUKON, manufactured by Owens Corning (Toledo, Ohio), is a continuous-filament fiberglass-insulating material with a specific gravity of 2.6. Before use in these tests, the batts of NUKON were stored outdoors and exposed to atmospheric conditions. For use during testing, small quantities of the NUKON batts were removed and weighed using a 0.01-g balance. Then the NUKON was placed in boiling tap water for 5 min; this process made the fiberglass particles more flexible. The wet NUKON was removed from boiling water and immediately placed in a

kitchen blender (Black and Decker, Model BL6000). Cold tap water was added in sufficient quantity to cover the NUKON fiber. The NUKON and water first were mixed at low speed for 2 min. Then the blender was turned off, and any NUKON fiber was flushed from the sides of the blender chamber. Then the NUKON and water was mixed at medium speed for 3 min. This process produced a slurry mix of NUKON and water, as shown in Figure 2-22. The NUKON and water slurry then was placed in a separate container before testing. All of the NUKON on the blender was flushed from the blender with water. The NUKON quickly settled to the bottom of the container. The NUKON slurry may have sat for several hours or days before being used in a test. When the NUKON slurry was to be placed in the debris insertion manifold, it was first mixed using a metal spoon. Some of the water that was in the manifold had to be removed to provide space for the NUKON slurry. This process was accomplished by draining the manifold before testing or by using a portable wet-dry vacuum. When the NUKON slurry was added to the debris insertion manifold, any space remaining was filled with tap water so that large air pockets were not created in the manifold. On several tests, the volume of the NUKON slurry exceeded the volume available in the manifold. With these tests, any excess NUKON slurry was oven-dried so that the weight of the excess could be subtracted from the original weight of the NUKON.

Figure 2-22. NUKON after Processing by Kitchen Blender

2.4.3 CalSil

CalSil is a high-temperature calcium silicate insulation manufactured by RATH Performance Fibers, Inc. (Wilmington, Delaware). CalSil contains >90% synthetic calcium silicate, >1% aluminum silicate, >1% inorganic fiber, >1% cellulose, and >0.1% crystalline silica. The material normally is found as a yellow or white solid block or solid pipe insulation.

A sample of CalSil that consisted of broken pieces and fine powdery debris was available in the UNM laboratory (Figure 2-23). For the throttle valve tests, the CalSil was processed further by

passing the material through a #4 [4.75-mm (0.19 in.)] or #8 [2.36-mm (0.09-in.)] sieve; the material that passed through the sieve was retained for testing. The material remaining on the sieve was removed, further crushed with a rubber-tipped pestle, and returned to the sieve. After several passes of crushing and sieving, any material remaining on the sieve was discarded. Except for one test, all of the CalSil used in the throttle valve test had passed a #4 or #8 sieve. For one test (test 5sc9) unsieved CalSil from the initial broken sample was tested. Most of the CalSil that had passed through the sieves was much finer than the sieve size, and little visual difference was observed between the CalSil that had passed the #4 sieve and the CalSil that had passed the #8 sieve. Before testing in the throttle valve apparatus, the appropriate quantity of dry CalSil was obtained with a 0.01-g balance. Then tap water was added in a sufficient quantity and mixed with the CalSil to form a slurry. Water in the debris insertion manifold was removed to provide space for the CalSil slurry using the same procedure as with the NUKON insulation.

Figure 2-23. CalSil Sample

2.4.4 Mixtures of RMI, NUKON, and CalSil

Some tests called for a mixture of RMI and CalSil, RMI and NUKON, NUKON and CalSil, or a mixture of all three debris types. In all of these tests, the debris was prepared first as described for each of the three single debris types. Then the debris types were mixed together by hand. The combined debris was added to the debris insertion manifold in a manner similar to that described with the NUKON testing. For mixtures of all three debris types, different insertion sequences were specified for different tests.

2.5 Test Parameters

The test procedure is described in detail in Appendix A. The types of data recorded during each test, as well as the nomenclature used to refer to them in subsequent sections, are described in this section.

Stem: The valve-stem/ring combination used (one of three possibilities: 45L, 5L, or 5S). This combination was noted before the start of each test.

Gap: The valve opening (in inches) specified for each test in the test matrix. The gap was measured perpendicular to the face of the seat plug. The range of valve-opening sizes for the 5L and 5S configurations was significantly lower than that for 45L. This disparity was the result of differences in the design of the configurations and the need to maintain similar flow over the range of valve openings for a given stem configuration.

N1: The number of RMI pieces introduced in the system (for tests where a specified number of pieces of RMI was introduced in the system).

W1: The mass of RMI introduced in the system, in grams, for tests where a specified mass of RMI was introduced.

WN: The mass of NUKON introduced in the system (grams).

WC: The mass of CalSil introduced in the system (grams).

Sieve #: The mesh size of the screen used to sieve the CalSil. The two sieves used were #4 and #8.

RMI size: The size of the RMI pieces introduced (uniform for any given single-debris test and possibly a combination of two sizes in the mixed-debris tests). Examples of square and rectangular pieces of RMI are shown in Figure 2-21.

K: Valve loss coefficient.

K before: The average *K* before introduction of debris. Typically, the averaging was done over a time window between ~500 ms after the start of data acquisition and ~0.1 s before the introduction of debris. Averages also were calculated for intermediate time windows within this interval and generally were found to be within the margin of error for the tests; thus, only the result for the full pre-test time interval as described previously was presented.

K after: The average *K* after introduction of debris. Typically, the averaging was done over a time window between ~30 s after debris insertion and the end of data acquisition. Averages also were calculated for intermediate time windows within this interval and generally were found to be within the margin of error for the tests; thus, only the result for the full post-test time interval as described previously was presented.

$\Delta K\%$: The percent increase in average *K* after debris insertion. Only values >5% were included. Values less than this value were considered to be within the range of uncertainty in the calculation of *K* and thus were not considered to be meaningful (these are indicated by "<5" in the tables).

W2: The mass of debris recovered in the recovery bucket during the test and after post-test flushing. The recovery bucket was located inside the flume at the outlet of the vertical segment of pipe shown in Figure 2-18b. The debris recovered following an example test is shown in Figure 2-20. The procedure is described in Section 2.2.5.

Wf: The mass of debris not recovered during the test and after post-test flushing. This measurement was taken as the difference between the initial debris mass and the mass of debris recovered in the bucket. The mass of the RMI contained within the valve after the test is included in this measurement.

NR: The number of RMI pieces recovered from the throttle valve after a test. This RMI mass is included in Wf.

2.6 Test Matrix

The test matrix for debris testing is divided into three tables, representing the three phases of testing, single debris, mixed debris, and debris accumulation. Baseline tests were performed before each phase of testing and at the end of the test program. Baseline data for known blockage conditions were obtained for selected valve configurations at the start of the test program and at the end of testing.

The test matrix for the single-debris tests, Table 2-1, provides the test conditions established for the first test series. The key test conditions that were established were the gap size, mass (and size for RMI) of debris, type of debris, and stem configuration (45L, 5L, or 5S). The RMI test conditions are provided first, followed by NUKON and CalSil. Similarly, the test matrix for the mixed-debris tests, Table 2-2, provides the conditions established for the second test series. The gap, debris mass, debris type, and debris sizes are provided for the different debris combinations and stem configurations tested. The addition sequence is also provided for the sequentially mixed debris. The test matrix for the debris accumulation tests, Table 2-3, established the test conditions for the third test series. A complete test matrix listing every test along with the observed increase in K is provided in Appendix D.

2.7 Data Analysis

The approach used to analyze the data and present the results is outlined in this section.

2.7.1 Valve Pressure Loss

The valve pressure drop is the indicator of flow resistance in the valve. When debris gets trapped in the valve, the flow resistance increases. If the flow rate through the valve remains the same, this translates to a higher pressure drop across the valve. The flow resistance of the valve can be expressed as either a valve-loss coefficient, K, or equivalently a valve-flow coefficient, Cv.

Table 2-1. Single Debris Test Matrix

RMI Tests, Stem # 45L

Gap 0.317 cm (0.125 in.)											
RMI Type [cm × cm (in. × in.)]											
0.317 × 0.317 (1/8 × 1/8)				**0.63 × 0.63 (1/4 × 1/4)**				**0.317 × 1.27 (1/8 × 1/2)**			
1 g	5 g	10 g	10 pieces	1 g	5 g	10 g	10 pieces	1 g	5 g	10 g	10 pieces
Gap 0.159 cm (0.0625 in.)											
RMI Type [cm × cm (in. × in.)]											
0.317 × 0.317 (1/8 × 1/8)				**0.63 × 0.63 (1/4 × 1/4)**				**0.63 × 0.63 (1/4 × 1/4)**			
1 g	5 g	10 g	10 pieces	1 g	5 g	10 g	10 pieces	1 g	5 g	10 g	10 pieces
Gap 0.63 cm (0.25 in.)											
RMI Type [cm × cm (in. × in.)]											
0.317 × 0.317 (1/8 × 1/8)				**0.63 × 0.63 (1/4 × 1/4)**				**0.63 × 0.63 (1/4 × 1/4)**			
--	--	10 g	--	--	--	--	--	--	--	10 g	--

RMI Tests, Stem # 5L

Gap 0.13 cm (0.050 in.)											
RMI Type [cm × cm (in. × in.)]											
0.317 × 0.317 (1/8 × 1/8)				**0.63 × 0.63 (1/4 × 1/4)**				**0.317 × 1.27 (1/8 × 1/2)**			
1 g	5 g	10 g	10 pieces	1 g	5 g	10 g	10 pieces	1 g	5 g	10 g	10 pieces

RMI Tests, Stem # 5S

Gap 0.25 cm (0.10 in.)											
RMI Type [cm × cm (in. × in.)]											
0.317 × 0.317 (1/8 × 1/8)				**0.63 × 0.63 (1/4 × 1/4)**				**0.317 × 1.27 (1/8 × 1/2)**			
1 g	5 g	10 g	10 pieces	1 g	5 g	10 g	10 pieces	1 g	5 g	10 g	10 pieces
Gap 0.159 cm (0.0625 in.)											
RMI Type [cm × cm (in. × in.)]											
0.317 × 0.317 (1/8 × 1/8)				**0.63 × 0.63 (1/4 × 1/4)**				**0.317 × 1.27 (1/8 × 1/2)**			
1 g	5 g	10 g	10 pieces	1 g	5 g	10 g	10 pieces	1 g	5 g	10 g	10 pieces

Table 2-1. Single-Debris Test Matrix (cont)

CalSil Tests, Stem # 5L		CalSil Tests, Stem # 5S	
Gap	**Mass (g)**	**Gap**	**Mass (g)**
0.13 cm (0.050 in.)	50	0.159 cm (0.0625 in.)	50
	100		100
		0.25 cm (0.10 in.)	50
			100
			50 (Unsieved)

NUKON Tests, Stem # 45L		NUKON Tests, Stem # 5L	
Gap	**Mass (g)**	**Gap**	**Mass (g)**
0.159 cm (0.0625 in.)	25	0.13 cm (0.050 in.)	50
	50		100
	100	0.25 cm (0.10 in.)	50
NUKON Tests, Stem # 5S		0.159 cm (0.0625 in.)	50
Gap	**Mass (g)**	0.317 cm (0.125 in.)	50
0.25 cm (0.10 in.)	100		

Table 2-2. Mixed-Debris Test Matrix

	Stem	Gap [cm (in.)]	CalSil (g)	NUKON (g)	RMI (g)	RMI Type [cm × cm (in. × in.)]
RMI Mixture	45L	0.63 (0.25)	--	--	5	0.317 × 1.27 (1/8 × 1/2)
					5	0.63 × 0.63 (1/4 × 1/4)
NUKON-RMI Mixture	45L	0.63 (0.25)	--	50	10	0.317 × 1.27 (1/8 × 1/2)
	45L	0.317 (0.125)	--	50	10	0.317 × 1.27 (1/8 × 1/2)
	45L	0.159 (0.0625)	--	25	5	0.63 × 0.63 (1/4 × 1/4)
	5L	0.13 (0.05)	--	50	10	0.317 × 0.317 (1/8 × 1/8)
CalSil-NUKON Mixture	45L	0.317 (0.125)	25	25	--	--
	45L	0.159 (0.0625)	25	25	--	--
CalSil-RMI Mixture	45L	0.159 (0.0625)	50	--	5	0.63 × 0.63 (1/4 × 1/4)
CalSil-NUKON-RMI Mixture (Homogeneous)	45L	0.63 (0.25)	25	25	5	0.317 × 1.27 (1/8 × 1/2)
	45L	0.317 (0.125)	25	25	10	0.317 × 1.27 (1/8 × 1/2)
	45L	0.159 (0.0625)	25	25	5	0.63 × 0.63 (1/4 × 1/4)
	45L	0.159 (0.0625)	25	25	10	0.317 × 1.27 (1/8 × 1/2)
	5L	0.13 (0.05)	25	25	5	0.317 × 0.317 (1/8 × 1/8)
					5	0.317 × 1.27 (1/8 × 1/2)
CalSil-NUKON-RMI Mixture (Sequential)	45L	0.159 (0.0625)	25 (3rd)	25 (2nd)	5 (1st)	0.63 × 0.63 (1/4 × 1/4)
	45L	0.159 (0.0625)	25 (3rd)	25 (1st)	5 (2nd)	0.63 × 0.63 (1/4 × 1/4)
	45L	0.159 (0.0625)	25 (3rd)	25 (1st)	10 (2nd)	0.317 × 1.27 (1/8 × 1/2)

Table 2-3. Debris Accumulation Test Matrix

Test	Stem	Gap [cm (in.)]	CalSil (g)	NUKON (g)	RMI (g)	RMI Type [cm × cm (in. × in.)]
A-1	45L	0.159 (0.0625)	25 g every 15 min	25 g every 15 min	10 g at t = 0	0.317 × 1.27 (1/8 × 1/2)
A-2	45L	0.159 (0.0625)	12 g every 15 min	13 g every 15 min	10 g at t = 0	0.317 × 1.27 (1/8 × 1/2)
A-3	45L	0.159 (0.0625)	25 g every 15 min	25 g once (t=3 min)	10 g at t = 0	0.317 × 1.27 (1/8 × 1/2)

The energy equation (Ref. 6) applied between the upstream and downstream pressure measurement points (denoted by suffixes 1 and 2, respectively) of the throttle valve can be written as

$$P_1 + \frac{\rho_1 V_1^2}{2} + \rho_1 g z_1 = P_2 + \frac{\rho_2 V_2^2}{2} + \rho_2 g z_2 + K\frac{\rho_1 V_1^2}{2} + \frac{2 f L V^2}{\rho_1 D} \quad , \tag{2-1}$$

where the fourth term on the right-hand side denotes the pressure loss in the valve and the fifth term denotes the frictional loss between points 1 and 2. Because the pipe diameters upstream and downstream of the valve were the same and the temperature rise in the valve was negligible, the fluid density and flow velocity upstream and downstream of the valve were nearly equal. The difference in elevation was negligible [~0.62 kPa (0.09 psi), which translates to ~0.09 m (0.3 ft) of head], and the friction pressure drop in the piping was also negligible [~0.90 kPa (0.13 psi), which translates to ~0.06 m (0.2 ft) of head]. The pressure drop between the measurement locations was composed almost entirely of the pressure loss that occurred as the fluid flowed through the valve itself [~448 kPa (65 psi), which translates to ~45.7 m (150 ft) of head]. Therefore, Equation 2-1 is simplified as

$$\Delta P = P_1 - P_2 = K\frac{\rho_1 V_1^2}{2} \quad , \tag{2-2}$$

and the valve-loss coefficient for the valve, *K*, is described by

$$K = 2\frac{\Delta P}{\rho V^2} . \tag{2-3}$$

For a pipe diameter of 5.08 m (2 in.), using a water density of 995.8 kg/m^3 (62.17 lbm/ft^3), the above equation can be rewritten in terms of the measurement quantities (pressure drop ΔP in pounds per square inch and flow rate *Q* in gallons per minute) as

$$K = 14269.2\frac{\Delta P_{psi}}{Q_{gpm}^2} . \tag{2-4}$$

In the remainder of the report, *K* calculated using the above equation was used to present the test data.

The valve flow coefficient (Ref. 7) is described by the equation

$$C_v = C_0 \sqrt{\frac{Q_{\text{gpm}}^2}{\Delta P_{\text{psi}}}} \ , \tag{2-5}$$

where C_0 is a constant that depends on the density of the fluid. Comparing Eqs. (2-4) and (2-5), it is noted that

$$K \propto \frac{1}{C_v^2} \ ; \tag{2-6}$$

therefore, K and C_v are equivalent ways to describe the flow resistance.

2.7.2 Using *K* to Present Results

Raw data from a typical debris test are shown in Figure 2-24. The figure shows the transient variation of pressure drop across the valve and the flow rate measured at the upstream and downstream flow meters for test 45LDT4. In this and all subsequent similar plots, the vertical line indicates the time of debris insertion. In this test, 1 g of RMI measuring 6.35 mm × 6.35 mm (0.25 in. × 0.25 in.) was introduced at t = 1.64 min. The downstream flow-meter reading showed a pronounced dip after the debris was inserted, evidently the result of temporary lodging of debris in the meter. The upstream flow meter was relatively unchanged during the test. In this test, the pressure drop across the valve increased from ~242.7 to 267.5 kPa (35.2 to 38.8 psi) following debris insertion. Figure 2-25 shows the transient variation of the valve-loss-coefficient *K*, which was calculated based on the measured pressure difference and the flow rate from the upstream flow meter. *K* increased from ~88.0 to 98.4 following debris introduction. Thus, the pressure drop data and the *K* data exhibit similar behavior in this test.

Raw data from another debris test are shown in Figure 2-26. The figure shows the transient variation of valve pressure drop and upstream and downstream flow-meter data for test 45LDT6, in which 10 g of RMI measuring 0.63 cm × 0.63 cm (0.25 in. × 0.25 in.) was introduced at t = 1.89 min. In this case, both the downstream and upstream flow meters recorded a pronounced dip after the debris was inserted. The upstream flow-meter data recovered to a higher value than the downstream meter, again presumably because of some temporary clogging of the downstream flow meter by the debris. In this test, the pressure drop data were relatively unchanged immediately after debris insertion, and they later stabilized to a lower value. The average pressure drop was ~239.9 kPa (34.8 psi) before debris insertion and 233 kPa (33.8 psi) following debris insertion. Although this reduction in pressure may appear to be counterintuitive, a more accurate assessment of clogging can be obtained by examining Figure 2-27, which shows the transient variation of the valve-loss-coefficient *K*. *K* increased from ~86.9 to 110.9 following debris introduction. The pressure drop reduced because the flow rate in the system dropped after debris introduction, possibly as a result of valve blockage and increased head loss in the system. The inferred valve blockage is supported by the 33 pieces of RMI that were found within the valve body after this test. Thus, although increased losses could be found in the valve as a result

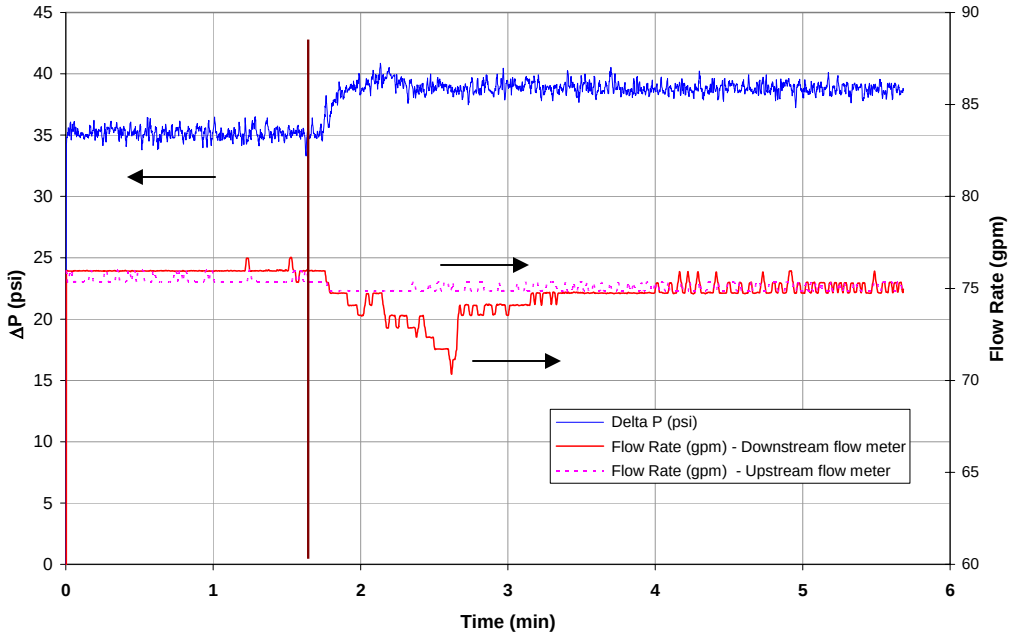

Figure 2-24. Transient Variation of Pressure Drop (psi) and Flow Rate (gpm) for Test 45LDT4*

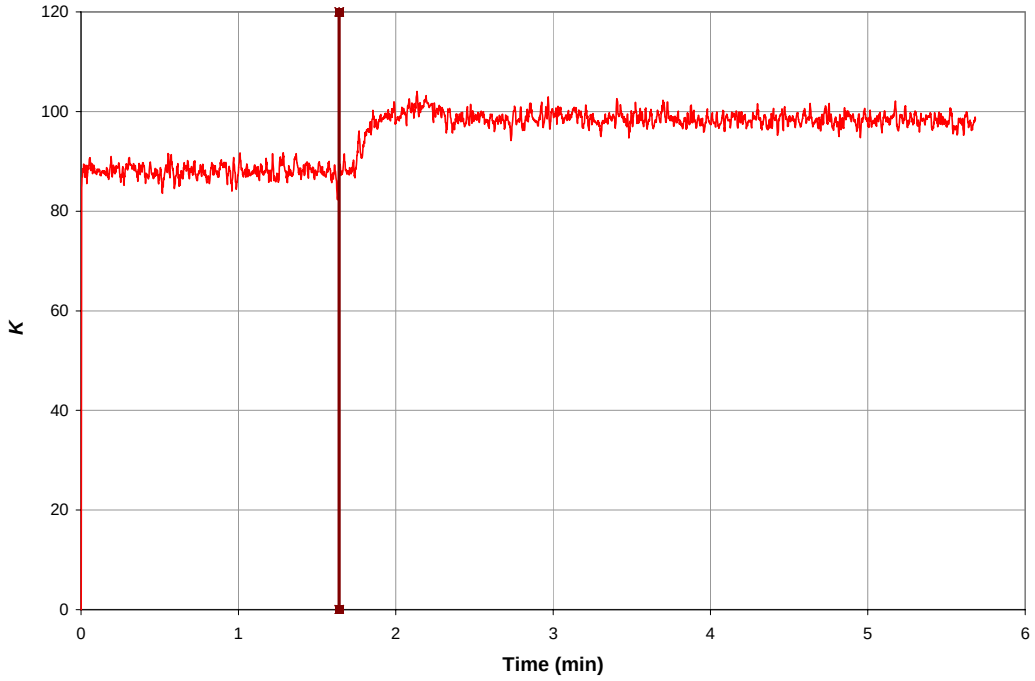

Figure 2-25. Transient Variation of Valve-Loss-Coefficient *K* for Test 45LDT4

* In this and all similar plots, pressure drop is plotted in pounds per square inch (1 psi = 6.89 kPa) and flow rate is plotted in gallons per minute (100 gpm = 6.31 l/s).

of clogging, it was compensated for by the reduction in the pressure drop as a result of the reduction in system flow. This result suggests that the valve-loss-coefficient *K*, rather than the valve pressure drop itself, is the appropriate indicator of debris clogging in these tests. The discussion of results in the remainder of the report is based on the valve-loss-coefficient *K*.

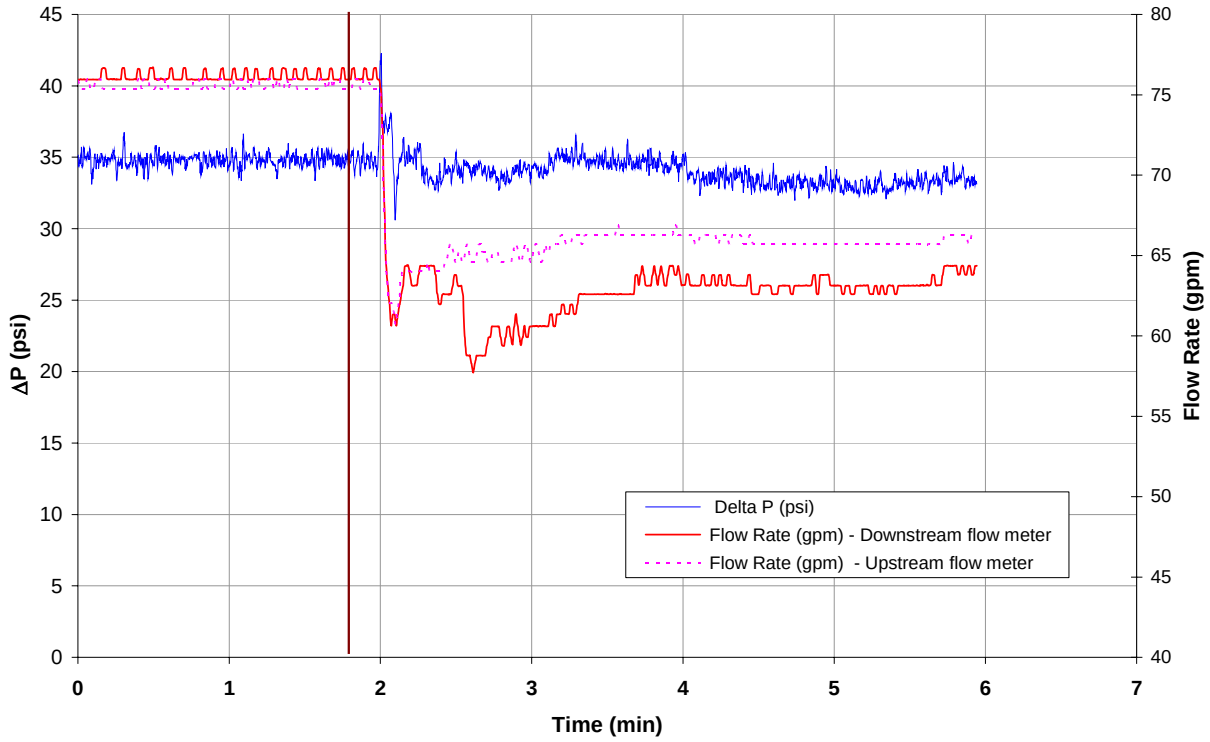

Figure 2-26. Transient Variation of Pressure Drop and Flow Rate for Test 45LDT6

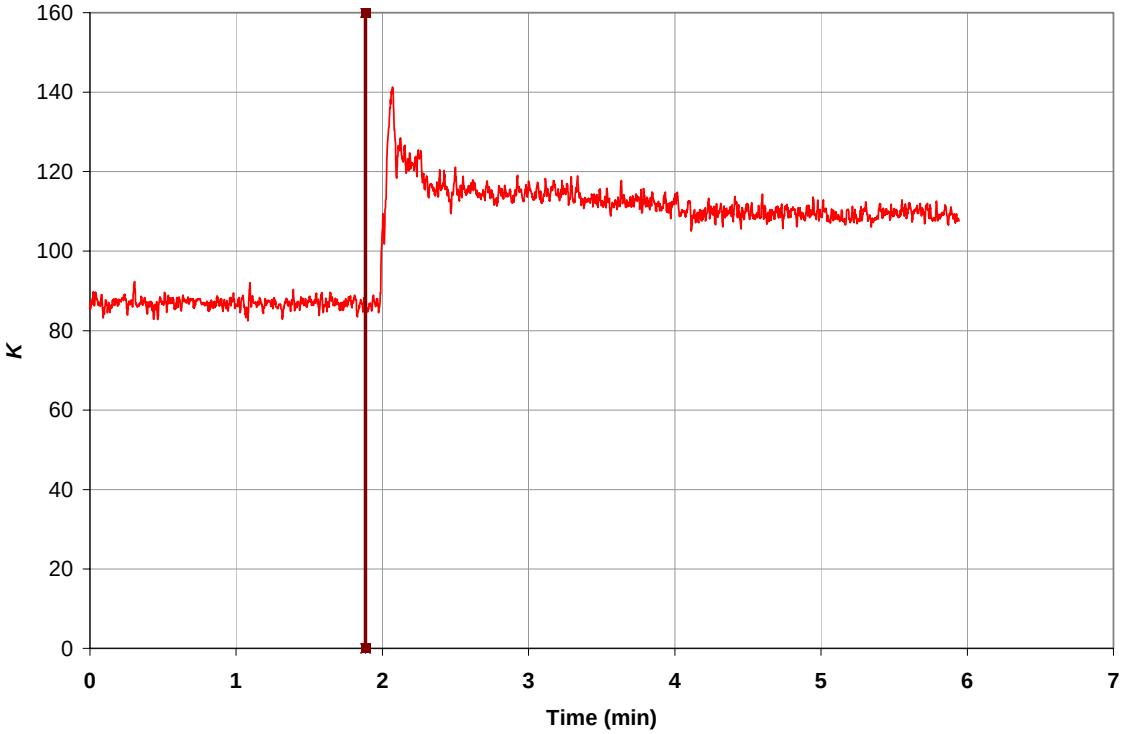

Figure 2-27. Transient Variation of Valve-Loss-Coefficient *K* for Test 45LDT6

3 RESULTS OF BASELINE TESTS

3.1 Baseline for Unblocked Flow

Baseline tests for unblocked flow involved determining the flow loss characteristics of the valve at different valve openings for each valve configuration. The baseline performance of the valve configurations was initially determined at the beginning of the test program. Baseline testing was then repeated twice through the test program to track potential changes in the baseline as a result of wear or other processes.

Baseline data for the 45L, 5L, and 5S valve stem configurations are shown in Figures 3–1 through 3–3. Each figure contains data taken at different times through the test program. The first set of measurements was made in December 2004. Post-measurement inspection of the valve internals revealed evidence of marked galling at the stem-ring interface for the 5L configuration. The 5L configuration had been brought to full closure before taking measurements for the smallest opening condition. The galling evidently had occurred when the valve was fully closed. The subsequent measurement of the flow resistance for the smallest valve configuration was compromised by the surface defect. The 5S configuration also was observed to have evidence of galling, but to a much smaller extent. As a precaution, the surfaces of the stems and rings for all three valve configurations were machined. Data labeled "Dec-04" in Figures 3–1 through 3–3 indicate tests that were done before the resurfacing. Data labeled "Jan-05-Run 1" and "Jan-05-Run 2" indicate tests that were done after resurfacing. Two runs were made to examine the repeatability of the data. The last two baseline tests for each stem were taken using single-point sampling rather than five-point averaging, as discussed in Section 2.3.

Figure 3-1 shows the baseline data for the 45L valve configuration. Except for the smallest valve opening, K remained relatively unchanged over time. The value for the smallest valve opening appeared to increase with time. This observation was consistent with the fact that the smallest valve opening was most susceptible to changes in the wear conditions of the surface. As seen in Figures 3–2 and 3–3, K for the smallest opening also changed significantly after machining of the surfaces for the 5L and 5S valve configurations. Table 3-1 provides tabulated data for converting valve gap opening to flow area through the valve for the 45L, 5L, and 5S valve configurations.

The changes in K over time discussed previously did not impact the results of the current study adversely. The objective of evaluating debris blockage effects primarily required consideration of the change in K relative to the baseline established just before each test. Therefore, the absolute value at the beginning of the test is not that important. Additionally, most testing was conducted using larger valve gaps where K values do not vary much throughout the various baseline measurements (Figures 3–1 to 3–3).

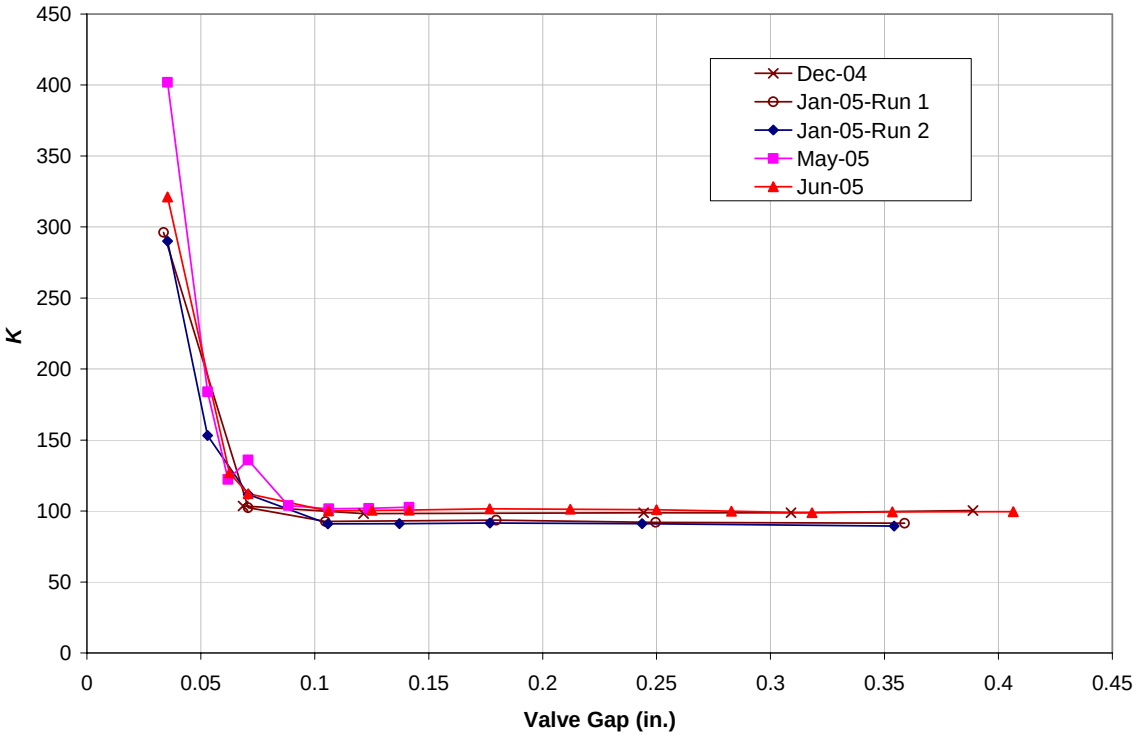

Figure 3-1. Baseline Data for 45L

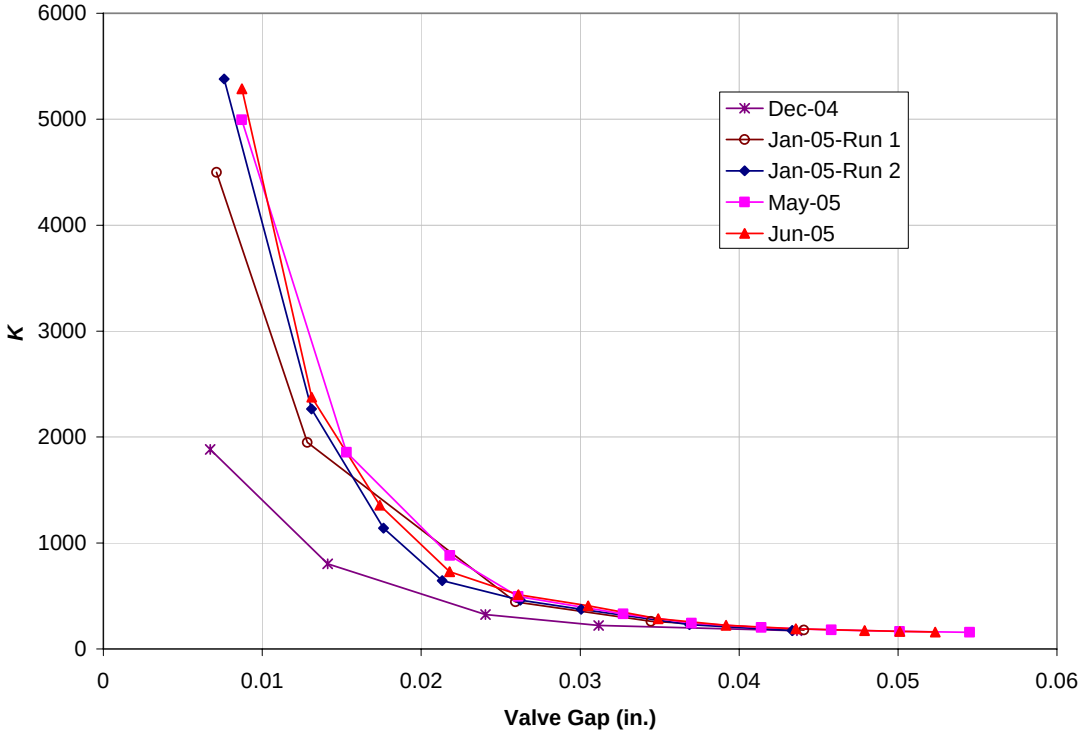

Figure 3-2. Baseline Data for 5L

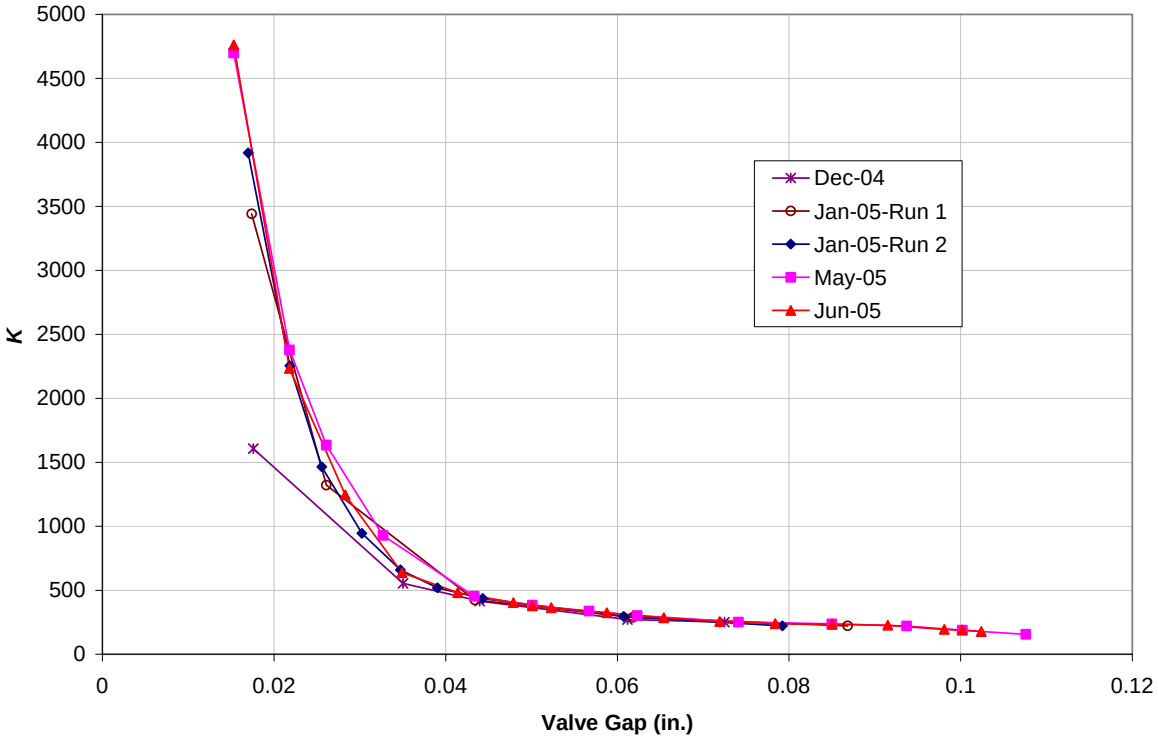

Figure 3-3. Baseline Data for 5S Stem

Table 3-1. Throttle Valve Flow Area Conversions

45L		5L		5S	
Throttle Valve Gap (in.)	**Throttle Valve Flow Area ($in.^2$)**	**Throttle Valve Gap (in.)**	**Throttle Valve Flow Area ($in.^2$)**	**Throttle Valve Gap (in.)**	**Throttle Valve Flow Area ($in.^2$)**
0.035400	0.200422	0.007600	0.050543	0.016980	0.073898
0.053000	0.318540	0.013100	0.087890	0.021844	0.096202
0.070700	0.449704	0.017620	0.119067	0.025554	0.113555
0.105746	0.746015	0.021316	0.144885	0.030236	0.135875
0.137152	1.052883	0.026232	0.179678	0.034724	0.157709
0.176800	1.496073	0.030060	0.207129	0.039024	0.179034
0.243606	2.383682	0.036874	0.256768	0.044304	0.205759
0.354304	4.243595	0.043336	0.304760	0.060736	0.292745
--	--	--	--	0.079236	0.397590

3.2 Baseline Data for Known Blockage Area

A series of blockage tests was performed in the beginning of the test program using the 45L valve configuration. These tests were performed by placing shims of known areas on the valve ring so that a predetermined portion of the flow area in the valve throat could be blocked. Figure

3-4 illustrates the use of a shim to simulate blockage in the valve. The shim consisted of a thin piece of rubber gasket material affixed to the valve seating ring via epoxy.

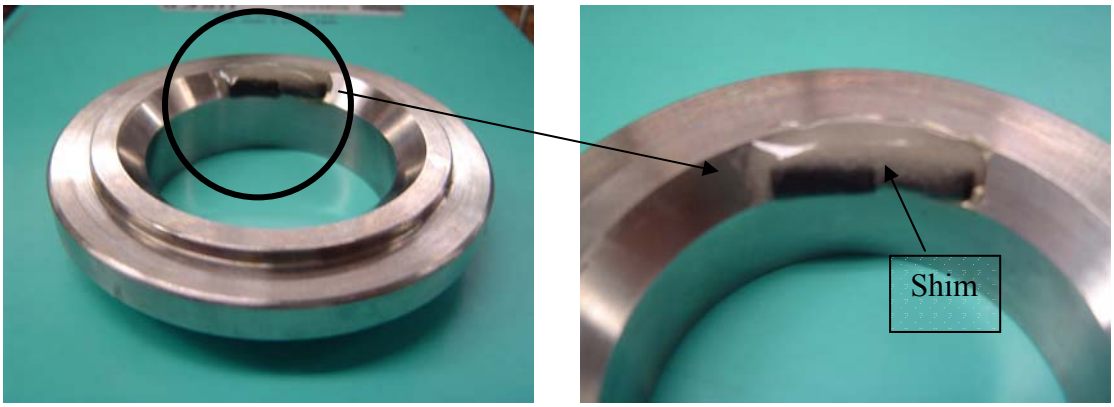

Figure 3-4. Detail Showing Placement of a Shim on the Valve Ring

Data from these tests helped to establish the threshold of blockage detection. In addition, *K* determined for the different blocked area fractions was compared with the baseline data to establish the relation between an increase in *K* and the blocked area. Tests were conducted at the beginning and end of the test program for the 45L and 5L valve. No shim tests were performed for the 5S stem. All blockage tests were performed for two flow rates—4.73 l/s (75 gpm) and 6.12 l/s (97 gpm). The 6.12 l/s (97 gpm) corresponded approximately to the highest flow rate possible in the system with the set of downstream orifice plates installed (see discussion in Section 2.2.5).

Figure 3-5 shows the transient variation of calculated *K* for different blockage conditions in the 45L/0.159-cm (0.0625-in.)-opening configuration. For clarity, only segments of the transient data for each case are shown. All test times were >3 min. The average values of *K* calculated for each case also are indicated in Figure 3-5. The standard deviation in all cases was ~0.8. The change from an unblocked condition to 6.2% blockage resulted in an increase in the average *K* of 9.8. To conclude that the 6.2%-blockage condition could be detected by the measurement system, it had to be ascertained that the increase in *K* was substantially greater than the uncertainty in the data itself.

The measurement standard deviation of the *K* data contained uncertainties, which theoretically could be propagated from first principles as in Eq. (3-1),

$$\frac{\Delta K}{K} = \frac{\Delta(P_1)}{P_1} + \frac{\Delta(P_2)}{P_2} + 2\frac{\Delta Q}{Q} = 2\left[\frac{\Delta P}{P} + \frac{\Delta Q}{Q}\right] \quad . \tag{3-1}$$

A ΔK of 9.8 corresponded to a blocked area of 6.2%, which was greater than two standard deviations (4.8) from the baseline *K* as calculated using Eq. (3-1). Thus, the shim blockage test data showed that the 6.2% blockage in the 45L valve configuration was detectable by the system (i.e., the detection threshold was between 0% and 6.2%). Because no tests were done for blockages in this range, a more definitive estimate of the detection threshold was not possible,

but it is reasonable to estimate that the detection threshold for the 45L valve configuration was on the order of 5% blockage of the flow area.

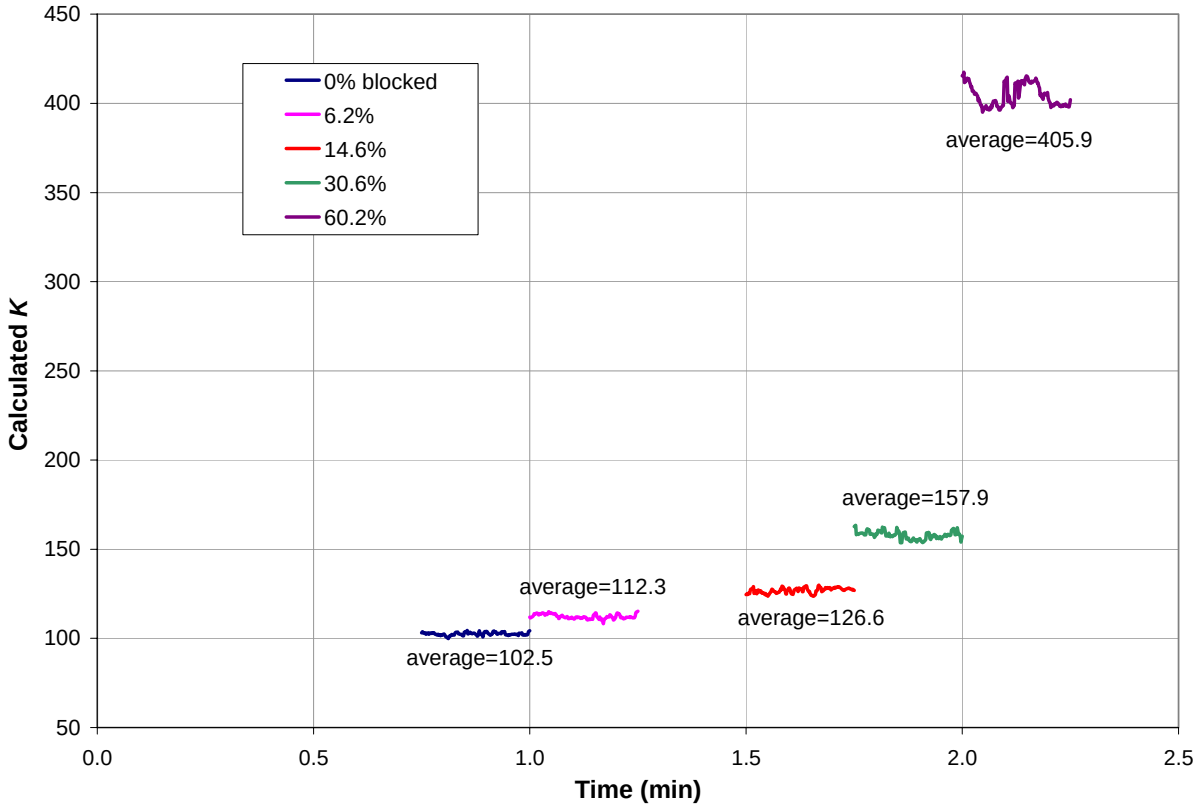

Figure 3-5. Transient Variation of *K* for Different Blockage Conditions

Figure 3-6 also shows the shim test data for the 45L valve configuration, and Figure 3-7 presents the same data as a plot of the increase in *K* relative to unblocked flow ($\Delta K\%$). As seen in Figure 3-6 and Figure 3-7, the data for 45L, especially at 60% blockage, show a pronounced increase in *K* between the beginning and end of the test program. This increase is due to the combined effects of the pieces being remachined early in the test program followed by wear processes introduced during testing. However, there is essentially no *K* dependence on flow rate.

A fourth-order polynomial fit for the $\Delta K\%$ end of test program data (Figure 3-7) for the 45L configuration at 4.73 l/s (75 gpm) is

$$\Delta K\% = -3E-05\, A_B^4 + 0.0055\, A_B^3 - 0.1638\, A_B^2 + 4.0011\, A_B \quad , \tag{3-2}$$

where $\Delta K\%$ is the increase in *K* and A_B is the percentage of blocked area.

Figure 3-8 and Figure 3-9 show the corresponding data for the 5L stem for a valve opening of 0.13 cm (0.05 in.) The data for 4.73 l/s (75 gpm) indicated no appreciable increase in *K* for a

blocked area of 5.7%, so the detection threshold for 5L was between 5.7% and 10%. A more precise estimate of the detection threshold for the 5L case could be established through additional testing. However, based on a detection threshold of two standard deviations, a reasonable estimate for the threshold for the 5L configuration was ~8%. For the 5L data at 4.73 l/s (75 gpm), the corresponding equation is

$$\Delta K\% = 8E-05\, A_B^4 - 0.0079\, A_B^3 + 0.3109\, A_B^2 - 1.2808\, A_B \quad . \tag{3-3}$$

Figure 3-10 shows a comparison of the two polynomial curve fits (Equations 3-2 and 3-3) with the 45L and 5L data. Both equations show similar trends in valve blockage behavior. Additional data would be required to confirm the applicability of these equations to cases other than those used to develop them.

Figure 3-11 and Figure 3-12 compare the valve loss coefficients between the shim blockage and baseline tests for the 45L and 5L stems, respectively. The comparisons are made on the basis of flow area. The flow area for the baseline tests was varied by changing the throttle valve gap opening. The flow area for the shim blockage tests was varied by changing the percent of the opening blocked by the shim while maintaining a constant gap opening for a given stem configuration. The agreement between the shim blockage and baseline data is very good for both the 45L and 5L stems. This agreement implies that debris blockage increases the valve loss coefficient primarily by decreasing the flow area. Consequently, blockage asymmetry has minimal or no effect.

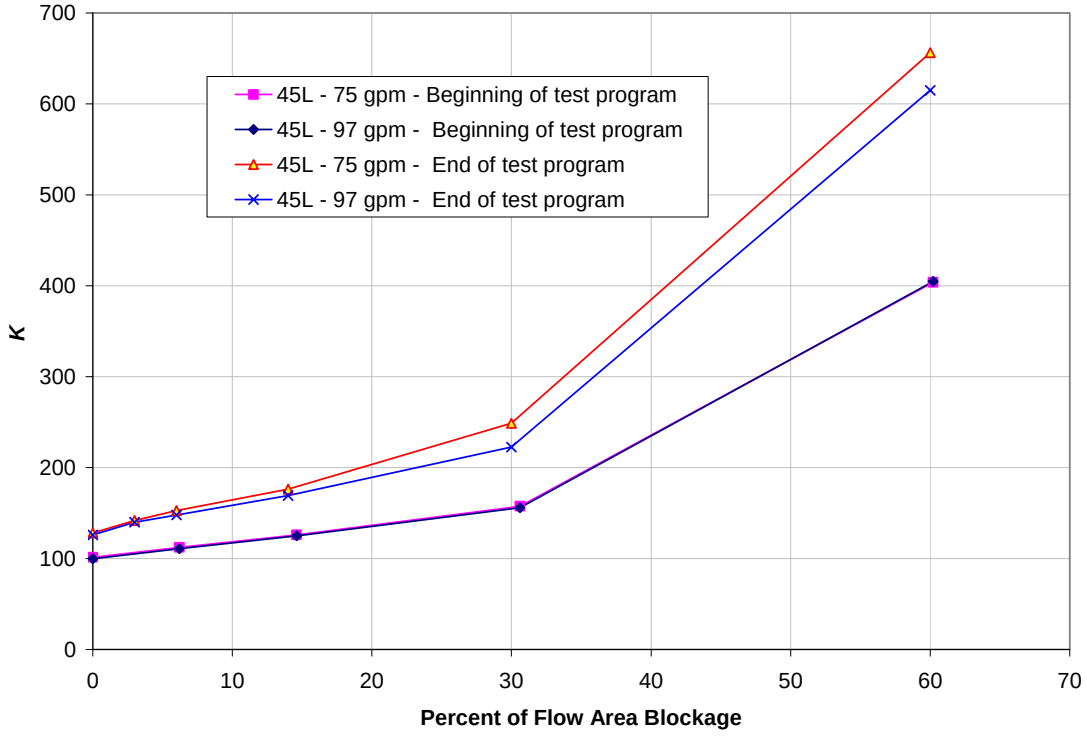

Figure 3-6. Blockage Test Data for 45L, Valve Opening = 0.159 cm (0.0625 in.)

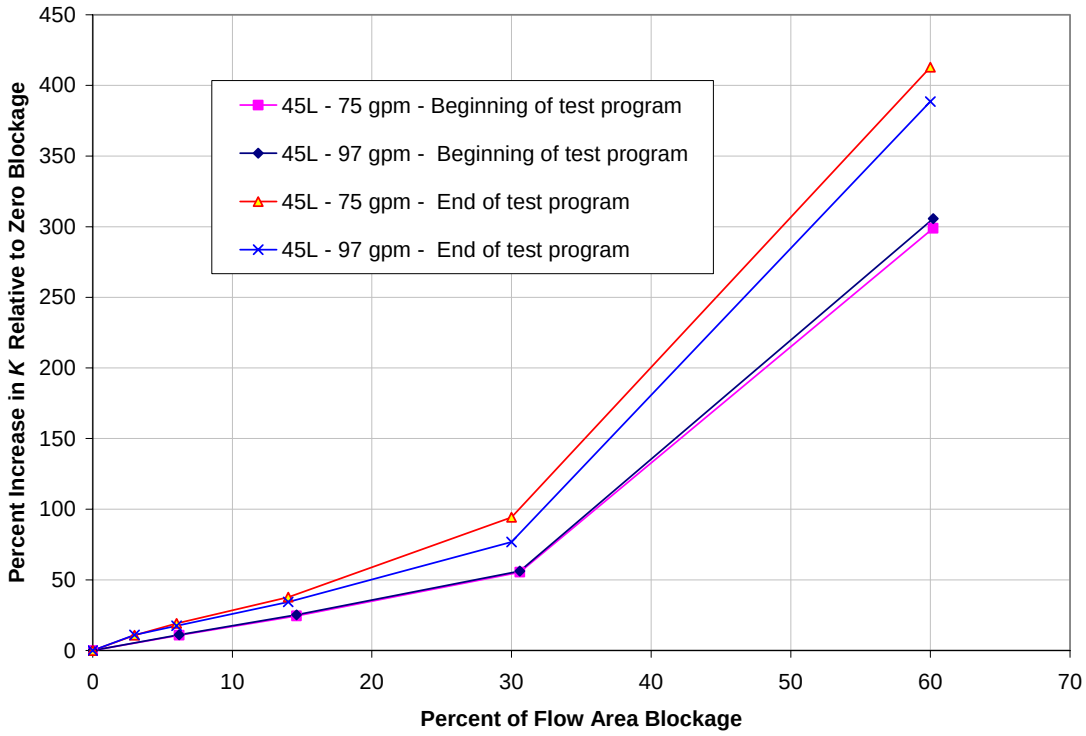

Figure 3-7. Percentage Increase in *K* as a Result of Blockage [45L, 0.159-cm (0.0625-in.) Opening]

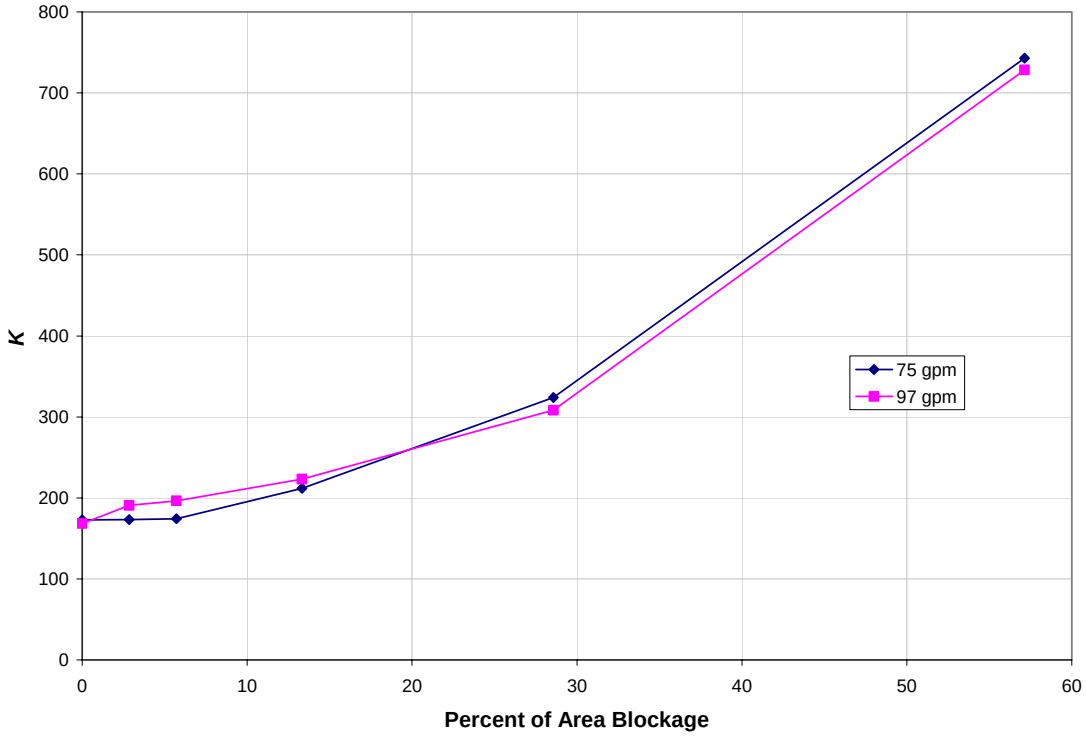

Figure 3-8. Blockage Test Data for 5L, Valve Opening = 0.13 cm (0.05 in.)

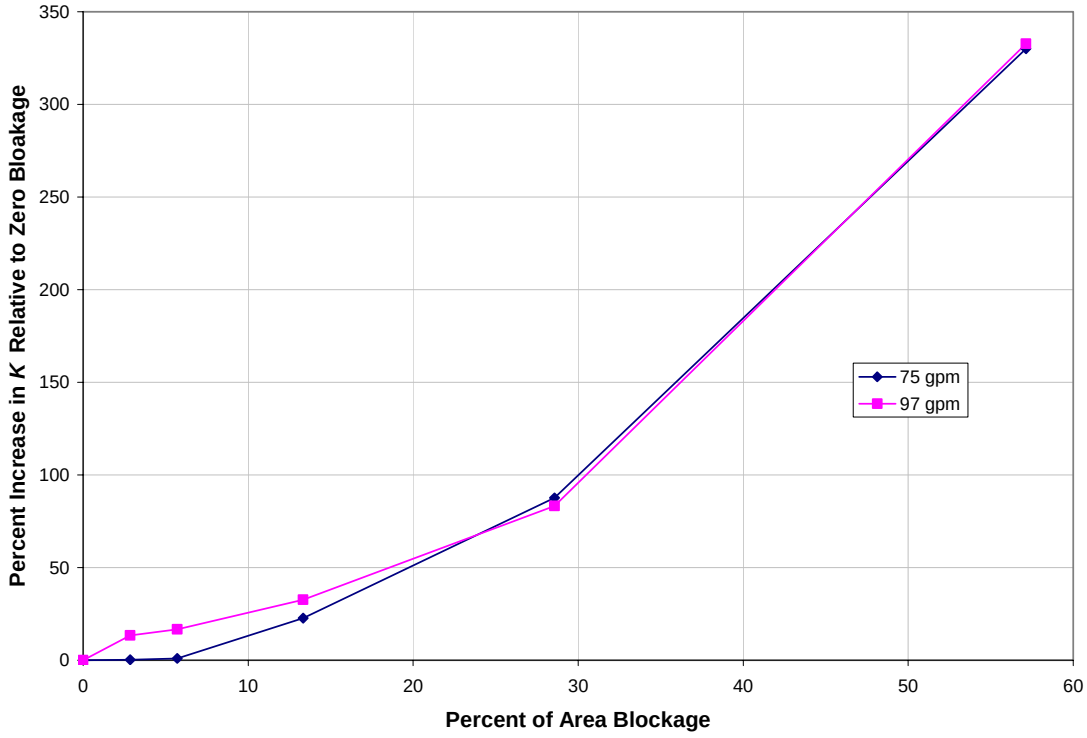

Figure 3-9. Percentage Increase in *K* as a Result of Blockage [5L, 0.13-cm (0.05-in.) Opening]

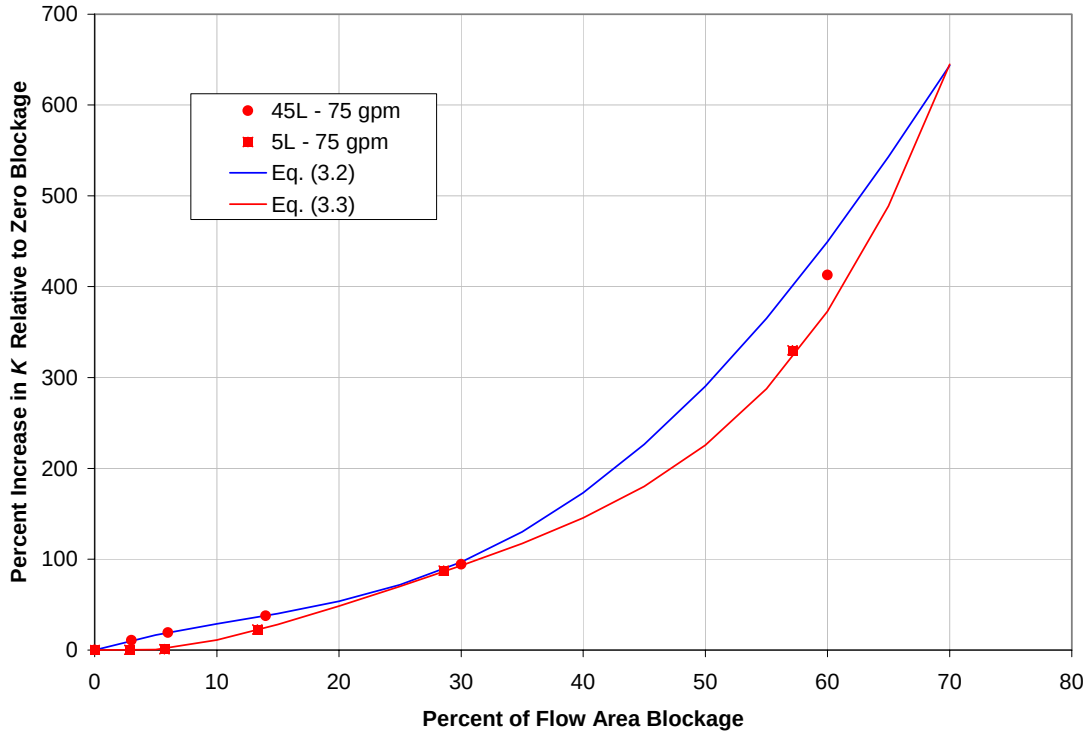

Figure 3-10. Comparing Curve Fits for $\Delta K\%$ vs A_B

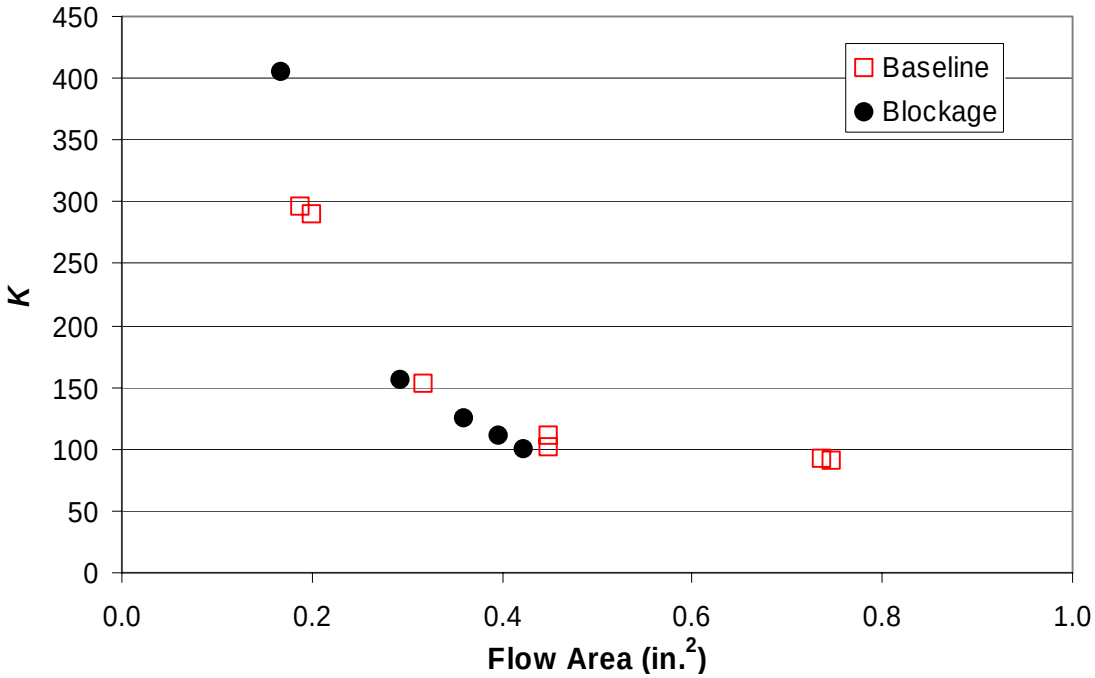

Figure 3-11. Comparing Shim Blockage to Baseline (45L Stem, Beginning of Test Program, 75 gpm)

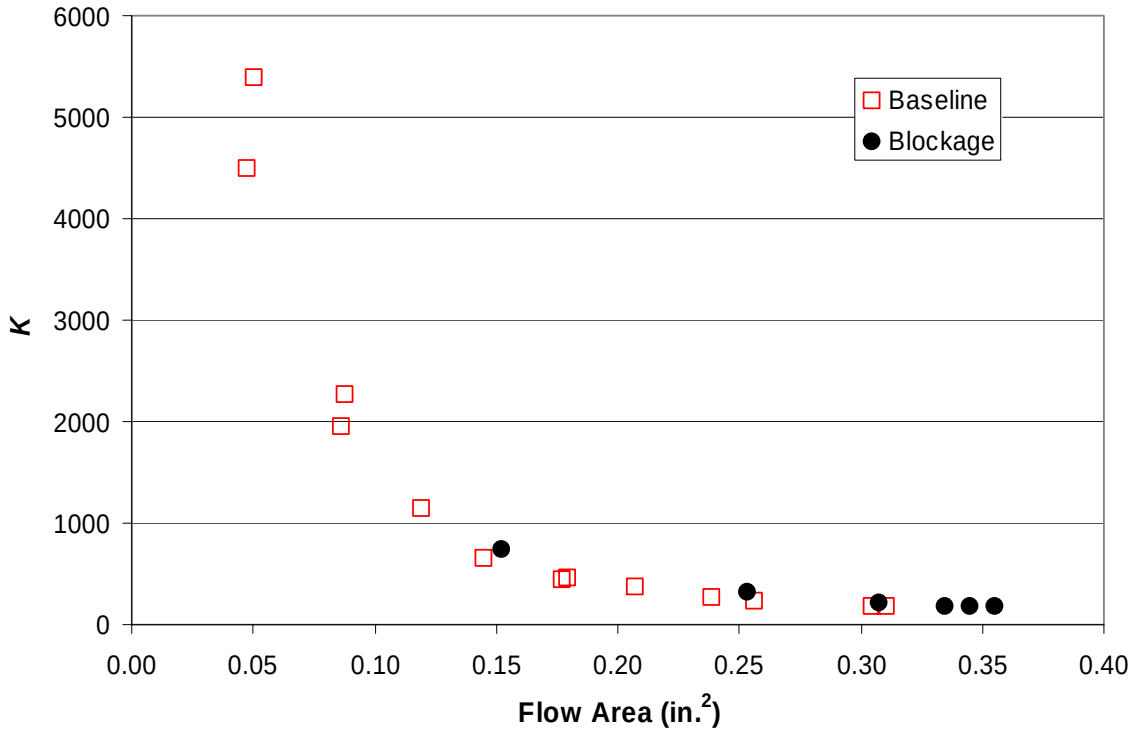

Figure 3-12. Comparing Shim Blockage to Baseline (5L Stem, Beginning of Test Program, 75 gpm)

This page intentionally left blank.

4 RESULTS OF SINGLE-DEBRIS TESTS

The results of single-debris tests with RMI, NUKON, and CalSil are presented in this section. In each case, a single batch of debris was introduced into the system and the hydraulic behavior of the valve was recorded to infer any resulting blockage. The upstream temperature was for each test fell between 15°C (59ºF) and 26°C (78ºF).

4.1 RMI Tests

The results of single debris tests with RMI are presented in three categories:

- Tests with a specified number of pieces of RMI: These initial scoping tests were performed early in the test program to test system performance and identify follow-up tests. All tests in this category used 10 pieces of RMI—the valve stem/ring combination and valve gap were varied.
- Tests with a specified mass of RMI: These tests used between 1 and 10 g of RMI. In addition to the mass of RMI introduced, the valve stem/ring combination and valve gap also were varied.
- Tests to examine repeatability of data: A limited number of replicate RMI tests with a specified mass were conducted to assess data repeatability.

4.1.1 Tests with a Specified Number of Pieces of RMI

These tests were performed early in the test program. All tests in this category used 10 pieces of RMI. The valve stem/ring combination and valve gap were varied. Post-test collection of debris was not recorded for these tests, so no data are available regarding how many of the debris pieces were recovered either downstream of the valve or in the valve itself.

The results of this series of tests are summarized in Table 4-1.* The increase in K was found to be significant (>5%) only when the pieces had at least one characteristic dimension >0.63 cm (0.25 in.) and only for the 5L stem when the smallest gap setting [0.13 cm (0.05 in.)] was evaluated. For the two cases that had measurable increases in loss coefficient, the greatest increase was ~7%. Test data in this category were limited, but they indicated that a small number of RMI pieces would not normally cause appreciable valve blockage.

* The ΔK% data for the full data set are compiled in Appendix D. The plots of measured valve pressure drop and calculated K are compiled in Appendix E.

Table 4-1. Results of Tests with Specified Number of Pieces of RMI Introduced

Test ID	Stem	Gap [cm (in.)]	Number of RMI Pieces Inserted N1	RMI Size [cm × cm (in. × in.)]	*K*		
					Before	After	% Change
5SDT1a	5S	0.158 (0.0622)	10	0.32 × 0.32 (1/8 × 1/8)	293	293	<5
5SDT1b	5S	0.158 (0.0622)	10	0.63 × 0.63 (1/4 × 1/4)	291	289	<5
5SDT1c	5S	0.158 (0.0622)	10	0.32 × 1.27 (1/8 × 1/2)	290	289	<5
5SDT2a	5S	0.2543 (0.1001)	10	0.32 × 0.32 (1/8 × 1/8)	179	178	<5
5SDT2b	5S	0.2543 (0.1001)	10	0.63 × 0.63 (1/4 × 1/4)	180	178	<5
5SDT2c	5S	0.2543 (0.1001)	10	0.32 × 1.27 (1/8 × 1/2)	178	178	<5
5LDT1a	5L	0.127 (0.0499)	10	0.32 × 0.32 (1/8 × 1/8)	154	154	<5
5LDT1b	5L	0.127 (0.0499)	10	0.63 × 0.63 (1/4 × 1/4)	152	157	<5
5LDT1c	5L	0.127 (0.0499)	10	0.32 × 1.27 (1/8 × 1/2)	153	165	7
45LDT1a	45L	0.180 (0.0707)	10	0.32 × 0.32 (1/8 × 1/8)	107	107	<5
45LDT1b	45L	0.180 (0.0707)	10	0.63 × 0.63 (1/4 × 1/4)	107	109	<5
45LDT1c	45L	0.180 (0.0707)	10	0.32 × 1.27 (1/8 × 1/2)	107	106	<5
45LDT2a	45L	0.3124 (0.1230)	10	0.32 × 0.32 (1/8 × 1/8)	88.4	87.9	<5
45LDT2b	45L	0.3124 (0.1230)	10	0.63 × 0.63 (1/4 × 1/4)	88.6	89.2	<5
45LDT2c	45L	0.3124 (0.1230)	10	0.32 × 1.27 (1/8 × 1/2)	88.3	88.2	<5

Transient data from two typical tests in this category are shown in Figure 4-1 and Figure 4-2. Figure 4-1 shows the data for Test 45LDT1a, which had essentially no evidence of blockage, and Figure 4-2 shows data from test 5LDT1c, which had a 7% increase in *K*.

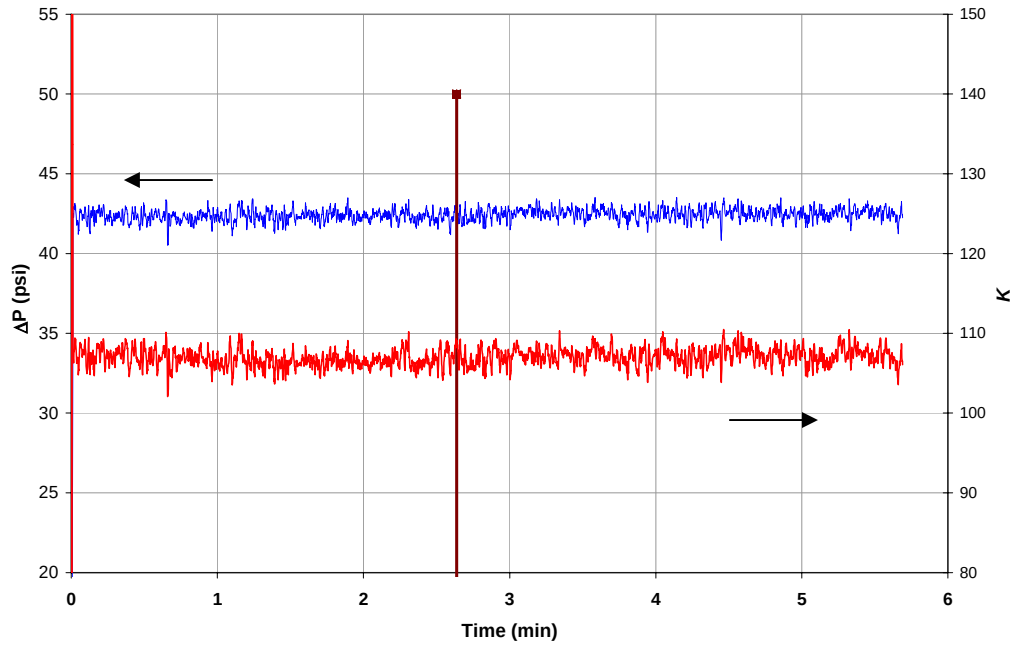

Figure 4-1. Transient Variation of Valve Pressure Drop and Calculated *K* for Test 45LDT1a*

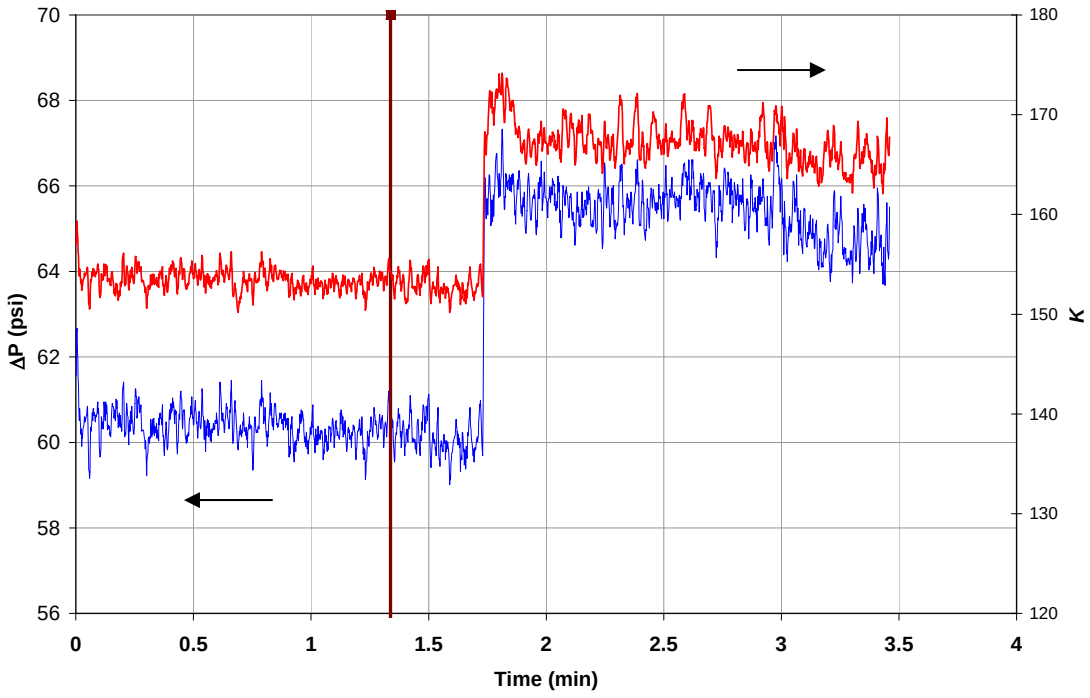

Figure 4-2. Transient Variation of Valve Pressure Drop and Calculated *K* for Test 5LDT1c

*NOTE: In this and all similar plots, unless otherwise indicated, the blue (or lighter) curve denotes ΔP and the red (or darker) curve denotes *K*. Also, the vertical line marks the time of debris addition.

4.1.2 Tests with Specified Mass of RMI

These tests used between 1 and 10 g of RMI. In addition to the mass of RMI introduced, the valve stem/ring combination and valve gap also were varied. For tests in this class, debris was collected during the test and when the system was flushed following the test. The procedure is described in Sections 2.2.5 and A.3. For some of the tests, an additional debris recovery step was added by opening the trap and back flushing the system. The valve was opened and inspected after each test, and the number of RMI pieces recovered from the valve was recorded. Note that the recovery of RMI debris from the valve body does not necessarily mean that the RMI was trapped in the gap between the valve stem and seat.

The results of this series of tests are summarized in Table 4-2. In general, a correlation is apparent between the number of RMI pieces recovered from the valve following a test and the increase in the valve-loss-coefficient *K*. The higher the number of pieces found in the valve, the larger the calculated increase in the valve-loss-coefficient *K*. This general trend is evident from the data shown in Figure 4-3.

A companion plot, Figure 4-4, presents the percent increase in *K* for different debris loadings as a function of the ratio of the maximum RMI dimension to the valve gap size. If Figure 4-3 and Figure 4-4 are considered together; the following general trends are apparent. The performance of the 5S valve configuration was only minimally degraded by RMI debris (smallest observed increase in *K*), regardless of the initial RMI loading, the ratio of RMI size tested to the gap size, or the number of RMI pieces recovered from the valve body. The implication of this result is that the geometry of the 5S valve configuration was such that RMI was less likely to be trapped within the valve and that those pieces that were recovered from the valve may have been trapped in areas other than the gap and did not affect the flow area through the valve.

The 5L valve configuration appears to have been less likely to trap RMI than the 45L valve configuration for the same initial RMI loadings. However, once the RMI was trapped within the 5L valve configuration, the performance degradation appeared to have been higher for the 5L valve configuration for the same number of recovered RMI pieces. In light of the inherent data variability, as well as the discrepancy in the number of tests between the 45L and 5L valve configurations, this apparent trend may not be actual. The physical size of the RMI debris was not as important as the debris loading quantity for degrading valve performance for debris size to gap ratios greater than ~3.

The 45L valve configuration appears to have trapped the most number of RMI pieces and subsequently suffered the most performance degradation (exhibited the greatest increase in *K*) for a given debris quantity and size. The 45L test data also exhibited the most variability, but the number of tests using this configuration far exceeded the other configurations. Sample loadings of 1 g were generally not large enough to cause valve clogging of any significance, regardless of the valve configuration or the RMI sizes tested. This result indicates that a loading threshold may exist below which valve performance degradation will not occur. However, this result does not address the potential for cumulative effects from a continuous stream of small quantities of RMI debris.

4.1.3 RMI Repeatability Tests

A limited number of RMI tests were performed with test conditions identical to those in the above category to investigate the repeatability of data. Eight tests from Table 4-2 were selected for repeating—these included three cases where the original test showed a negligible change in *K* (<5%), two for which the original test showed a detectable change in *K* (5%–12%), and two cases where the original tests showed a significant change in *K* (>50%). In addition, one test was repeated using a smaller debris size (a debris size slightly smaller than the valve gap). The results are summarized in Table 4-3.

For test 45LDT5, the original test yielded a *K* increase of <5%, whereas the repeat test yielded 24%. The increase in *K* was 51% for the original run of test 45LDT9. The repeated tests showed a great deal of variability (5%, 19%, and 54%). For test 45LDT11, the original run resulted in virtually no change in *K*, whereas the repeat run showed a moderate increase in *K* of 6%. For test 45LDT18, the original run resulted in an increase in *K* of 51%, whereas the repeat run resulted in an increase of 20%. The data for test 5LDT3 were the most reproducible among cases where detectable increases in *K* were observed although only a single replicate test was performed. Repeat tests of the null tests (N-1_45L and N-4_45L), where the gap size was larger than the debris dimension, consistently showed no appreciable indication of clogging.

The above results clearly show that debris clogging data are difficult to reproduce. This conclusion largely is consistent with the fact that debris clogging of the valve has an inherent randomness associated with it. The likelihood of debris getting trapped in the valve opening depends on the orientation of the debris piece relative to the flow in the valve throat; this process is random, especially when the flow is turbulent. In addition, the orientation of the pieces has an effect on whether, and by how much, the pieces get bent inside the valve; in turn, the change in shape of the pieces has an effect on their ability to pass through the valve or to be trapped inside it. A larger number of repeatability tests would be necessary to quantitatively assess variability. This was beyond the objective of these scoping tests.

4.1.4 Estimating the Blockage Area

As discussed in Section 3, baseline data for known blockage conditions were obtained for the 45L and the 5L valve configurations for valve openings of 0.159 cm (0.0625 in.) and 0.13 cm (0.05 in.), respectively. Blockage-area fractions estimated using Eq. (3-2) for the RMI tests using the 45L/0.159-cm (0.0625-in.)-opening and Eq. (3-3) for the 5L/0.13-cm (0.05-in.)-opening combinations are listed in Table 4-4. The highest estimated blocked area fraction is ~20% and occurred with the largest RMI pieces tested [0.63 cm × 0.63 cm (1/4 in. × 1/4 in.)] in the 45L configuration.

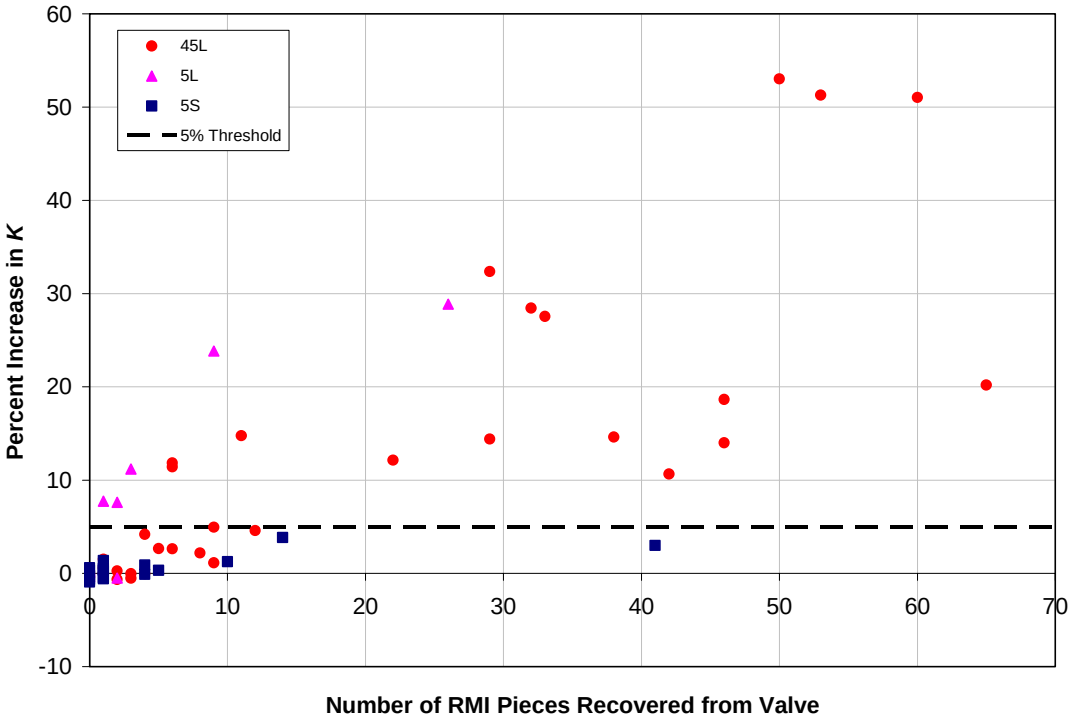

Figure 4-3. Observed Correlation between the Increase in *K* and the Number of RMI Pieces Recovered in the Valve

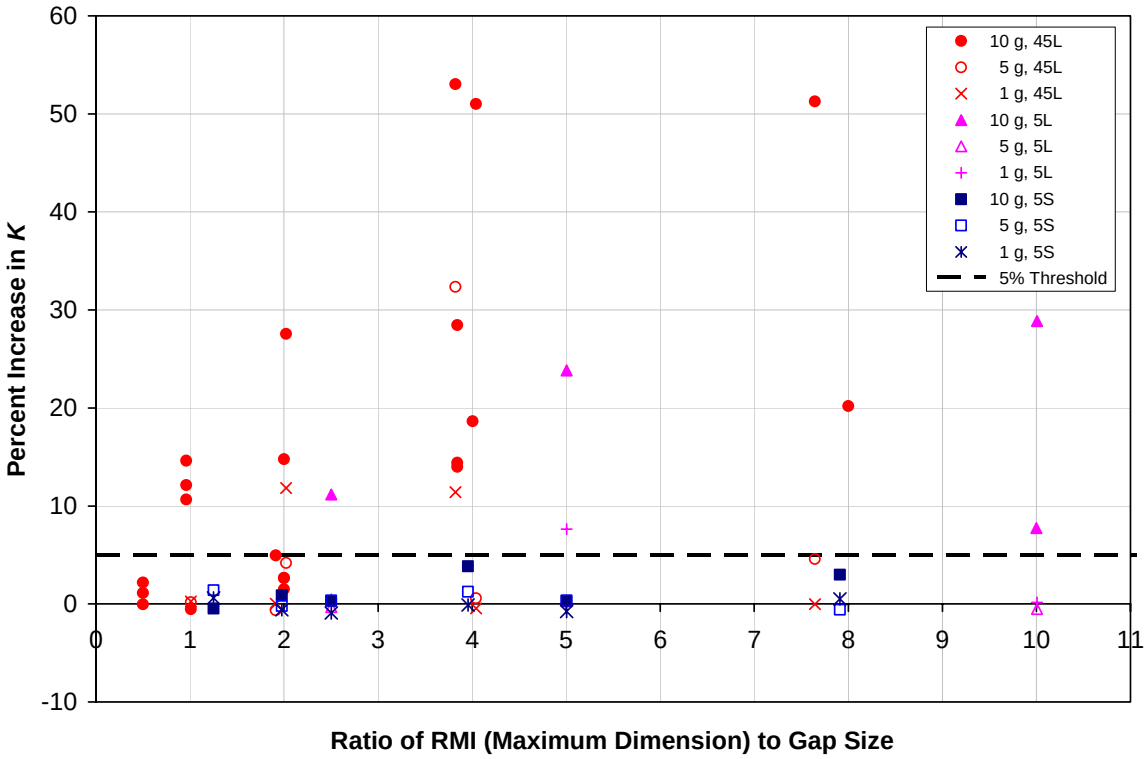

Figure 4-4. Relation between the Increase in *K* and the Ratio of RMI Size to Gap Size

Table 4-2. Results of Tests with Specified Mass of RMI Introduced

Test ID	Stem	Gap [cm (in.)]	Mass of RMI Inserted (g)W1	RMI Size [cm × cm (in. × in.)]	*K*			RMI Recovered in Bucket (g) W2	RMI Unaccounted for Wf=W1-W2	Number of RMI Pieces Recovered from Valve after Test NR
					Before	After	% Change			
45LDT1	45L	0.3142 (0.1237)	1.00	0.32 × 0.32 (1/8 × 1/8)	88.7	88.9	<5	0.79	0.21	2
45LDT2	45L	0.3142 (0.1237)	5.00	0.32 × 0.32 (1/8 × 1/8)	89.0	89.2	<5	4.33	0.67	0
45LDT3	45L	0.3142 (0.1237)	10.01	0.32 × 0.32 (1/8 × 1/8)	87.9	87.4	<5	7.90	2.11	3
45LDT4	45L	0.3142 (0.1237)	1.02	0.63 × 0.63 (1/4 × 1/4)	88.0	98.4	12	0.85	0.17	6
45LDT5	45L	0.3142 (0.1237)	5.00	0.63 × 0.63 (1/4 × 1/4)	88.9	92.6	<5	4.82	0.18	4
45LDT6	45L	0.3142 (0.1237)	10.02	0.63 × 0.63 (1/4 × 1/4)	86.9	111	28	8.95	1.07	33
45LDT7	45L	0.3142 (0.1237)	0.99	0.32 × 1.27 (1/8 × 1/2)	92.5	92.1	<5	0.98	0.01	0
45LDT8	45L	0.3142 (0.1237)	5.03	0.32 × 1.27 (1/8 × 1/2)	89.9	90.4	<5	4.57	0.46	1
45LDT9	45L	0.3142 (0.1237)	10.00	0.32 × 1.27 (1/8 × 1/2)	88.1	133	51	8.92	1.08	60
45LDT10	45L	0.166 (0.0654)	1.02	0.32 × 0.32 (1/8 × 1/8)	126	126	<5	0.97	0.05	1
45LDT11	45L	0.166 (0.0654)	4.99	0.32 × 0.32 (1/8 × 1/8)	125	124	<5	4.24	0.75	2
45LDT12	45L	0.166 (0.0654)	10.00	0.32 × 0.32 (1/8 × 1/8)	124	130	<5	7.84	2.16	9
45LDT13	45L	0.166 (0.0654)	1.00	0.63 × 0.63 (1/4 × 1/4)	122	136	11	0.98	0.02	6
45LDT14	45L	0.166 (0.0654)	5.00	0.63 × 0.63 (1/4 × 1/4)	124	165	32	4.54	0.46	29
45LDT15	45L	0.166 (0.0654)	10.01	0.63 × 0.63 (1/4 × 1/4)	121	186	53	8.68	1.33	50
45LDT16	45L	0.166 (0.0654)	1.01	0.32 × 1.27 (1/8 × 1/2)	126	126	<5	0.90	0.11	3
45LDT17	45L	0.166 (0.0654)	5.02	0.32 × 1.27 (1/8 × 1/2)	127	133	<5	4.95	0.07	12
45LDT18	45L	0.166 (0.0654)	10.00	0.32 × 1.27 (1/8 × 1/2)	127	192	51	9.42	0.58	53
5LDT1	5L	0.1269 (0.04997)	1.01	0.32 × 0.32 (1/8 × 1/8)	174	175	<5	0.92	0.09	0

Table 4-2. Results of Tests with Specified Mass of RMI Introduced (cont)

Test ID	Stem	Gap [cm (in.)]	Mass of RMI Inserted (g)W1	RMI Size [cm × cm (in. × in.)]	*K*			RMI Recovered in Bucket (g) W2	RMI Unaccounted for Wf=W1-W2	Number of RMI Pieces Recovered from Valve after Test NR
					Before	After	% Change			
5LDT2	5L	0.1269 (0.04997)	5.01	0.32 × 0.32 (1/8 × 1/8)	174	174	<5	4.56	0.45	0
5LDT3	5L	0.1269 (0.04997)	10.01	0.32 × 0.32 (1/8 × 1/8)	173	192	11	9.24	0.77	3
5LDT4	5L	0.1269 (0.04997)	1.01	0.63 × 0.63 (1/4 × 1/4)	173	186	8	0.77	0.24	2
5LDT5	5L	0.1269 (0.04997)	5.01	0.63 × 0.63 (1/4 × 1/4)	173	174	<5	4.75	0.26	0
5LDT6	5L	0.1269 (0.04997)	10.01	0.63 × 0.63 (1/4 × 1/4)	170	211	24	9.14	0.87	9
5LDT7	5L	0.1269 (0.04997)	1.01	0.32 × 1.27 (1/8 × 1/2)	172	173	<5	0.91	0.10	0
5LDT8	5L	0.1269 (0.04997)	5.01	0.32 × 1.27 (1/8 × 1/2)	172	171	<5	4.53	0.48	2
5LDT9	5L	0.1269 (0.04997)	10.01	0.32 × 1.27 (1/8 × 1/2)	171	220	29	8.61	1.40	26
5SDT1	5S	0.254 (0.0999)	1.00	0.32 × 0.32 (1/8 × 1/8)	203	204	<5	0.97	0.03	0
5SDT2	5S	0.254 (0.0999)	5.00	0.32 × 0.32 (1/8 × 1/8)	203	206	<5	4.52	0.48	1
5SDT3	5S	0.254 (0.0999)	10.00	0.32 × 0.32 (1/8 × 1/8)	203	202	<5	9.18	0.82	1
5SDT4	5S	0.254 (0.0999)	1.00	0.63 × 0.63 (1/4 × 1/4)	205	204	<5	0.8	0.18	0
5SDT5	5S	0.254 (0.0999)	5.01	0.63 × 0.63 (1/4 × 1/4)	205	205	<5	4.5	0.47	0
5SDT6	5S	0.254 (0.0999)	10.00	0.63 × 0.63 (1/4 × 1/4)	204	205	<5	9.0	1.00	1
5SDT7	5S	0.254 (0.0999)	1.01	0.32 × 1.27 (1/8 × 1/2)	204	203	<5	0.8	0.18	0
5SDT8	5S	0.254 (0.0999)	5.01	0.32 × 1.27 (1/8 × 1/2)	201	202	<5	4.6	0.42	1
5SDT9	5S	0.254 (0.0999)	10.01	0.32 × 1.27 (1/8 × 1/2)	202	203	<5	9.0	1.05	5
5SDT10	5S	0.161 (0.0632)	1.00	0.32 × 0.32 (1/8 × 1/8)	311	309	<5	1.0	0.05	0

Table 4-2. Results of Tests with Specified Mass of RMI Introduced (cont)

Test ID	Stem	Gap [cm (in.)]	Mass of RMI Inserted (g)W1	RMI Size [cm × cm (in. × in.)]	*K*			RMI Recovered in Bucket (g) W2	RMI Unaccounted for Wf=W1-W2	Number of RMI Pieces Recovered from Valve after Test NR
					Before	After	% Change			
5SDT11	5S	0.161 (0.0632)	5.00	0.32 × 0.32 (1/8 × 1/8)	311	310	<5	4.6	0.42	0
5SDT12	5S	0.161 (0.0632)	10.00	0.32 × 0.32 (1/8 × 1/8)	310	313	<5	9.0	0.98	4
5SDT13	5S	0.161 (0.0632)	1.02	0.63 × 0.63 (1/4 × 1/4)	316	316	<5	0.9	0.16	4
5SDT14	5S	0.161 (0.0632)	5.00	0.63 × 0.63 (1/4 × 1/4)	313	317	<5	4.6	0.42	10
5SDT15	5S	0.161 (0.0632)	10.02	0.63 × 0.63 (1/4 × 1/4)	314	326	<5	9.1	0.93	14
5SDT16	5S	0.161 (0.0632)	1.01	0.32 × 1.27 (1/8 × 1/2)	315	317	<5	0.9	0.08	1
5SDT17	5S	0.161 (0.0632)	5.00	0.32 × 1.27 (1/8 × 1/2)	313	311	<5	4.5	0.51	1
5SDT18	5S	0.161 (0.0632)	10.00	0.32 × 1.27 (1/8 × 1/2)	327	337	<5	9.2	0.75	41
N-1_45L	45L	0.6350 (0.2500)	10.01	0.32 × 0.32 (1/8 × 1/8)	105	108	<5	9.7	0.30	8
N-4_45L	45L	0.6350 (0.2500)	10.01	0.32 × 1.27 (1/8 × 1/2)	103	105	<5	9.9	0.13	5
N-7_45L	45L	0.6350 (0.2500)	5	0.32 × 1.27 (1/8 × 1/2)	104	120	15	10.2	-0.21	6
			5	0.63 × 0.63 (1/4 × 1/4)						5
D-2_45L	45L	0.159 (0.0625)	10.01	0.32 × 1.27 (1/8 × 1/2)	166	200	20	9.9	0.12	65
D-3_5L	5L	0.127 (0.0500)	10.05	0.32 × 1.27 (1/8 × 1/2)	173	186	8	9.9	0.15	1
N-11_45L	45L	0.3305 (0.1301)	10.03	0.32 × 0.32 (1/8 × 1/8)	104	119	15	9.5	0.50	38
N-21_45L	45L	0.3305 (0.1301)	10.00	0.32 × 0.32 (1/8 × 1/8)	103	114	11	9.7	0.30	42
N-31_45L	45L	0.3305 (0.1301)	10.01	0.32 × 0.32 (1/8 × 1/8)	102	115	12	9.8	0.16	22
N-41_45L	45L	0.3305 (0.1301)	10.00	0.32 × 1.27 (1/8 × 1/2)	107	122	14	9.78	0.32	29

Table 4-2. Results of Tests with Specified Mass of RMI Introduced (cont)

Test ID	Stem	Gap [cm (in.)]	Mass of RMI Inserted (g)W1	RMI Size [cm × cm (in. × in.)]	*K*			RMI Recovered in Bucket (g) W2	RMI Unaccounted for Wf=W1-W2	Number of RMI Pieces Recovered from Valve after Test NR
					Before	After	% Change			
N-51_45L	45L	0.3305 (0.1301)	10.00	0.32 × 1.27 (1/8 × 1/2)	104	133	28	9.8	0.16	32
N-61_45L	45L	0.3305 (0.1301)	10.00	0.32 × 1.27 (1/8 × 1/2)	103	117	14	9.9	0.05	46

Table 4-3. Results of Repeatability Tests

No.	Test ID	Case	Stem	Gap [cm (in.)]	Mass of RMI Inserted (g)W1	RMI Size [cm × cm (in. × in.)]	*K*			RMI Recovered in Bucket (g) W2	RMI Unaccounted for Wf=W1-W2	Number of RMI Pieces Recovered from Valve after Test NR
							Before	After	% Change			
1	45LDT5	Original	45L	0.3142 (0.1237)	5.00	0.63 × 0.63 (1/4 × 1/4)	88.9	92.6	<5	4.82	0.18	4
	45LDTR5	Repeat	45L	0.3124 (0.1230)	5.01	0.63 × 0.63 (1/4 × 1/4)	107	133	24	4.39	0.37	0
	45LDTR5x	Gap>Debris Size	45L	0.3269 (0.1287)	5.07	0.32 × 0.32 (1/8 × 1/8)	105	105	<5	4.35	0.54	7
2	45LDT9	Original	45L	0.3142 (0.1237)	10.00	0.32 × 1.27 (1/8 × 1/2)	88.1	133	51	8.92	1.08	60
	45LDTR9	Repeat	45L	0.3124 (0.1230)	10.05	0.32 × 1.27 (1/8 × 1/2)	105	111	5	4.98	0.52	14
	D-1_45L	Repeat	45L	0.3170 (0.1248)	10.00	0.32 × 1.27 (1/8 × 1/2)	104	124	19	9.88	0.12	46
	D-1-2_45L	Repeat	45L	0.3180 (0.1252)	10.00	0.32 × 1.27 (1/8 × 1/2)	99.0	152	54	10.12	-0.12	46
3	45LDT11	Original	45L	0.166 (0.0654)	4.99	0.32 × 0.32 (1/8 × 1/8)	125	124	<5	4.24	0.75	2
	45LDTR11	Repeat	45L	0.156 (0.0615)	5.03	0.32 × 0.32 (1/8 × 1/8)	126	133	6	9.99	1.33	11

Table 4-3. Results of Repeatability Tests (cont)

No.	Test ID	Case	Stem	Gap [cm (in.)]	Mass of RMI Inserted (g)W1	RMI Size [cm × cm (in. × in.)]	*K*			RMI Recovered in Bucket (g) W2	RMI Unaccounted for Wf=W1-W2	Number of RMI Pieces Recovered from Valve after Test NR
							Before	After	% Change			
4	45LDT18	Original	45L	0.166 (0.0654)	10.00	0.32 × 1.27 (1/8 × 1/2)	127	192	51	9.42	0.58	53
	D-2_45L	Repeat	45L	0.159 (0.0625)	10.01	0.32 × 1.27 (1/8 × 1/2)	166	200	20	9.88	0.12	65
5	45LDT14	Original	45L	0.166 (0.0654)	5.0	0.63 × 0.63 (1/4 × 1/4)	124	165	32	4.54	0.46	29
	D-6_45L	Repeat	45L	0.159 (0.0626)	5.00	0.63 × 0.63 (1/4 × 1/4)	155	194	25	5.07	-0.07	33
6	5LDT3	Original	5L	0.127 (0.0500)	10.01	0.32 × 0.32 (1/8 × 1/8)	173	192	11	9.24	0.77	3
	D-3_5L	Repeat	5L	0.127 (0.0500)	10.05	0.32 × 0.32 (1/8 × 1/8)	173	186	8	9.90	0.15	1
7	N-1_45L	Original	45L	0.6350 (0.2500)	10.01	0.32 × 0.32 (1/8 × 1/8)	105	108	<5	9.71	0.30	8
	N-2_45L	Repeat	45L	0.6350 (0.2500)	10.00	0.32 × 0.32 (1/8 × 1/8)	102	102	<5	9.73	0.27	4
	N-3_45L	Repeat	45L	0.6350 (0.2500)	10.01	0.32 × 0.32 (1/8 × 1/8)	105	106	<5	9.83	0.18	9
8	N-4_45L	Original	45L	0.6350 (0.2500)	10.01	0.32 × 1.27 (1/8 × 1/2)	103	105	<5	9.88	0.13	5
	N-5_45L	Repeat	45L	0.6350 (0.2500)	10.02	0.32 × 1.27 (1/8 × 1/2)	99.5	102	<5	9.78	0.24	6
	N-6_45L	Repeat	45L	0.6350 (0.2500)	10.01	0.32 × 1.27 (1/8 × 1/2)	99.3	101	<5	9.82	0.19	1

Table 4-4. Estimates of Blockage-Area Fraction for RMI Tests

Test ID	Stem	Gap [cm (in.)]	Mass of RMI Inserted (g)W1	RMI Size [cm × cm (in. × in.)]	*K*			Estimate of Blocked Area Fraction
					Before	After	% Change	
45LDT12	45L	0.166 (0.0654)	10.00	0.32 × 0.32 (1/8 × 1/8)	124	130	<5	<5%
45LDT13	45L	0.166 (0.0654)	1.00	0.63 × 0.63 (1/4 × 1/4)	122	136	11	<5%
45LDT14	45L	0.166 (0.0654)	5.00	0.63 × 0.63 (1/4 × 1/4)	124	165	32	12
45LDT15	45L	0.166 (0.0654)	10.01	0.63 × 0.63 (1/4 × 1/4)	121	186	53	20
45LDT17	45L	0.166 (0.0654)	5.02	0.32 × 1.27 (1/8 × 1/2)	127	133	<5	<5%
45LDT18	45L	0.166 (0.0654)	10.00	0.32 × 1.27 (1/8 × 1/2)	127	192	51	19
D-2_45L	45L	0.159 (0.0625)	10.01	0.32 × 1.27 (1/8 × 1/2)	166	200	20	6.4
D-6_45L	45L	0.159 (0.0626)	5.00	0.63 × 0.63 (1/4 × 1/4)	155	194	25	19
45LDTR11	45L	0.156 (0.0615)	5.03	0.32 × 0.32 (1/8 × 1/8)	126	133	6	<5%
5LDT3	5L	0.1269 (0.04997)	10.01	0.32 × 0.32 (1/8 × 1/8)	173	192	11	10
5LDT4	5L	0.1269 (0.04997)	1.01	0.63 × 0.63 (1/4 × 1/4)	173	186	8	8.7
5LDT6	5L	0.1269 (0.04997)	10.01	0.63 × 0.63 (1/4 × 1/4)	170	211	24	14
5LDT9	5L	0.1269 (0.04997)	10.01	0.32 × 1.27 (1/8 × 1/2)	171	220	29	15
D-3_5L	5L	0.127 (0.0500)	10.05	0.32 × 0.32 (1/8 × 1/8)	173	186	8	8.7

4.2 CalSil Tests

Single-debris tests with CalSil used 50 or 100 g of material prepared, as described in Section 2.4. The results are summarized in Table 4-5. The various columns in the CalSil data table are explained below.

Table 4-5. Results of CalSil Tests

Test ID	Stem	Gap [cm (in.)]	Mass of CalSil (g) WC	Sieve #	*K*		
					Before	After	% Change
5sc1	5S	0.161 (0.0632)	50.04	4	312	319	<5
5sc2	5S	0.161 (0.0632)	100.04	4	313	310	<5
5sc3	5S	0.161 (0.0632)	51.01	8	314	314	<5
5sc4	5S	0.161 (0.0632)	100.00	8	312	321	<5
5sc5	5S	0.254 (0.0999)	50.06	4	205	202	<5
5sc6	5S	0.254 (0.0999)	100.04	4	205	204	<5
5sc7	5S	0.254 (0.0999)	49.98	8	205	204	<5
5sc8	5S	0.254 (0.0999)	100.08	8	205	205	<5
5LC1	5L	0.127 (0.0499)	50.08	4	177	179	<5
5LC2	5L	0.127 (0.0499)	100.56	4	177	182	<5
5LC3	5L	0.127 (0.0499)	50.12	8	177	179	<5
5LC4	5L	0.127 (0.0499)	101.25	8	177	199	12

Only one of the CalSil tests (5LC4) showed an appreciable increase in the valve-loss coefficient. This test used 101 g of #8-sieved CalSil with valve stem 5L and a valve gap of 1.3 mm (0.05 in.). For this case, the blocked area fraction, based on Eq. (3-3), is 10%. Transient data from the 5LC4 test are shown in Figure 4-5.

In addition to the tests listed in Table 4-5, a test was performed with unsieved CalSil (Figure 2-23) using the 45L stem and an opening of 0.1 in. This bounding test was performed for the purpose of demonstrating test procedures to visiting NRC personnel, so the CalSil could not be characterized sufficiently before the test. The transient data are shown in Figure 4-6. The loss coefficient, *K*, increased by ~25% shortly after debris introduction but then decreased gradually over the remainder of the test. It appeared that unsieved CalSil clogged the valve initially but that the clogged debris eroded gradually over time, resulting in a reduction in the loss coefficient.

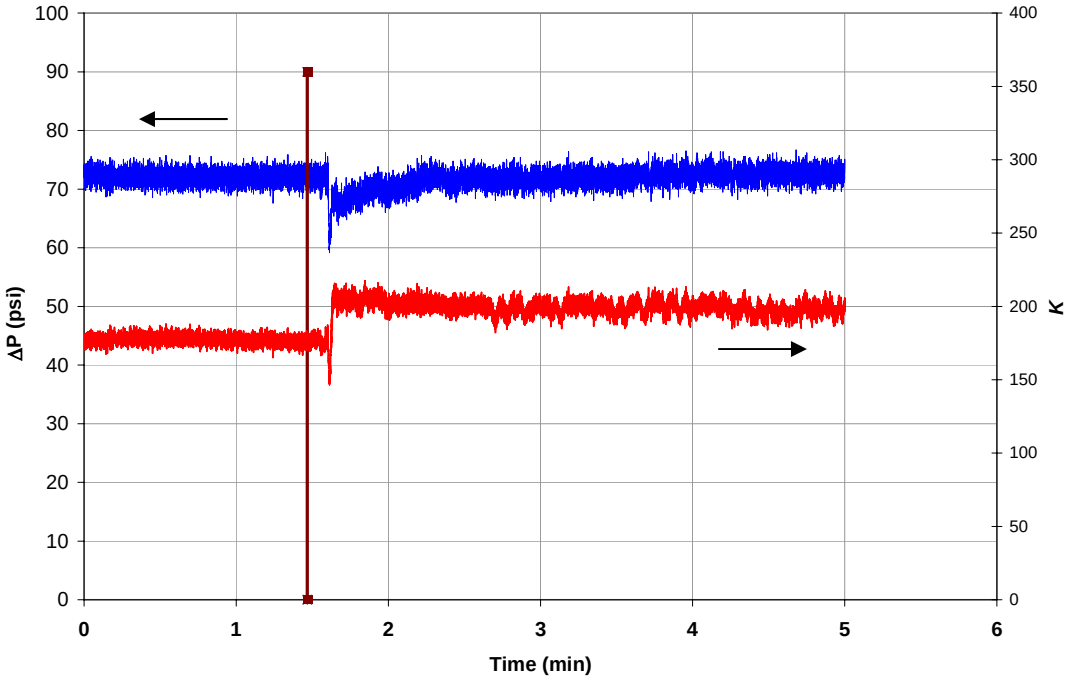

Figure 4-5. Transient Variation of Valve Pressure Drop and Calculated *K* for Test 5LC4

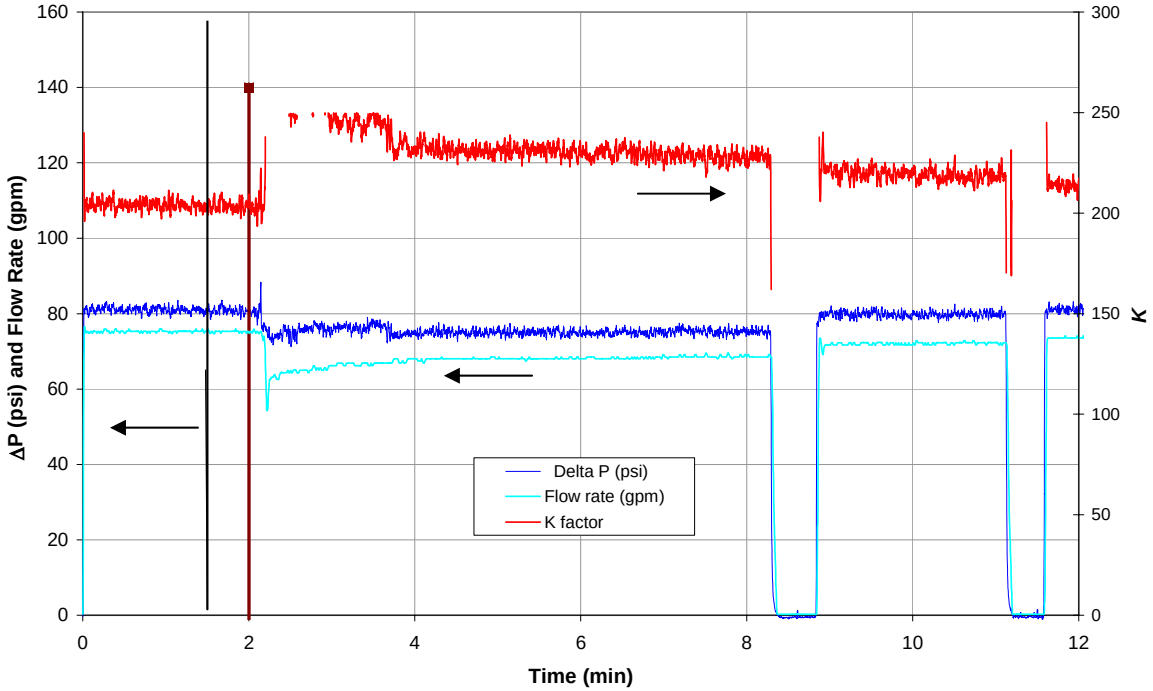

Figure 4-6. Transient Variation of Valve Pressure Drop, Flow Rate, and Calculated *K* for Test 5sc9

4.3 NUKON Tests

4.3.1 Tests with Specified Mass of NUKON

Single-debris NUKON tests used ~50 or 100 g of material, prepared as described in Section 2.4. One test used 25 g of NUKON. The results are summarized in Table 4-6.

Transient data from two typical tests in this category are shown in Figure 4-7, Figure 4-8, and Figure 4-9. Figure 4-7 presents the data for Test 45LN1, which showed a very small increase in the loss-coefficient *K*. Figure 4-8 shows the data for test 5LN3, which showed a significant increase in *K* following debris introduction. The average steady-state *K* value over the post-debris test interval was 186% higher than the baseline value. Unlike RMI and sieved CalSil, *K* could be observed to decrease gradually over time in this test, possibly as a result of erosion of the debris trapped in the valve. Figure 4-9 shows data from test 45LN3, which showed a 222% increase in average steady-state *K* over the test interval following debris introduction. The erosion effects were pronounced in this case, as well.

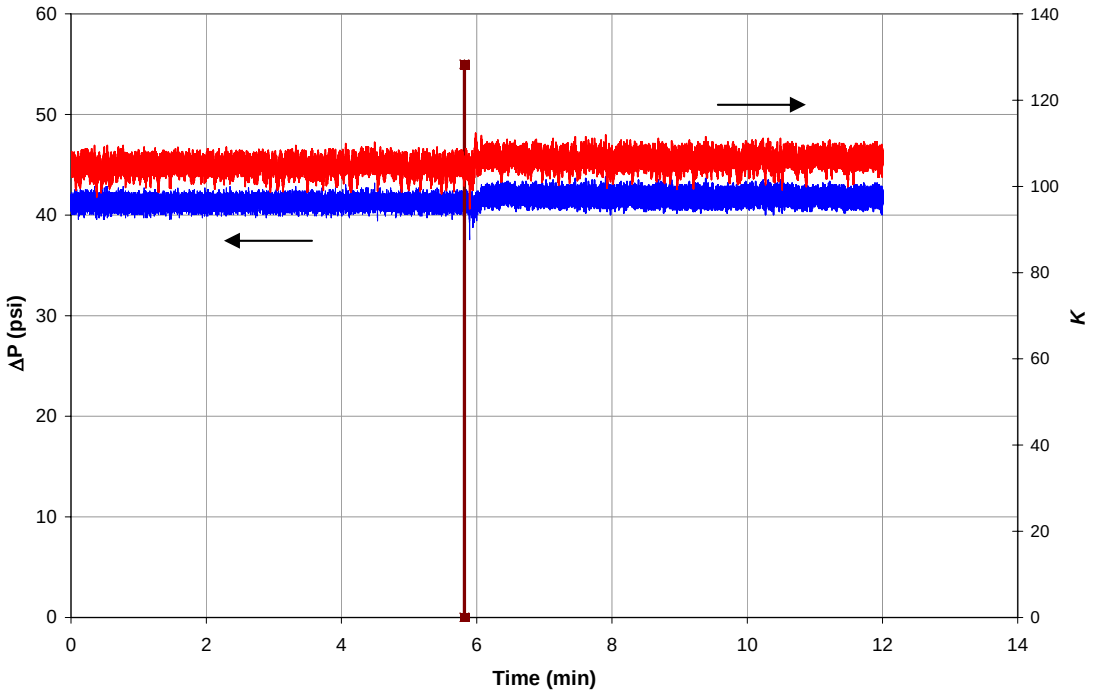

Figure 4-7. Transient Variation of Valve Pressure Drop and Calculated *K* for NUKON Test 45LN1

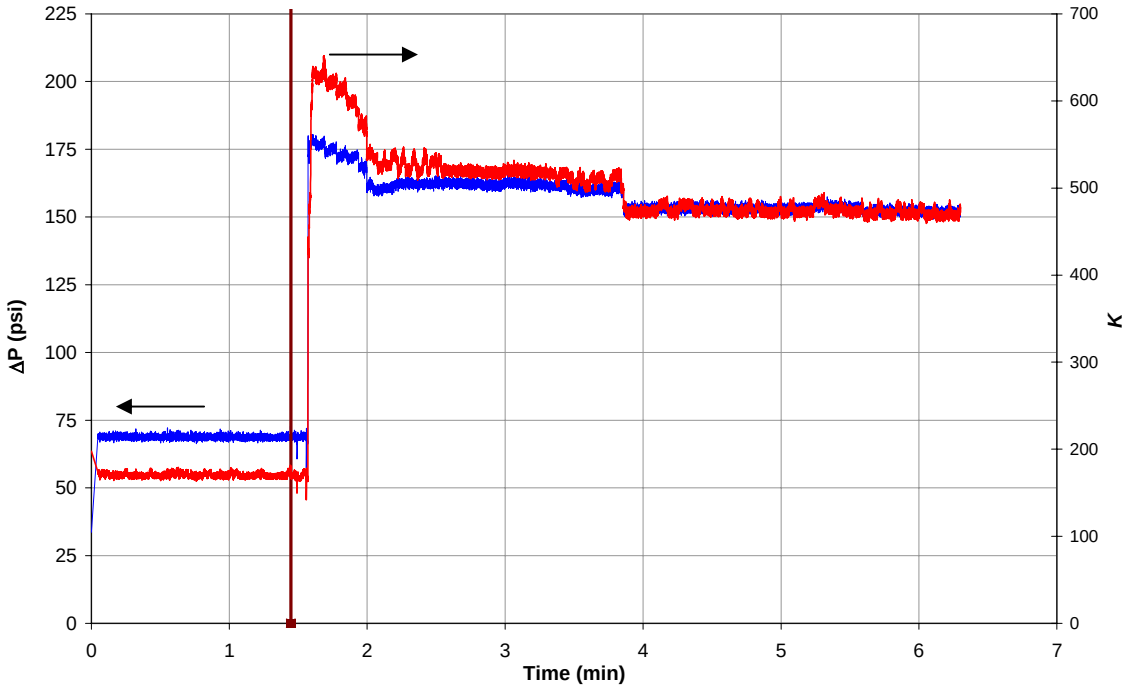

Figure 4-8. Transient Variation of Valve Pressure Drop and Calculated *K* for NUKON Test 5LN2

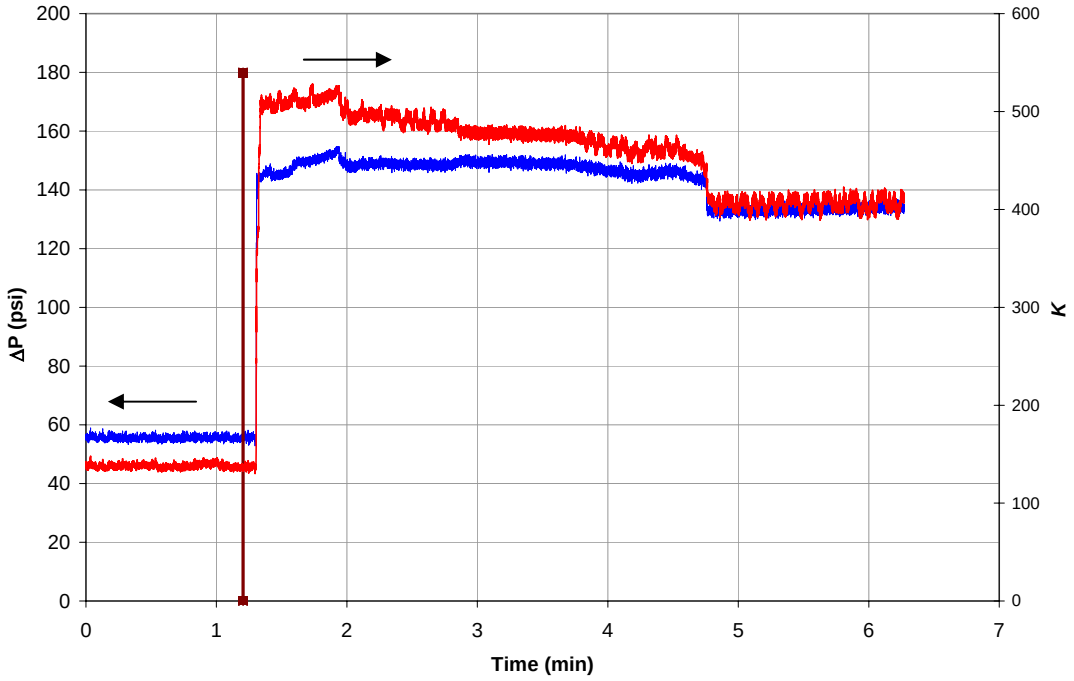

Figure 4-9. Transient Variation of Valve Pressure Drop and Calculated *K* for NUKON Test 45LN3

The results summarized in Table 4-6 and portrayed graphically in Figure 4-10 show that NUKON can cause significant clogging in the valve, as evidenced by the large increases in *K* in many of the tests. The effect was pronounced in tests with valve gaps less than 0.16 cm (0.063 in.) for the 45L and 5L configuration. Gaps larger than 0.16 cm (0.063 in.) did not result in significant clogging. The single test performed using a smaller quantity (25 g) of NUKON (D-17_45L) showed no significant evidence of clogging; however, insufficient data exists to establish any possible clogging threshold.

In addition to the observed gap-dependent behavior, the stem geometry affected the observed increase in *K*. The 5S stem showed essentially no increase in *K* for any quantity of NUKON introduced. The 5L and 45L stems showed substantial increases in *K*, with the 45L stem being somewhat higher than the 5L stem for comparable gap sizes.

Table 4-6. Results of NUKON Tests

Test ID	Stem	Gap [cm (in.)]	Mass of NUKON (g) WN	*K*		
				Before	After	% Change
45LN1	45L	0.3152 (0.1241)	49.92	105	106	<5
45LN2	45L	0.162 (0.0636)	49.85	124	182	47
45LN3	45L	0.160 (0.0629)	95.67	138	445	222
45LN4	45L	0.160 (0.0629)	98.23	140	421	201
D-17_45L	45L	0.159 (0.0626)	25.05	154	155	<5
5LN1	5L	0.126 (0.0497)	50.07	175	198	14
5LN2	5L	0.127 (0.0500)	97.99	170	488	187
5LN3	5L	0.127 (0.0500)	97.47	170	385	126
5SN1	5S	0.2540 (0.1000)	50.15	195	196	<5
5SN4	5S	0.2543 (0.1001)	98.05	196	197	<5
5SN2	5S	0.159 (0.0627)	50.07	313	318	<5
5SN3	5S	0.159 (0.0627)	95.83	317	340	7

4.3.2 NUKON Repeatability Tests

A single test was done to gauge the repeatability of the NUKON data. The results are summarized in Table 4-7, and the transient data from the two tests are compared in Figure 4-11. It should be noted that the baseline *K* values were different in the two tests but, as discussed in Section 3.1, only the relative change in *K* is important for making inferences about debris-clogging effects. The table and the figure show that, as in the case of RMI data presented earlier, the results of these two nominally identical tests were highly variable.

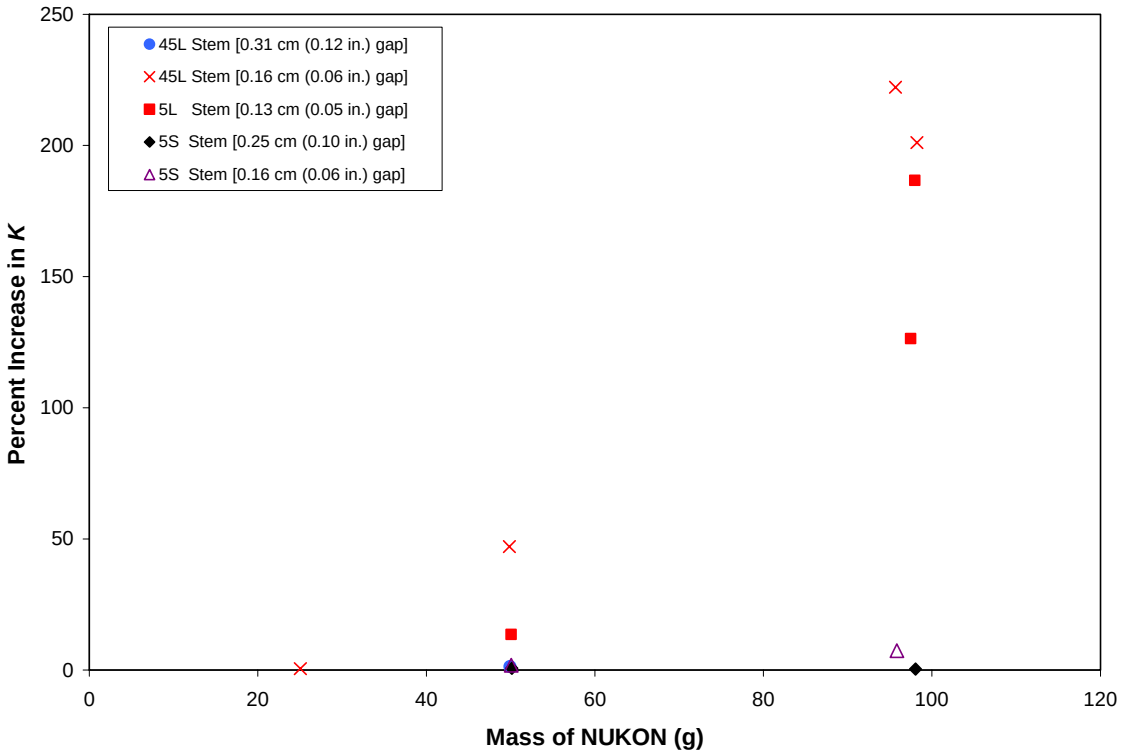

Figure 4-10. Observed Correlation between Mass of NUKON Introduced and the Increase in *K*.

Table 4-7. Results of NUKON Repeatability Test

Test ID	Case	Stem	Gap [cm (in.)]	Mass of NUKON (g) WN	*K*		
					Before	After	% Change
45LN2	Original	45L	0.162 (0.0636)	49.85	124	182	47
D-16	Repeat	45L	0.159 (0.0626)	50.01	158	375	137

4.3.3 Estimating Blockage Area

As discussed in Section 3, baseline data for known blockage conditions were obtained for the 45L and the 5L valve configurations for valve openings of 0.159 cm (0.0625 in.) and 0.13 cm (0.05 in.), respectively. Blockage-area fractions estimated using Eq. (3-2) for the NUKON tests using the 45L/0.159-cm (0.0625-in.)-opening and Eq. (3-3) for the 5L/0.13-cm (0.05-in.)-opening combinations are listed in Table 4-8. It should be noted that the shape of the blockage curves, as shown in Figure 3-6 and Figure 3-8, indicates

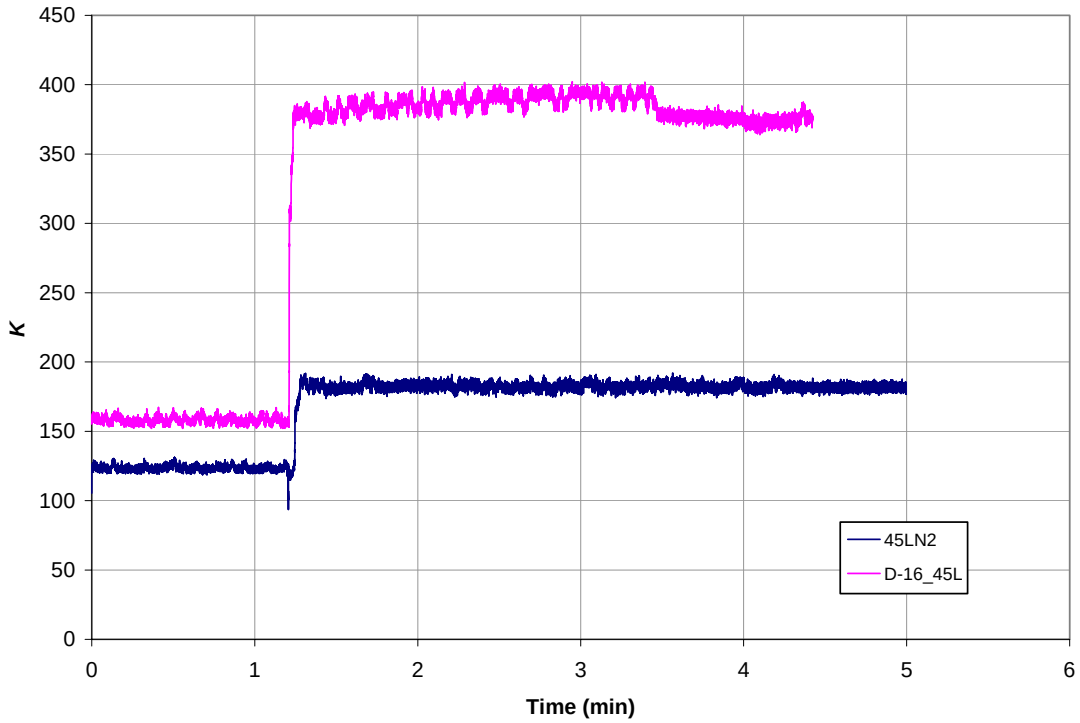

Figure 4-11. Transient Variation of *K* for NUKON Repeatability Tests

that the sensitivity of the estimated blockage area decreases with increasing *K*. The highest estimated blocked area fraction was ~45%. Typically, the blockage fractions with NUKON were substantially higher than the largest fractions estimated for the RMI tests.

Table 4-8. Estimates of Blocked Area Fraction for NUKON Tests

Test ID	Stem	Gap [cm (in.)]	Mass of NUKON (g) WN	*K*			Blocked Area Fraction (%)
				Before	After	% Change	
5LN1	5L	0126 (0.0497)	50.07	175	198	14	11
45LN2	45L	0.162 (0.0636)	49.85	124	182	47	18
5LN2	5L	0.127 (0.0500)	97.99	170	488	187	46
5LN3	5L	0.127 (0.0500)	97.47	170	385	126	37
45LN3	45L	0.160 (0.0629)	95.67	138	445	222	45
45LN4	45L	0.160 (0.0629)	98.23	140	421	201	43

4.4 Discussion

Data from the tests discussed in this chapter provided some overall qualitative information on the potential clogging of the throttle valves by unmixed debris. In general, higher loading of larger debris sizes (relative to the throttle valve opening) resulted in the highest observed increase in valve-loss-coefficient *K*.

In RMI tests, the highest observed increase in *K* was ~50%. In tests for which an estimate of the corresponding blockage-area fraction could be estimated, this increase translated to a blocked area fraction of ~20% for RMI pieces 0.63 cm × 0.63 cm (1/4 in. × 1/4 in.) and valve openings of 0.159 cm (0.0625 in.). For RMI pieces smaller than 0.63 cm × 0.63 cm (1/4 in. × 1/4 in.), blockage in the valve appeared to be minimal for the valve clearances studied here.

Based on the results of the screen penetration tests (Ref. 3), 0.63 cm × 0.63 cm (1/4-in. × 1/4-in.) RMI pieces typically were less likely to penetrate screens with screen openings of 0.63 cm (1/4 in.)—the data showed that <20% of the RMI pieces of this size penetrated the 0.63-cm (1/4-in.) screen for the highest flow velocities tested, as described in Ref. 3. A similar result was seen for 0.32-cm (1/8-in.) RMI pieces and a 0.32-cm (1/8-in.) screen. When the RMI debris had dimensions smaller than the screen size, a larger fraction of RMI penetrated the screen, but the current results show that the smaller-size RMI debris was able to clear the throttle valve, as well—at least for the range of valve openings tested here. The results for RMI debris alone (without any other debris) indicated that the smaller debris, which was more likely to pass through the sump screen, was also less likely to get caught in the valve.

The screen penetration tests showed that a significant fraction of CalSil passed through the screen, regardless of the screen opening. The current results show that the same occurs in the valve, as well—practically all of the CalSil passed through the valve without causing appreciable blockage.

As much as 80% of blender-processed NUKON debris was found to penetrate the screen, as described in Ref. 3. The current results show that *K* increases of between 7% and 220% occurred when a stream of blender-processed NUKON reached the valve. For cases where an estimate of the corresponding blockage-area fraction was possible, this increase translated to between 10% and 45% blockage in the valve opening. Based on these results, NUKON is judged to be more likely then RMI or CalSil to cause throttle valve blockage. A large fraction of blender-processed NUKON was able to penetrate the screen, and a large fraction of this NUKON, in turn, could get trapped in the valve, resulting in significant increases in valve pressure loss. Note that this finding was based on tests involving a single batch or slug of NUKON. It is possible that the blockage effects of NUKON could be magnified in combination with other ingested materials or when a steady debris stream of NUKON over time is considered; these effects are examined in Section 6.

The data also showed a high degree of variability in the valve-clogging data for RMI and NUKON. This observation was consistent with the inherent randomness involved in the process; the propensity for trapping of debris in the valve gap is a function of the random orientation of the individual pieces as they enter the valve gap. Further, the bending or thrashing of the debris pieces inside the valve is also a random process.

5 RESULTS OF MIXED-DEBRIS TESTS

Section 4 focused on the clogging of the throttle valve by separate insulation components of the debris stream. This section now addresses the potential for clogging of the valve by mixtures of insulation debris. All of the mixed-debris tests were conducted within a temperature range of 19°C (66ºF) and 27°C (80ºF). All of the mixed-debris tests (Appendix D, Test Series 2) were taken using single-point sampling rather than five-point averaging, as discussed in Section 2.3.

The debris mixtures tested included the following:

1. NUKON combined with RMI;
2. CalSil combined with RMI;
3. NUKON combined with CalSil;
4. homogeneous mixtures of CalSil, NUKON, and RMI; and
5. CalSil, NUKON, and RMI introduced separately in a specific sequence.

5.1 Mixtures of NUKON and RMI

A series of tests was performed in which homogeneous mixtures of NUKON and RMI were introduced in the flow. The test conditions and results are summarized in Table 5-1. One test was repeated; the results are provided in Table 5-2. Blockage-area fraction estimates could be made only for the two tests that corresponded with the valve gap openings used in the shim blockage measurements. The results are listed in Table 5-3.

The mixture test data are compared with the single-debris data in Table 5-4 and Figure 5-1. Data Set 1 in Table 5-4 shows the results for a valve opening of 0.63 cm (0.25 in.) and an RMI of size 0.32 cm × 1.27 cm (1/8 in. × 1/2 in.) did not result in any appreciable increase in the valve-loss coefficient; however, the addition of 50 g of NUKON showed a nearly 13% increase in the loss coefficient. Single-debris tests were not performed with NUKON with this valve opening; however, a single-debris NUKON test performed for a smaller opening [0.317 cm (0.125 in.)] indicated no appreciable blockage. Based on this result, the increase in K for the RMI and NUKON mixture (test N-8_45L) may be attributed to the debris combination. Additionally, a total of 17 RMI pieces were recovered from the valve after the mixture test, whereas only between 1 and 6 pieces were recovered after the single-debris RMI tests. It is possible that some of the NUKON trapped in the valve also trapped some RMI pieces, resulting in an increased blockage compared to either debris form acting alone. However, given the inherent variability in the data discussed previously, additional repeatability tests would be necessary to determine if a statistically significant effect exists. Other mixture combinations (Data sets 2, 3, and 4 in Table 5-4) showed relatively no effect when NUKON and RMI were combined. In all of these cases, the valve-loss-coefficients for the individual mixed-debris tests were within the range of variability for the single-debris cases. The number of RMI pieces recovered from the valve following the tests also was generally consistent with the RMI-only tests. As before, more testing is required to quantify any differences.

Table 5-1. Results of Tests with NUKON-RMI Mixtures

Test ID	Stem	Valve Opening [cm (in.)]	W1	RMI Size [cm × cm (in. × in.)]	WN	*K*			W2	Wf	NR
						Before	After	% Change			
N-8_45L	45L	0.6350 (0.2500)	10.03	0.32 × 1.27 (1/8 × 1/2)	48.25	102	115	13	38.19	20.09	17
D-4_45L	45L	0.3170 (0.1248)	10.00	0.32 × 1.27 (1/8 × 1/2)	50.24	101	152	51	39.87	20.37	30
D-7_45L	45L	0.159 (0.0626)	5.01	0.63 × 0.63 (1/4 × 1/4)	25.14	154	180	17	21.23	8.92	16
D-5_5L	5L	0.127 (0.0500)	10.00	0.32 × 0.32 (1/8 × 1/8)	50.16	168	177	6	28.01	32.15	26

Table 5-2. Results of Repeatability Test with NUKON RMI Mixtures

Test ID	Stem	Valve Opening [cm (in.)]	W1	RMI Size [cm × cm (in. × in.)]	WN	*K*			W2	Wf	NR
						Before	After	% Change			
D-4_45L	45L	0.3170 (0.1248)	10.00	0.32 × 1.27 (1/8 × 1/2)	50.24	101	152	51	39.87	20.37	30
D-4-2_45L	45L	0.3180 (0.1252)	10.03	0.32 × 1.27 (1/8 × 1/2)	50.00	98.1	132	35	40.21	19.82	32

Table 5-3. Estimates of Blocked Area Fraction for Tests with NUKON-RMI Mixtures

Test ID	Stem	Valve Opening [cm (in.)]	W1	RMI Size [cm × cm (in. × in.)]	WN	*K*			Blocked Area Fraction (%)
						Before	After	% Change	
D-7_45L	45L	0.159 (0.0626)	5.01	0.63 × 0.63 (1/4 × 1/4)	25.14	154	180	17	5.3
D-5_5L	5L	0.127 (0.0500)	10.00	0.32 × 0.32 (1/8 × 1/8)	50.16	168	177	6	7.9

Table 5-4. Comparing NUKON-RMI Mixture Test Data with Baseline Single-Debris Test Data

Data Set	Stem	Valve Opening [cm (in.)][1]	W1	RMI Size [cm × cm (in. × in.)]	WN[2]	Debris Type	Test ID	*K*			NR
								Before	After	% Change	
1	45L	0.6350 (0.2500)	10.00	0.32 × 1.27 (1/8 × 1/2)	50	RMI only	N-4_45L	103	105	<5	5
							N-5_45L	99.5	102	<5	6
							N-6_45L	99.3	101	<5	1
						RMI + NUKON	N-8_45L	102	115	13	17
2	45L	0.3175 (0.1250)	10.00	0.32 × 1.27 (1/8 × 1/2)	50	RMI only	45LDT9	88.1	133	51	60
							45LDTR9	105	111	5	14
							D-1_45L	104	124	19	46
							D-1-2_45L	99.0	152	54	46
						NUKON only	45LN1	105	106	<5	-
						RMI + NUKON	D-4_45L	101	152	51	30
3	45L	0.159 (0.0626)	5.00	0.63 × 0.63 (1/4 × 1/4)	25	RMI only	45LDT14	124	165	32	29
							D-6_45L	155	194	25	35
						NUKON only	D-17_45L	154	155	<5	-
						RMI + NUKON	D-7_45L	154	180	17	16
4	5L	0.127 (0.0500)	10.00	0.32 × 0.32 (1/8 × 1/8)	50	RMI only	5LDT3	173	192	11	3
							D-3_5L	173	186	8	13
						NUKON only	D-17_45L	175	198	14	-
						RMI + NUKON	D-5_45L	168	177	6	26

Note 1: Valve opening value cited is approximate. Tests in each set did not all have identical valve openings but varied over a small range, typically within 0.003 cm (0.001 in.).

Note 2: Mass cited is approximate. Tests in each set did not all have identical mass but varied over a small range, typically within 0.1 g.

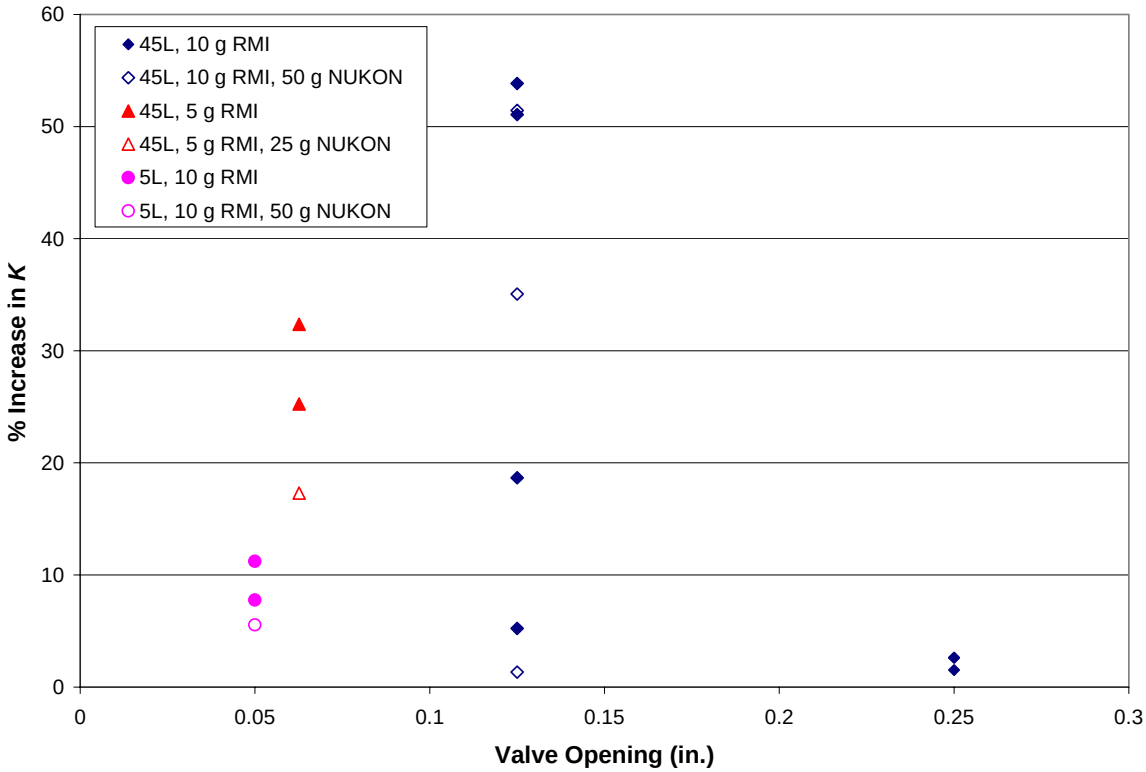

Figure 5-1. Comparison of RMI-NUKON Mixed Debris to RMI Alone

5.2 Mixtures of CalSil and RMI

One test was performed with a mixture of CalSil and RMI (Table 5-5). The test used 50 g of CalSil mixed with 5 g of 0.63-cm × 0.63-cm (1/4-in. × 1/4-in.) RMI and a valve opening of 0.159 cm (0.0625 in.) in the 45L stem. The single-debris RMI tests showed an increase in *K* of between 25% and 32%. The mixed-debris test showed an increase of 57%. A single-debris CalSil test was not performed for this valve opening; however, corresponding data for the 5S stem exhibited no blockage due to CalSil alone.

The limited data in this category suggested a possible mixture effect, but additional testing would be necessary to establish this more conclusively.

5.3 Mixtures of NUKON and CalSil

Two tests were performed with a mixture of NUKON and sieved CalSil (Table 5-6). Both used 25 g each of NUKON and CalSil. The single-debris NUKON test and the mixed-debris tests showed no appreciable differences in light of the test to test variability in the results. When the mixture tests were repeated using unsieved CalSil mixed with NUKON, *K* increased by 27% to 33% relative to a <5% increase for the NUKON-only case. This increase was roughly equivalent to the increase observed earlier for unsieved CalSil and was most likely attributed to the unsieved CalSil rather than the mixture

effect. This increase is illustrated in the test 5sc9 (Figure 4-6), which also used unsieved CalSil.

The transient data measured in one of the unsieved CalSil tests (D-19c_45L) are shown in Figure 5-2. Unlike in test 5sc9, *K* appears to be constant within several seconds after inserting debris, and does not degrade with time.

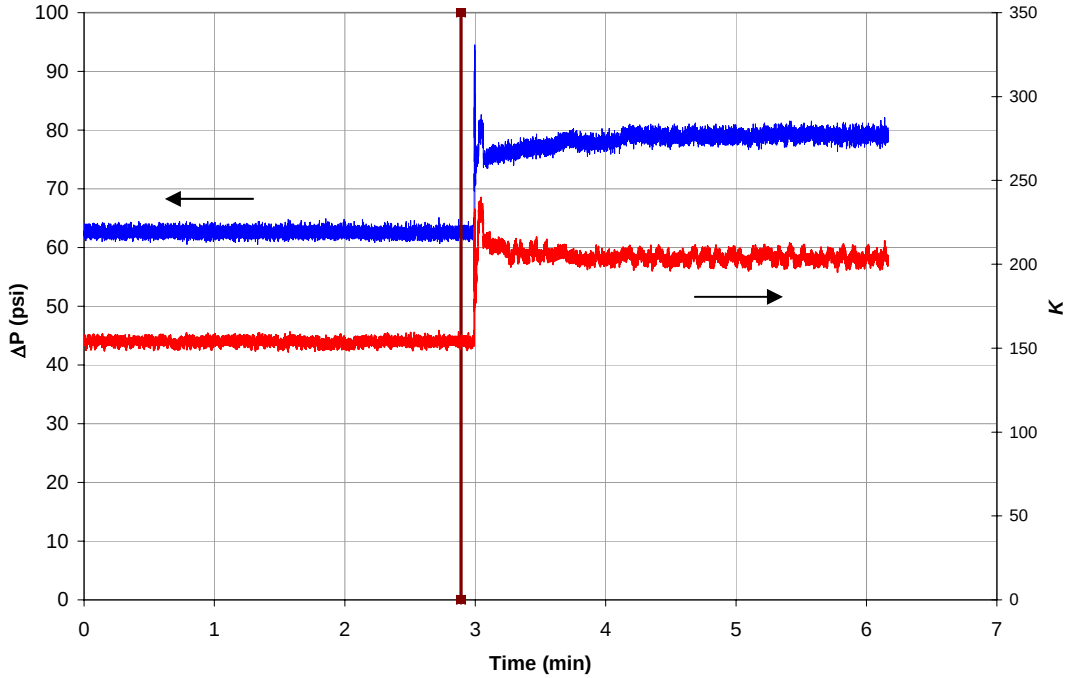

Figure 5-2. Transient Variation of Pressure Drop and *K* for Test D-19c_45L

5.4 Mixtures of RMI, NUKON, and CalSil

A series of tests was performed with mixtures of all three debris types. Most of the tests in this category used homogeneous combinations of the three debris types. A few tests were conducted with the debris types introduced sequentially. These two types are discussed separately below.

5.4.1 Homogeneous Combination of RMI, NUKON, and CalSil

In this series of tests, RMI, NUKON, and CalSil were premixed and introduced into the flow as a homogeneous mixture. A total of seven tests were conducted. The results of these tests are summarized in Figure 5-3 and Table 5-7. Four of the tests utilized two sizes of RMI. For these tests, the number of RMI pieces recovered from the valve following the tests is presented separately for each RMI size. Test D-15-2_5L was a replicate of test D-15_5L.

Table 5-5. Comparing CalSil-RMI Mixture Test Data with Baseline Single-Debris Test Data

Data Set	Stem	Valve Opening [cm (in.)][1]	Mass of RMI [2] (g) W1	RMI Size (in. × in.)	Mass of CalSil[2] (g) WC	Debris Type	Test ID	*K*			
								Before	After	% Change	NR
1	45L	0.159 (0.0625)	5.00	0.63 × 0.63 (1/4 × 1/4)	50	RMI only	45LDT14	124	165	32	29
							D-6_45L	155	194	25	35
						RMI + CalSil	D-8_45L	152	239	57	42

Table 5-6. Comparing NUKON-CalSil Mixture Test Data with Baseline Single-Debris Test Data

Data Set	Stem	Valve Opening [cm (in.)][1]	Mass of CalSil[2] (g) WC	Mass of NUKON[2] (g) WN	Debris Type	Test ID	*K*		
							Before	After	% Change
1	45L	0.159 (0.0625)	25.00	25.00	NUKON only	D-17_45L	154	155	<5
					#8 sieved CalSil + NUKON	D-18_45L	154	154	<5
					Unsieved CalSil + NUKON	D-19a_45L	154	196	27
						D-19b_45L			
						D-19c_45L	154	203	32
2	45L	0.3175 (0.1250)	25.00	25.00	NUKON only	45LN1	105	106	<5
					#8 sieved CalSil + NUKON	D-13_45L	100	102	<5

Note 1: Valve opening value cited is approximate. Tests in each set did not all have identical valve openings but varied over a small range, typically within 0.003 cm (0.001 in.).

Note 2: Mass cited is approximate. Tests in each set did not all have identical mass but varied over a small range, typically within 0.1 g.

Substantial increases in *K* were observed for all tests, except in test N-9_45L, which had a valve opening of 0.63 cm (0.25 in.). The two D-15 replicate tests yielded *K* increases of 187% and 68%, indicating the high variability of this data as well.

5.4.2 Sequential Addition of RMI, NUKON, and CalSil

In this series of tests, the three types of debris were added in a sequence, rather than as a homogeneous composition. The objective was to examine whether the effect of a particular debris type would be enhanced by the debris type introduced previously and potentially already trapped in the valve. All tests in this category used the 45L stem with a valve opening of 0.159 cm (0.0625 in.).

The results of this series of tests are summarized in Table 5-8. The increase in *K* ranged between 8% and 46%. The test where RMI was introduced first showed greater blockage than when NUKON was introduced first. The results of the tests summarized in Table 5-7 and Table 5-8 are compared with analogous baseline single- and two-component debris tests in Table 5-9. When the variability exhibited in replicate tests was considered, there are no significant differences between either homogeneous or sequential mixtures of RMI, NUKON, and CalSil.

5.4.3 Estimating Blockage-Area Fractions

As discussed in Section 3, baseline data for known blockage conditions were obtained for the 45L and the 5L valve configurations for valve openings of 0.159 cm (00625 in.) and 0.13 cm (0.05 in.), respectively. Blockage-area fractions estimated using Eq. (3-2) and Eq. (3-3) are listed in Table 5-10. The highest estimated blocked area fraction is ~42%.

5.5 Discussion

Tests using CalSil-RMI mixtures were the only combination that exhibited clear increases in *K* when compared with results from analogous single-debris CalSil and RMI tests. The results of tests performed using NUKON-RMI or CalSil-NUKON mixtures did not differ significantly from results for analogous separate tests, with one possible exception. One mixture test performed using unsieved CalSil with NUKON showed an appreciable increase in valve blockage compared to single-debris NUKON tests. However, it is unclear if this result is attributed to clumping within the unsieved CalSil or to retention by NUKON fibers within the valve.

The three-component mixture tests were divided into two types of tests; homogeneous mixtures of RMI, CalSil, and NUKON and sequential additions of each debris type using different ordering. Tests using homogeneous mixtures of RMI, CalSil, and NUKON showed an increase in valve blockage when compared with analogous single-debris RMI tests. However, there was no particular debris introduction sequence that resulted in increases in valve blockage compared with results for homogeneous mixtures. Further, in the tests where NUKON was introduced first in the debris sequence, the blockage was much less than for homogeneous mixtures. The highest estimated blockage-area fraction when NUKON was introduced first was 46%—in the same range as the NUKON single-

debris tests. Due to the high degree of variability observed it is difficult to identify trends in the data from these tests.

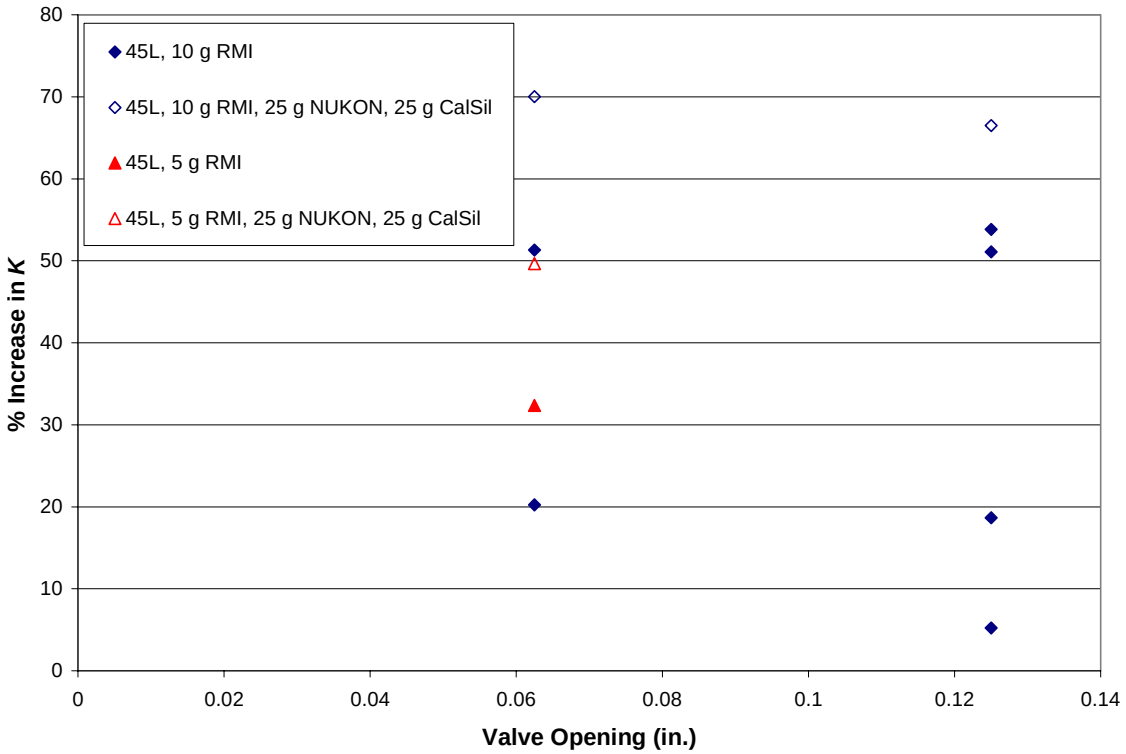

Figure 5-3. Comparison of RMI-NUKON-CalSil Mixed Debris to RMI Alone

Table 5-7. Results of Tests with Homogeneous RMI-NUKON-CalSil Mixtures

Test ID	Stem	Valve Opening [cm (in.)]	W1	RMI Size [cm × cm (in. × in.)]	WN	WC	*K*			W2	Wf	NR
							Before	After	Δ*K*%			
N-9_45L	45L	0.6350 (0.2500)	5.02	0.32 × 1.27 (1/8 × 1/2)	25.17	25.02	101	107	5	28.71	31.53	6
			5.03	0.63 × 0.63 (1/4 × 1/4)								9
D-9_45L	45L	0.159 (0.0626)	5.01	0.63 × 0.63 (1/4 × 1/4)	25.14	25.16	157	234	50	24.16	31.15	38
D-11_5L	5L	0.127 (0.0500)	5.01	0.32 × 0.32 (1/8 × 1/8)	25.06	25.12	170	307	81	44.26	15.93	74
			5.00	0.32 × 1.27 (1/8 × 1/2)								24
D-12_45L	45L	0.3175 (0.1250)	10.00	0.32 × 1.27 (1/8 × 1/2)	25.15	25.02	102	169	67	27.84	32.37	44
D-14_45L	45L	0.159 (0.0625)	10.02	0.32 × 1.27 (1/8 × 1/2)	25.14	25.00	152	259	70	28.15	32.01	58
D-15_5L	5L	0.127 (0.0500)	5.03	0.32 × 1.27 (1/8 × 1/2)	25.01	25.02	169	485	187	28.95	31.12	48
			5.01	0.63 × 0.63 (1/4 × 1/4)								70
D-15-2_5L	5L	0.127 (0.0500)	5.00	0.32 × 1.27 (1/8 × 1/2)	25.00	25.00	174	293	68	23.33	36.70	11
			5.03	0.63 × 0.63 (1/4 × 1/4)								16

Table 5-8. Results of Tests with Sequential Addition of RMI-NUKON-CalSil Mixtures

Test ID	Stem	Valve Opening [cm (in.)]	W1	RMI Size [cm × cm (in. × in.)]	WN	WC	Order of Debris Introduction	*K*			W2	Wf	NR
								Before	After	Δ*K*%			
D-10_45L	45L	0.159 (0.0626)	5.03	0.63 × 0.63 (1/4 × 1/4)	25.01	25.05	1. RMI 2. NUKON 3. CalSil	154	224	46	23.34	31.75	25
D-10-2_45L	45L	0.159 (0.0626)	5.05	0.63 × 0.63 (1/4 × 1/4)	25.22	25.54	1. NUKON 2. RMI 3. CalSil	153	165	8	20.81	35.00	13
D-12-2_45L	45L	0.159 (0.0626)	10.02	0.32 × 1.27 (1/8 × 1/2)	25.00	25.00	1. NUKON 2. RMI 3. CalSil	137	155	13	24.19	35.83	11

Table 5-9. Comparing RMI-NUKON-CalSil Mixture Test Data with Baseline 1- and 2-Component Debris Test Data

Data Set	Stem	Gap[1] [cm (in.)]	W1	RMI Size [cm × cm (in. × in.)]	WN[2]	WC[2]	Debris Type	Test ID	*K*			NR
									Before	After	Δ*K*%	
1	45L	0.6350 (0.2500)	5 5	0.32 × 1.27 (1/8 × 1/2) 0.63 × 0.63 (1/4 × 1/4)	25	25	RMI only	N-7_45L	104	120	15	11
							RMI + NUKON + CalSil	N-9_45L	101	107	5	15
2	45L	0.159 (0.0625)	5	0.63 × 0.63 (1/4 × 1/4)	25	25	RMI only	45LDT14	124	165	32	29
							NUKON only	D-17_45L	154	155	<5	-
							RMI + NUKON	D-7_45L	154	180	17	16
							RMI + CalSil	D-8_45L	152	239	57	42
							NUKON + CalSil	D-18_45L	154	154	<5	-
							Mixed together: RMI + NUKON + CalSil	D-9_45L	157	234	50	38
							Sequence: RMI, NUKON, CalSil	D-10_45L	154	224	46	25
							Sequence: NUKON, RMI, CalSil	D-10-2_45L	153	165	8	13
3	45L	0.3175 (0.1250)	10	0.32 × 1.27 (1/8 × 1/2)	25	25	RMI only	45LDT9	88.1	133	51	60
								45LDTR9	105	111	6	14
								D-1_45L	104	124	19	46
								D-1-2_45L	99.0	152	54	46
							NUKON only	45LN1	105	106	<5	-
							RMI + NUKON	D-4_45L	101	152	51	30
							RMI + NUKON + CalSil	D-12_45L	102	169	67	44
4	45L	0.159 (0.0625)	10	0.32 × 1.27 (1/8 × 1/2)	25	25	RMI only	45LDT18	127	192	51	53
								D-2_45L	166	200	20	65
							Mixed together: RMI + NUKON + CalSil	D-14_45L	152	259	70	58
							Sequence: NUKON, RMI, CalSil	D-12-2_45L	137	155	13	11

Note 1: Valve opening value cited is approximate. Tests in each set did not all have identical valve openings but varied over a small range, typically within 0.003 cm (0.001 in.)

Note 2: Mass cited is approximate. Tests in each set did not all have identical mass but varied over a small range, typically within 0.1 g.

Table 5-10. Estimates of Blockage-Area Fractions for RMI-NUKON-CalSil Mixtures

Test ID	Stem	Valve Opening [cm (in.)]	W1	RMI Size [cm × cm (in. × in.)]	WN	WC	Order of Introduction	*K*			Estimated Blockage-Area Fraction %
								Before	After	Δ*K*%	
D-9_45L	45L	0.159 (0.0626)	5.01	0.63 × 0.63 (1/4 × 1/4)	25.14	25.16	homogenized	157	234	50	19
D-11_5L	5L	0.127 (0.0500)	5.01	0.32 × 0.32 (1/8 × 1/8)	25.06	25.12	homogenized	170	307	81	27
			5.00	0.32 × 1.27 (1/8 × 1/2)							
D-14_45L	45L	0.159 (0.0625)	10.02	0.32 × 1.27 (1/8 × 1/2)	25.14	25.00	homogenized	152	259	70	25
D-15_5L	5L	0.127 (0.0500)	5.03	0.32 × 1.27 (1/8 × 1/2)	25.01	25.02	homogenized	169	485	187	46
			5.01	0.63 × 0.63 (1/4 × 1/4)							
D-15-2_5L	5L	0.127 (0.0500)	5.00	0.32 × 1.27 (1/8 × 1/2)	25.00	25.00	homogenized	174	293	68	25
			5.03	0.63 × 0.63 (1/4 × 1/4)							
D-10_45L	45L	0.159 (0.0626)	5.03	0.63 × 0.63 (1/4 × 1/4)	25.01	25.03	1. RMI 2. NUKON 3. CalSil	154	224	46	17
D-10-2_45L	45L	0.159 (0.0626)	5.05	0.63 × 0.63 (1/4 × 1/4)	25.22	25.54	1. NUKON 2. RMI 3. CalSil	153	165	8	<5
D-12-2_45L	45L	0.159 (0.0626)	10.02	0.32 × 1.27 (1/8 × 1/2)	25.00	25.00	1. NUKON 2. RMI 3. CalSil	137	155	13	<5

6 ACCUMULATION TESTS

All of the tests described until now involved the addition of debris either as a single batch or, in some tests, as a sequential addition over 5 min. An additional series of tests was performed to examine the potential for clogging of the valve as a result of sustained addition of debris over a period of 3 h. All tests in this category were done for the 45L configuration with a valve opening of 0.159 cm (0.0625 in.) and were taken using single-point sampling rather than five-point averaging, as discussed in Section 2.3.

Tests in this category introduced an additional complication that had to be addressed. As described in Section 2.2.3, the fluid temperature difference across the pump was between 1.1°C (2ºF) and 1.7°C (3ºF) for the range of flow rates of interest. Sustained operation of the loop over 3 h therefore resulted in significant temperature increases in the fluid. For the tests of interest, it was desirable to avoid such an upward drift in the temperature. Additionally, operation at the high temperatures required evaluation of the potential for pump cavitation. For these reasons, temperature control was necessary. Moderate temperature variations would not affect either pump operation or the valve performance results, so precise temperature control schemes, such as the use of a chiller, were deemed unnecessary. The temperature control option chosen for the tests was to drain a fraction of the system water periodically and replace it with colder water from the reservoir. Some of the debris that passed through the valve was drained, along with the water at each drain-and-replace step. The objective of these tests was to assess the potential for valve clogging as a result of a series of debris additions and not from recirculation of previously introduced debris. The fine-mesh screen installed upstream of the flow meter on the pump suction side was used to trap debris from recirculating back to the valve. Three accumulation tests were performed and are subsequently described.

6.1 Test A-1

In this test, 10 g of RMI, 0.32 cm × 1.27 cm (1/8 in. × 1/2 in.), was introduced into the flow at time = 0 (when data acquisition started). Then a mixture of 25 g of NUKON and 25 g of CalSil was added at time = 2 min and every 15 min thereafter, for a total test duration of ~3 h. This series of additions corresponded to 13 successive introductions of the NUKON-CalSil mixture, totaling 325 g each of NUKON and CalSil. The transient variation of the valve-loss-coefficient K is shown in Figure 6-1. The addition times of the NUKON-CalSil mixture are indicated by vertical dashed lines in the figure.

K increased from approximately 132 to 233 at the end of the 3-h test. Segments of the full transient are shown in Figure 6-2 and Figure 6-3. Figure 6-2 shows data for the first 10 min of the test. K increased ~21% from an initial value of 132 to 160 after the introduction of the RMI. The corresponding single-debris test (45LDT18) showed an increase of 51%. This difference is consistent with the range of variability of data that has been observed in other tests. K can be seen to spike briefly following the first introduction of the NUKON-CalSil mixture, presumably as a result of a plug of the mixture being slowed down in the valve throat, but K decreases to approximately 155 shortly thereafter, yet remains within the threshold of discernable K differences (~5%)

Figure 6-3 shows the data between t = 15 min and t = 50 min. A definite increase in *K* can be seen following the introduction of the second batch of the debris mixture. However, at about t = 28.3 min, *K* decreases sharply to the values seen before the introduction of the debris mixture. A similar pattern can be seen following the introduction of the third batch of the debris mixture. Evidently, plugs of the debris mixture were trapped in the valve throat for short periods of time and then were dislodged. Not all debris additions showed this behavior. Additions 6, 7, 10, and 11 do not show any increase in *K* while debris insertions 5, 8, and 12 result in *K* increases that do not erode over the course of the test. Overall, the valve-loss-coefficient *K* increases gradually over time as more debris progressively reaches the valve.

Temperature data were taken at 5-min intervals to verify that the drain-and-replace method was controlling the temperature adequately. The data are shown in Figure 6-4. The upstream and downstream temperatures were within 1.8°C (3.3ºF) for the duration of the test, which was more than adequate temperature control for these tests.

6.2 Test A-2

All test conditions for test A-2 were identical to those for A-1, except for reducing the quantity of the NUKON-CalSil mixture added in the batch. The 10 g of RMI, 0.32 cm × 1.27 cm (1/8 in. × 1/2 in.), was introduced into the flow at time = 0 (when data acquisition started). Then a mixture of 13 g of NUKON and 12 g of CalSil was added at time = 2 min and every 15 min thereafter, for a total test duration of ~3 h. This series of additions corresponded to 13 successive introductions of the NUKON-CalSil mixture, totaling 169 g of NUKON and 156 g of CalSil. The transient variation of *K* is shown in Figure 6-5. The times of addition of the NUKON-CalSil mixture are indicated by vertical dashed lines in the figure.

Figure 6-6 shows the data for the first 10 min of the test. The loss coefficient increased from 130 to 260 following RMI addition but then decreased to about 160 within one minute. This initial increase is very similar to the increase from the RMI debris in Test A-1. The loss coefficient decreased further following the addition of the first batch of debris mixture. As seen in Figure 6-5, subsequent additions resulted in only small increases in the loss coefficient. The highest value was not more than approximately 160.

This test was continued for ~1 h following the addition of the last batch of the NUKON-CalSil mixture to investigate whether any existing debris in the valve might be eroded by the flow. The data showed no evidence of erosion during this time period.

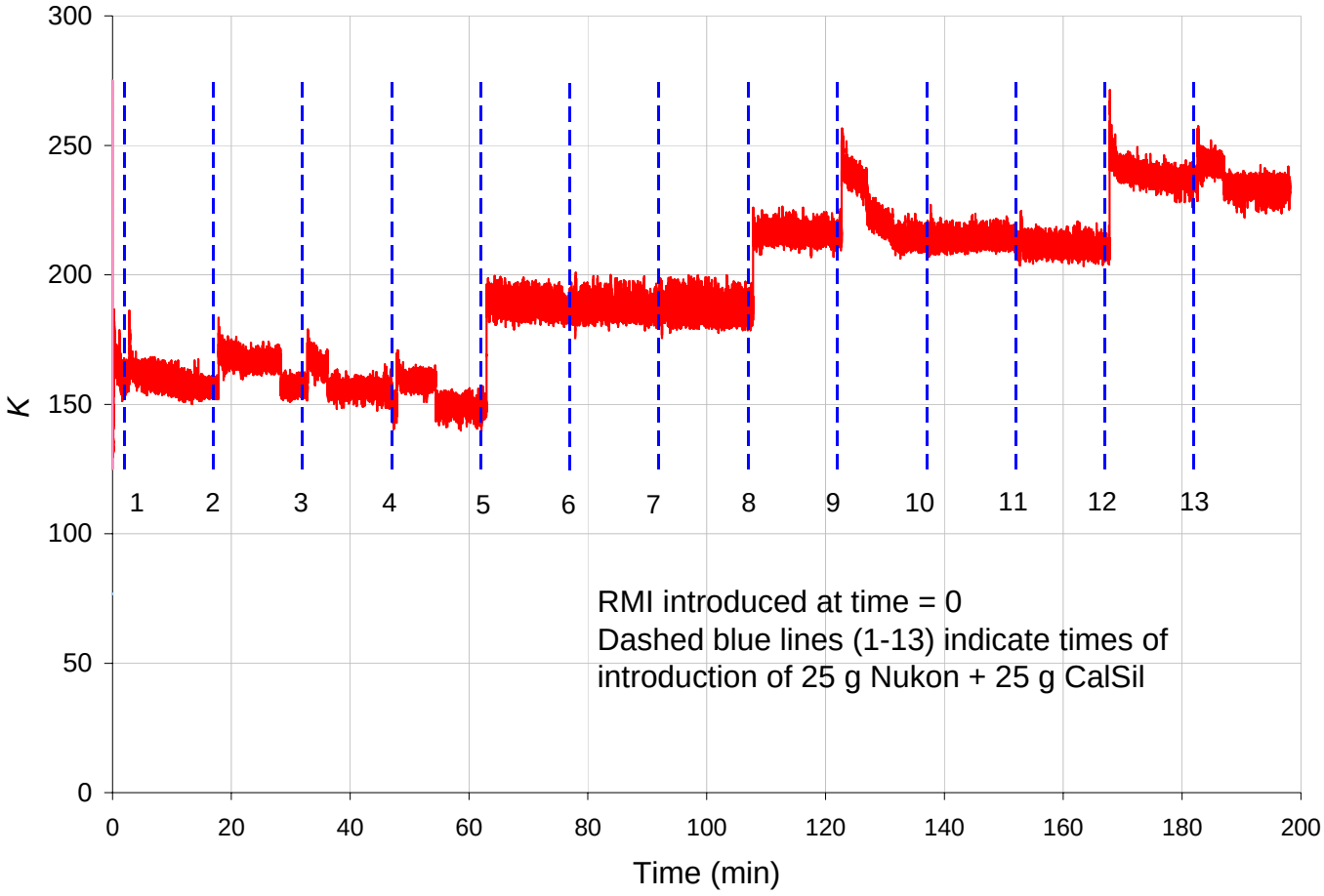

Figure 6-1. Transient Variation of *K* for Debris Accumulation Test A-1

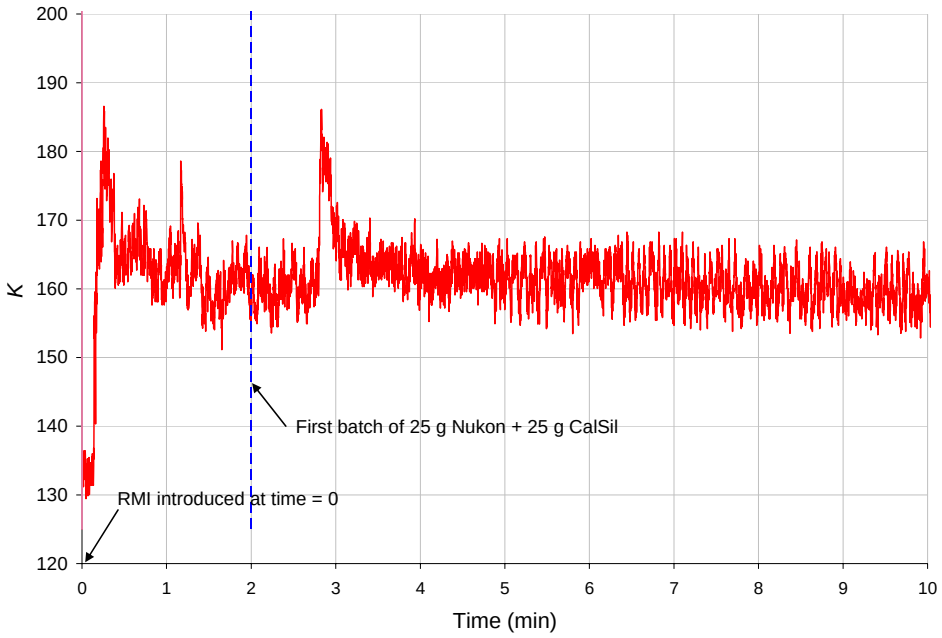

Figure 6-2. Transient Data for RMI Addition, Followed by First Addition of NUKON-CalSil

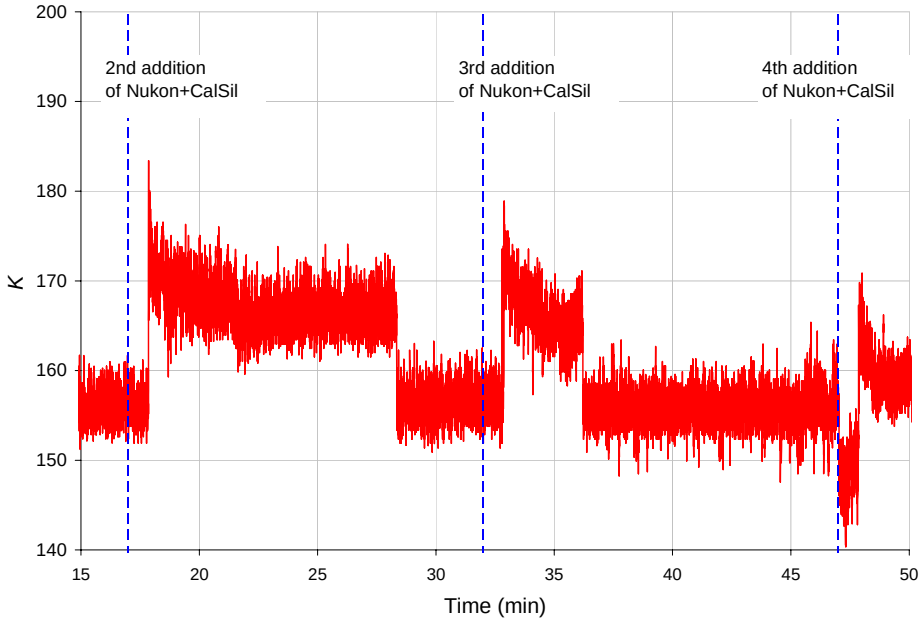

Figure 6-3. Transient Data for Three Additions of NUKON-CalSil Mixture

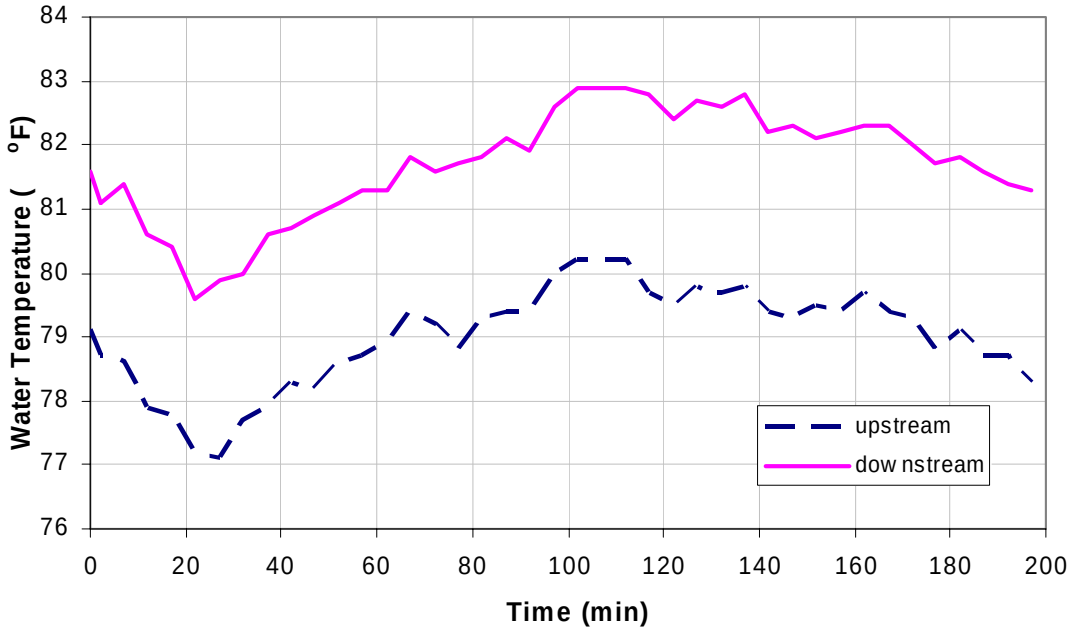

Figure 6-4. Temperature Data for Test A-1

6.3 Test A-3

In Test A-3, 10 g of RMI, 0.32 cm × 1.27 cm (1/8 in. × 1/2 in.), was introduced into the flow at time = 0 (when data acquisition started). Then a mixture of 25 g of NUKON and 25 g of CalSil was added at time = 3 min. Then 25 g of CalSil was added at time 17 min and every 15 min thereafter, for a total test duration of ~3 h. This series of additions corresponded to a total addition of 325 g of CalSil. The transient variation of K is shown in Figure 6-8. The times of addition of the debris are indicated by vertical dashed lines in the figure.

Figure 6-9 shows the data for the first 20 min of the test. In contrast to Tests A-1 and A-2, the loss coefficient shows no appreciable change after the RMI addition but increases from 138 to 260 following the addition of the NUKON-CalSil mixture. As seen from Figure 6-8, some additions of CalSil result in increases in the loss coefficient, whereas some do not. Overall, the highest average loss coefficient during the test was about 310. The data indicate the potential for buildup of CalSil over NUKON that was previously trapped in the valve. Single-debris tests with CalSil showed no appreciable buildup, but this test indicates that the presence of NUKON in the valve may cause some trapping of CalSil in the valve.

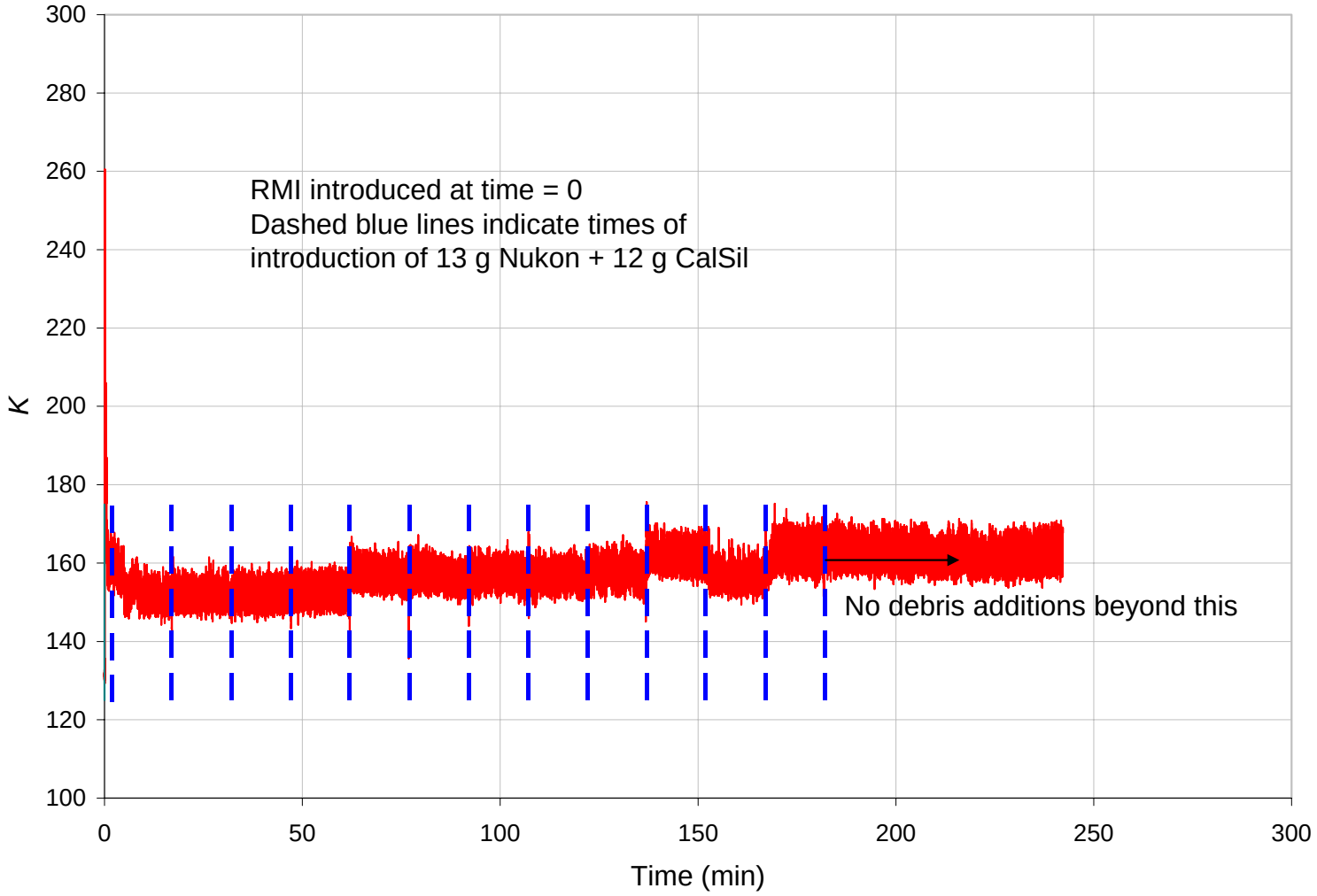

Figure 6-5. Transient Data for Test A-2

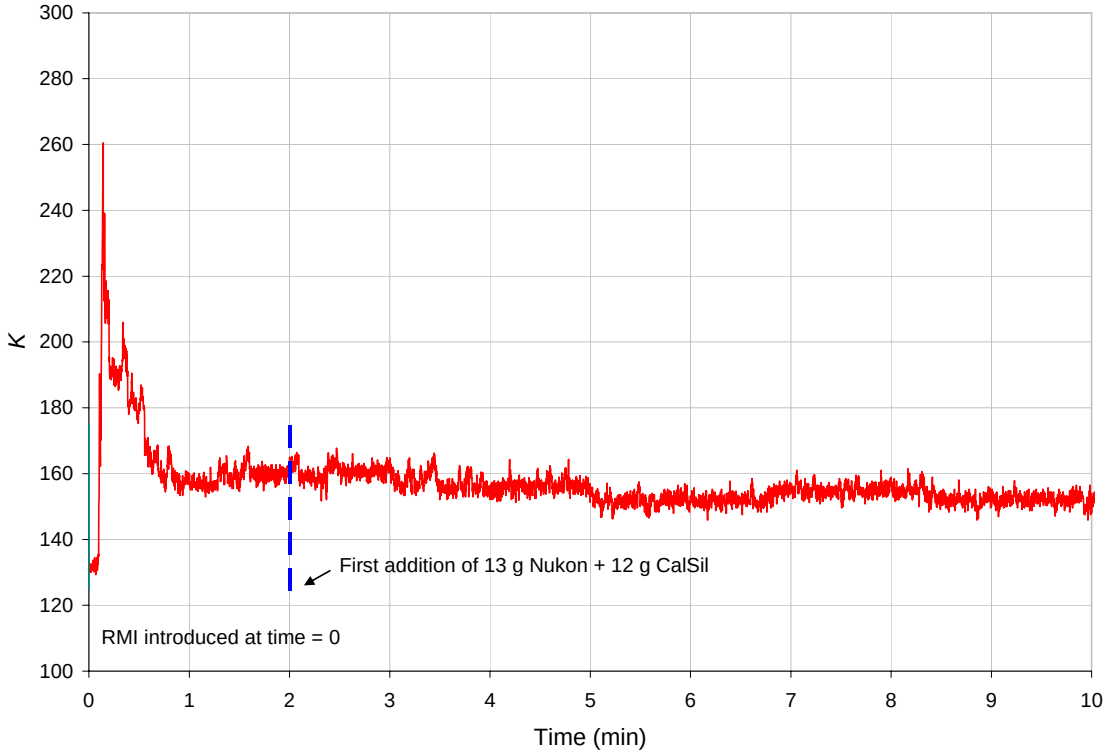

Figure 6-6. Early Transient Data for Test A-2

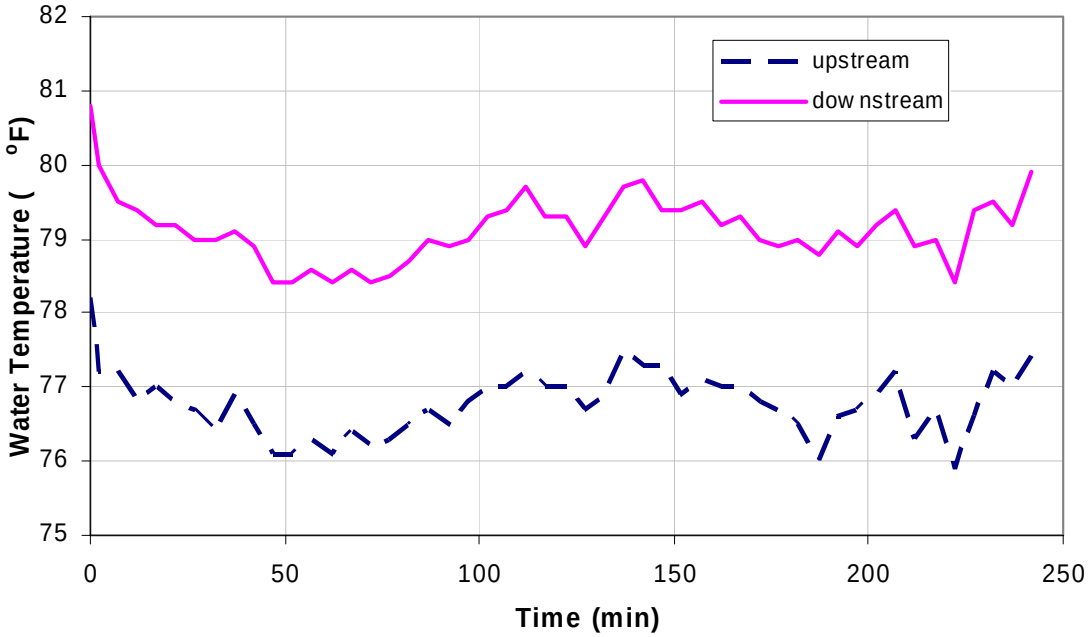

Figure 6-7. Temperature Data for Test A-2

As with Test A-2, Test A-3 was continued for ~1 h following the addition of the last batch of CalSil to investigate whether any existing debris in the valve might be eroded by the flow. In this case, appreciable erosion did occur, resulting in a decrease of the loss coefficient to approximately 235, below the *K* value after the initial NUKON-CalSil batch.

6.4 Discussion

The objective of the accumulation tests described in this section was to investigate the potential for cumulative increase in valve clogging as a result of a sustained stream or debris batches reaching the valve. Tests were done for three types of debris types; in each case, 10 g of RMI was added at the outset of testing to attempt to initiate blockage; then different combinations of NUKON and CalSil debris were introduced at 15-min intervals, for a total duration of 3 h.

The test with batches of 25 g each of NUKON and CalSil showed a sustained increase in *K* over time as more and more debris reached the valve. However, consistent with the randomness described in previous sections, the increase in *K* was not observed following all additions of debris—some debris additions did not result in any increase in *K*, suggesting no net increase in valve blockage at that step.

The test with smaller quantities of NUKON and CalSil introduced at each step (13 g each) showed a similar random behavior, except that the net increase over time was smaller than with the 25 g additions. This observation was consistent with single-debris results, which indicated relatively small blockage effects for lower debris loadings.

Tests with periodic additions of CalSil alone also showed similar behavior—some debris addition events triggered increases in *K*, whereas others did not. Relative to single-debris CalSil tests, larger *K* increases were observed for some debris addition events, suggesting some potential for CalSil to be trapped in the valve by NUKON or RMI that may already be present there. When the test was continued for 1 h following the final addition of debris, *K* decreased precipitously at one point, suggesting erosion of the previously trapped CalSil debris.

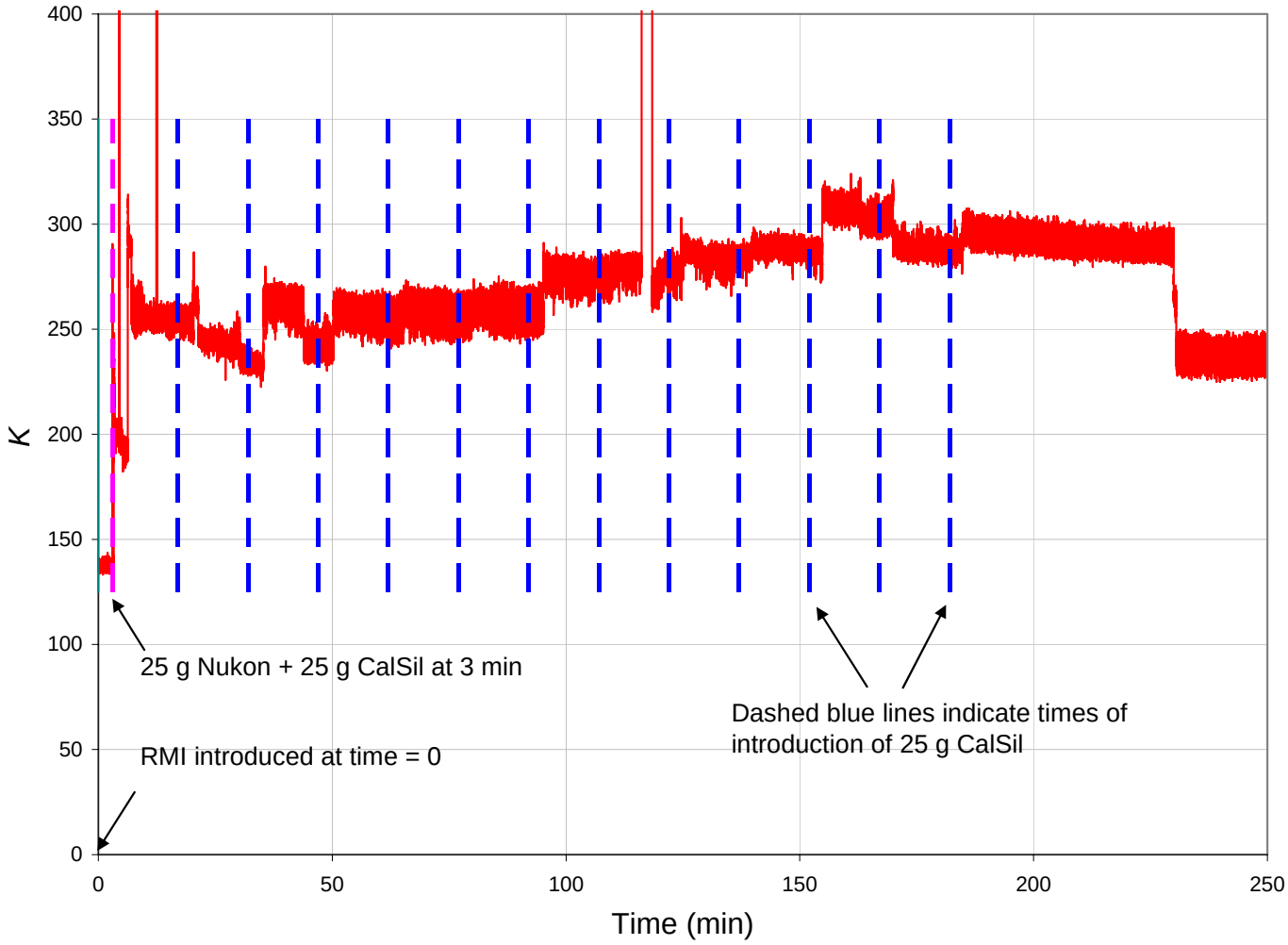

Figure 6-8. Transient Data for Test A-3

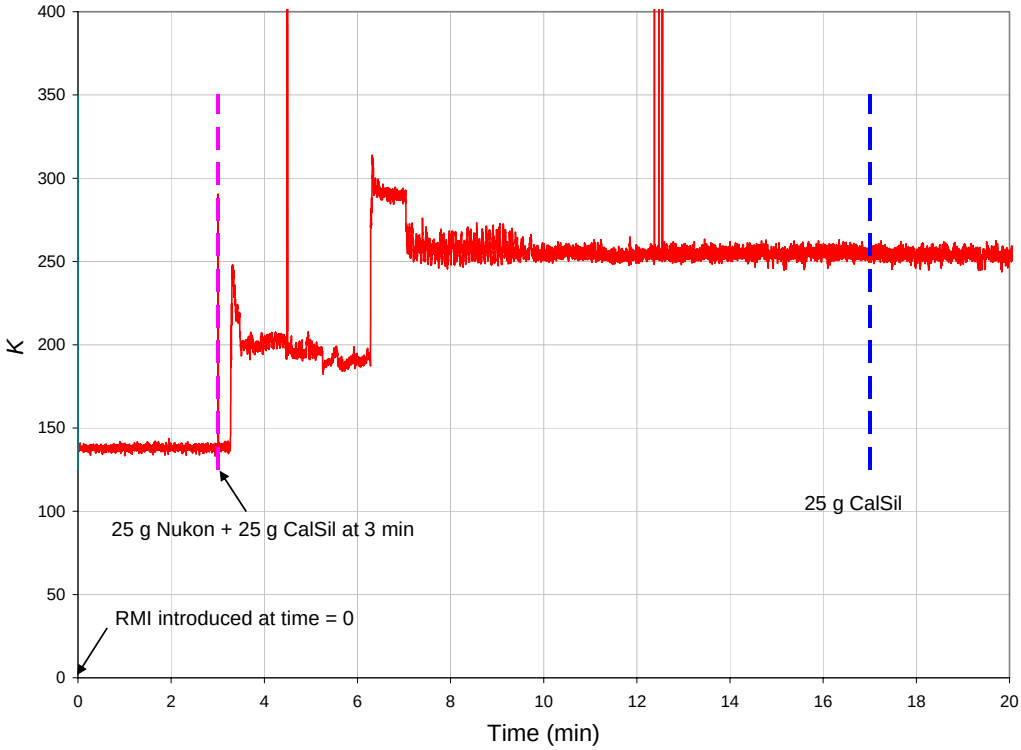

Figure 6-9. Early Stage of Test A-3

7 CONCLUSIONS

A series of tests was performed using the UNM Civil Engineering test facilities to investigate the effects of insulation debris streams composed of RMI, NUKON, and CalSil on PWR HPSI throttle valves. The current tests addressed the downstream effects of debris types and sizes that may penetrate sump screens. The test data provided information on the potential clogging of the throttle valves by unmixed debris and by combinations of debris types.

Baseline tests were performed at the outset of the test program to determine the valve-loss coefficient, *K*, for the valve stem configurations for different valve openings and flow rates. Limited tests also were performed with simulated blockage conditions using shims to correlate increases in the valve loss coefficient with the blocked area and determine the blockage detection threshold of the system. The data indicated that blockages on the order of ~5%–8% should be detectable.

Data from tests with single batches of unmixed debris showed that, in general, higher RMI debris loadings and larger debris sizes (relative to the throttle valve opening) resulted in higher observed increases in *K*. In single-debris RMI tests, the highest observed increase in *K* was ~50% (corresponding to a blocked area fraction of ~20%) for RMI pieces of 0.63 cm × 0.63 cm (1/4 in. × 1/4 in.) and a valve opening of 0.159 cm (0.0625 in.). For RMI pieces smaller than 0.63 cm × 0.63 cm (1/4 in. × 1/4 in.), valve blockage appeared to be minimal for the valve clearances studied here.

Based on the results of the screen penetration tests (Ref. 3), 0.63-cm × 0.63-cm (1/4-in. × 1/4-in.) RMI pieces typically were less likely to penetrate screens with screen openings of 0.63 cm (1/4 in.)—the data showed that <20% of the RMI pieces of this size penetrated the 0.63-cm (1/4-in.) screen for the highest flow velocities tested, as described in Ref. 3 (20% may be significant, depending on the total mass of debris loading). A similar result was seen for 0.32-cm (1/8-in.) RMI pieces impinging on a 0.32-cm (1/8-in.) screen. When the RMI debris had dimensions smaller than the screen size, a larger fraction of RMI penetrated the screen; however, the current results show that the smaller-size RMI debris was able to clear the throttle valve as well—at least for the range of valve openings tested. The results for RMI debris alone (without any other debris) indicated that the smaller debris, which was more likely to pass through the sump screen, was also less likely to get caught in the valve.

The screen penetration tests showed that a significant fraction of CalSil passed through the screen, regardless of the screen opening. The current results show that the same occurred in the valve, as well—when CalSil was the only debris present, practically all of the CalSil passed through the valve without causing appreciable blockage.

As much as 80% of blender-processed NUKON debris was found to penetrate the screen, as described in Ref. 3. The current results show that NUKON can cause significant clogging in the valve, depending on the combination of stem geometry, gap spacing, and NUKON loading used. The increase in *K* was pronounced in tests with valve gaps of 0.13 and 0.16 cm (0.05 and 0.063 in.) for NUKON loadings of 50–100 g in the 45L and 5L

configurations. Larger gaps [0.16 cm (0.063 in.)] or smaller NUKON loadings (25 g) did not result in significant clogging. The 5S stem showed essentially no increase in *K* for any quantity of NUKON introduced. The 5L and 45L stems showed substantial increases in *K*, with the 45L stem being somewhat higher than the 5L stem for roughly comparable gap sizes.

The highest *K* increase observed (220%) occurred when the valve encountered a stream of NUKON. This increase translated to ~45% blockage in the valve-opening flow area. A large fraction of blender-processed NUKON was able to penetrate the screen, and a large fraction of this NUKON, in turn, could get trapped in the valve, resulting in significant increases in valve pressure loss. These results indicate that NUKON is more likely than RMI or CalSil to cause throttle valve blockage when each debris type is tested separately.

Tests using CalSil-RMI mixtures were the only combinations that exhibited clear increases in *K* when compared with results from analogous single-debris CalSil and RMI tests. The results of tests performed using NUKON-RMI or CalSil-NUKON mixtures did not differ significantly from results for analogous separate tests for each debris component, with one possible exception. One mixture test performed using unsieved CalSil with NUKON showed an appreciable increase in valve blockage compared with single-debris NUKON tests. However, it is unclear if this result is attributed to clumping within the unsieved CalSil or to retention by NUKON fibers within the valve.

The three-component mixture tests were divided into two types of tests: (1) homogeneous mixtures of RMI, CalSil, and NUKON; and (2) sequential additions of each debris type using different ordering. Tests using homogeneous mixtures of RMI, CalSil, and NUKON showed an increase in valve blockage when compared with analogous single-debris RMI tests. However, no particular debris introduction sequence resulted in increases in valve blockage compared with results for homogeneous mixtures. Further, in the tests where NUKON was introduced first in the debris sequence, the blockage was much less than for homogeneous mixtures.

Three accumulation tests were performed to investigate the potential for a cumulative increase in valve clogging as a result of multiple debris batches reaching the valve sequentially. Tests were done for three types of debris types and loadings using the 45L configuration with a valve gap of 0.159 cm (0.0625 in); in each case, 10 g of 0.32 cm × 1.27 cm (1/8 in. × 1/2 in.) RMI was added at the outset of testing in an attempt to initiate blockage. Then different combinations of debris were introduced at 15-min intervals, for a total duration of 3 h.

Test A-1, with batches of 25 g each of NUKON and CalSil, showed a sustained increase in *K* over time as more and more debris reached the valve. However, consistent with the randomness observed in other tests, the increase in *K* was not observed following all additions of debris. Some debris additions did not result in any increase in *K*, suggesting no net increase in valve blockage at that step.

Test A-2, with batches of 13 g each of NUKON and CalSil, showed a similar random behavior to Test A-1, except that the net increase over time was smaller. This observation

was consistent with single-debris results, which indicated smaller blockage effects for lower debris loadings.

Test A-3, the accumulation test with periodic additions of CalSil alone, also showed similar behavior. Some debris addition events triggered increases in *K*, whereas others did not. Larger *K* increases were observed for some debris addition events compared with single-debris CalSil tests, suggesting that CalSil may have been trapped by NUKON or RMI that was already present in the valve. However, when the test was continued for 1 h following the final addition of debris, *K* decreased precipitously at one point, suggesting erosion of the previously trapped debris.

The results for replicated single-debris, multiple-debris, and accumulation tests exhibit significant test-to-test variability. This variability was consistent with the inherent randomness involved in the process; the propensity for trapping of debris in the valve gap is a function of the random orientation of the individual pieces as they enter the valve gap. Further, the bending or thrashing of the debris pieces inside the valve also is a random process.

This page intentionally left blank.

8 REFERENCES

1. C. J. Shafer, M. T. Leonard, B. C. Letellier, D. V. Rao, A. K. Maji, K. Howe, A. Ghosh, J. Garcia, W. A. Roesch, and J. D. Madrid, "GSI-191: Experimental Studies of Loss-of-Coolant-Accident-Generated Debris Accumulation and Head Loss with Emphasis on the Effects of Calcium Silicate Insulation," United States Nuclear Regulatory Commission report NUREG/CR-6874 (May 2005), Los Alamos National Laboratory report LA-UR-04-1227 (April 2004).

2. D. V. Rao, B. Letellier, C. Shaffer, S. Ashbaugh, and L. Bartlein, "GSI-191: Parametric Evaluations for Pressurized Water Reactor Recirculation Sump Performance," United States Nuclear Regulatory Commission report NUREG/CR-6762 (August 2002), Los Alamos National Laboratory report LA-UR-01-4083 (August 2001).

3. C. B. Dale, B. C. Letellier, A. K. Maji, K. Howe, and F. Carles, "Screen Penetration Test Report," United States Nuclear Regulatory Commission report NUREG/CR-6885 (October 2005), Los Alamos National Laboratory report LA-UR-04-5416 (initial draft November 2004).

4. ARES Corporation drawing No. 0391511.17-1-001, Revision A.

5. Nuclear Energy Institute, "Condition Assessment Guidelines: Debris Sources inside PWR Containment," Nuclear Energy Institute report NEI 02-01, Revision 1 (September 2002).

6. B. R. Munson, D. F. Young, and T. H. Okiishi, *Fundamentals of Fluid Mechanics,* 4th ed. (John Wiley & Sons, Hoboken, New Jersey, November 2001).

7. *Flow of Fluids through Valves, Fittings, and Pipe* (CRANE Company Engineering Department, King of Prussia, Pennsylvania, Crane Co., 1988).

This page intentionally left blank.

APPENDIX A: TEST PROCEDURE

The procedures used to perform the various types of tests discussed in Sections 3 through 6 are outlined in this appendix. Figure A-1 shows the valve identification numbers referred to in the procedures.

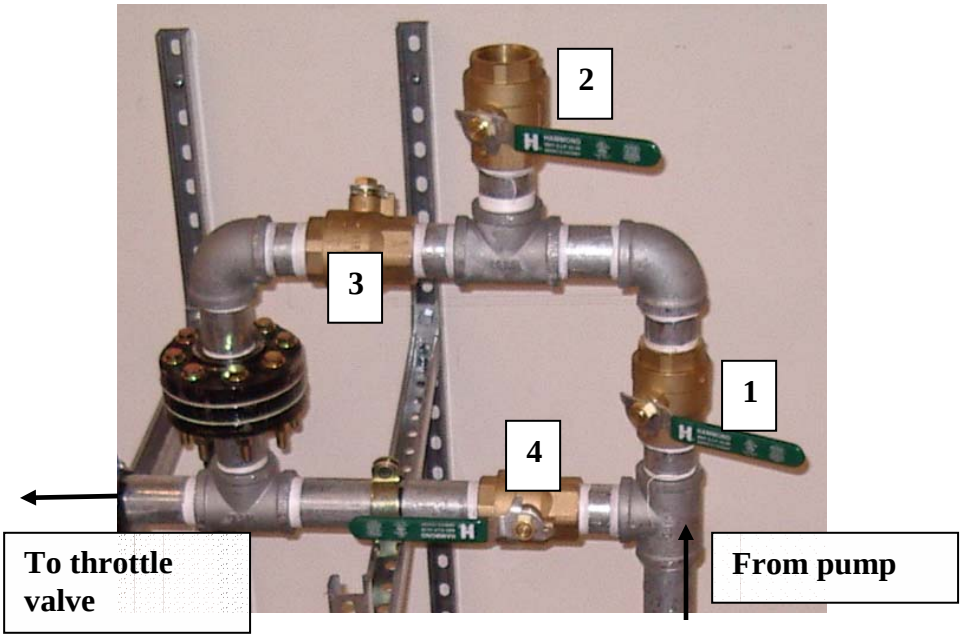

Figure A-1. Valve Identification Numbers Used in the Procedures

Following each test, the throttle valve was opened and the debris trapped in the valve was recovered (see definition of variable NR in Section 2.6). Typically, the debris pieces were recovered from the bottom of the valve body. Debris found in the valve body following an RMI test is shown in Figure A-2, and that following a NUKON test is shown in Figure A-3. It is difficult to estimate how much of this debris actually was trapped in the valve throat during the test and how much was trapped elsewhere in the valve. The recovered debris was oven-dried, and the weight was recorded.

Figure A-2. Debris Found in the Valve Body Following an RMI Single-Debris Test

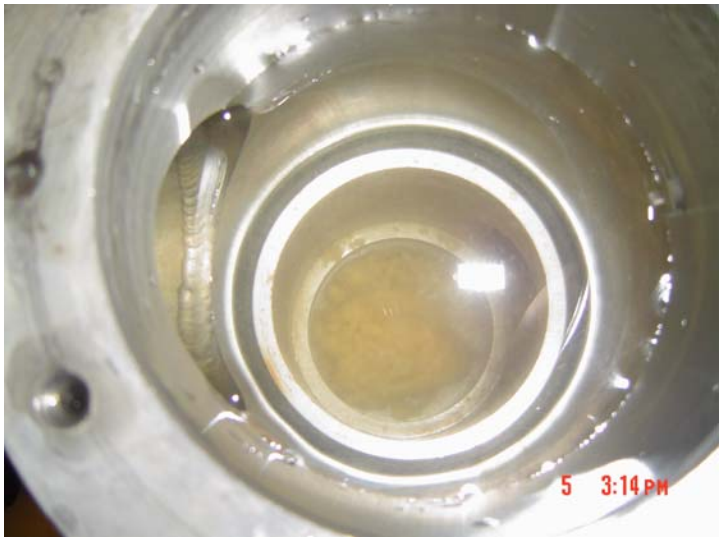

Figure A-3. Debris Found in Valve Body Following a NUKON Single-Debris Test

A.1 Baseline Tests

1. Close gate valve at drain, close debris insertion port (valve 2 in Figure A-1), and open all other valves in debris insertion manifold (valves 1, 3, and 4 in Figure A-1). Open globe valves downstream of throttle valve.
2. Fill flume with water up to 22 in.
3. Relieve air from the system by opening and closing air relief valve.
4. Use desired stem.
5. Set desired opening of the throttle valve.
6. Set up computer station (via data logger).
7. Turn system on and wait ~1 min until steady flow is read on the flow meter.
8. Run desired test for ~3 min.
    a. Read temperatures from thermocouples upstream and downstream of the pump.
    b. Verify that pressure gauges and pressure transducers are reading approximately the same values.
    c. Verify that the flow meter is reading approximately the same value as the data logger.
9. Turn off the system.
10. Repeat steps 4 through 9 for different flows and openings for the same stem.
11. Repeat steps 1 through 10 for different stems (45L, 5L and 5S).

A.2 Shim Blockage Tests

1. Close gate valve at drain, close debris insertion port (valve 2 in Figure A-1), and open all other valves in debris insertion manifold (valves 1, 3, and 4 in Figure A-1). Open globe valves downstream of throttle valve.
2. Fill flume with water up to 22 in.
3. Relieve air from the system by opening and closing air relief valve.
4. Use desired stem.
5. Set desired opening of the throttle valve.
6. Set up shim.
7. Attach shim to the ring using a thin layer of epoxy.
8. Attach shim to the ring, rather than to the stem, to minimize machining required in case of damage during attachment and detachment of the shim.
9. Clean surface with acetone and soft lens-cleaning tissue after removal of the shim.
10. If the epoxy cannot be removed, leaving a smooth ring surface, machine and rebaseline a new ring before proceeding to debris testing.
11. Set up computer station (via data logger).
12. Turn system on and wait ~1 min until steady flow is read on the flow meter.
13. Run desired test for ~3 min.
    a. Read temperatures from thermocouples upstream and downstream of the pump.
    b. Verify that pressure gauges and pressure transducers are reading approximately the same values.

c. Verify that the flow meter is reading approximately the same value as the data logger.

14. Turn off the system.
15. Repeat steps 6 through 10 for different flows and percent blockage for the same stem.

A.3 Tests with One Batch of Single Debris or Mixed Debris

1. Close gate valve at drain, close debris insertion port (valve 2 in Figure A-1), and open all other valves in debris insertion manifold (valves 1, 3, and 4 in Figure A-1). Open globe valves downstream of throttle valve.
2. Fill flume with water up to 22 in.
3. Relieve air from the system by opening and closing air relief valve.
4. Use desired stem (45^o large stem in this case).
5. Set opening of the throttle valve.
6. Set up computer station (via data logger).
7. Turn system on and wait ~1 min until steady flow is read on the flow meter.
8. Run desired test for ~6-10 min.
    a. Read temperatures from thermocouples upstream and downstream of the pump.
    b. Verify that pressure gauges and pressure transducers are reading approximately the same values.
    c. Verify that the flow meter is reading approximately the same value as the data logger.
9. Close valves 1 and 3 (Figure A-1). Open valve 2, and insert the debris.
10. Close valve 2. Open valves 1 and 3 (Figure A-1).
11. Turn off the system, and collect debris from the discharge bucket screens.
12. Repeat steps 8 through 10 for different flows and debris types for the same stem.

A.4 Accumulation Tests

1. Close gate valve at drain, close debris insertion port (valve 2 in Figure A-1), and open all other valves in debris insertion manifold (valves 1, 3, and 4 in Figure A-1). Open globe valves downstream of throttle valve.
2. Fill flume with water up to 22 in.
3. Relieve air from the system by opening and closing air relief valve.
4. Use desired stem (45^o large stem in this case).
5. Set opening of the throttle valve.
6. Set up computer station (via data logger).
7. Continuously drain water from the flume at a rate of 0.946-1.26 l/s (15-20 gpm).
8. Run the pump to fill the flume as needed so that a minimum depth of 21 in. and a maximum depth of 24 in. are maintained. (The purpose of steps 7 and 8 are to regulate temperature.)
9. Verify that the temperature in the system has reached a near steady-state condition. The water exiting the throttle valve is ~10°C hotter than the water

entering the flume at steady state. The exact difference will depend on the drain rate, temperature of the inflow water, pumping rate, and air temperature.

10. Wait until steady flow is read on the flow meter and steady temperature is measured by the thermocouples.
11. Run desired test for ~180-240 min.
    a. Read temperatures from thermocouples upstream and downstream of the pump every 5 min.
    b. Verify that pressure gauges and pressure transducers are reading approximately the same values.
    c. Verify that the flow meter is reading approximately the same value as the data logger.
12. Close valves 1 and 3. Open valve 2 and insert the debris (Figure A-1). (Trigger data acquisition coincident with the initial insertion of RMI debris.)
13. Close valve 2. Open valves 1 and 3 (Figure A-1).
14. Repeat steps 8-13 for each debris type with the pump continuously in operation. Periodically collect debris from the discharge bucket screens.
15. Continue to monitor the flow, pressure, and temperature for 10-60 min after the last debris insertion, depending on the test specification.
16. Turn off the system and collect debris from the discharge bucket screens.

This page intentionally left blank.

APPENDIX B: CALIBRATION

B.1. Flow-Meter Calibration

The upstream flow meter was calibrated simply by allowing a measured quantity of water to flow from a uniform tank while measuring the elapsed time using a stop watch. Starting at an initial depth of ~101.6 cm (40 in.) in a 275-gal. cylindrical tank, the water level in the tank was allowed to drop by roughly half of the initial depth over a period of ~2 min. The flow rate was calculated based on the measured change in water level in the tank over the measured time period. The depth in the tank was measured to the nearest 0.158 cm (1/16 in.), and the time was measured to the nearest 0.01 s. The tank had a diameter of 1.07 m (42 in.), which resulted in a cross-sectional area of 0.894 m^2 (1385.4 $in.^2$). The calculated values were compared with the corresponding flow-meter readings in Figure B-1. All results show <1% difference.

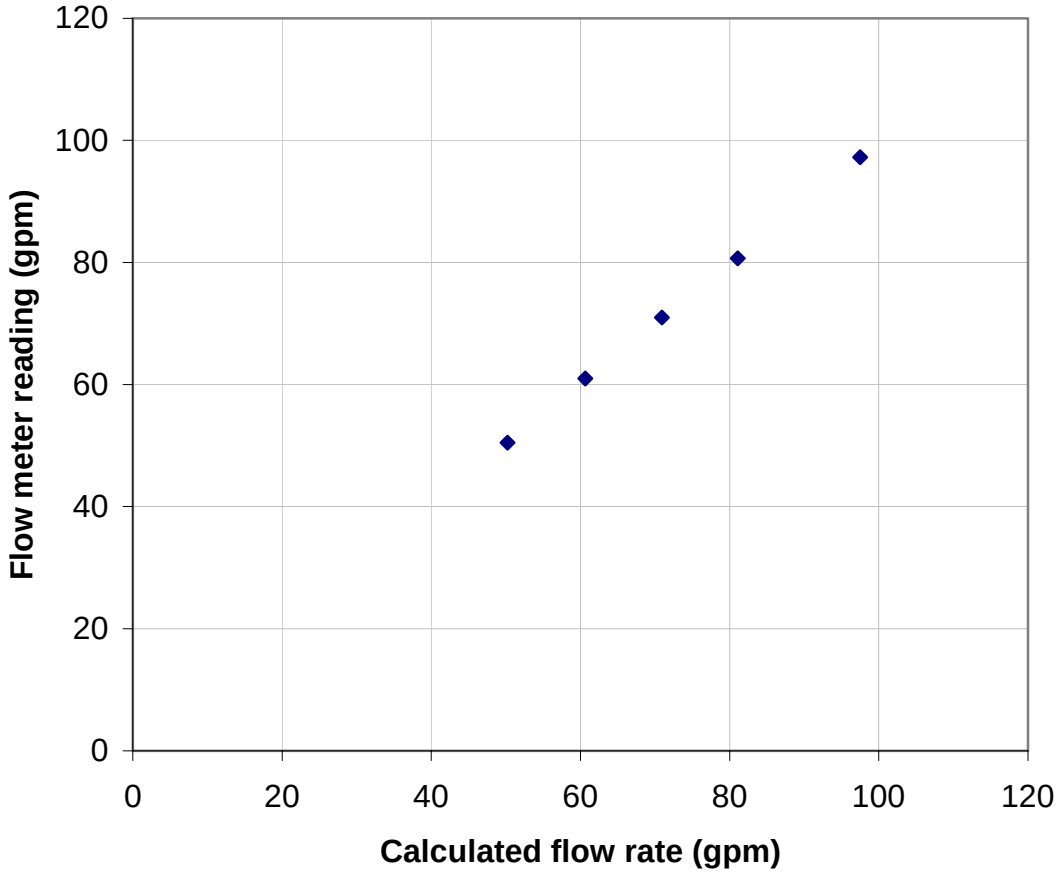

Figure B-1. Measured Flow vs Flow-Meter Reading

B.2 Pressure Device Calibration

The upstream and downstream pressure transducers and accompanying pressure gauges were calibrated by an external vendor.* The calibration test determined that both pressure transducers had accuracies consistent with the advertised values—within ±0.13% of the full range of the transducers [±0.0013 × 3.45 MPa = 4.48 kPa (±0.0013 × 500 psi = 0.65 psi)].

B.3. Temperature Device Calibration

Two thermocouples were used to measure the temperature during testing. To establish the accuracy of the thermocouples, two different calibrations were performed (see Table B-1). The first calibration was performed by measuring the water temperature in a container. The thermocouples were compared against an American Society for Testing and Materials (ASTM) mercury thermometer. All of the results showed <1% difference between thermocouples and the reference thermometer.

Table B-1. Waterbath Thermocouple Calibration

Thermocouple Upstream [°C (°F)]	Thermocouple Downstream [°C (°F)]	Reference Thermometer [°C (°F)]	Percent Difference Upstream	Percent Difference Downstream
0.8 (33.4)	0.8 (33.4)	0.8 (33.4)	0	0
0.8 (33.4)	0.8 (33.4)	0.8 (33.4)	0	0
17.6 (63.7)	17.7 (63.9)	17.7 (63.9)	0.56	0
17.6 (63.7)	17.6 (63.7)	17.7 (63.9)	0.56	0.56
95.9 (204.6)	96 (204.8)	95.9 (204.6)	0	0.10
96 (204.8)	96 (204.8)	95.9 (204.6)	0.10	0.10

The second calibration was performed directly in the system. The linear hydraulic flume and pipe system were filled with water. An ASTM mercury thermometer was placed in the middle of the flume used in this calibration. The calibration was performed with no water flowing in the system. After 17 min, the temperature difference between the thermometer reading and the each of the thermocouples was <0.5°C. Table B-2 shows the results of this calibration.

* Instrument Service Laboratories, 680 Haines Avenue Northwest, Albuquerque, NM 87102.

Table B-2. In-Situ Thermocouple Calibration

Thermocouple 1 T_U [°C (°F)]	Thermocouple 2 T_D [°C (°F)]	Thermometer [°C (°F)]	Percent Difference 1	Percent Difference 2	Time (h)
15.2 (59.4)	15.5 (59.9)	15.9 (60.6)	4.40	2.52	8:57
15.3 (59.5)	15.5 (59.9)	15.8 (60.4)	3.16	1.90	9:02
15.4 (59.7)	15.6 (60.1)	15.8 (60.4)	2.53	1.27	9:07
15.5 (59.9)	15.7 (60.3)	15.9 (60.6)	2.52	1.26	9:14

This page intentionally left blank.

APPENDIX C: STEPS TAKEN TO MINIMIZE DATA FLUCTUATIONS

C.1 Background

After completion of some of the early tests, it was observed that the recorded pressure readings had fluctuations that were considerably larger than could be attributed to the inherent measurement uncertainty of the pressure transducers. The measurements were fluctuating at ±13.79 kPa (±2 psi) from a general trend line. The recorded flow rates varied by ±0.0126 l/s (±0.2 gpm) from the general trend line at a flow of 4.73 l/s (75 gpm). A concern was raised that the level of data fluctuation could obscure important physical conditions that needed to be measured with the throttle valve tests. Numerous diagnostic studies were done to address this issue.

C.2 Frequency Analyses

The raw data from the pressure and flow meters were analyzed using Fast Fourier Transforms to determine if the fluctuations had a dominant frequency. The original data were acquired at 100-ms intervals (at 10 Hz); therefore, based on the Nyquist criterion, the data would not be useful to extract frequencies >5 Hz. To examine whether there was an effect due to the alternating current frequency, additional diagnostic tests were performed (without debris additions) and data were recorded at frequencies >120 Hz. The results of these tests showed that the fluctuations in the data were random.

C.3 Mechanical Effects

The unstable measurements could have been caused by mechanical vibration and resonance caused by the structural configuration of the apparatus. Testing was performed while hammering on pipes and fittings to see if mechanical vibration would affect the characteristics of the fluctuations. No differences were found. Concrete block weights were hung from the pipes to see if the system mass would change the measurement variability. Again, no measurable differences were found.

C.4 Electrical Effects

Because mechanical system modifications were unlikely to provide improvements to the measurements, the electrical system was a major focus of further evaluation. The electrical system evaluations are summarized as follows.

The entire electrical system was inspected for loose wires, and all mechanical connections were checked. No loose connections were found, and retightening the connections did not change the measurement variability. It was noted that all gauge wiring in the system used shielded wires; thus, the type of wire used was considered appropriate for this application.

The power supply to the National Instruments Field Point Network Module (Model FP-1601) was a separate unit provided by National Instruments. An alternate laboratory-grade power supply was substituted temporarily; however, this alternate unit provided less-stable results. The power supply provided by National Instruments for the FP-1601 was used with all testing.

The original wiring for the pressure transducers did not include a connection to the ground terminal that was available with the instrument. The grounding for the instrumentation power supplies and the National Instruments Field Point power supply used the grounding of a standard three-prong electrical plug. The shield wire for the electrical cable to the instruments was not grounded. To modify this condition, a new main ground-wire cable was extended from an existing building ground connection. A ground wire was run to each of the pressure transducers. The shield wire for each of the instrument electrical cables was connected to the building ground wire. The ground port to each of the instrument power supplies was connected to the building ground wire. Grounding the instruments produced a substantial improvement in the measurement fluctuations, with the amplitude reduced to nearly half of the fluctuations in tests performed before grounding.

Some of the low-voltage cable to the instruments was parallel to and within a few feet of the three-phase, 208-230/460-V conductor and flexible conduit that supplied power to the 30-kw (40-hp) continuous-duty motor. A concern was raised that some of the variation in data measurements could be due to this condition. The instrument electrical cable was replaced temporarily with a much longer cable that could be rerouted away from the three-phase, 208-230/460-V conductor. No difference in the measurement variability was detected with this alternate location, and the original location for the instrument electrical cable was immediately restored.

The original electrical wiring to the pressure transducers and the flow meters used separate power supplies that were not directly connected to the National Instruments Field Point Analog Input Module (Model FP-AI-100). The electrical drawings for the FP-AI-100 showed that a single power supply connected to the FP-AI-100 module could be used to supply power to the all of the instruments and that this arrangement might be preferable because of simpler wiring and less power supply equipment. The wiring to the instruments was revised to use a single power supply to the FP-AI-100 module; this arrangement produced a very small improvement in data measurement variation.

When a single power supply was connected to the National Instruments Field Point Analog Input Module to supply power to the pressure transducers and flow meters, a separate power supply was used to supply power to the National Instruments Field Point Network Module (Model FP-1601). Tests were performed to determine if a single power supply to both instruments would provide improved results. Several different power supply units were tested, and it was found that in all cases, a single power supply produced greater data variation. Further consideration of a single power supply was abandoned.

If some of the measurement data variation came from the building electrical power system, then the use of an alternate source of stable electrical power could provide improved measurement. To test this hypothesis, the power supply to the FP-AI-100 was replaced with two 12-V wet-cell batteries connected in series. With this arrangement, it was found that the data variation was reduced slightly but not eliminated. Although the use of wet-cell batteries could be implemented, a concern was raised over the changes in instrument calibration with the change in battery voltage during power use. Because the benefits of using a wet-cell battery were small, the concern about instrument calibration caused this procedure to be abandoned.

The upstream and downstream pressure transducers provided threaded fittings that allowed the use of electrical metal tubing (EMT) conduit; however, EMT was not installed originally in the throttle valve apparatus. During the course of the diagnostic testing, EMT was installed at the electrical lines to both pressure transducers and to the flow transmitter. The EMT was connected to the building ground. The entire electrical system was rewired substantially during installation of the EMT. No measurable improvement to the data measurement variability was observed with the EMT in place. The EMT protected the electrical system wiring while personnel were working around the throttle valve; thus, the EMT provided a benefit to test operations.

Of all the methods tested, the grounding of the instruments was most efficacious in reducing the magnitude of the fluctuations in the data.

This page intentionally left blank.

APPENDIX D: COMPILATION OF *K* DATA

The full first and second test series, summarized in Table 2-1 and Table 2-2 is presented in Table D-1, with an additional column listing for Δ*K*%. The name associated with each test was intended as an identifier only and was not generally meant to be descriptive. For Test Series 1, the test name begins with 45L, 5L, or 5S for the stem designator. The stem designator is followed by the debris designator; DT, DTR, C, or N, which stands for RMI, RMI repeated, CalSil, and NUKON. The debris designator is followed by the test sequence number, 1, 2, 3, etc. In some cases, the sequence number is followed by a, b, or c, designating changes to the debris geometry for otherwise identical test conditions. Test Series 2 has no naming convention.

Table D-1. Summary of *K* Data

Test Series 1

No.	Test	Stem	Gap [cm (in.)]	CalSil (g)	NUKON (g)	RMI (g)	RMI Type [cm × cm (in. × in.)]	ΔK%
1	45LDT1	45L	0.3142 (0.1237)			1	0.32 × 0.32 (1/8 × 1/8)	0
2	45LDT2	45L	0.3142 (0.1237)			5	0.32 × 0.32 (1/8 × 1/8)	0
3	45LDT3	45L	0.3142 (0.1237)			10.01	0.32 × 0.32 (1/8 × 1/8)	0
4	45LDT4	45L	0.3142 (0.1237)			1.02	0.63 × 0.63 (1/4 × 1/4)	11.84
5	45LDT5	45L	0.3142 (0.1237)			5	0.63 × 0.63 (1/4 × 1/4)	4.19
6	45LDT6	45L	0.3142 (0.1237)			10.02	0.63 × 0.63 (1/4 × 1/4)	27.56
7	45LDT7	45L	0.3142 (0.1237)			0.99	0.32 × 1.27 (1/8 × 1/2)	0
8	45LDT8	45L	0.3142 (0.1237)			5.03	0.32 × 1.27 (1/8 × 1/2)	0
9	45LDT9	45L	0.3142 (0.1237)			10	0.32 × 1.27 (1/8 × 1/2)	51.03
10	45LDT10	45L	0.166 (0.0654)			1.02	0.32 × 0.32 (1/8 × 1/8)	0
11	45LDT11	45L	0.166 (0.0654)			4.99	0.32 × 0.32 (1/8 × 1/8)	0
12	45LDT12	45L	0.166 (0.0654)			10	0.32 × 0.32 (1/8 × 1/8)	4.95
13	45LDT13	45L	0.166 (0.0654)			1	0.63 × 0.63 (1/4 × 1/4)	11.41
14	45LDT14	45L	0.166 (0.0654)			5	0.63 × 0.63 (1/4 × 1/4)	32.36
15	45LDT15	45L	0.166 (0.0654)			10.01	0.63 × 0.63 (1/4 × 1/4)	53.03
16	45LDT16	45L	0.166 (0.0654)			1.01	0.32 × 1.27 (1/8 × 1/2)	0
17	45LDT17	45L	0.166 (0.0654)			5.02	0.32 × 1.27 (1/8 × 1/2)	4.59
18	45LDT18	45L	0.166 (0.0654)			10	0.32 × 1.27 (1/8 × 1/2)	51.29
19	5LDT1	5L	0.1269 (0.04997)			1.01	0.32 × 0.32 (1/8 × 1/8)	0
20	5LDT2	5L	0.1269 (0.04997)			5.01	0.32 × 0.32 (1/8 × 1/8)	0
21	5LDT3	5L	0.1269 (0.04997)			10.01	0.32 × 0.32 (1/8 × 1/8)	11.18
22	5LDT4	5L	0.1269 (0.04997)			1.01	0.63 × 0.63 (1/4 × 1/4)	7.63
23	5LDT5	5L	0.1269 (0.04997)			5.01	0.63 × 0.63 (1/4 × 1/4)	0
24	5LDT6	5L	0.1269 (0.04997)			10.01	0.63 × 0.63 (1/4 × 1/4)	23.84
25	5LDT7	5L	0.1269 (0.04997)			1.01	0.32 × 1.27 (1/8 × 1/2)	0

Table D-1. Summary of *K* Data, Test Series 1 (cont)

No.	Test	Stem	Gap [cm (in.)]	CalSil (g)	NUKON (g)	RMI (g)	RMI Type [cm × cm (in. × in.)]	ΔK%
26	5LDT8	5L	0.1269 (0.04997)			5.01	0.32 × 1.27 (1/8 × 1/2)	0
27	5LDT9	5L	0.1269 (0.04997)			10.01	0.32 × 1.27 (1/8 × 1/2)	28.87
28	5SDT1	5S	0.254 (0.0999)			1	0.32 × 0.32 (1/8 × 1/8)	0
29	5SDT2	5S	0.254 (0.0999)			5	0.32 × 0.32 (1/8 × 1/8)	0
30	5SDT3	5S	0.254 (0.0999)			10	0.32 × 0.32 (1/8 × 1/8)	0
31	5SDT4	5S	0.254 (0.0999)			1	0.63 × 0.63 (1/4 × 1/4)	0
32	5SDT5	5S	0.254 (0.0999)			5.01	0.63 × 0.63 (1/4 × 1/4)	0
33	5SDT6	5S	0.254 (0.0999)			10	0.63 × 0.63 (1/4 × 1/4)	0
34	5SDT7	5S	0.254 (0.0999)			1.01	0.32 × 1.27 (1/8 × 1/2)	0
35	5SDT8	5S	0.254 (0.0999)			5.01	0.32 × 1.27 (1/8 × 1/2)	0
36	5SDT9	5S	0.254 (0.0999)			10.01	0.32 × 1.27 (1/8 × 1/2)	0
37	5SDT10	5S	0.161 (0.0632)			1	0.32 × 0.32 (1/8 × 1/8)	0
38	5SDT11	5S	0.161 (0.0632)			5	0.32 × 0.32 (1/8 × 1/8)	0
39	5SDT12	5S	0.161 (0.0632)			10	0.32 × 0.32 (1/8 × 1/8)	0
40	5SDT13	5S	0.161 (0.0632)			1.02	0.63 × 0.63 (1/4 × 1/4)	0
41	5SDT14	5S	0.161 (0.0632)			5	0.63 × 0.63 (1/4 × 1/4)	0
42	5SDT15	5S	0.161 (0.0632)			10.02	0.63 × 0.63 (1/4 × 1/4)	3.84
43	5SDT16	5S	0.161 (0.0632)			1.01	0.32 × 1.27 (1/8 × 1/2)	0
44	5SDT17	5S	0.161 (0.0632)			5	0.32 × 1.27 (1/8 × 1/2)	0
45	5SDT18	5S	0.161 (0.0632)			10	0.32 × 1.27 (1/8 × 1/2)	0
46	45LDTR5-rep	45L	0.3124 (0.1230)			5.01	0.63 × 0.63 (1/4 × 1/4)	24.48
47	45LDTR9-rep	45L	0.3124 (0.1230)			10.05	0.32 × 1.27 (1/8 × 1/2)	5.27
48	45LDTR11-rep	45L	0.156 (0.0615)			5.03	0.32 × 0.32 (1/8 × 1/8)	5.61
49	45LDT×(gap)	45L	0.3269 (0.1287)			5.07	0.32 × 0.32 (1/8 × 1/8)	0
50	5sc1	5S	0.161 (0.0632)	50.04				0
51	5sc2	5S	0.161 (0.0632)	100.04				0
52	5sc3	5S	0.161 (0.0632)	51.01				0
53	5sc4	5S	0.161 (0.0632)	100				3.13
54	5sc5	5S	0.254 (0.0999)	50.06				0
55	5sc6	5S	0.254 (0.0999)	100.04				0
56	5sc7	5S	0.254 (0.0999)	49.98				0
57	5sc8	5S	0.254 (0.0999)	100.08				0
58	5sc9	5S	0.254 (0.0999)	*50 g Unsieved*				12.0
59	5LC1	5L	0.127 (0.0499)	50.08				0
60	5LC2	5L	0.127 (0.0499)	100.56				0
61	5LC3	5L	0.127 (0.0499)	50.12				0
62	5LC4	5L	0.127 (0.0499)	101.25				12.2
63	5LN1	5L	0.126 (0.0497)		50.07			13.61
64	5SN1	5L	0.254 (0.1000)		50.15			0
65	5SN2	5L	0.159 (0.0627)		50.07			0
66	45LN1	5L	0.3152 (0.1241)		49.92			0
67	45LN2	5L	0.162 (0.0636)		49.85			47.13

Table D-1. Summary of *K* Data, Test Series 1 (cont)

No.	Test	Stem	Gap [cm (in.)]	CalSil (g)	NUKON (g)	RMI (g)	RMI Type [cm × cm (in. × in.)]	ΔK%
68	5SDT1a	5S	0.158 (0.0622)			10 pieces	0.32 × 0.32 (1/8 × 1/8)	0
69	5SDT1b	5S	0.158 (0.0622)			10 pieces	0.63 × 0.63 (1/4 × 1/4)	0
70	5SDT1c	5S	0.158 (0.0622)			10 pieces	0.32 × 1.27 (1/8 × 1/2)	0
71	5SDT2a	5S	0.2543 (0.1001)			10 pieces	0.32 × 0.32 (1/8 × 1/8)	0
72	5SDT2b	5S	0.2543 (0.1001)			10 pieces	0.63 × 0.63 (1/4 × 1/4)	0
73	5SDT2c	5S	0.2543 (0.1001)			10 pieces	0.32 × 1.27 (1/8 × 1/2)	0
74	5LDT1a	5L	0.127 (0.0499)			10 pieces	0.32 × 0.32 (1/8 × 1/8)	0
75	5LDT1b	5L	0.127 (0.0499)			10 pieces	0.63 × 0.63 (1/4 × 1/4)	3.33
76	5LDT1c	5L	0.127 (0.0499)			10 pieces	0.32 × 1.27 (1/8 × 1/2)	7.30
77	45LDT1a	45L	0.180 (0.0707)			10 pieces	0.32 × 0.32 (1/8 × 1/8)	0
78	45LDT1b	45L	0.180 (0.0707)			10 pieces	0.63 × 0.63 (1/4 × 1/4)	0
79	45LDT1c	45L	0.180 (0.0707)			10 pieces	0.32 × 1.27 (1/8 × 1/2)	0
80	45LDT2a	45L	0.3124 (0.1230)			10 pieces	0.32 × 0.32 (1/8 × 1/8)	0
81	45LDT2b	45L	0.3124 (0.1230)			10 pieces	0.63 × 0.63 (1/4 × 1/4)	0
82	45LDT2c	45L	0.3124 (0.1230)			10 pieces	0.32 × 1.27 (1/8 × 1/2)	0
83	5LN2	5L	0.127 (0.0500)		97.99			186.67
84	5LN3	5L	0.127 (0.0500)		97.47			126.34
85	5SN3	5S	0.159 (0.0627)		95.83			7.4
86	5SN4	5S	0.2543 (0.1001)		98.05			0
87	45LN3	45L	0.160 (0.0629)		95.67			222.19
88	45LN4	45L	0.160 (0.0629)		98.23			201.08

Test Series 2—Single-Debris and Mixed-Debris Tests

No.	Test	Stem	Gap [cm (in.)]	CalSil (g)	NUKON (g)	RMI (g)	RMI Type [cm × cm (in. × in.)]	ΔK%
1	N-1	45L	0.63 (0.25)			10	0.317 × 0.317 (0.125 × 0.125)	0
2	N-2	45L	0.63 (0.25)			10	0.317 × 0.317 (0.125 × 0.125)	0
3	N-3	45L	0.63 (0.25)			10	0.317 × 0.317 (0.125 × 0.125)	0
4	N-4	45L	0.63 (0.25)			10	0.317 × 1.270 (0.125 × 0.500)	0
5	N-5	45L	0.63 (0.25)			10	0.317 × 1.270 (0.125 × 0.500)	0
6	N-6	45L	0.63 (0.25)			10	0.317 × 1.270 (0.125 × 0.500)	0
7	N-7	45L	0.63 (0.25)			5	0.317 × 1.270 (0.125 × 0.500)	14.77
						5	0.63 × 0.63 (0.25 × 0.25)	
8	D-1	45L	0.317 (0.125)			10	0.317 × 1.270 (0.125 × 0.500)	18.65
9	D-1-2	45L	0.317 (0.125)			10	0.317 × 1.270 (0.125 × 0.500)	53.67
10	D-2	45L	0.159 (0.0625)			10	0.317 × 1.270 (0.125 × 0.500)	20.19
11	D-3	5L	0.13 (0.05)			10	0.317 × 0.317 (0.125 × 0.125)	7.74
12	D-16	45L	0.159 (0.0625)		50		n/a	136.59
13	D-17	45L	0.159 (0.0625)		25		n/a	0
14	N-1-2	45L	0.33 (0.13)			10	0.317 × 0.317 (0.125 × 0.125)	14.62
15	N-2-2	45L	0.33 (0.13)			10	0.317 × 0.317 (0.125 × 0.125)	10.66
16	N-3-2	45L	0.33 (0.13)			10	0.317 × 0.317 (0.125 × 0.125)	12.14

Table D-1. Summary of *K* Data, Test Series 2 (cont)

No.	Test	Stem	Gap [cm (in.)]	CalSil (g)	NUKON (g)	RMI (g)	RMI Type [cm × cm (in. × in.)]	ΔK%
17	N-4-2	45L	0.33 (0.13)			10	0.317 × 1.270 (0.125 × 0.500)	14.4
18	N-5-2	45L	0.33 (0.13)			10	0.317 × 1.270 (0.125 × 0.500)	28.45
19	N-6-2	45L	0.33 (0.13)			10	0.317 × 1.270 (0.125 × 0.500)	14.01
20	N-8	45L	0.63 (0.25)		50	10	0.317 × 1.270 (0.125 × 0.500)	12.83
21	N-9	45L	0.63 (0.25)	25	25	5	0.317 × 1.270 (0.125 × 0.500)	5.07
22	D-4	45L	0.317 (0.125)		50	10	0.317 × 1.270 (0.125 × 0.500)	51.38
23	D-4-2	45L	0.317 (0.125)		50	10	0.317 × 1.270 (0.125 × 0.500)	35.5
24	D-5	5L	0.13 (0.05)		50	10	0.317 × 0.317 (0.125 × 0.125)	5.54
25	D-6	45L	0.159 (0.0625)			5	0.635 × 0.635 (0.250 × 0.250)	25.21
26	D-7	45L	0.159 (0.0625)		25	5	0.635 × 0.635 (0.250 × 0.250)	17.34
27	D-8	45L	0.159 (0.0625)	50		5	0.635 × 0.635 (0.250 × 0.250)	57.4
28	D-9	45L	0.159 (0.0625)	25	25	5	0.635 × 0.635 (0.250 × 0.250)	49.65
29	D-10	45L	0.159 (0.0625)	25 (3rd)	25 (2nd)	5 (1st)	0.635 × 0.635 (0.250 × 0.250)	45.94
30	D-10-2	45L	0.159 (0.0625)	25 (3rd)	25 (1st)	5 (2nd)	0.635 × 0.635 (0.250 × 0.250)	7.89
31	D-11	5L	0.13 (0.05)	25	25	5	0.317 × 0.317 (0.125 × 0.125)	80.54
						5	0.317 × 1.270 (0.125 × 0.500)	
32	D-12	45L	0.317 (0.125)	25	25	10	0.317 × 1.270 (0.125 × 0.500)	66.51
33	D-12-2	45L	0.159 (0.0625)	25 (3rd)	25 (1st)	10 (2nd)	0.317 × 1.270 (0.125 × 0.500)	13.03
34	D-13	45L	0.317 (0.125)	25	25		n/a	0
35	D-14	45L	0.159 (0.0625)	25	25	10	0.317 × 1.270 (0.125 × 0.500)	70.05
36	D-15	5L	0.13 (0.05)	25	25	5	0.317 × 1.270 (0.125 × 0.500)	186.88
						5	0.63 × 0.63 (0.25 × 0.25)	
37	D-15-2	5L	0.13 (0.05)	25	25	5	0.317 × 1.270 (0.125 × 0.500)	68.12
						5	0.63 × 0.63 (0.25 × 0.25)	
38	D-18	45L	0.159 (0.0625)	25	25		n/a	0
39	D-19a	45L	0.159 (0.0625)	25	25		n/a	27.5
40	D-19b	45L	0.159 (0.0625)	25	25		n/a	166.2
41	D-19c	45L	0.159 (0.0625)	25	25		n/a	32.36

APPENDIX E: COMPILATION OF PLOTS

Notes:

1. The order of the figures is the same as that in Table D-1.
2. In each figure, the blue or lighter curve shows pressure drop and the red or darker curve shows *K*.
3. In each figure, the vertical line denotes the time of debris addition.
4. Units for pressure drop are in pounds per square inch (1 psi = 6.89 kPa).

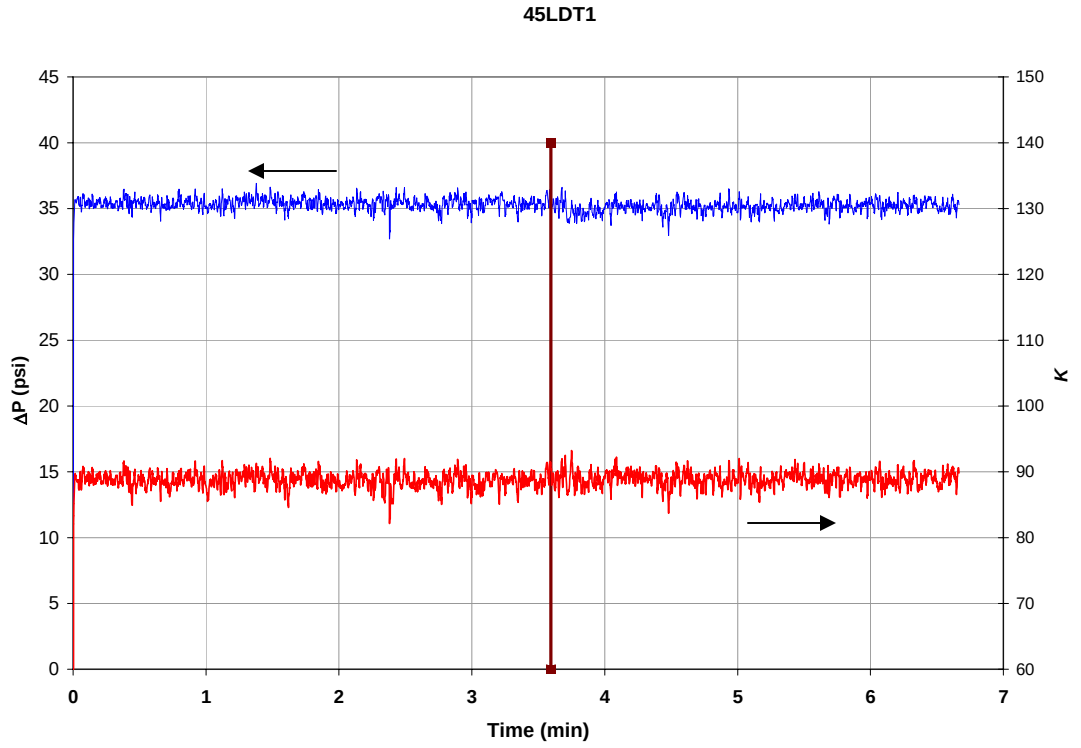
45LDT1
ΔP (psi)
K
Time (min)
0
5
10
15
20
25
30
35
40
45
60
70
80
90
100
110
120
130
140
150
0
1
2
3
4
5
6
7

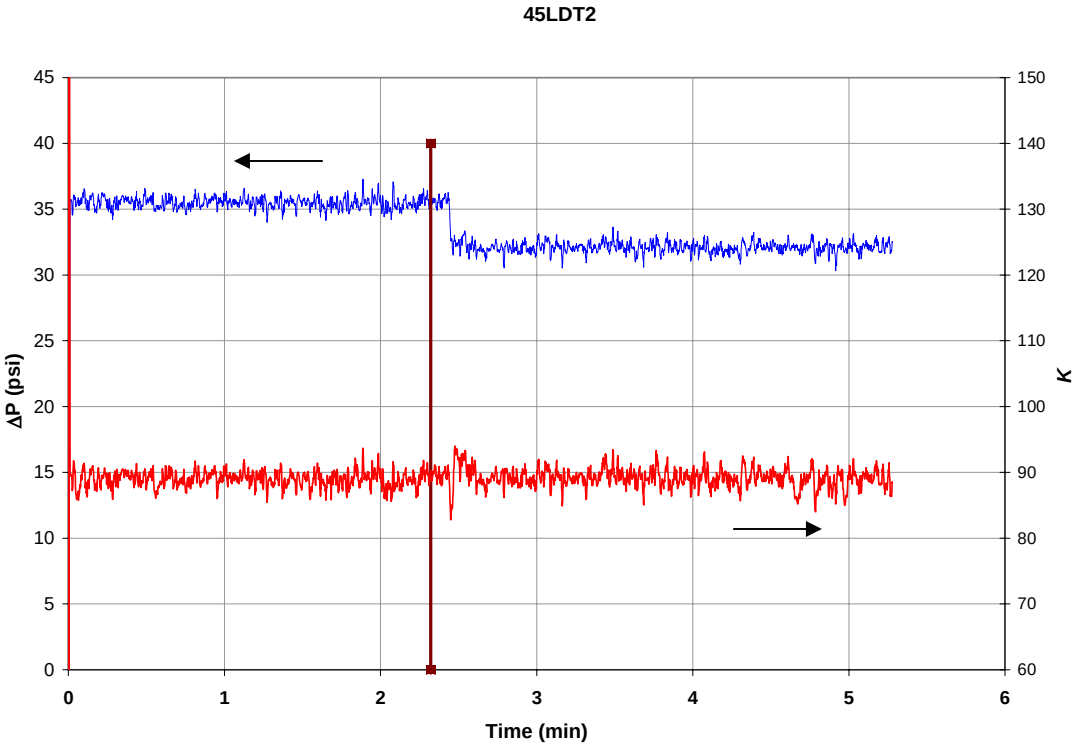
45LDT2
ΔP (psi)
K
Time (min)
0
5
10
15
20
25
30
35
40
45
60
70
80
90
100
110
120
130
140
150
0
1
2
3
4
5
6

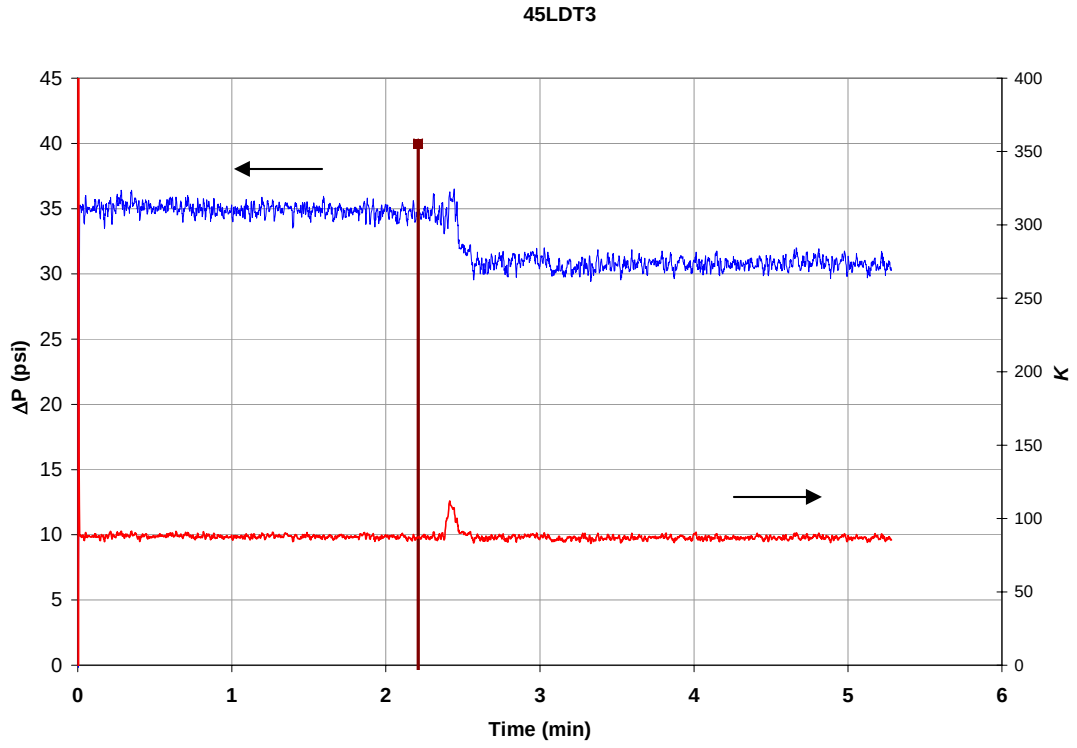
45LDT3
ΔP (psi)
K
Time (min)
0
5
10
15
20
25
30
35
40
45
50
100
150
200
250
300
350
400
1
2
3
4
6

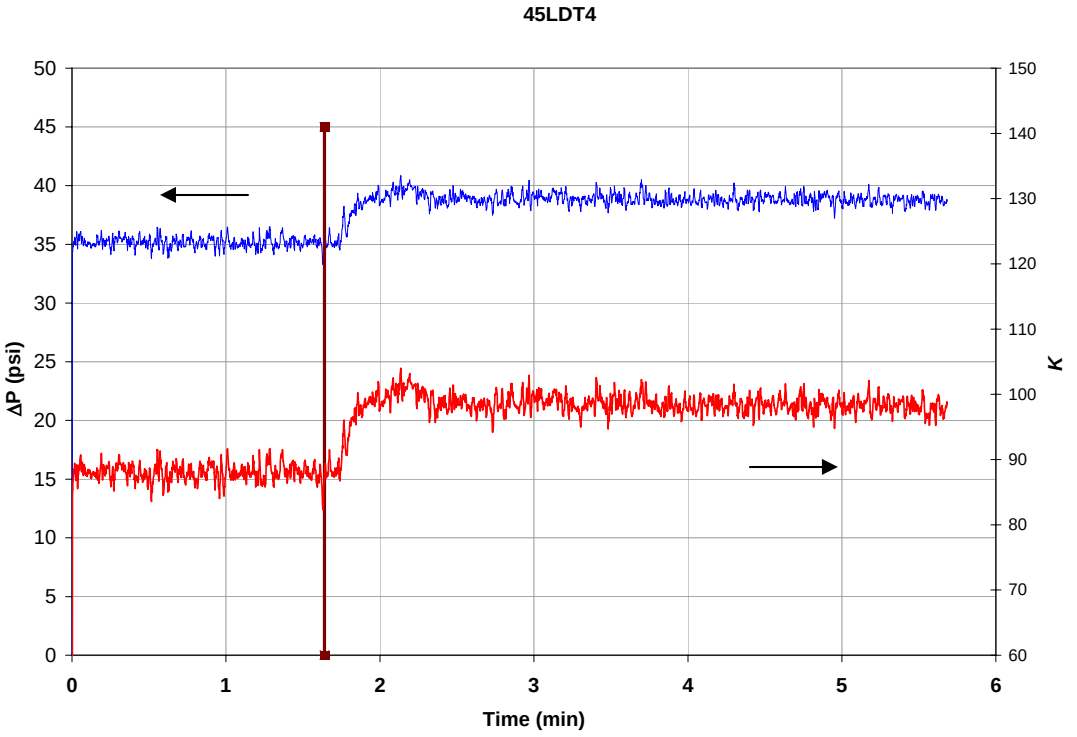
45LDT4
ΔP (psi)
K
Time (min)
0
5
10
15
20
25
30
35
40
45
50
60
70
80
90
100
110
120
130
140
150
1
2
3
4
6

45LDT5

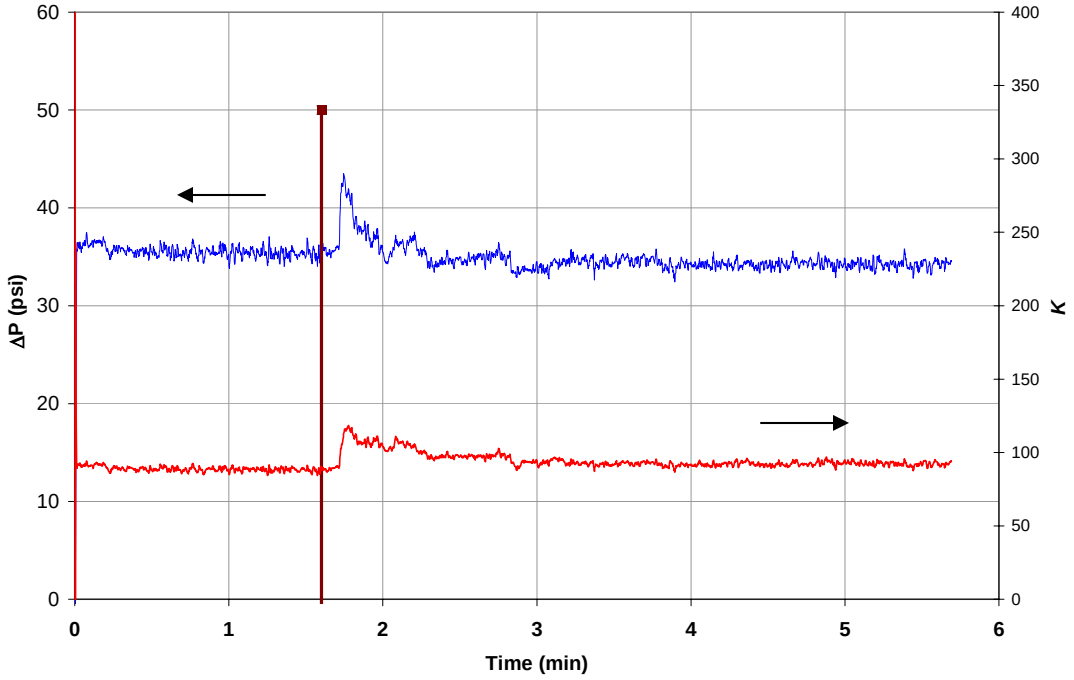

45LDT6

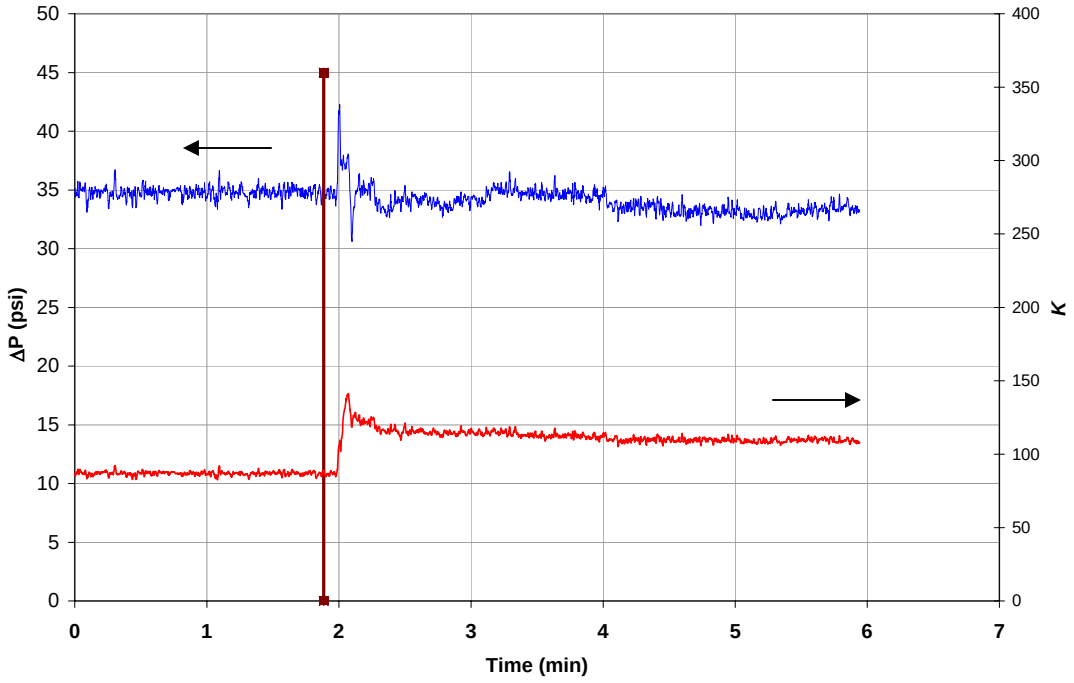

45LDT7

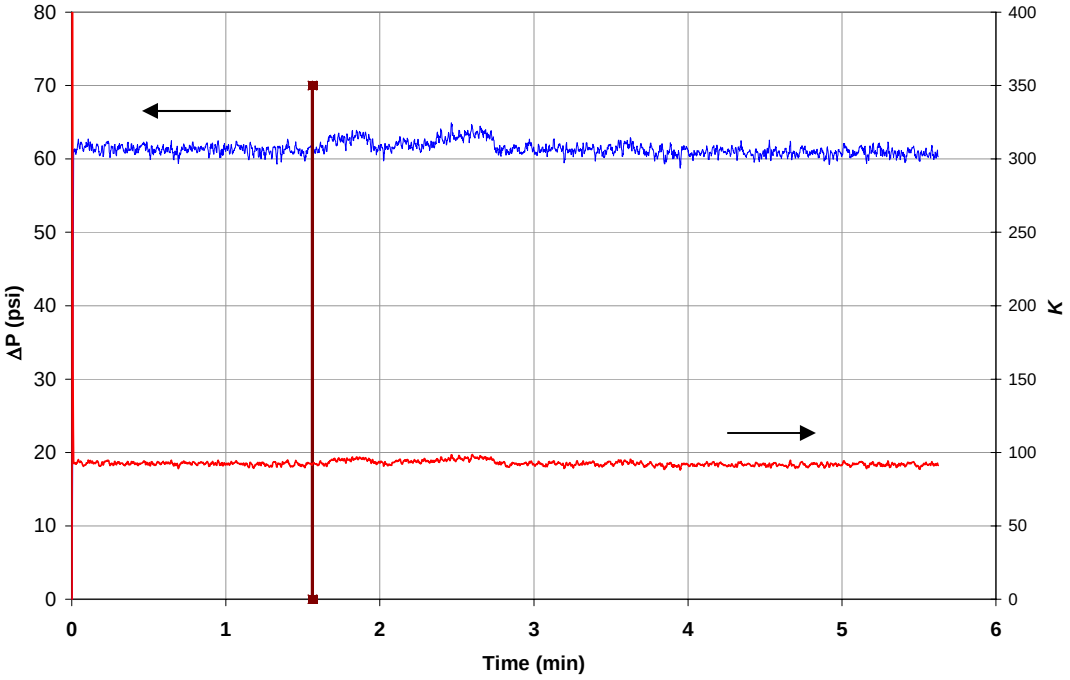

45LDT8

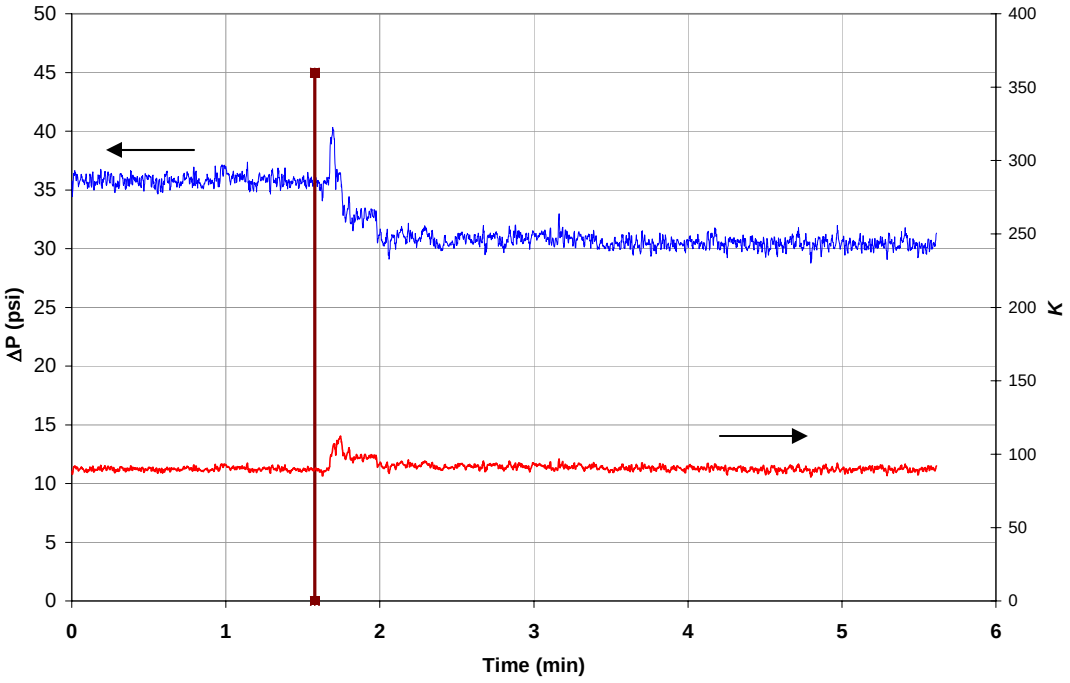

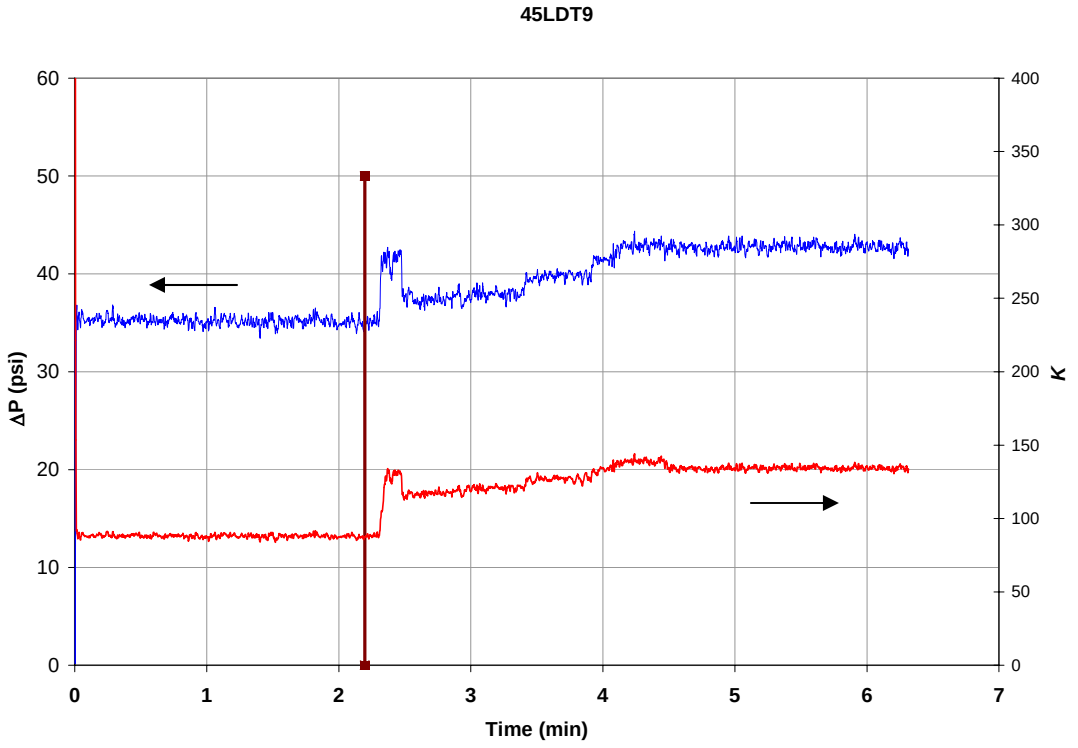
45LDT9
ΔP (psi)
K
Time (min)
0
10
20
30
40
50
60
0
50
100
150
200
250
300
350
400
0
1
2
3
4
5
6
7

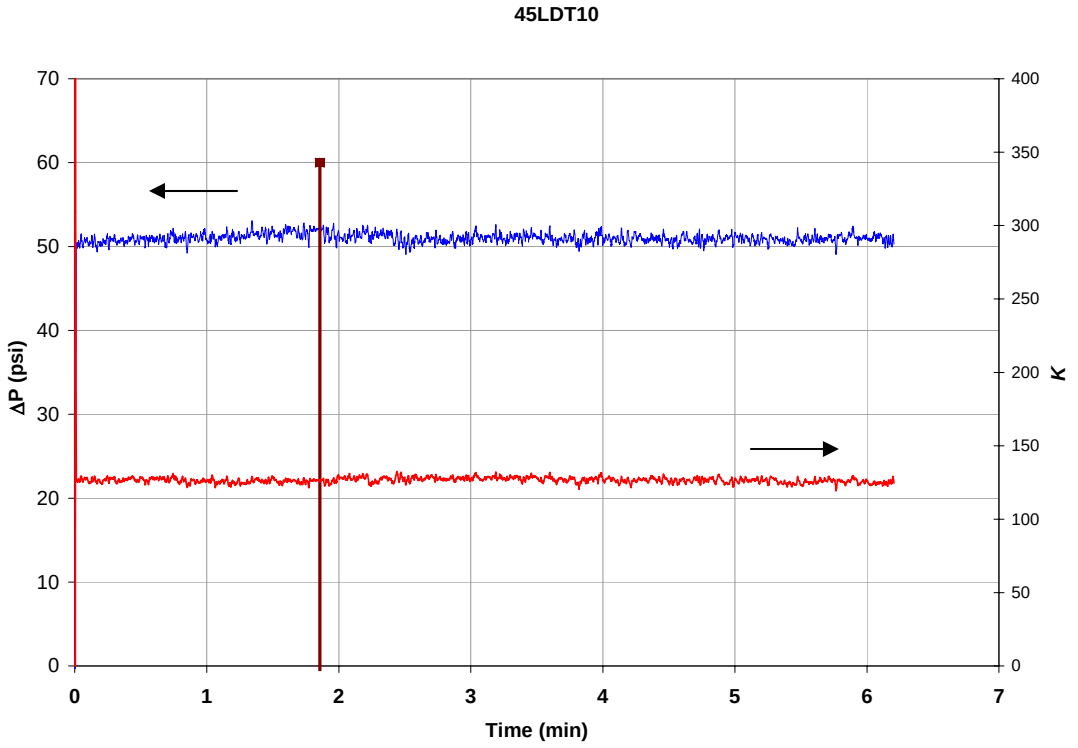
45LDT10
ΔP (psi)
K
Time (min)
0
10
20
30
40
50
60
70
0
50
100
150
200
250
300
350
400
0
1
2
3
4
5
6
7

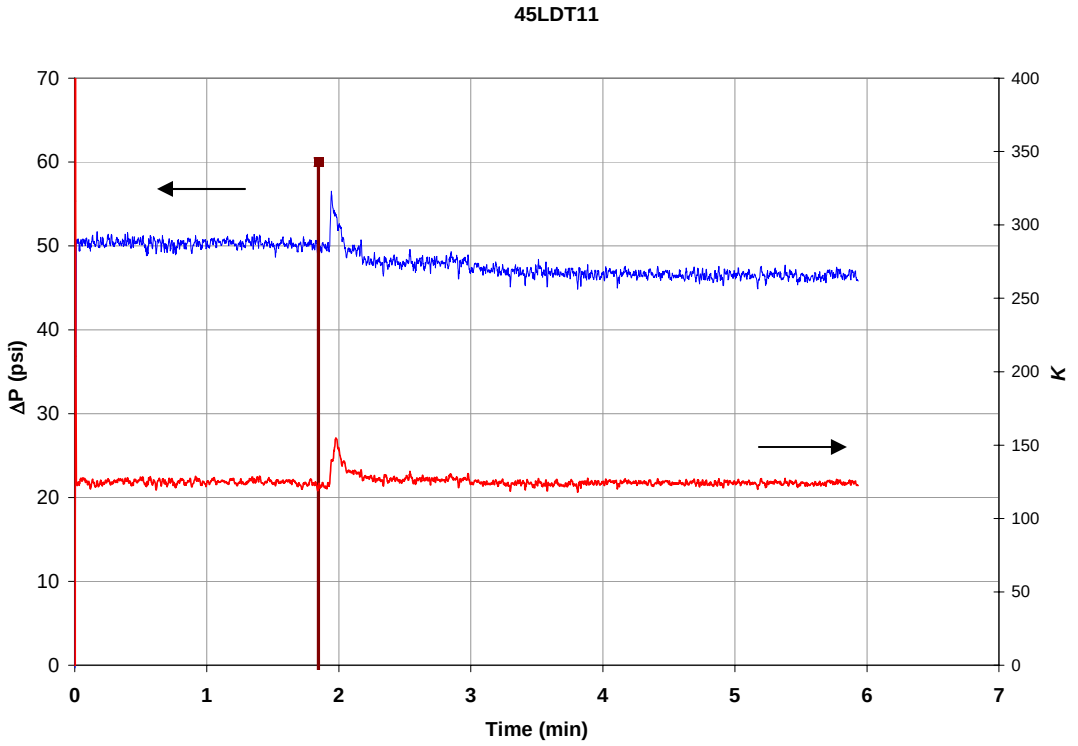
45LDT11
ΔP (psi)
K
Time (min)
0
10
20
30
40
50
60
70
0
50
100
150
200
250
300
350
400
0
1
2
3
4
5
6
7

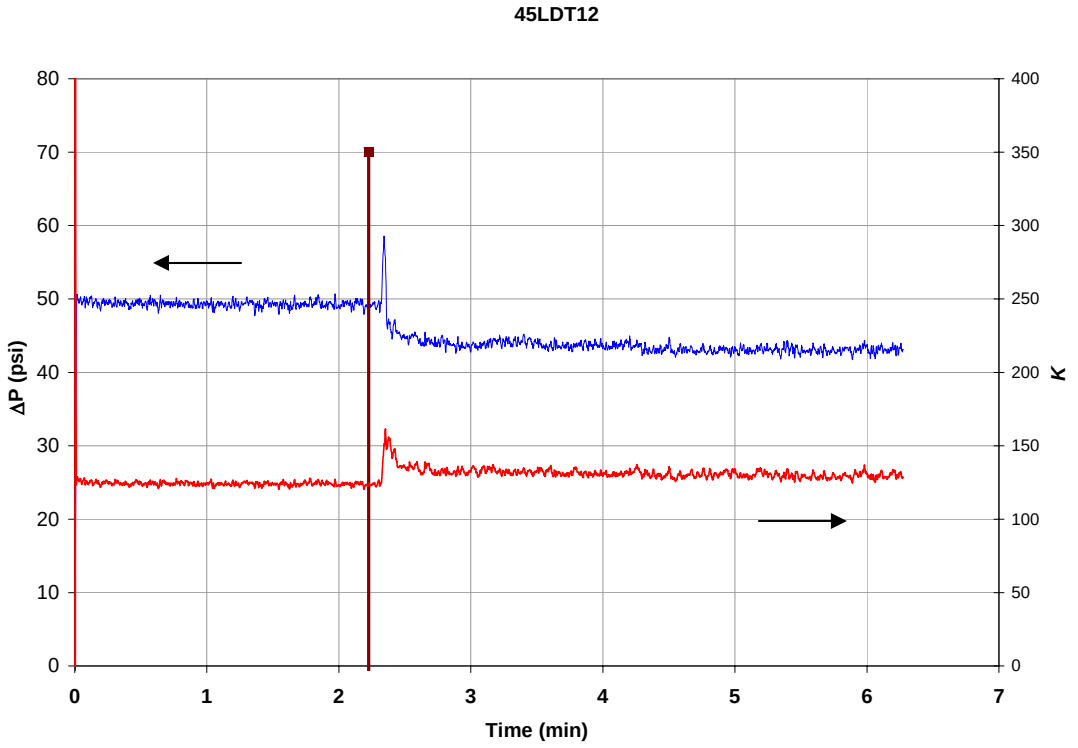
45LDT12
ΔP (psi)
K
Time (min)
0
10
20
30
40
50
60
70
80
0
50
100
150
200
250
300
350
400
0
1
2
3
4
5
6
7

45LDT13

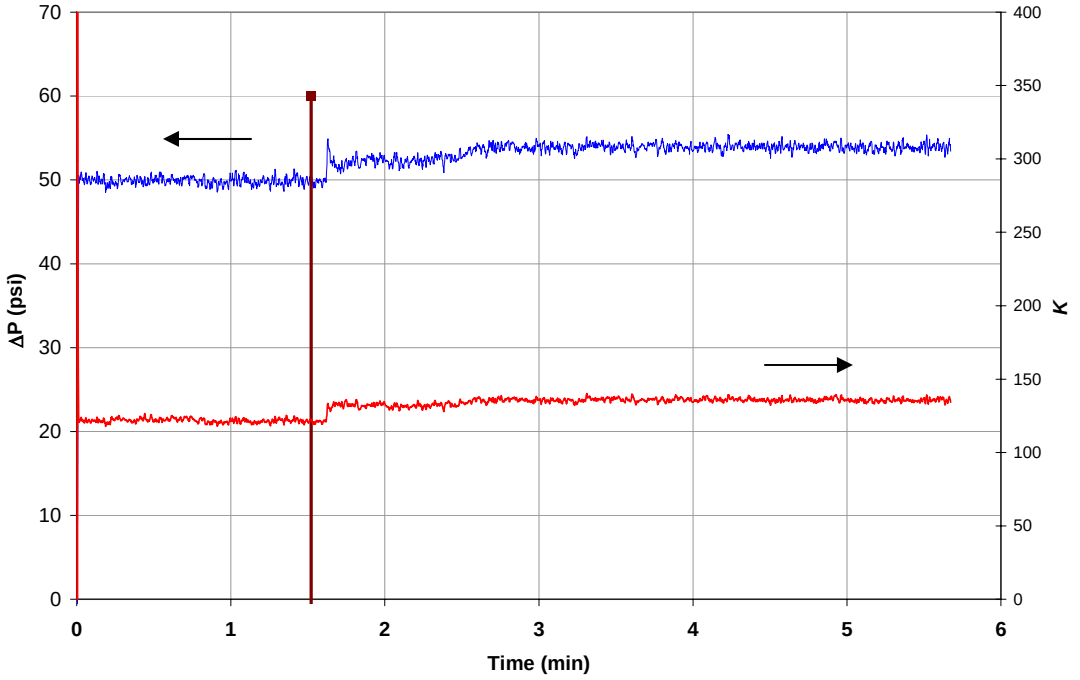

45LDT14

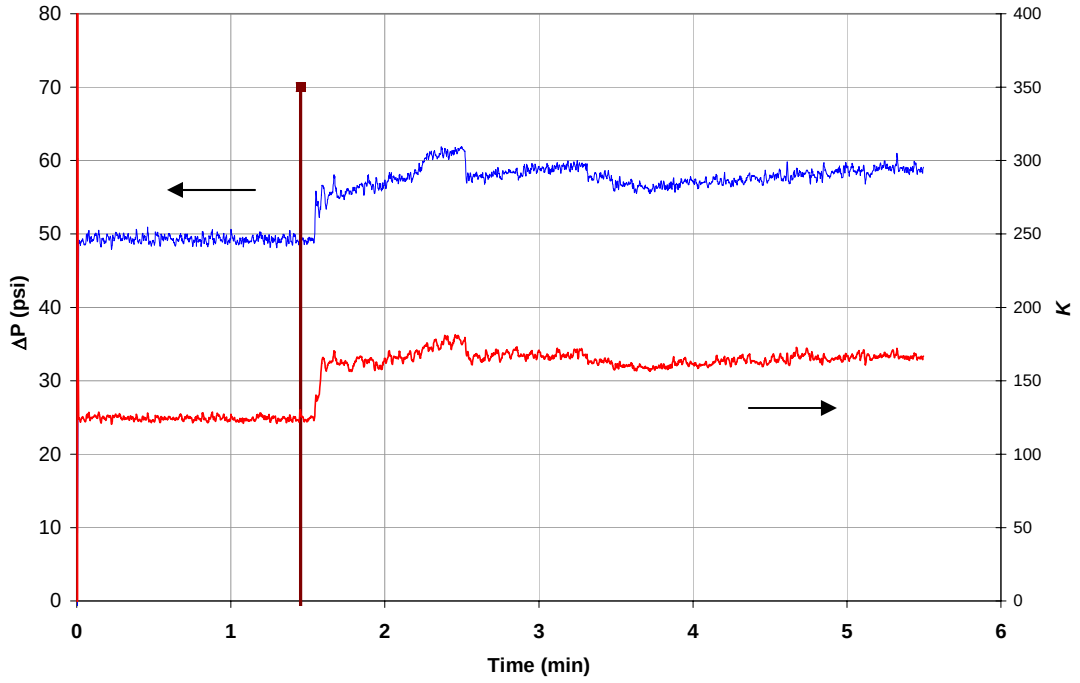

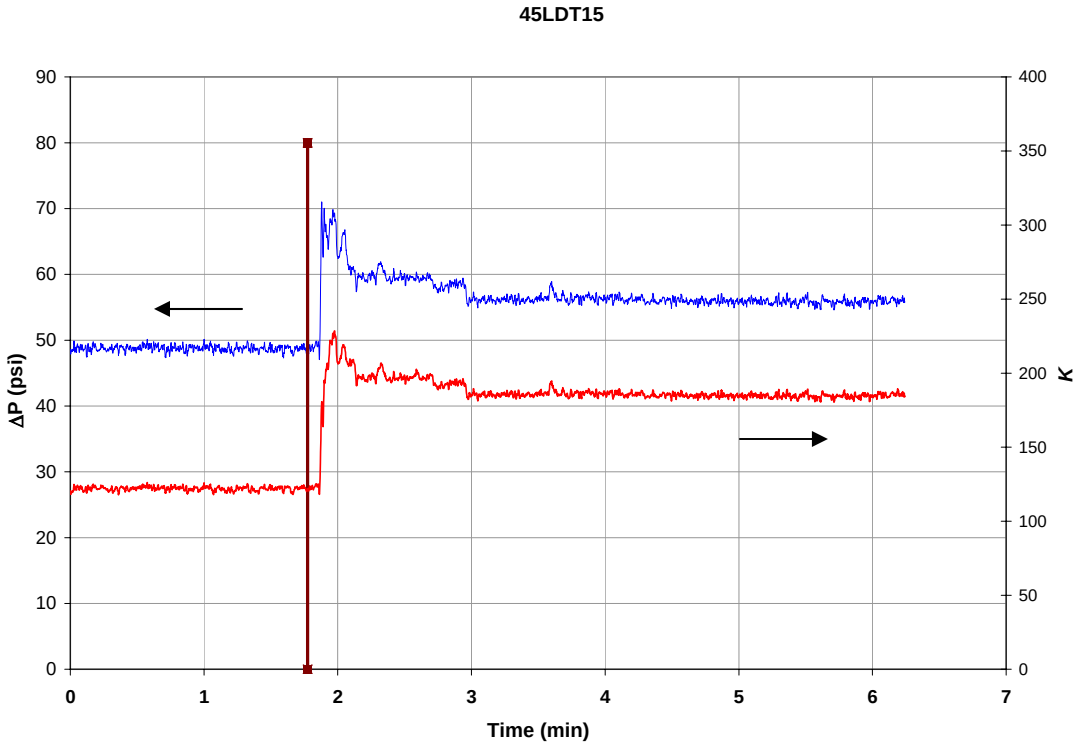
45LDT15
ΔP (psi)
K
Time (min)
0
10
20
30
40
50
60
70
80
90
0
50
100
150
200
250
300
350
400
0
1
2
3
4
5
6
7

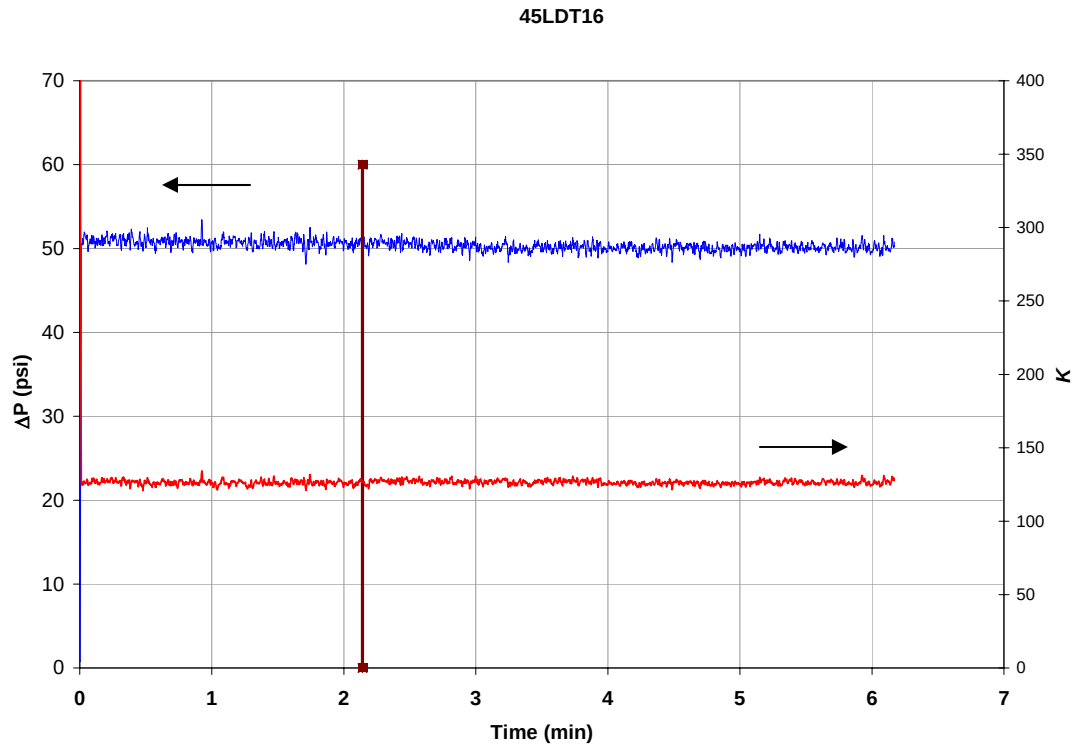
45LDT16
ΔP (psi)
K
Time (min)
0
10
20
30
40
50
60
70
0
50
100
150
200
250
300
350
400
0
1
2
3
4
5
6
7

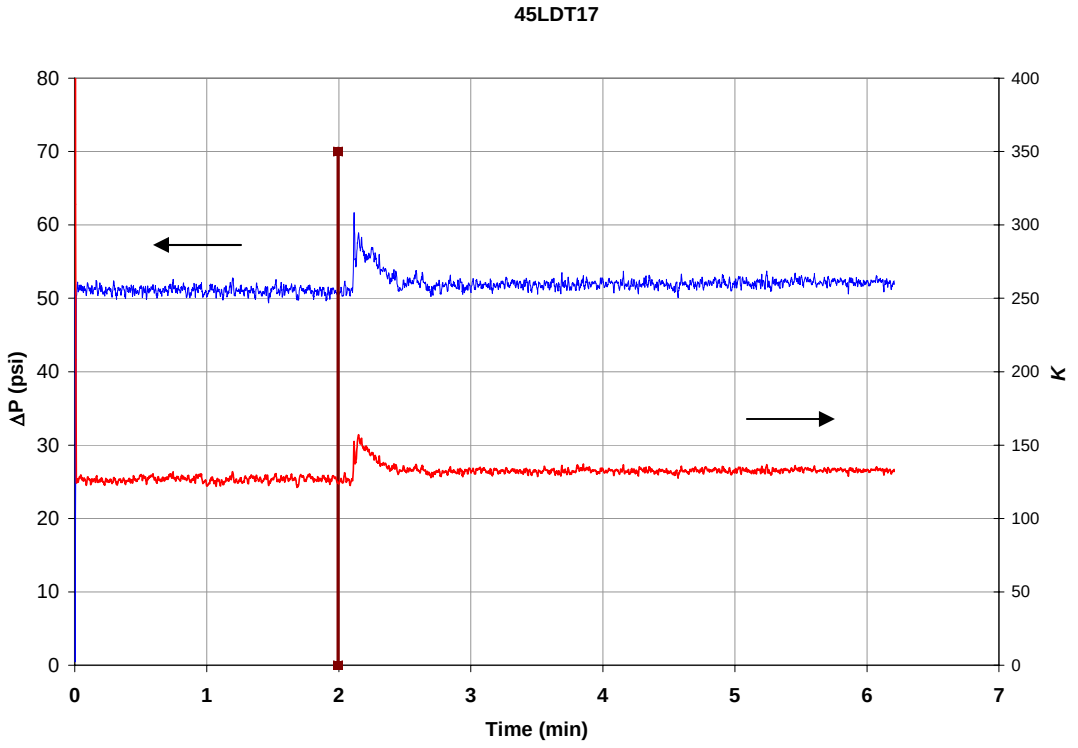
45LDT17
ΔP (psi)
K
Time (min)
0
10
20
30
40
50
60
70
80
0
50
100
150
200
250
300
350
400
0
1
2
3
4
5
6
7

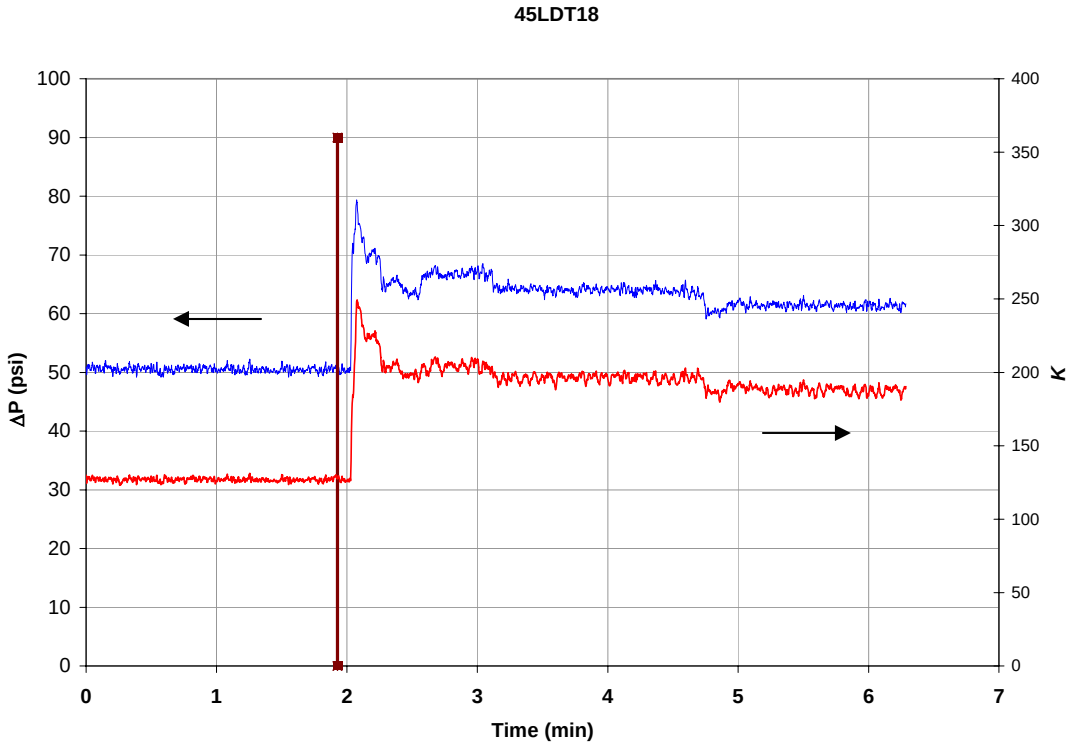
45LDT18
ΔP (psi)
K
Time (min)
0
10
20
30
40
50
60
70
80
90
100
0
50
100
150
200
250
300
350
400
0
1
2
3
4
5
6
7

5LDT1

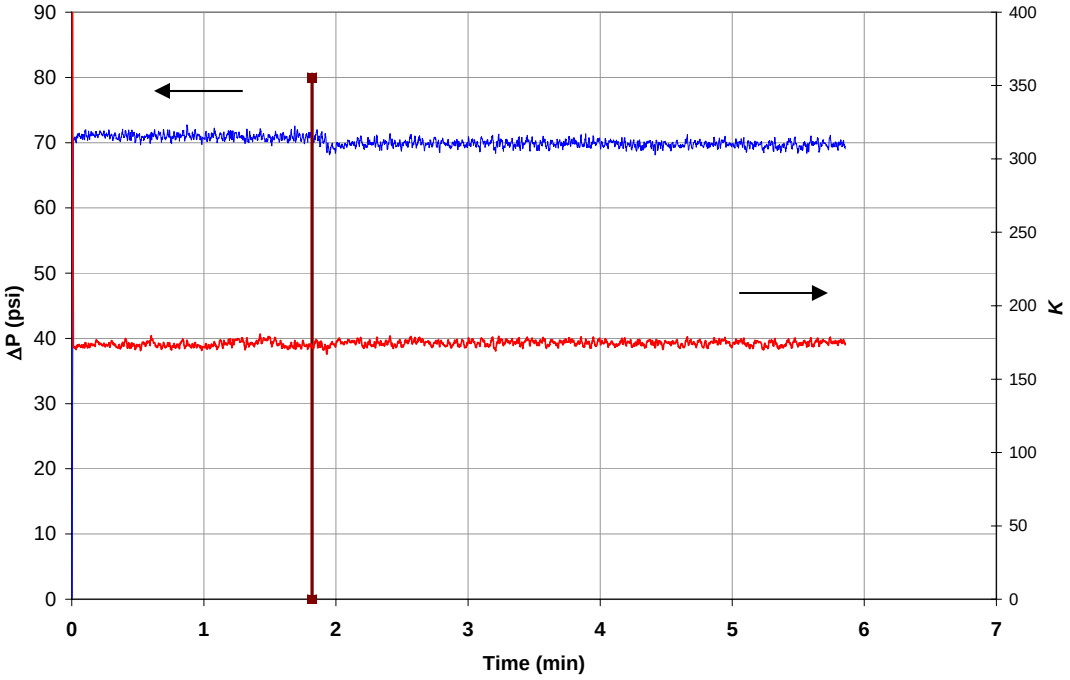
ΔP (psi)
K
Time (min)
0
10
20
30
40
50
60
70
80
90
0
50
100
150
200
250
300
350
400
0
1
2
3
4
5
6
7

5LDT2

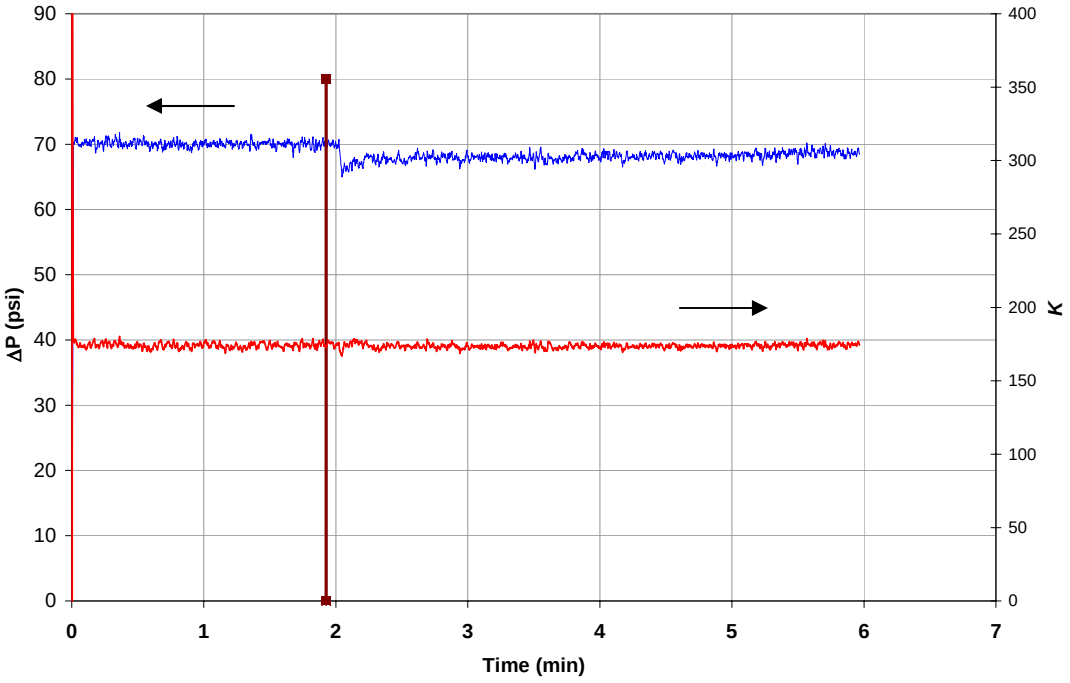
ΔP (psi)
K
Time (min)
0
10
20
30
40
50
60
70
80
90
0
50
100
150
200
250
300
350
400
0
1
2
3
4
5
6
7

5LDT3

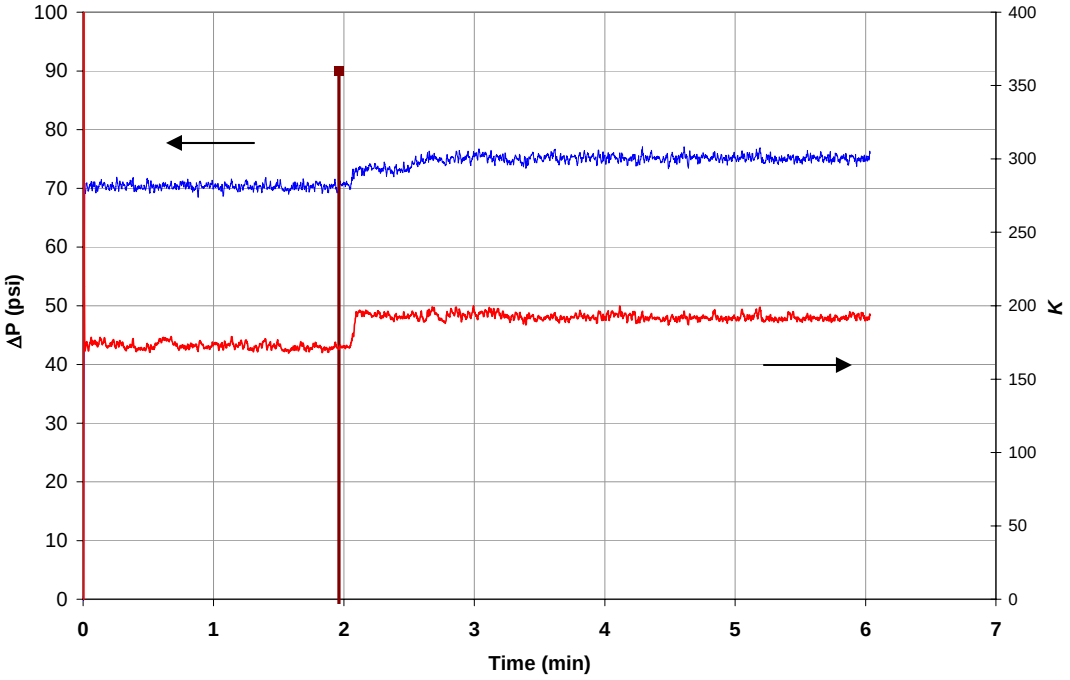
ΔP (psi)
K
Time (min)
100
90
80
70
60
50
40
30
20
10
0
400
350
300
250
200
150
100
50
0
0
1
2
3
4
5
6
7

5LDT4

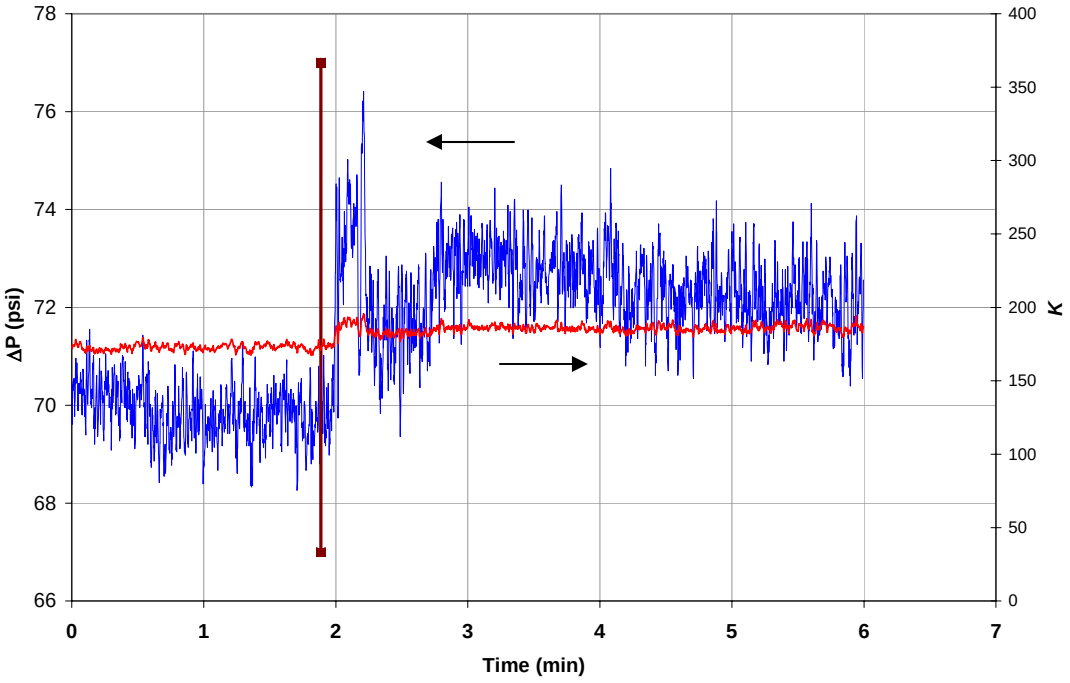
ΔP (psi)
K
Time (min)
78
76
74
72
70
68
66
400
350
300
250
200
150
100
50
0
0
1
2
3
4
5
6
7

5LDT5

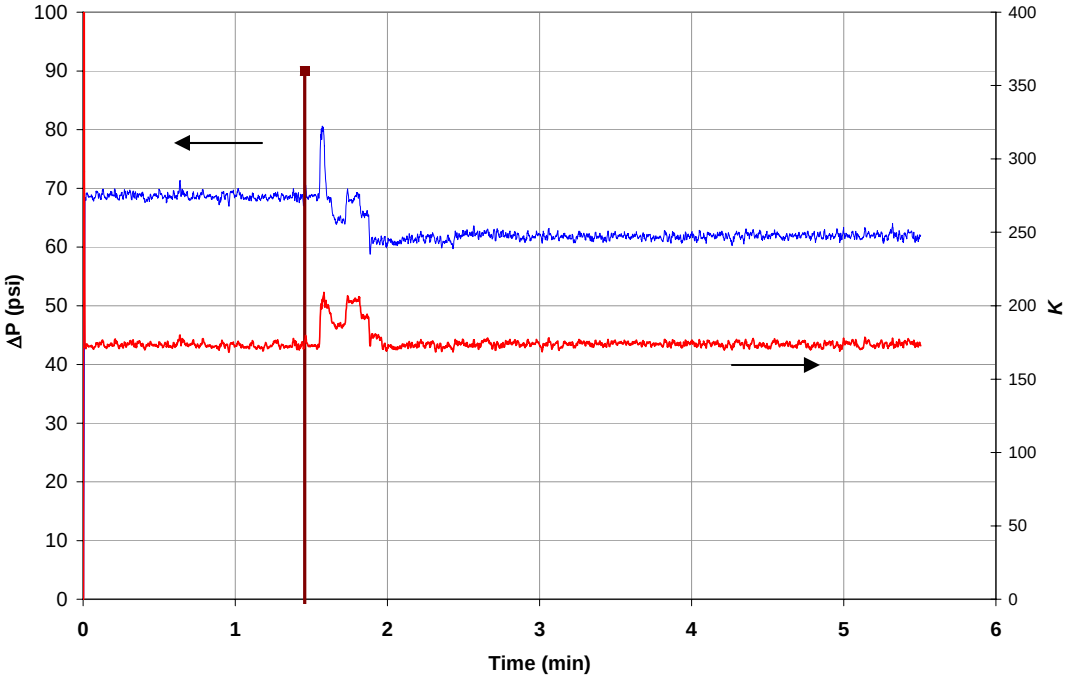
ΔP (psi)
K
Time (min)
0
10
20
30
40
50
60
70
80
90
100
0
50
100
150
200
250
300
350
400
0
1
2
3
4
5
6

5LDT6

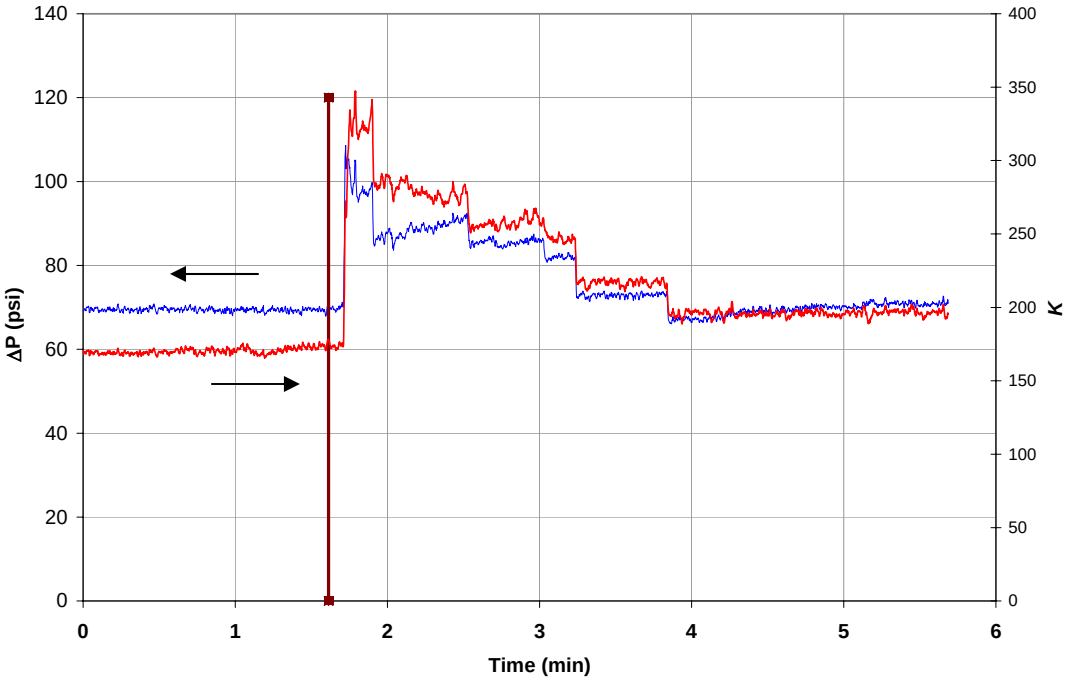
ΔP (psi)
K
Time (min)
0
20
40
60
80
100
120
140
0
50
100
150
200
250
300
350
400
0
1
2
3
4
5
6

5LDT7

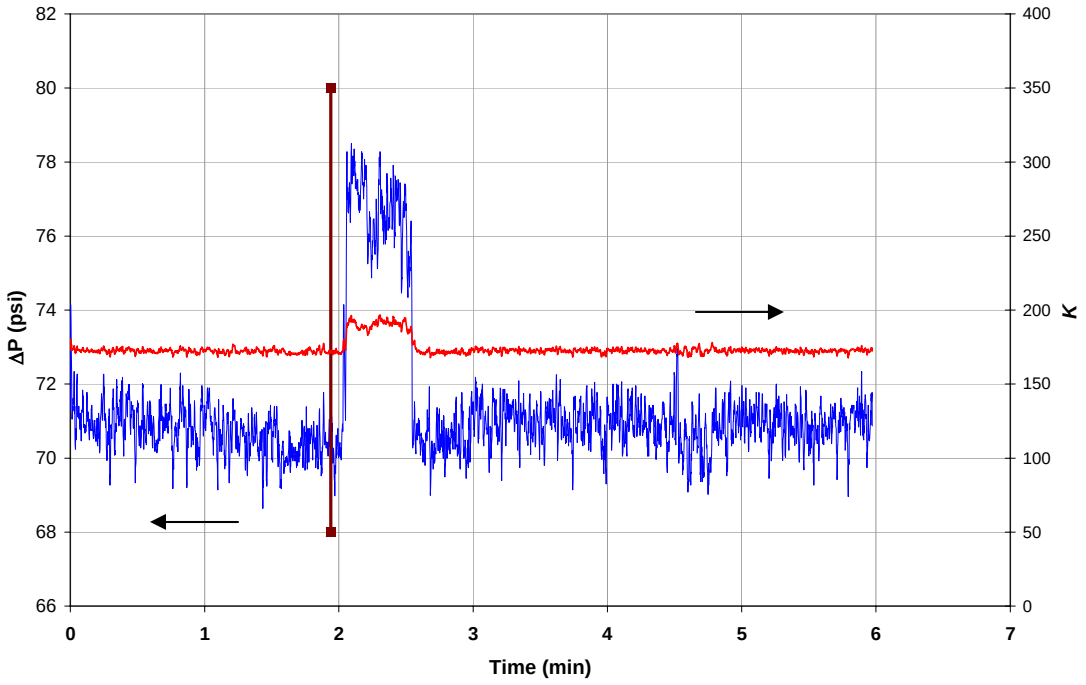
82
80
78
76
74
72
70
68
66
ΔP (psi)
400
350
300
250
200
150
100
50
0
K
0
1
2
3
4
5
6
7
Time (min)

5LDT8

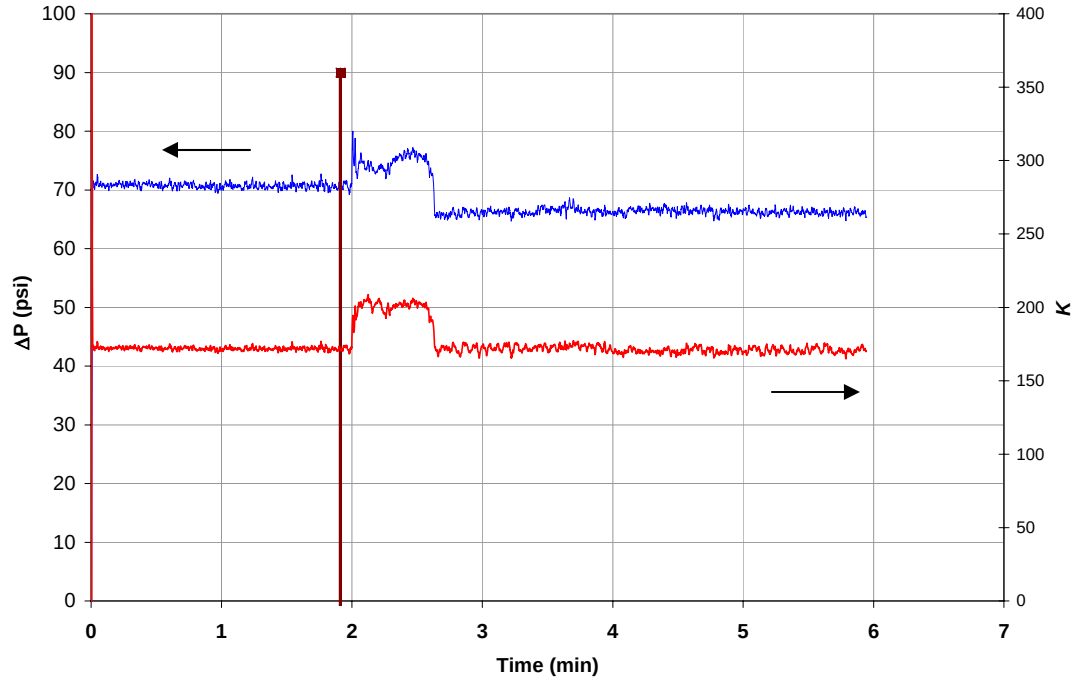
100
90
80
70
60
50
40
30
20
10
0
ΔP (psi)
400
350
300
250
200
150
100
50
0
K
0
1
2
3
4
5
6
7
Time (min)

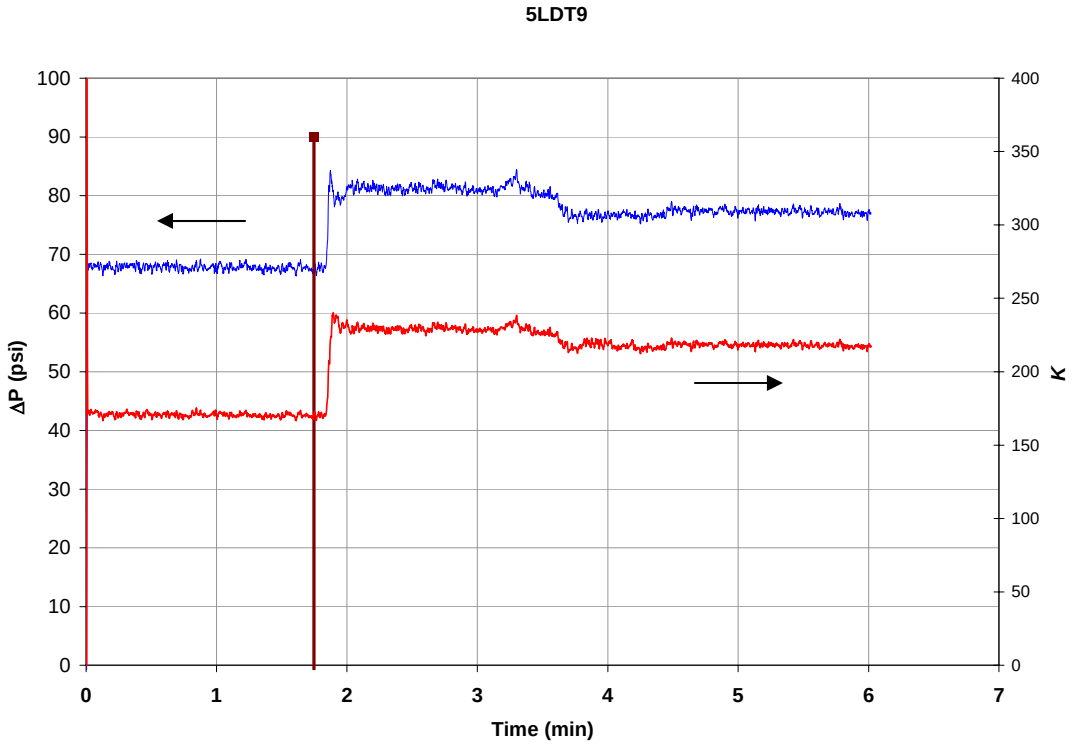
5LDT9
ΔP (psi)
K
Time (min)
0
10
20
30
40
50
60
70
80
90
100
0
50
100
150
200
250
300
350
400
0
1
2
3
4
5
6
7

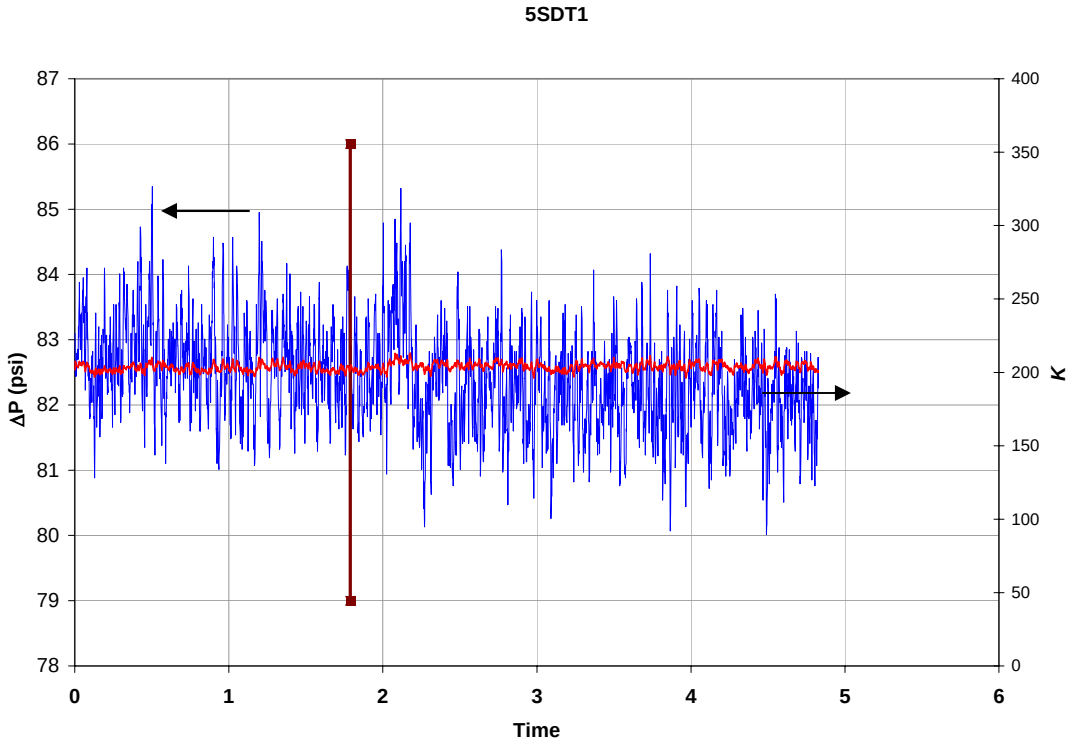
5SDT1
ΔP (psi)
K
Time
78
79
80
81
82
83
84
85
86
87
0
50
100
150
200
250
300
350
400
0
1
2
3
4
5
6

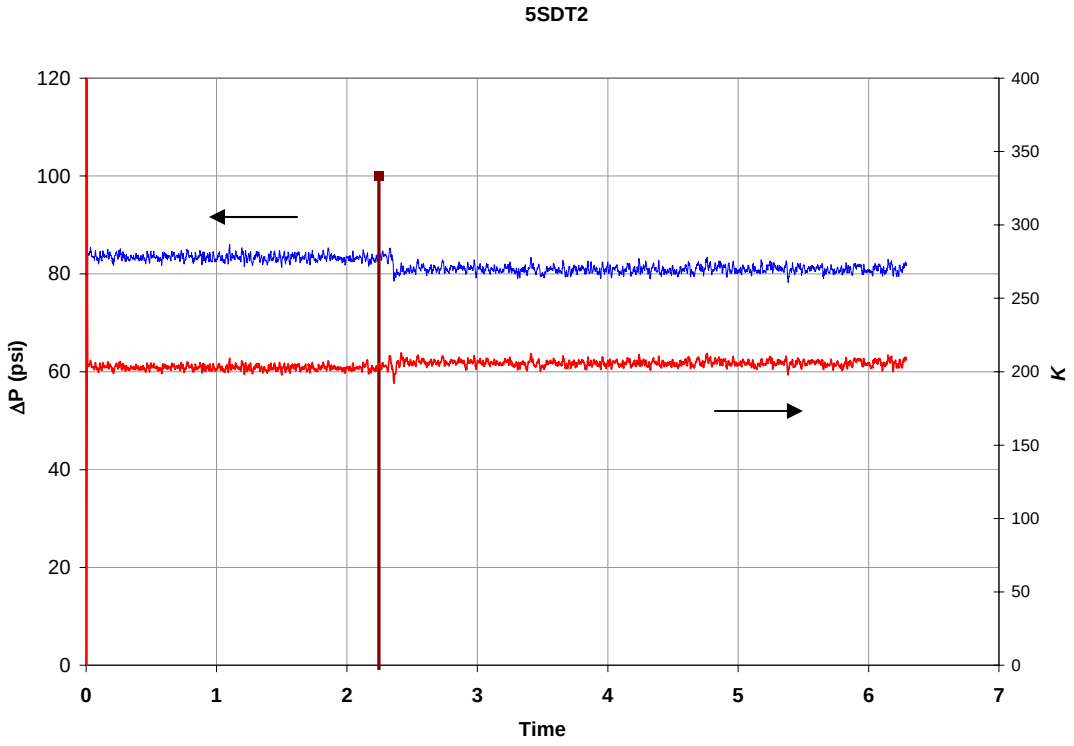
5SDT2
120
100
80
60
40
20
0
ΔP (psi)
400
350
300
250
200
150
100
50
0
K
0
1
2
3
4
5
6
7
Time

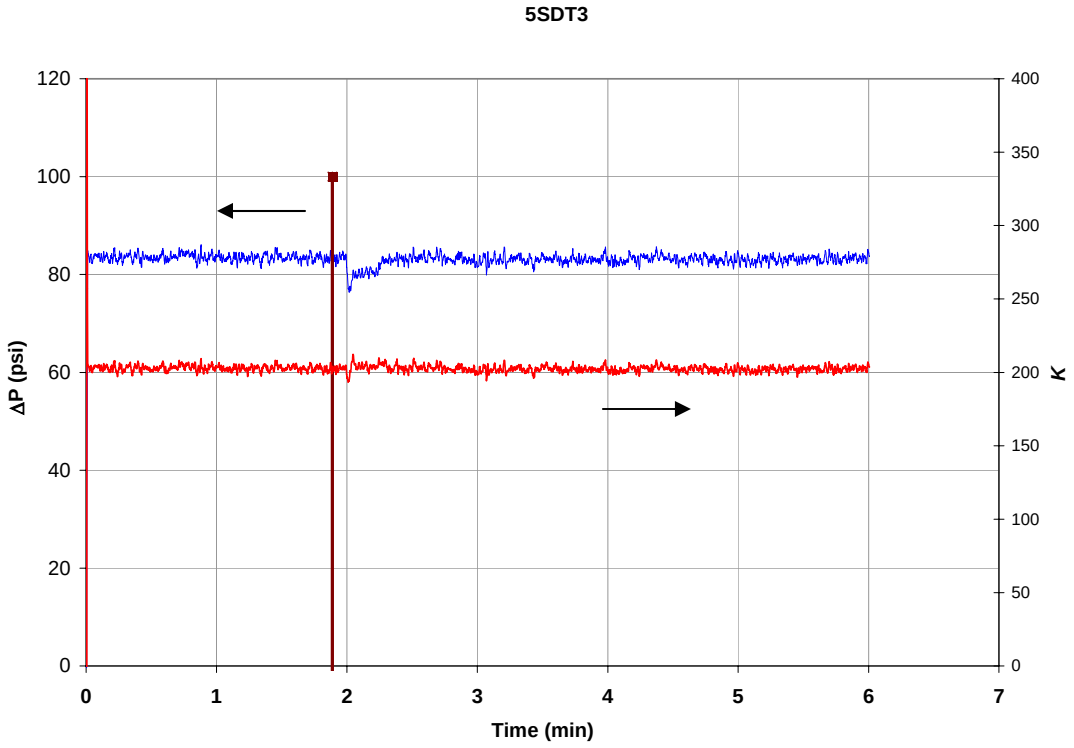
5SDT3
120
100
80
60
40
20
0
ΔP (psi)
400
350
300
250
200
150
100
50
0
K
0
1
2
3
4
5
6
7
Time (min)

5SDT4

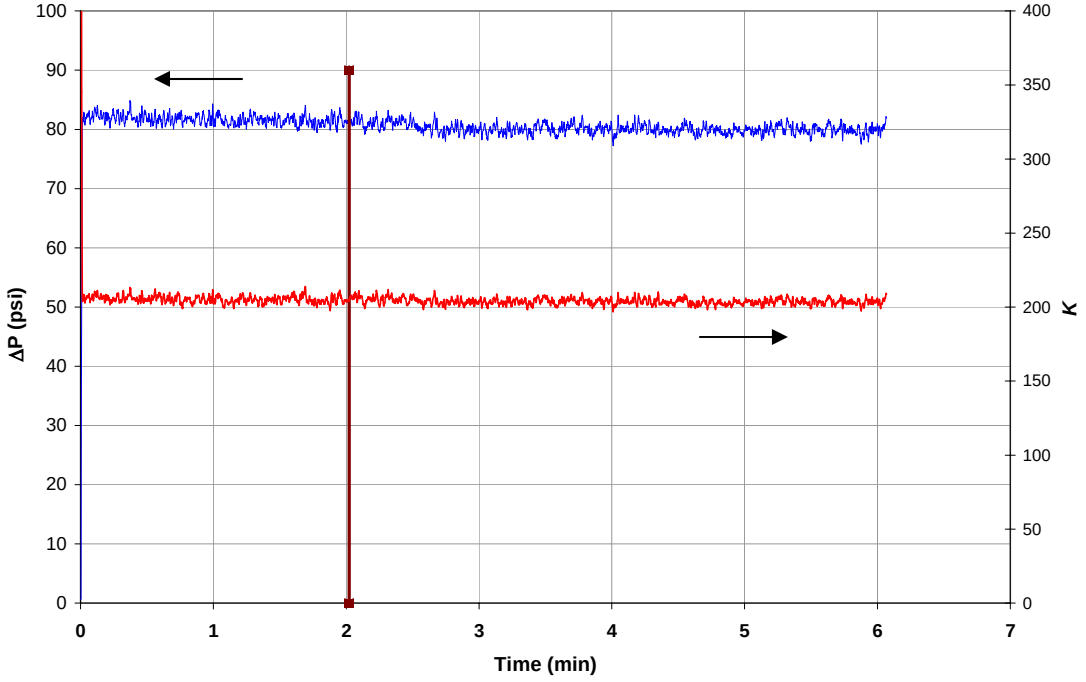
ΔP (psi)
K
Time (min)
0
10
20
30
40
50
60
70
80
90
100
0
50
100
150
200
250
300
350
400
0
1
2
3
4
5
6
7

5SDT5

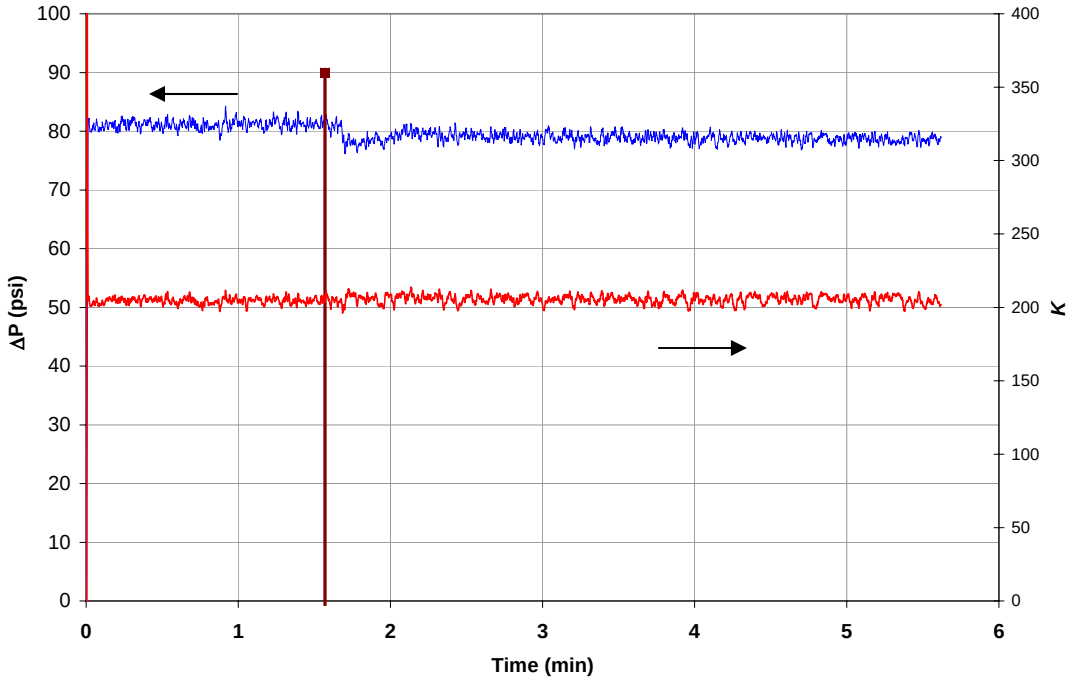
ΔP (psi)
K
Time (min)
0
10
20
30
40
50
60
70
80
90
100
0
50
100
150
200
250
300
350
400
0
1
2
3
4
5
6

5SDT6

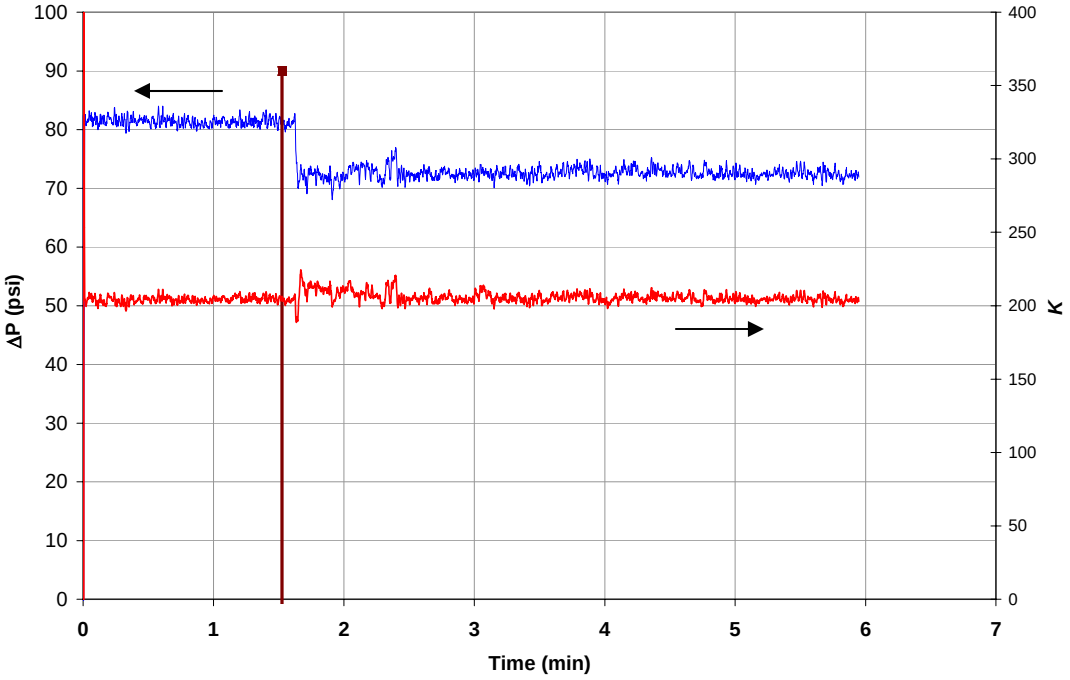
ΔP (psi)
K
Time (min)
0
10
20
30
40
50
60
70
80
90
100
0
50
100
150
200
250
300
350
400
0
1
2
3
4
5
6
7

5SDT7

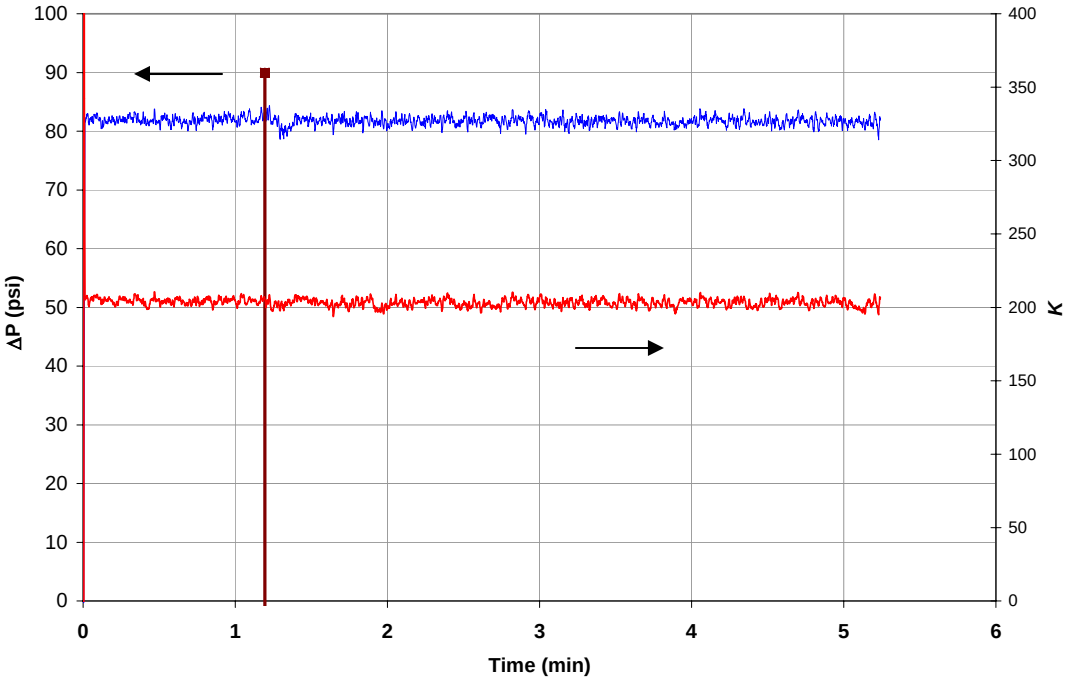
ΔP (psi)
K
Time (min)
0
10
20
30
40
50
60
70
80
90
100
0
50
100
150
200
250
300
350
400
0
1
2
3
4
5
6

5SDT8

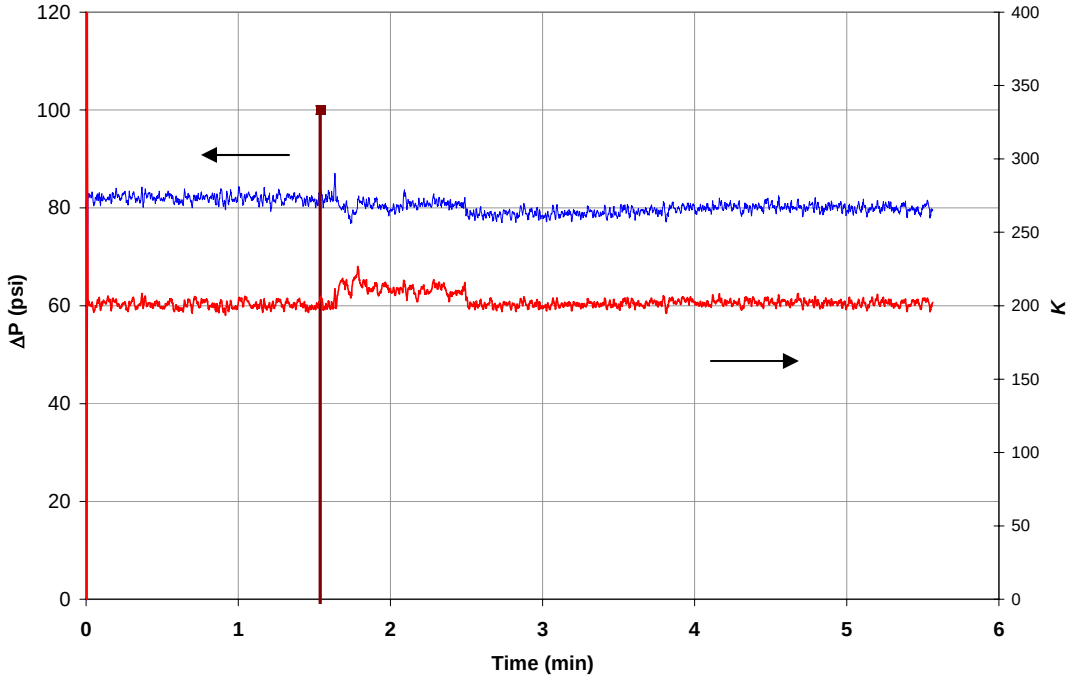
120
100
80
60
40
20
0
ΔP (psi)
400
350
300
250
200
150
100
50
0
K
0
1
2
3
4
5
6
Time (min)

5SDT9

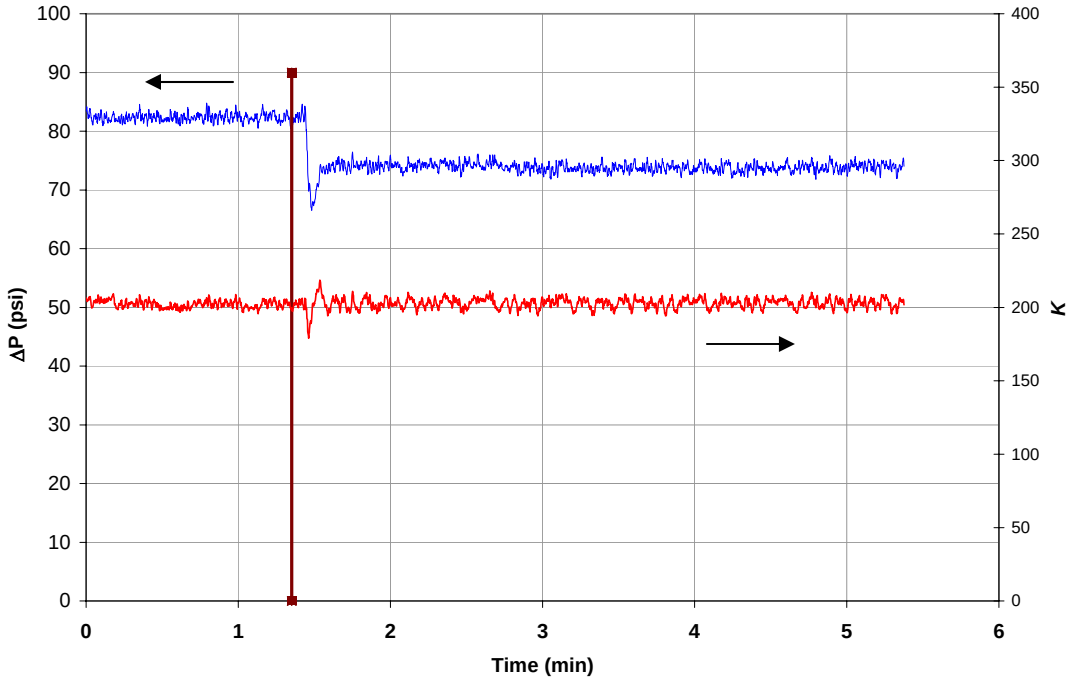
100
90
80
70
60
50
40
30
20
10
0
ΔP (psi)
400
350
300
250
200
150
100
50
0
K
0
1
2
3
4
5
6
Time (min)

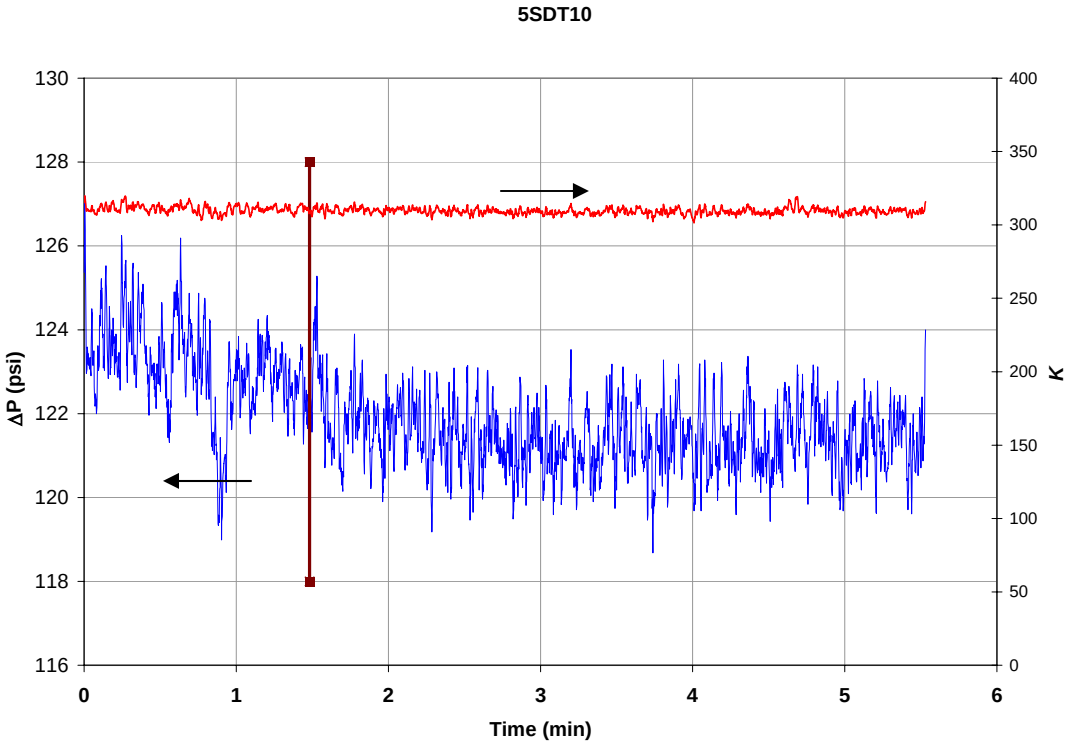
5SDT10
130
128
126
124
122
120
118
116
ΔP (psi)
400
350
300
250
200
150
100
50
0
K
0
1
2
3
4
5
6
Time (min)

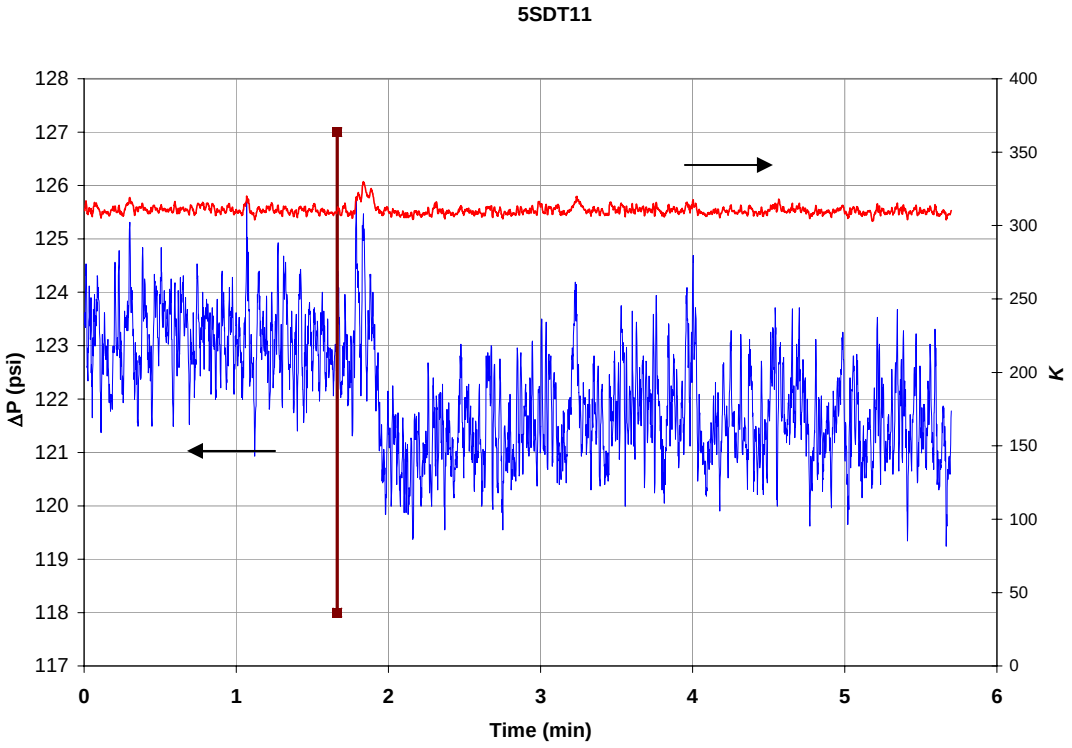
5SDT11
128
127
126
125
124
123
122
121
120
119
118
117
ΔP (psi)
400
350
300
250
200
150
100
50
0
K
0
1
2
3
4
5
6
Time (min)

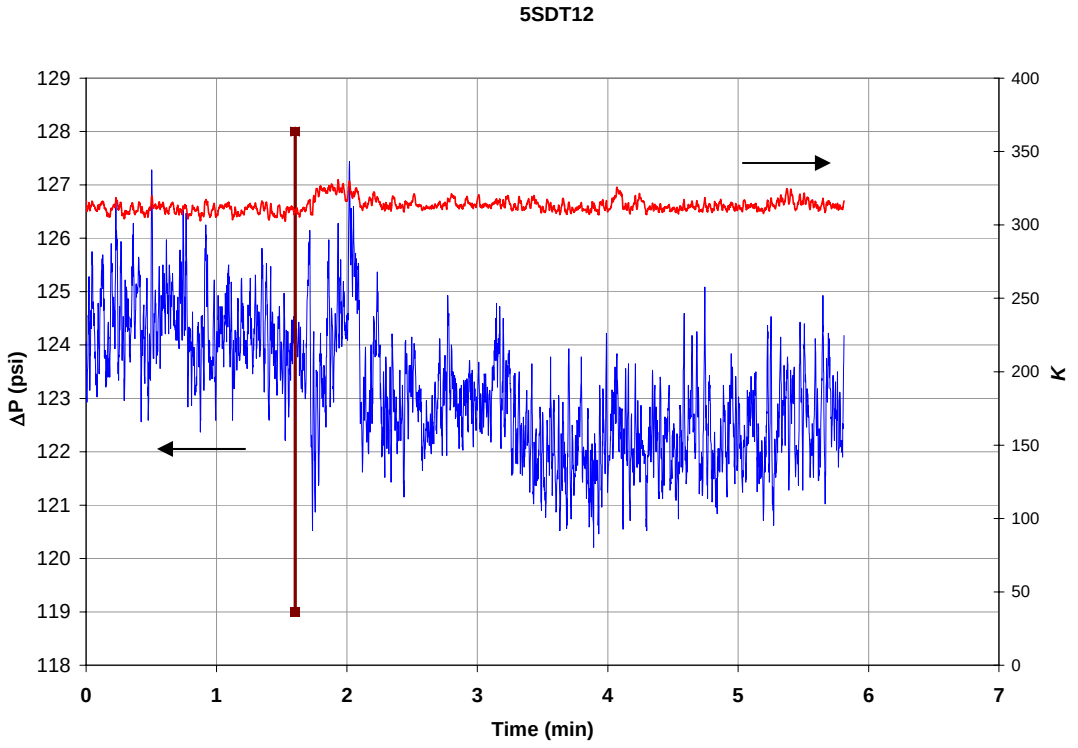
5SDT12
ΔP (psi)
K
Time (min)
129
128
127
126
125
124
123
122
121
120
119
118
400
350
300
250
200
150
100
50
0
0
1
2
3
4
5
6
7

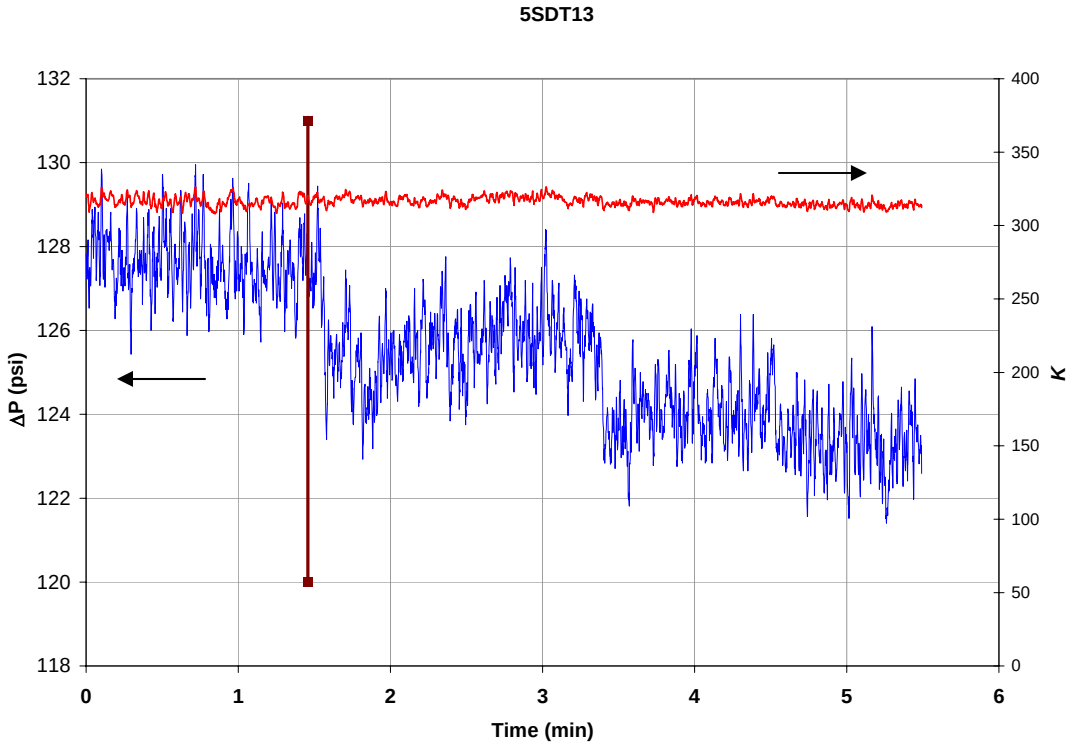
5SDT13
ΔP (psi)
K
Time (min)
132
130
128
126
124
122
120
118
400
350
300
250
200
150
100
50
0
0
1
2
3
4
5
6

5SDT14

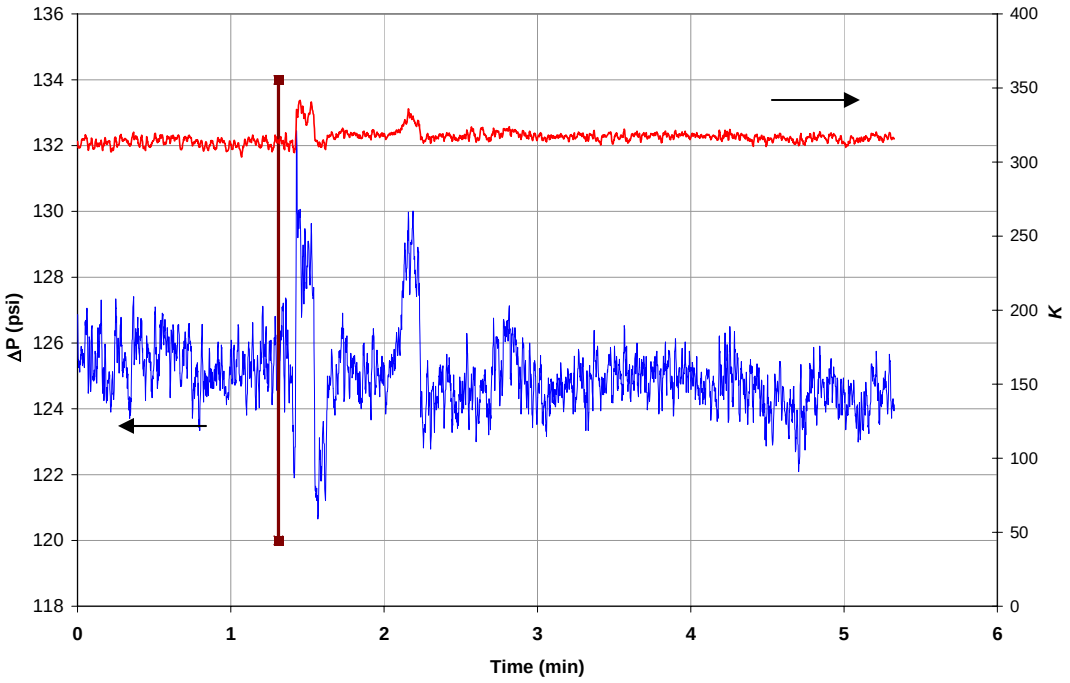

5SDT15

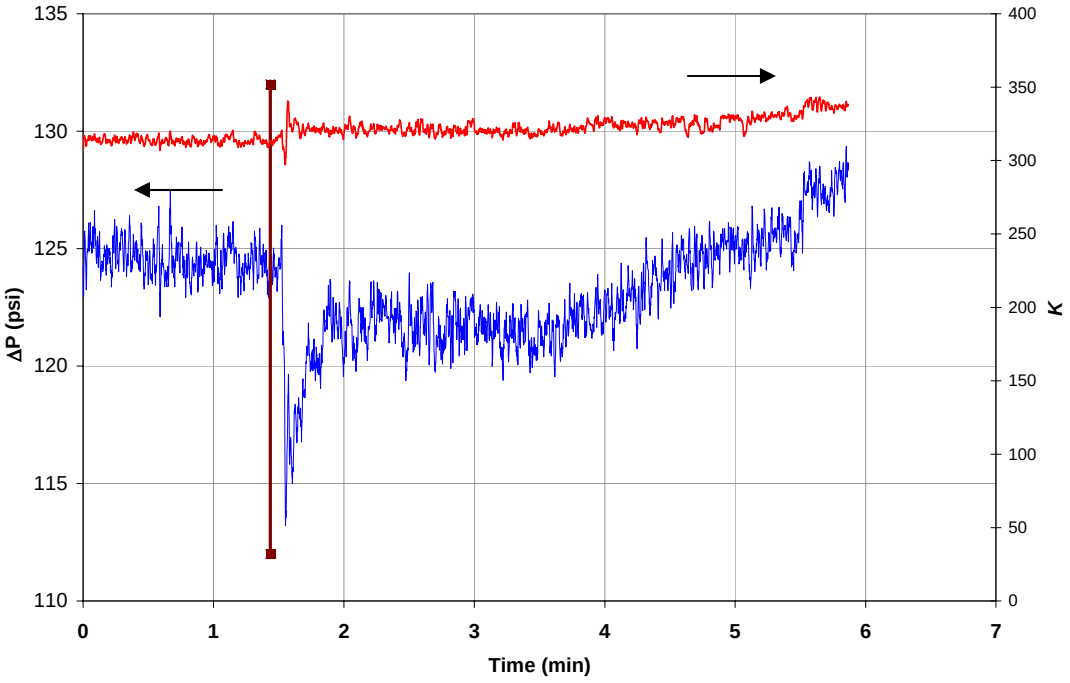

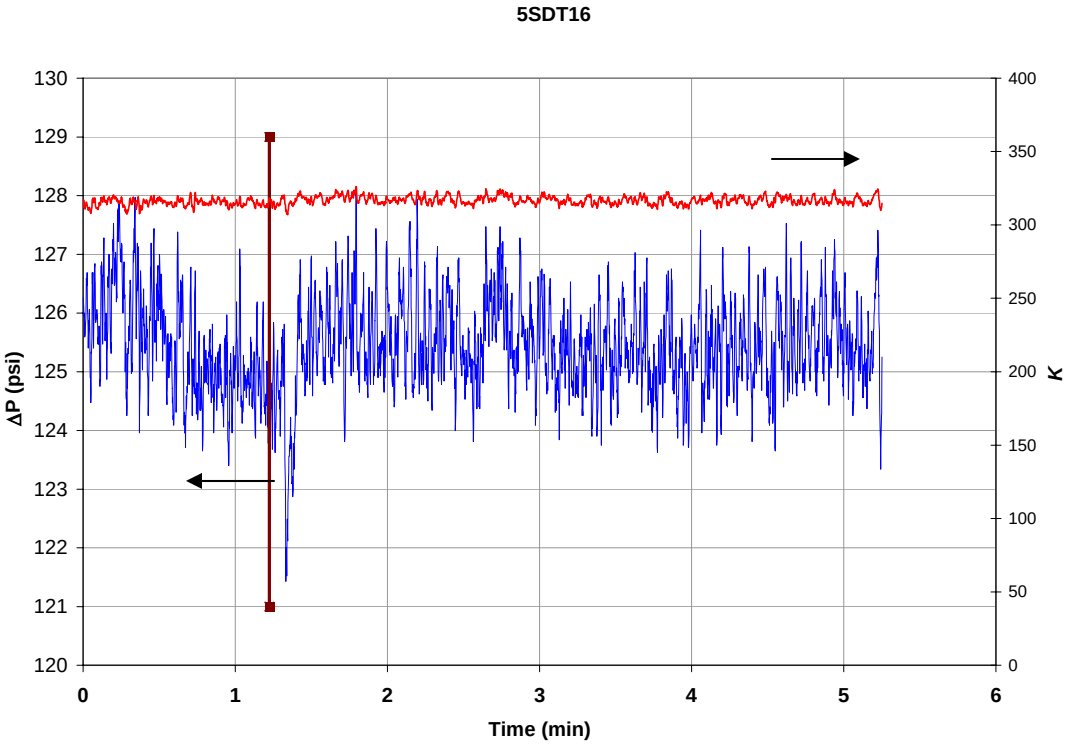
5SDT16
130
129
128
127
126
125
124
123
122
121
120
ΔP (psi)
400
350
300
250
200
150
100
50
0
K
0
1
2
3
4
5
6
Time (min)

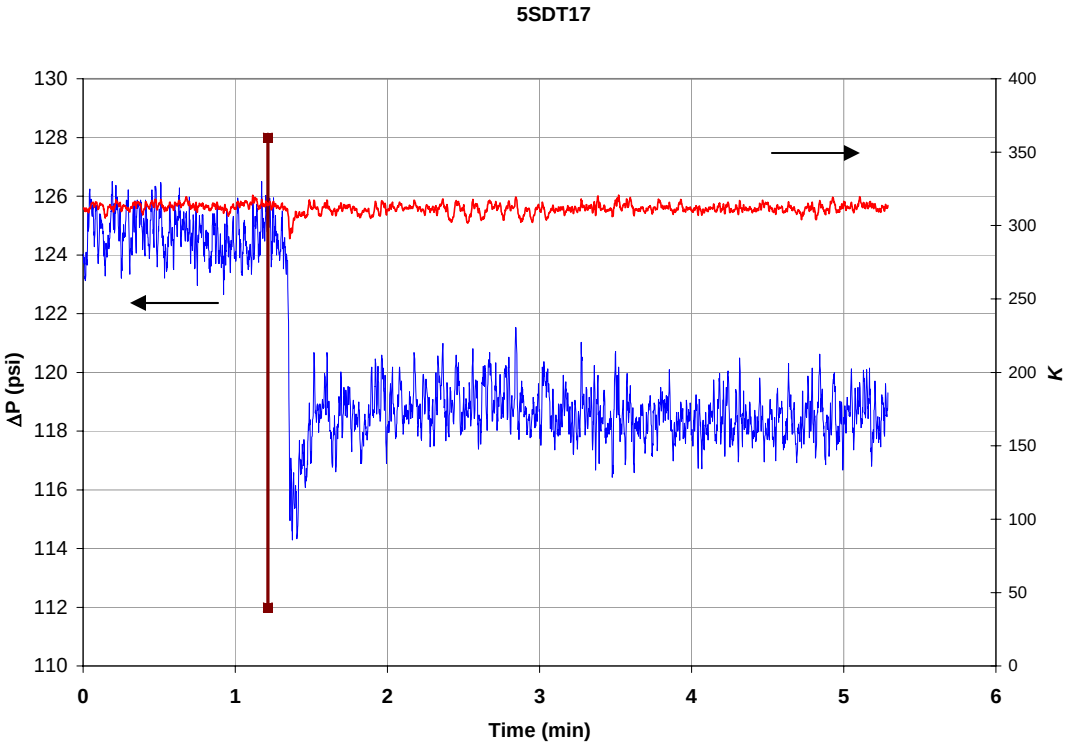
5SDT17
130
128
126
124
122
120
118
116
114
112
110
ΔP (psi)
400
350
300
250
200
150
100
50
0
K
0
1
2
3
4
5
6
Time (min)

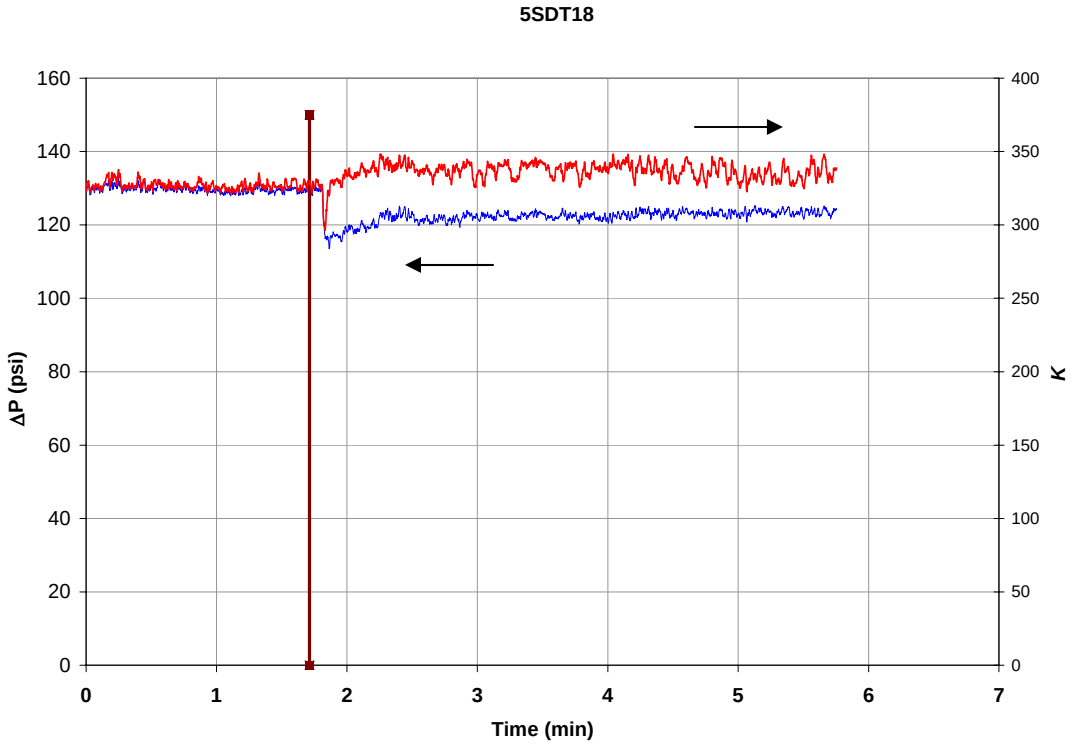
5SDT18
160
140
120
100
80
60
40
20
0
400
350
300
250
200
150
100
50
0
ΔP (psi)
K
0
1
2
3
4
5
6
7
Time (min)

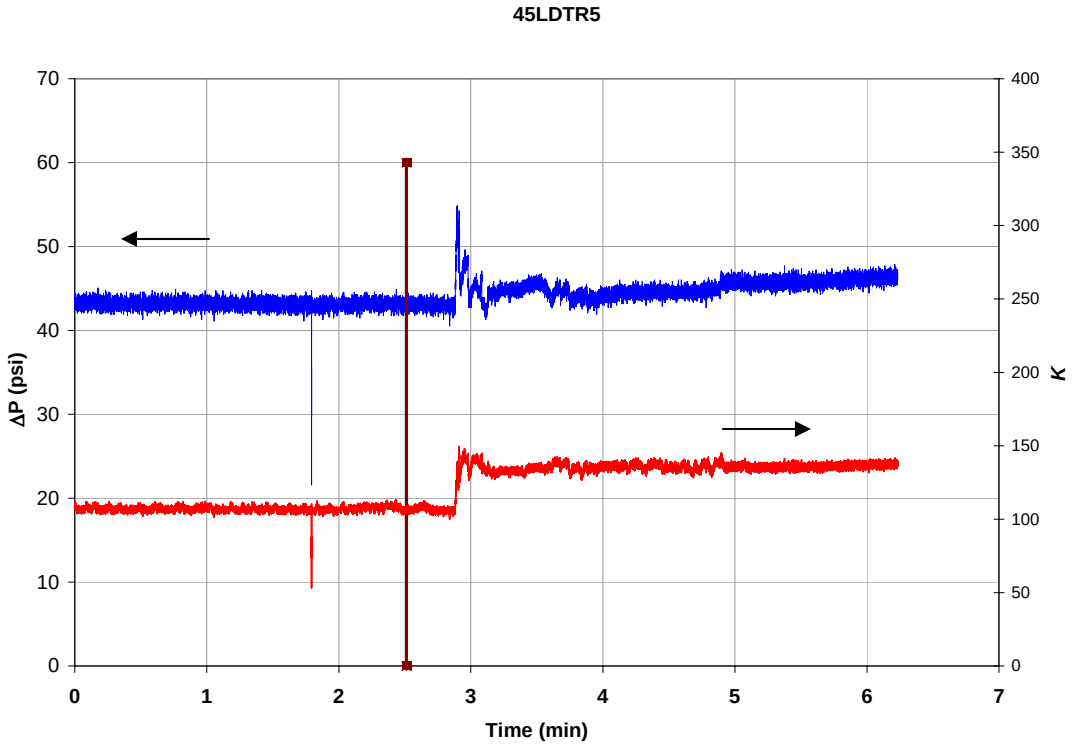
45LDTR5
70
60
50
40
30
20
10
0
400
350
300
250
200
150
100
50
0
ΔP (psi)
K
0
1
2
3
4
5
6
7
Time (min)

45LDTR9

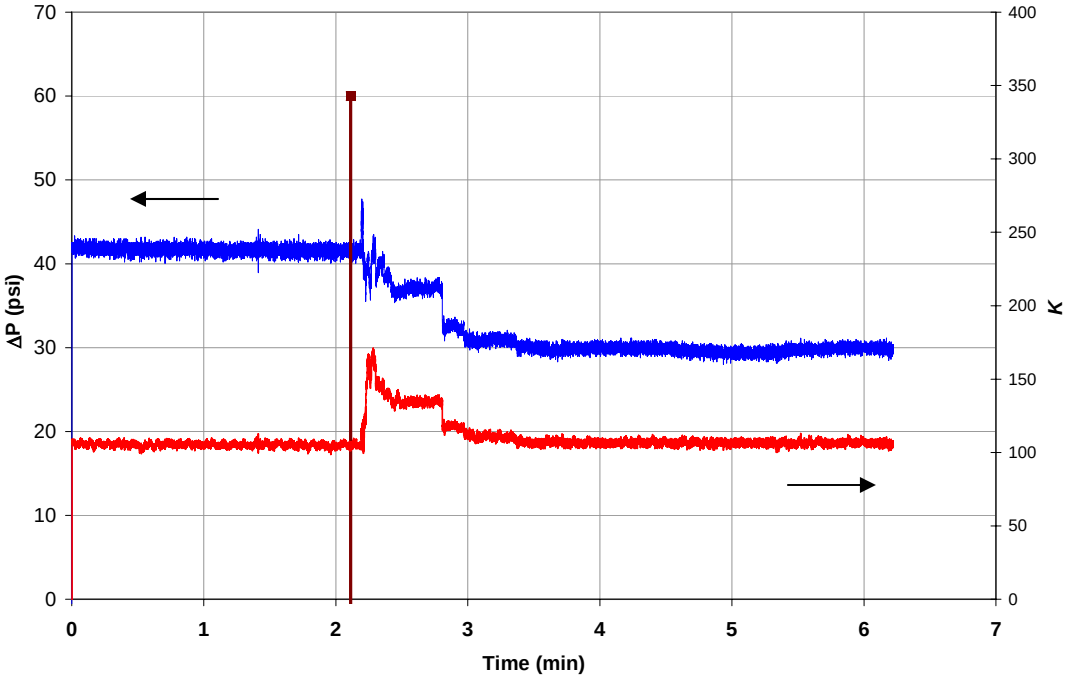

45LDTR11

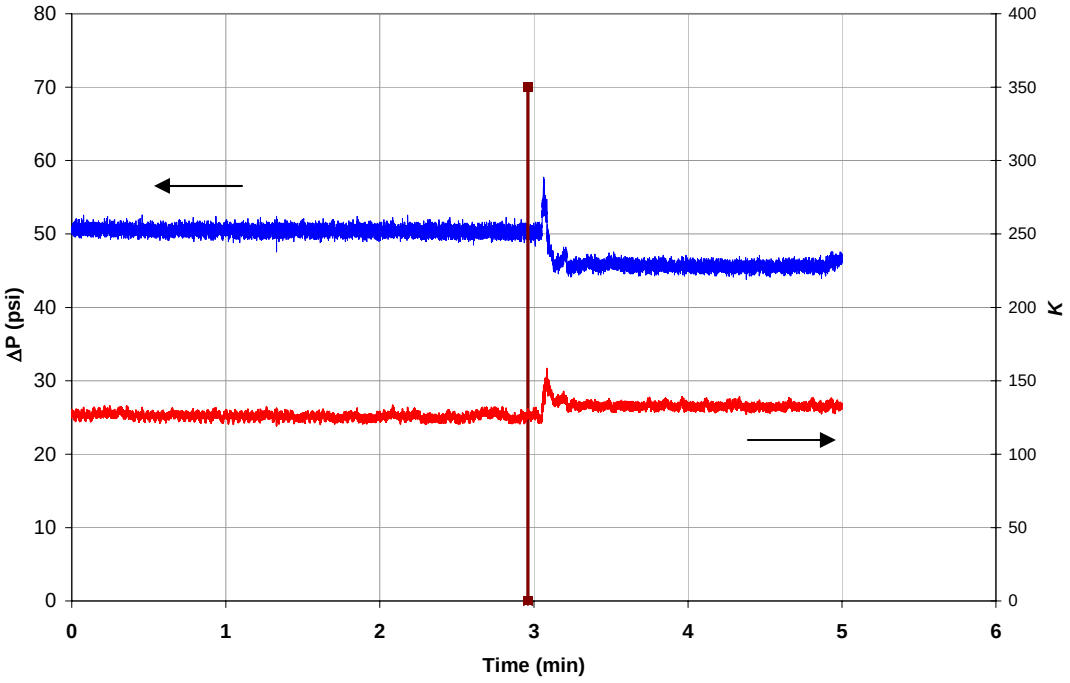

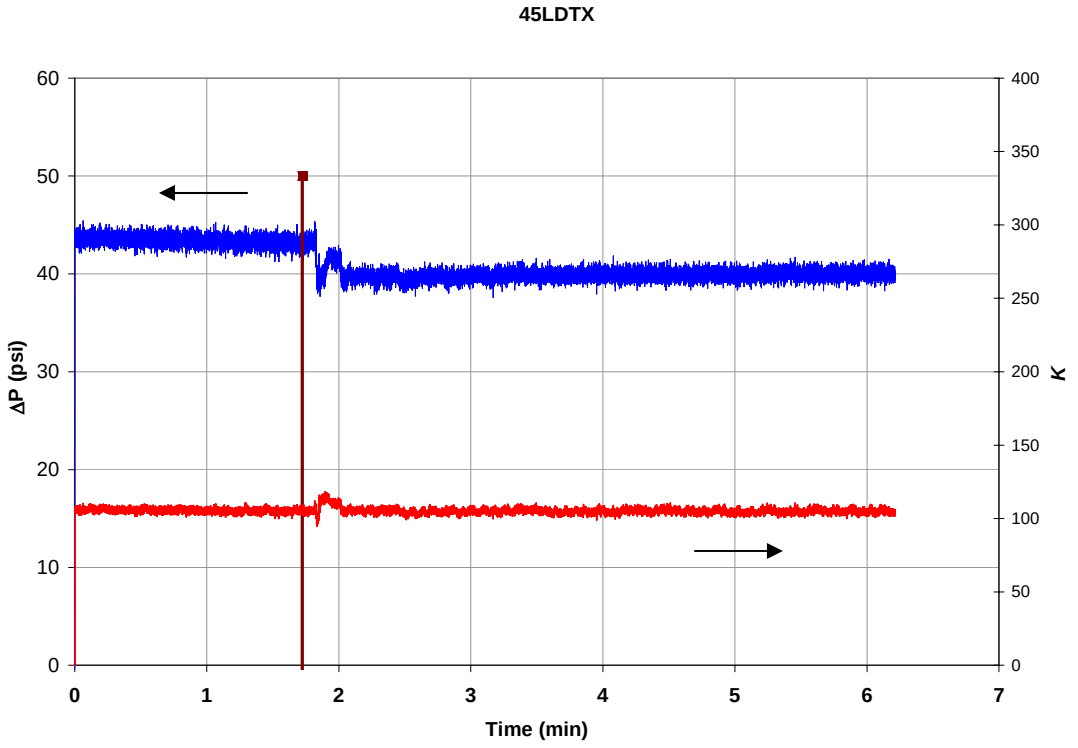
45LDTX
ΔP (psi)
K
Time (min)
0
10
20
30
40
50
60
0
50
100
150
200
250
300
350
400
0
1
2
3
4
5
6
7

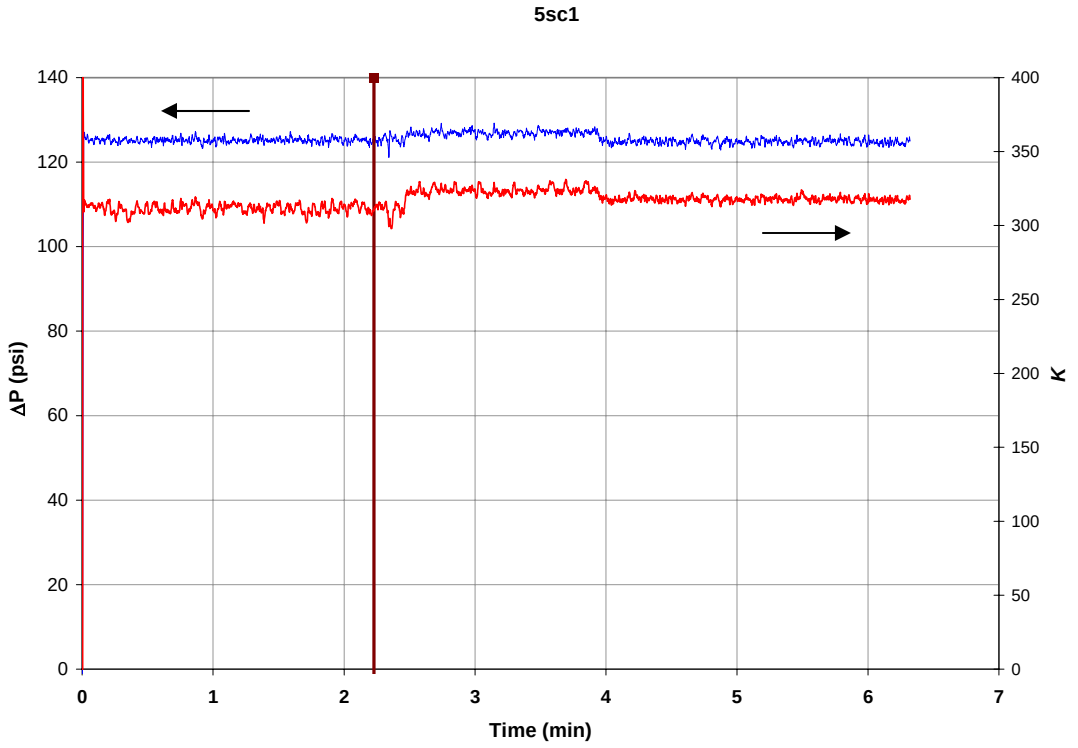
5sc1
ΔP (psi)
K
Time (min)
0
20
40
60
80
100
120
140
0
50
100
150
200
250
300
350
400
0
1
2
3
4
5
6
7

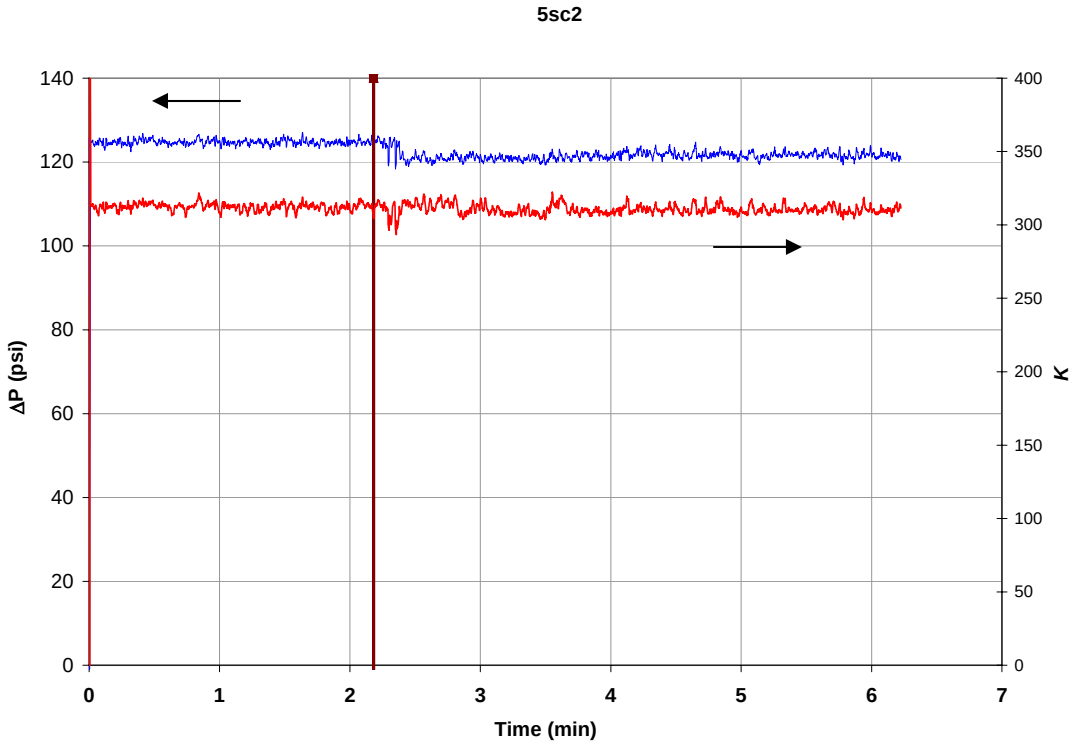
5sc2
ΔP (psi)
K
Time (min)
0
20
40
60
80
100
120
140
0
50
100
150
200
250
300
350
400
0
1
2
3
4
5
6
7

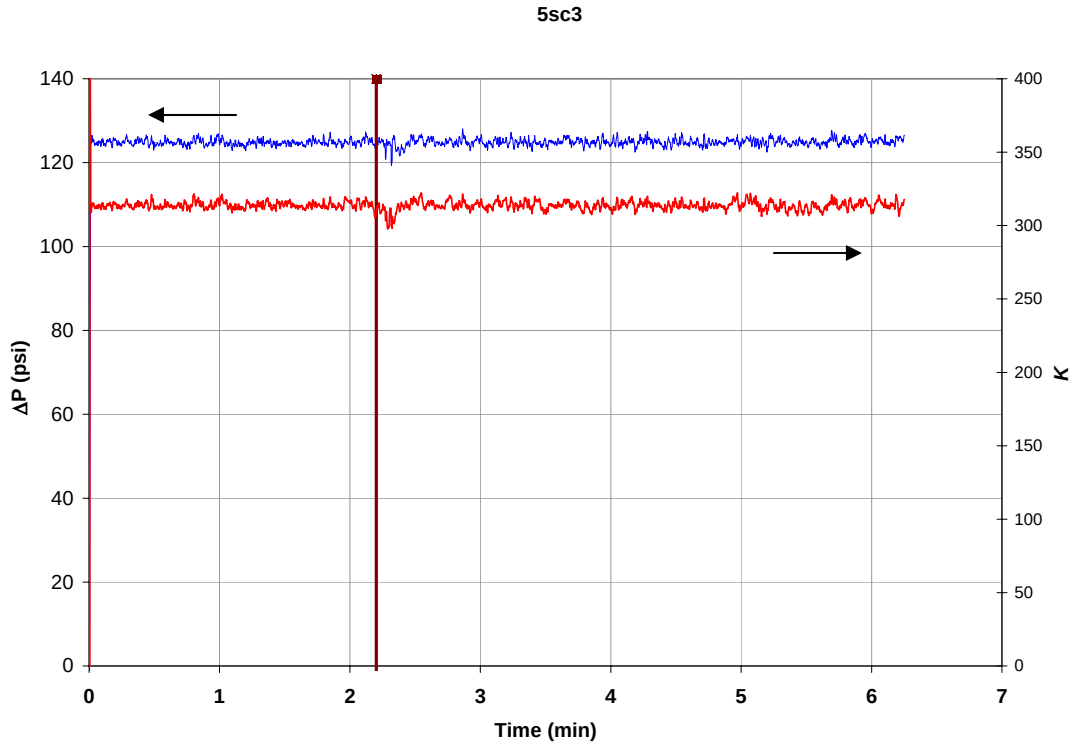
5sc3
ΔP (psi)
K
Time (min)
0
20
40
60
80
100
120
140
0
50
100
150
200
250
300
350
400
0
1
2
3
4
5
6
7

5sc4

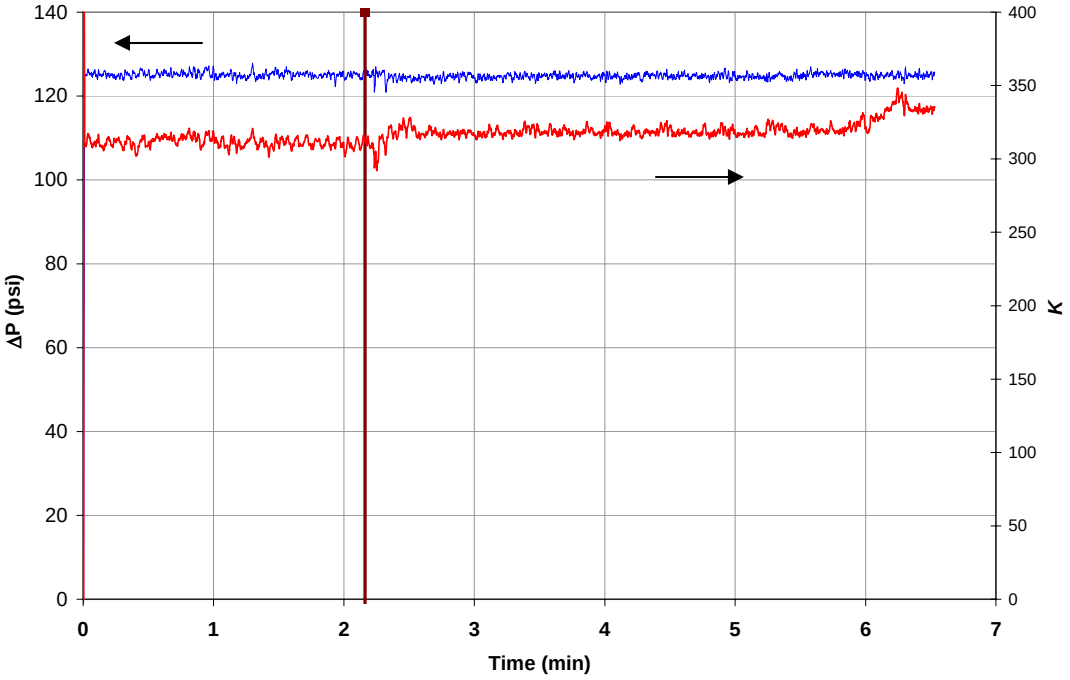
140
120
100
80
60
40
20
0
ΔP (psi)
400
350
300
250
200
150
100
50
0
K
0
1
2
3
4
5
6
7
Time (min)

5sc5

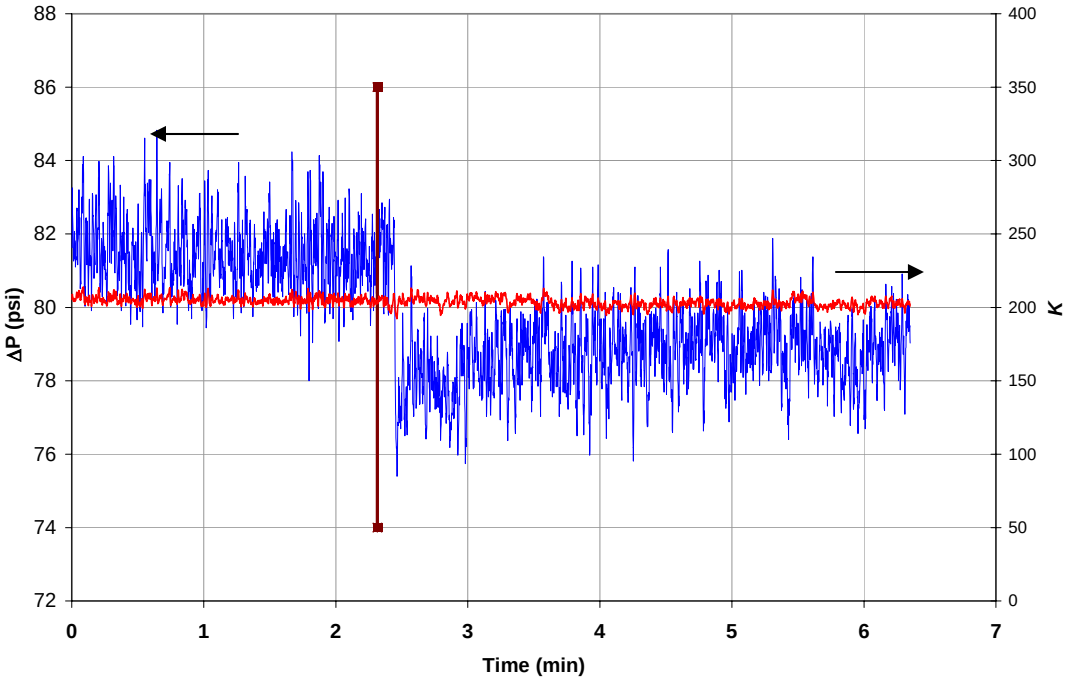
88
86
84
82
80
78
76
74
72
ΔP (psi)
400
350
300
250
200
150
100
50
0
K
0
1
2
3
4
5
6
7
Time (min)

5sc6

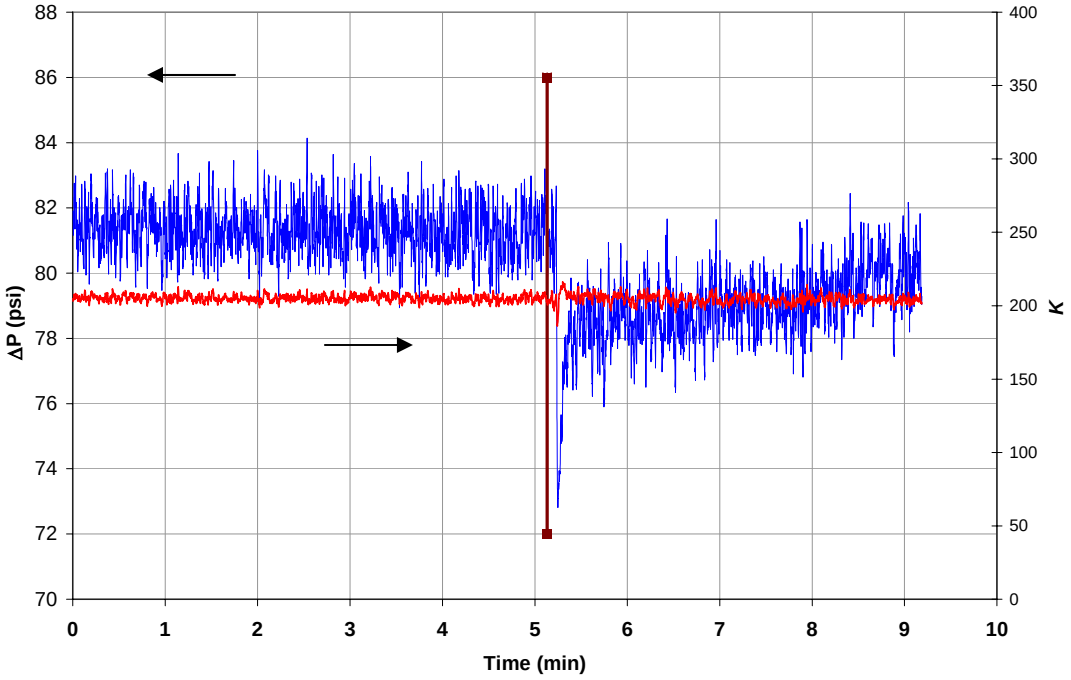
88
86
84
82
80
78
76
74
72
70
ΔP (psi)
400
350
300
250
200
150
100
50
0
K
0
1
2
3
4
5
6
7
8
9
10
Time (min)

5sc7

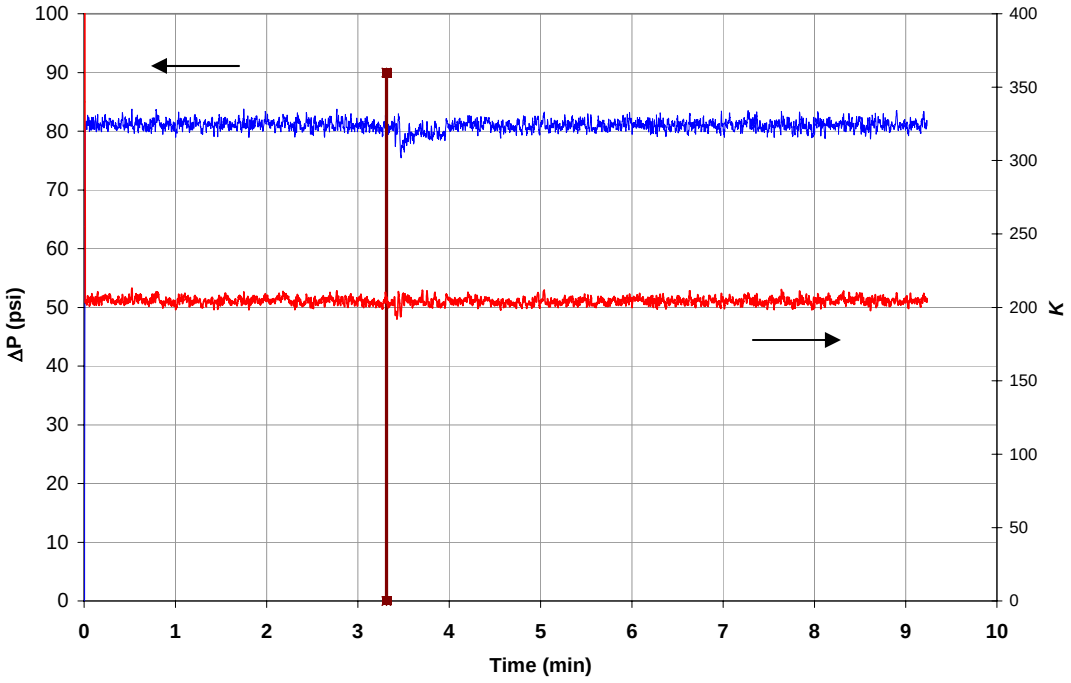
100
90
80
70
60
50
40
30
20
10
0
ΔP (psi)
400
350
300
250
200
150
100
50
0
K
0
1
2
3
4
5
6
7
8
9
10
Time (min)

5sc8

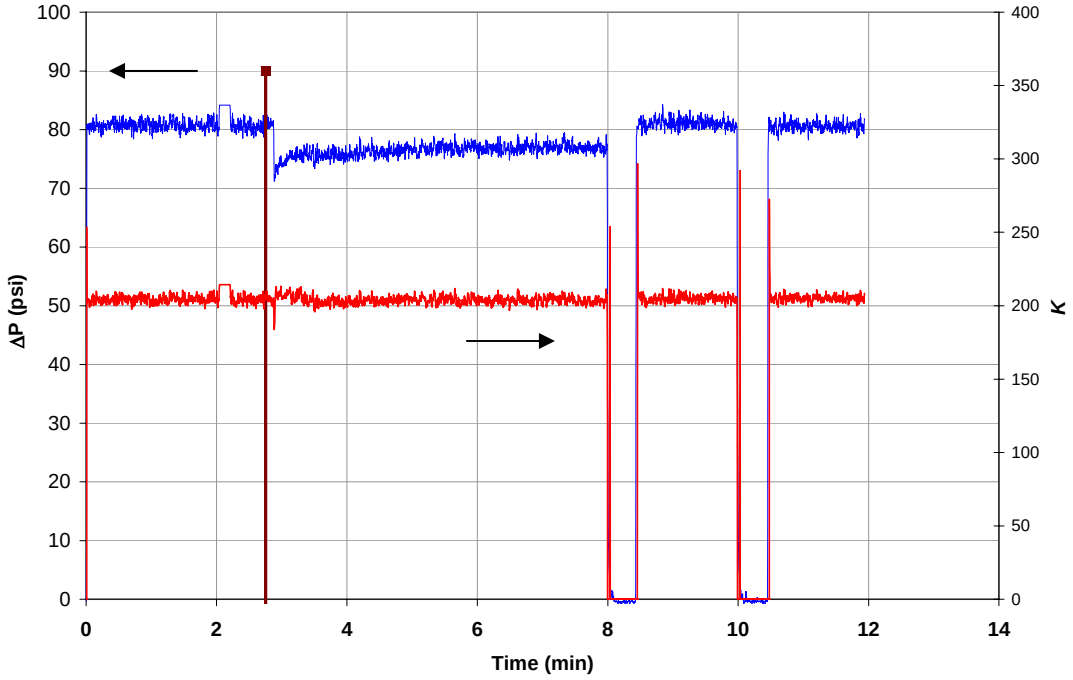
ΔP (psi)
K
Time (min)
0
10
20
30
40
50
60
70
80
90
100
0
50
100
150
200
250
300
350
400
0
2
4
6
8
10
12
14

5sc9

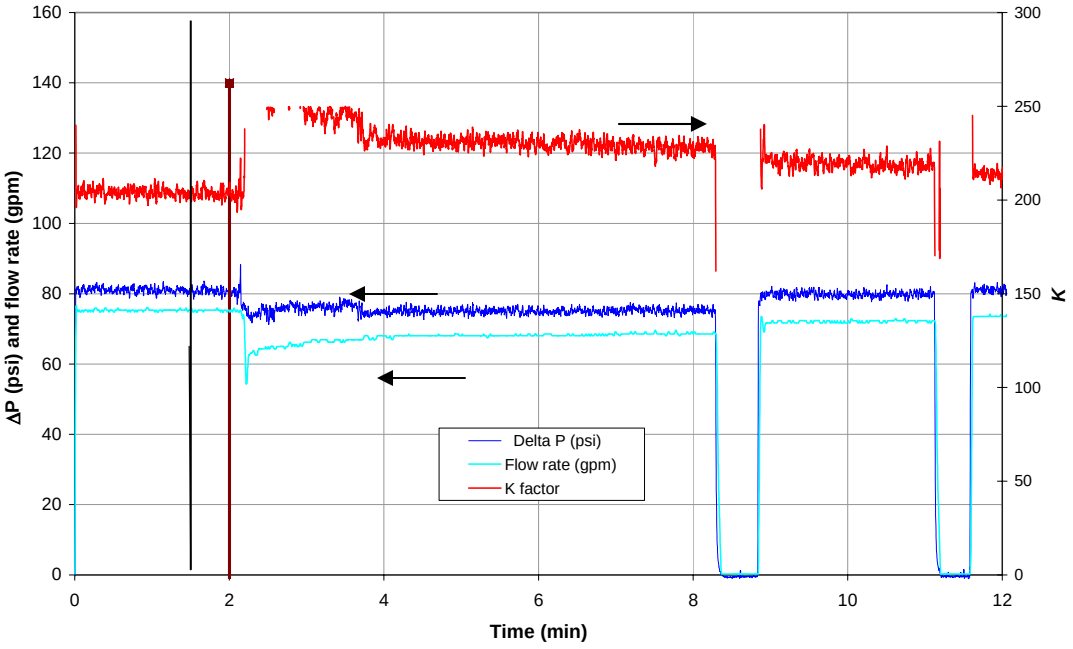
ΔP (psi) and flow rate (gpm)
K
Time (min)
Delta P (psi)
Flow rate (gpm)
K factor
0
20
40
60
80
100
120
140
160
0
50
100
150
200
250
300
0
2
4
6
8
10
12

5LC1

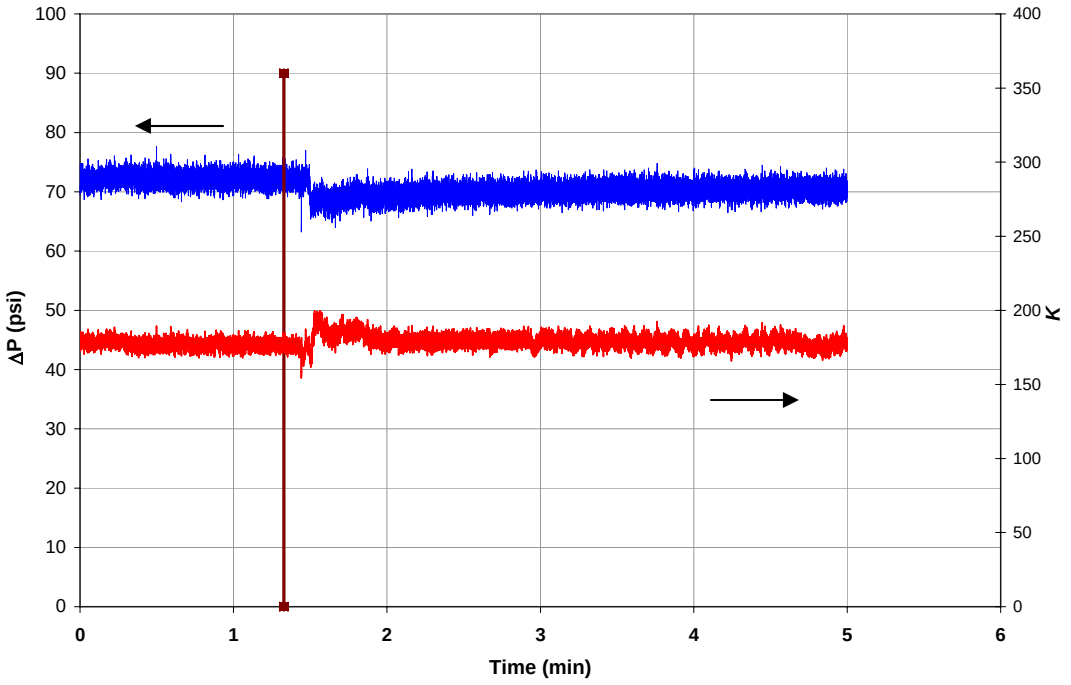
100
90
80
70
60
50
40
30
20
10
0
ΔP (psi)
400
350
300
250
200
150
100
50
0
K
0
1
2
3
4
5
6
Time (min)

5LC2

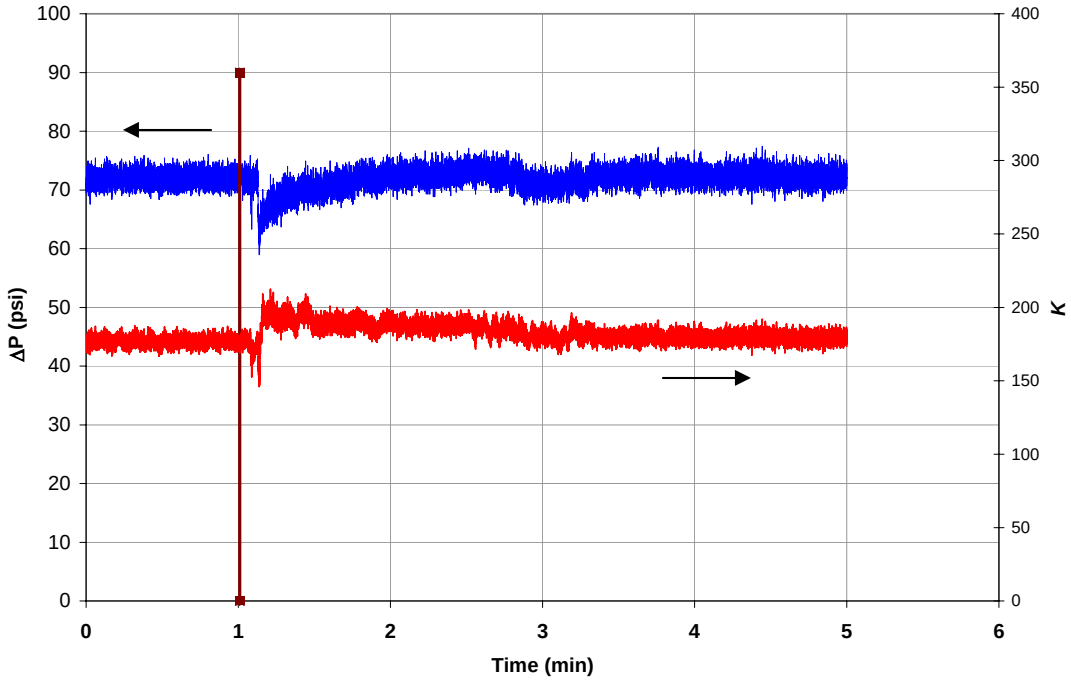
100
90
80
70
60
50
40
30
20
10
0
ΔP (psi)
400
350
300
250
200
150
100
50
0
K
0
1
2
3
4
5
6
Time (min)

5LC3

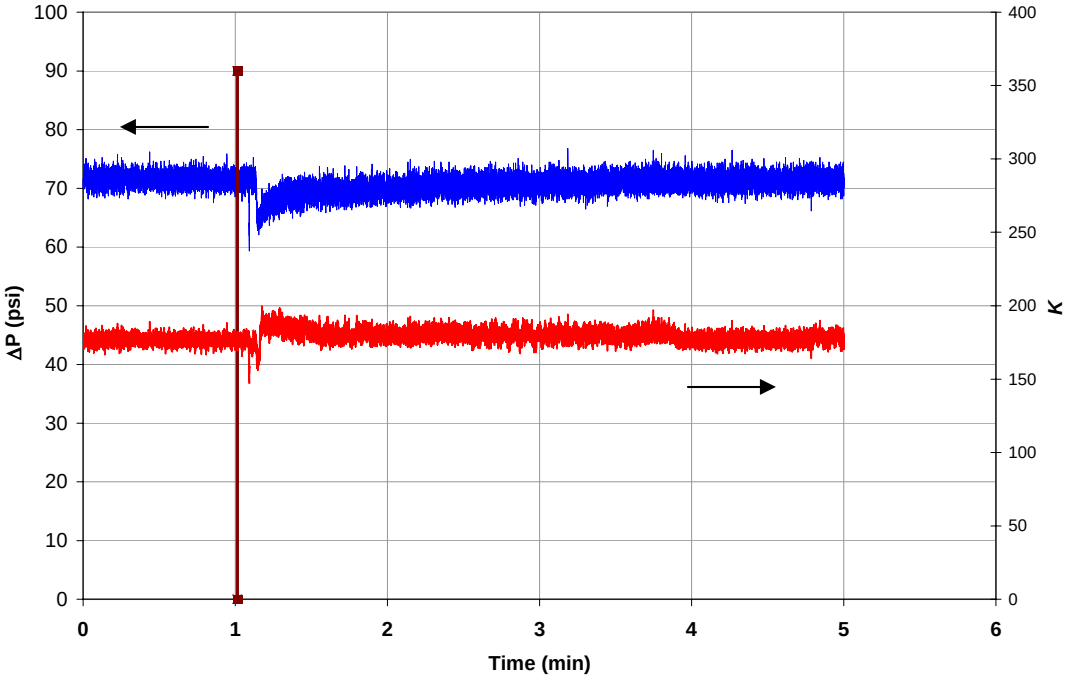
ΔP (psi)
K
Time (min)
0
10
20
30
40
50
60
70
80
90
100
0
50
100
150
200
250
300
350
400
0
1
2
3
4
5
6

5LC4

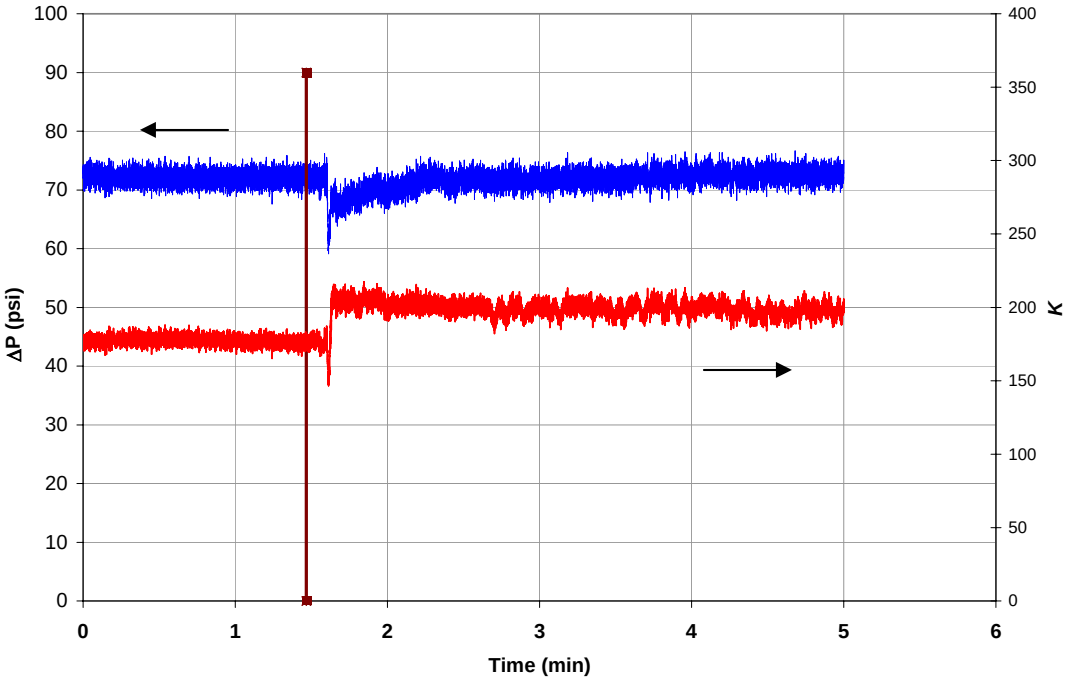
ΔP (psi)
K
Time (min)
0
10
20
30
40
50
60
70
80
90
100
0
50
100
150
200
250
300
350
400
0
1
2
3
4
5
6

5LN1

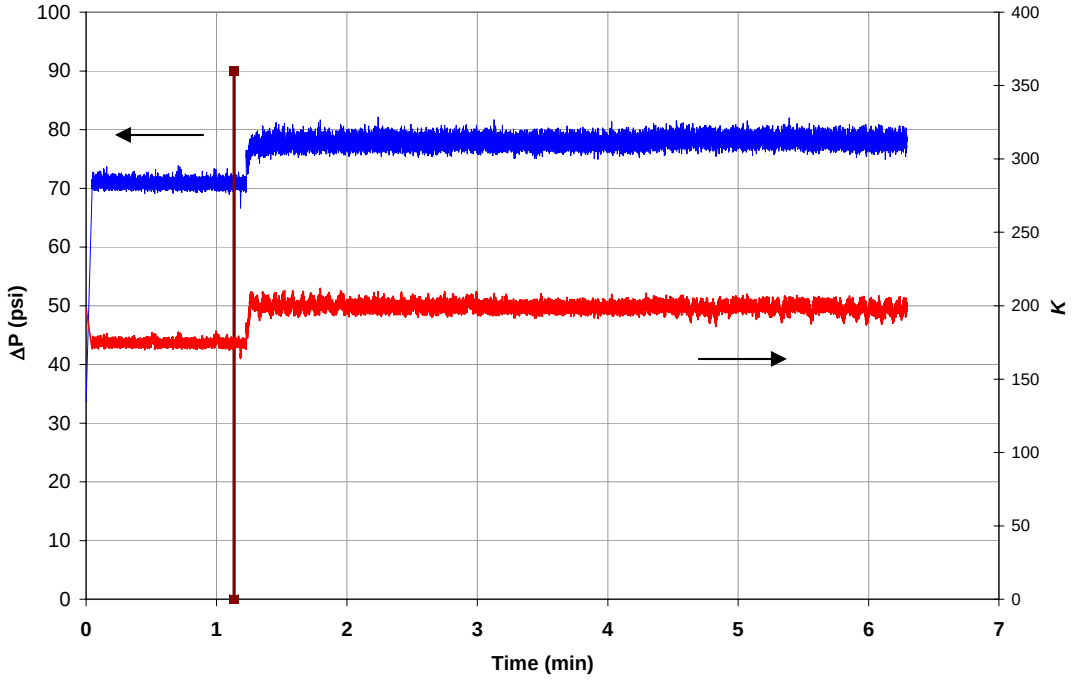
ΔP (psi)
K
Time (min)
0
10
20
30
40
50
60
70
80
90
100
0
50
100
150
200
250
300
350
400
0
1
2
3
4
5
6
7

5SN1

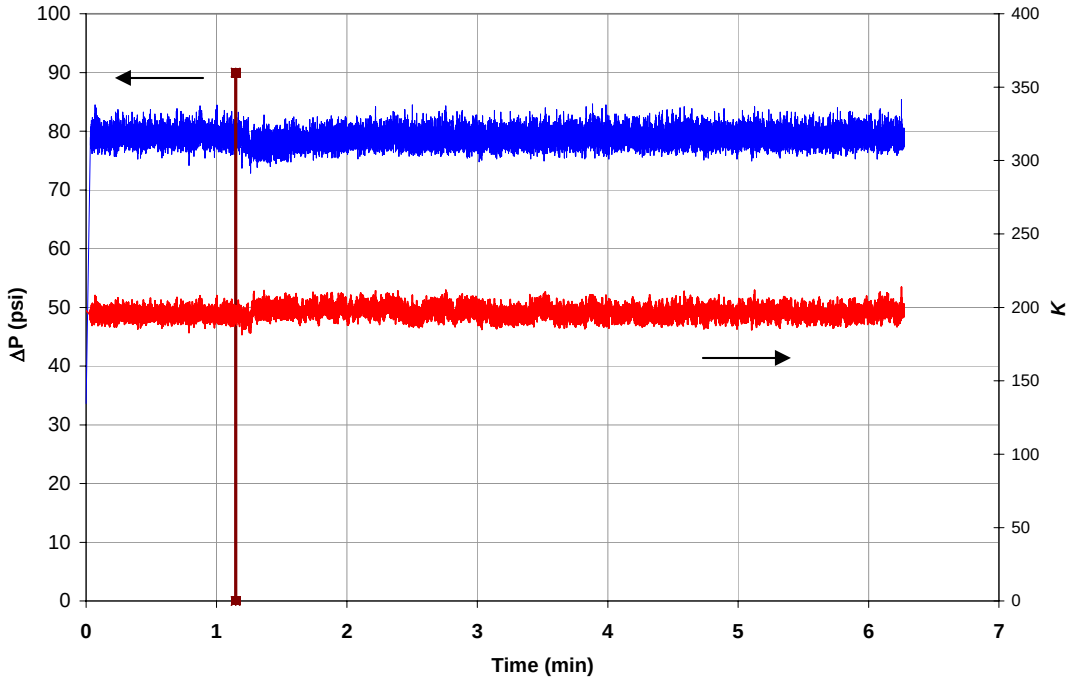
ΔP (psi)
K
Time (min)
0
10
20
30
40
50
60
70
80
90
100
0
50
100
150
200
250
300
350
400
0
1
2
3
4
5
6
7

5SN2

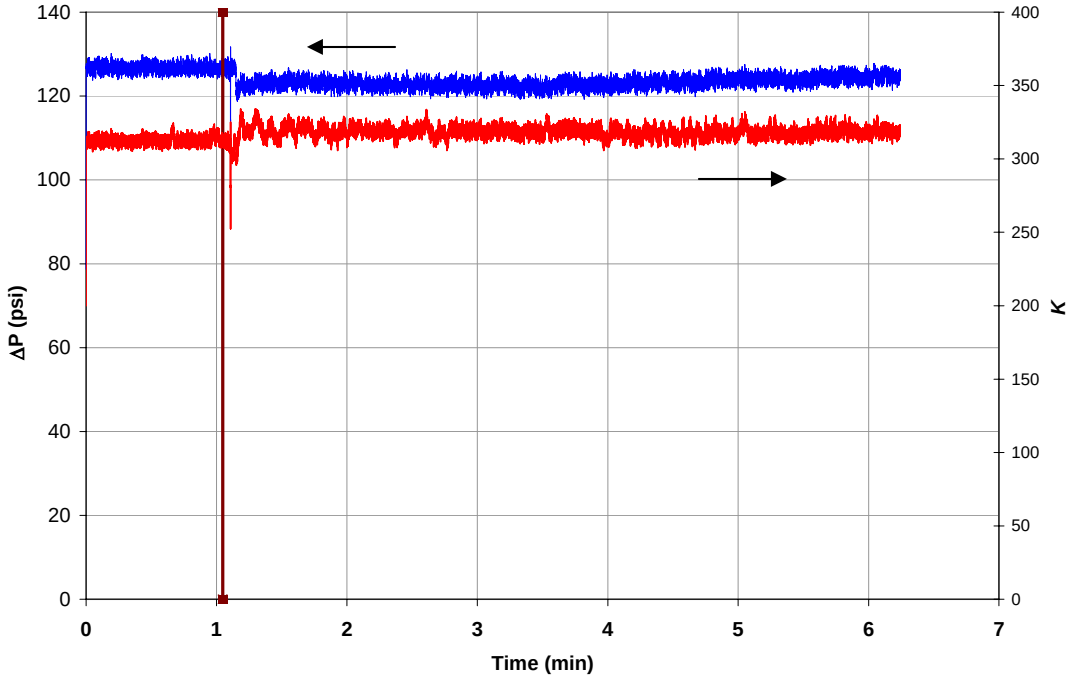
140
120
100
80
60
40
20
0
400
350
300
250
200
150
100
50
0
ΔP (psi)
K
0
1
2
3
4
5
6
7
Time (min)

45LN1

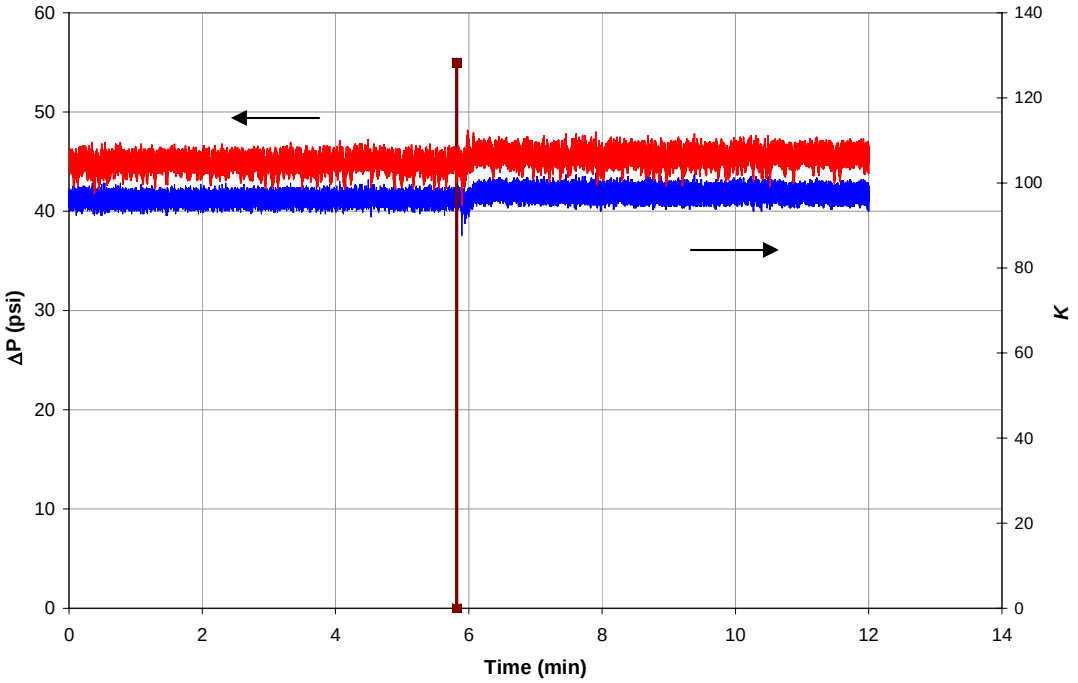
60
50
40
30
20
10
0
140
120
100
80
60
40
20
0
ΔP (psi)
K
0
2
4
6
8
10
12
14
Time (min)

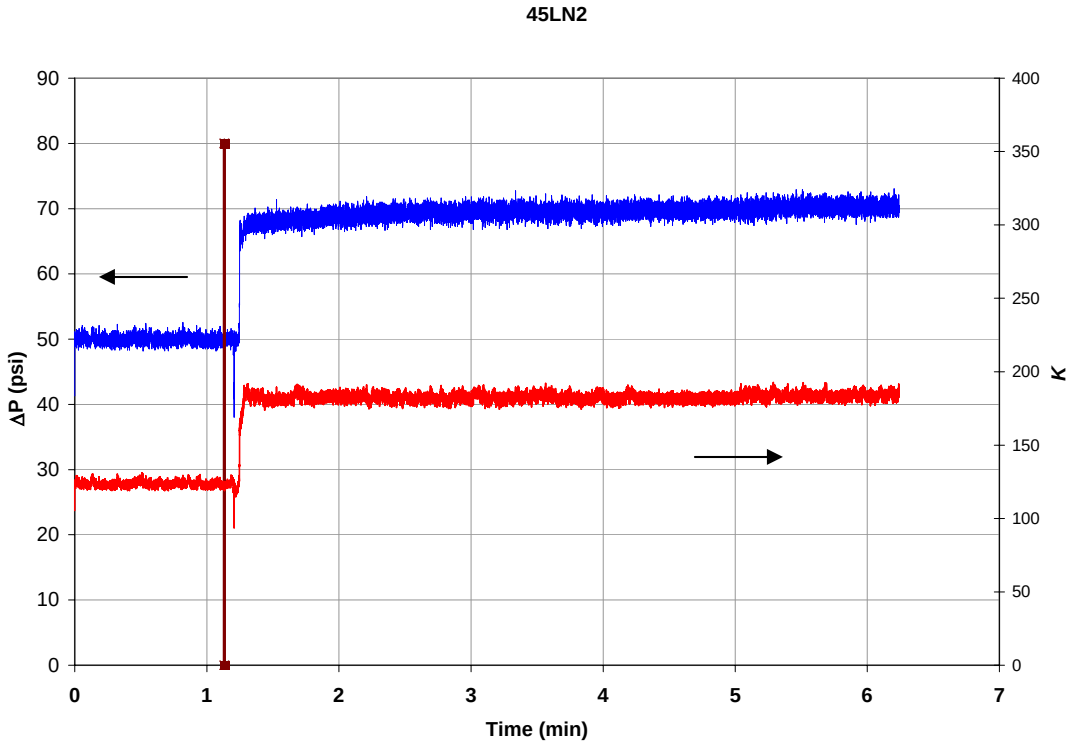
45LN2
ΔP (psi)
K
Time (min)
0
10
20
30
40
50
60
70
80
90
0
50
100
150
200
250
300
350
400
0
1
2
3
4
5
6
7

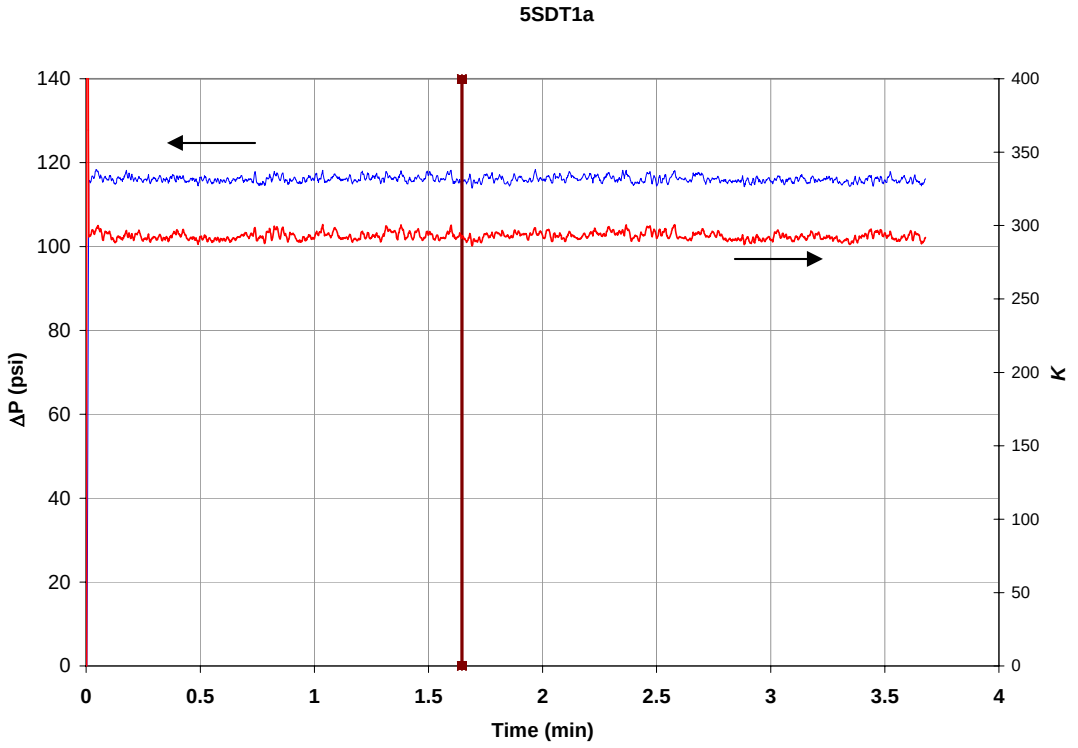
5SDT1a
ΔP (psi)
K
Time (min)
0
20
40
60
80
100
120
140
0
50
100
150
200
250
300
350
400
0
0.5
1
1.5
2
2.5
3
3.5
4

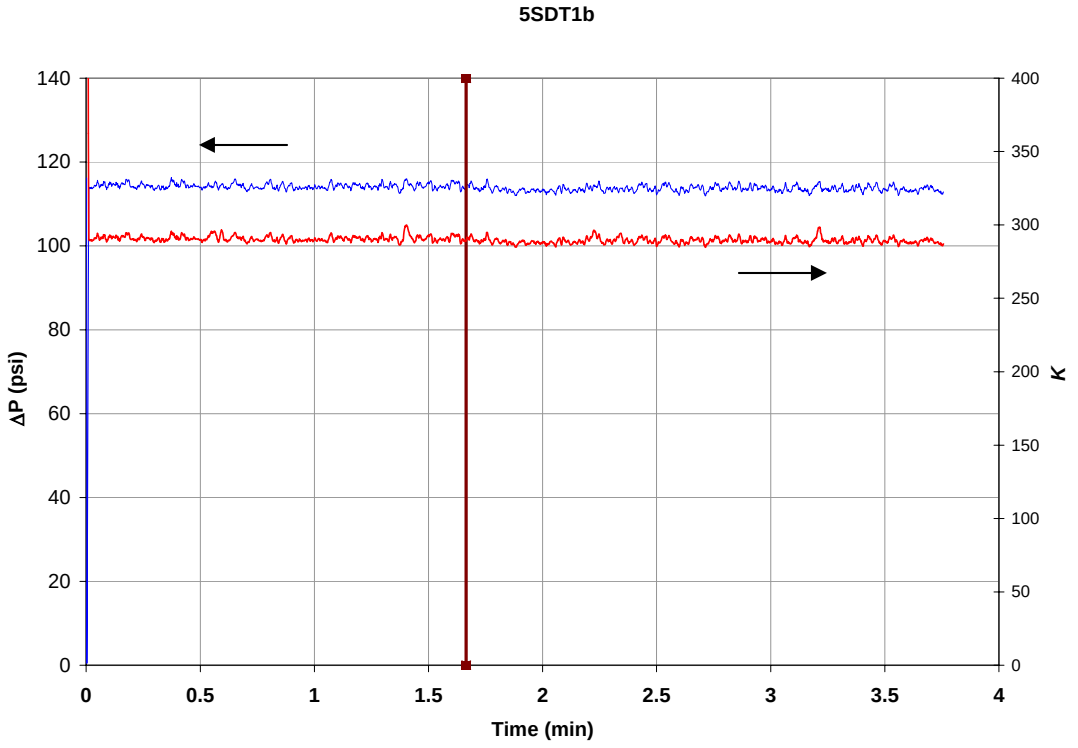
5SDT1b
ΔP (psi)
K
Time (min)
0
20
40
60
80
100
120
140
0
50
100
150
200
250
300
350
400
0
0.5
1
1.5
2
2.5
3
3.5
4

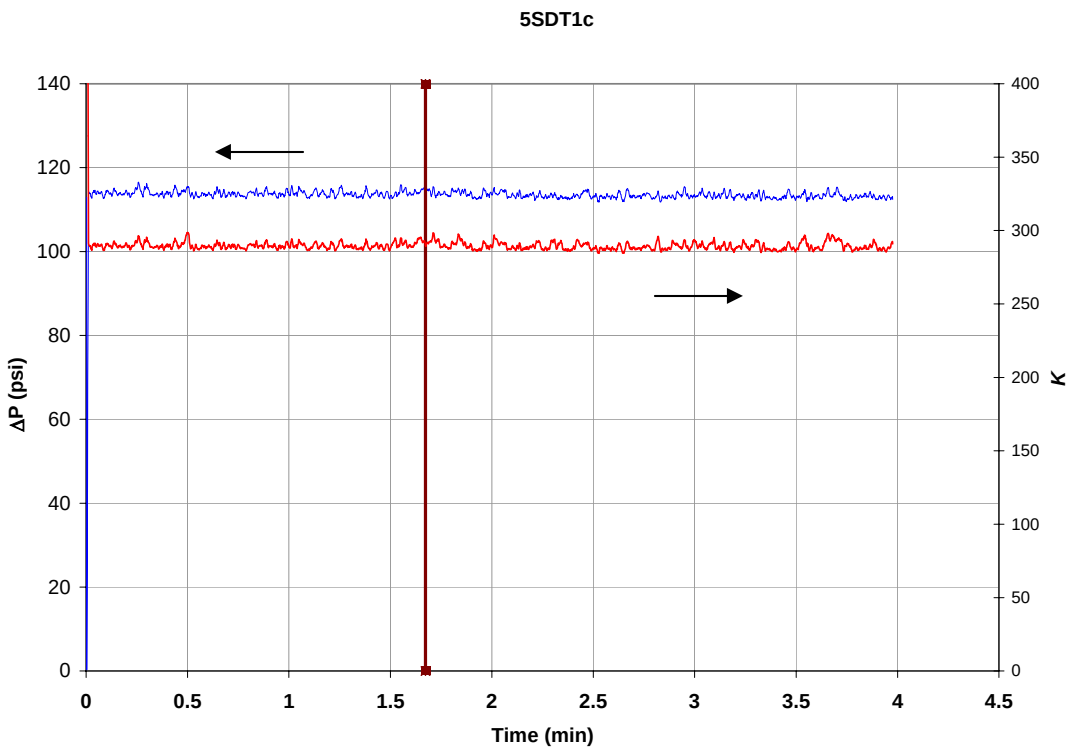
5SDT1c
ΔP (psi)
K
Time (min)
0
20
40
60
80
100
120
140
0
50
100
150
200
250
300
350
400
0
0.5
1
1.5
2
2.5
3
3.5
4
4.5

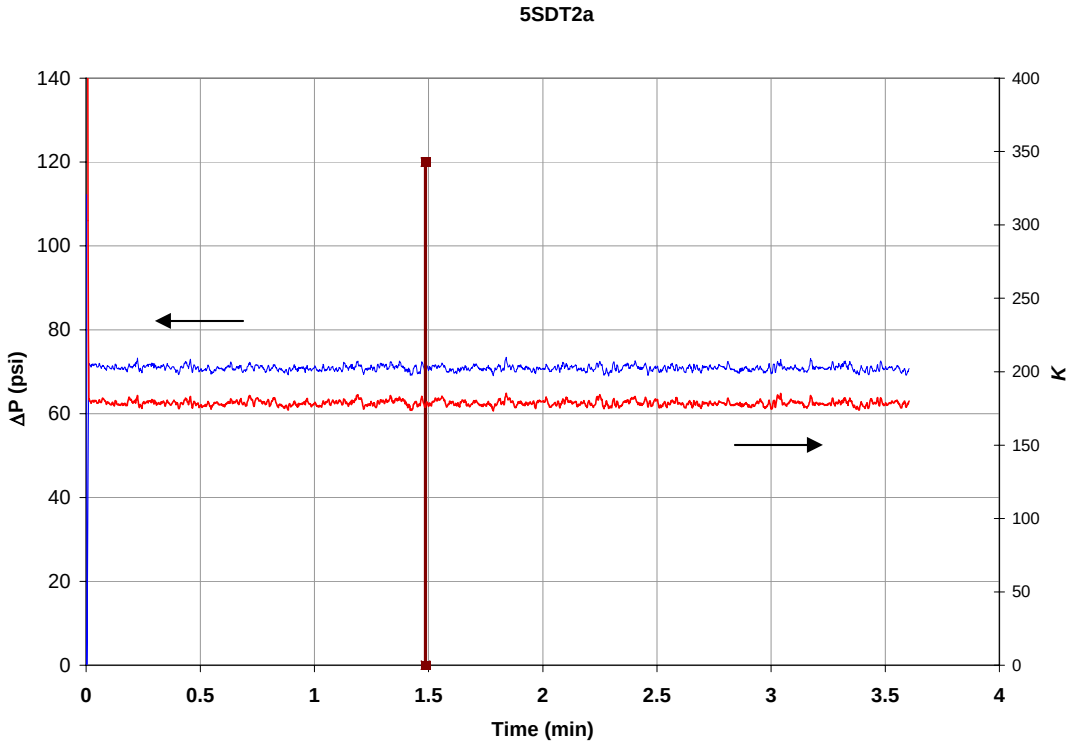
5SDT2a
ΔP (psi)
K
Time (min)
0
20
40
60
80
100
120
140
0
50
100
150
200
250
300
350
400
0
0.5
1
1.5
2
2.5
3
3.5
4

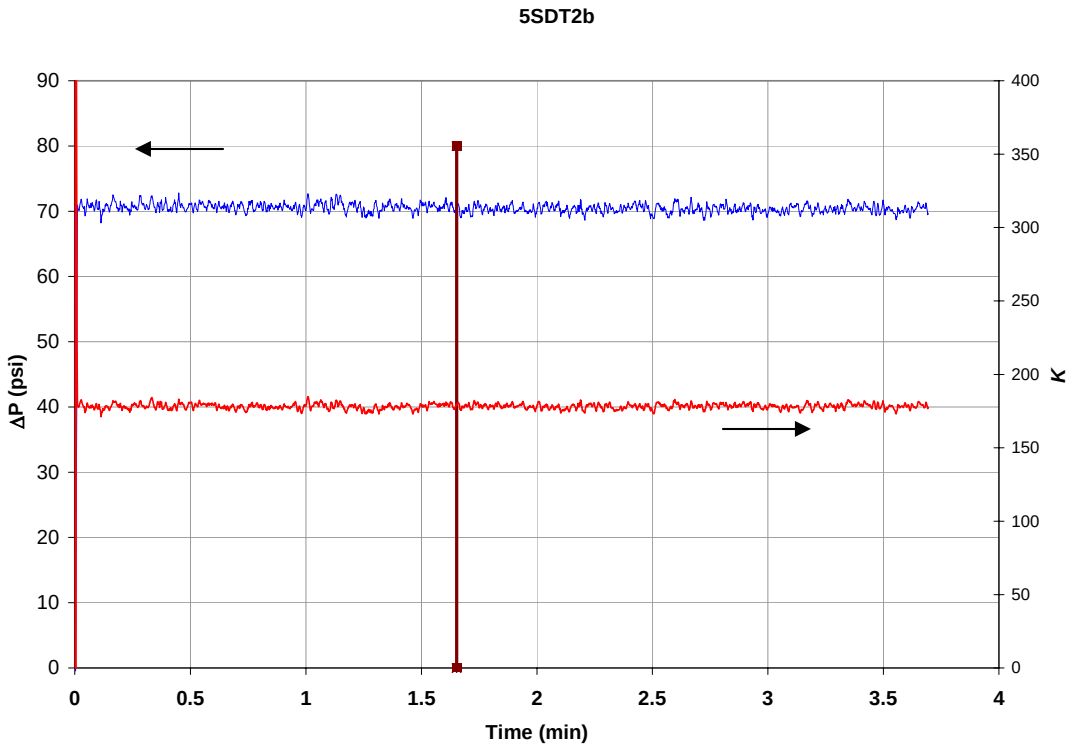
5SDT2b
ΔP (psi)
K
Time (min)
0
10
20
30
40
50
60
70
80
90
0
50
100
150
200
250
300
350
400
0
0.5
1
1.5
2
2.5
3
3.5
4

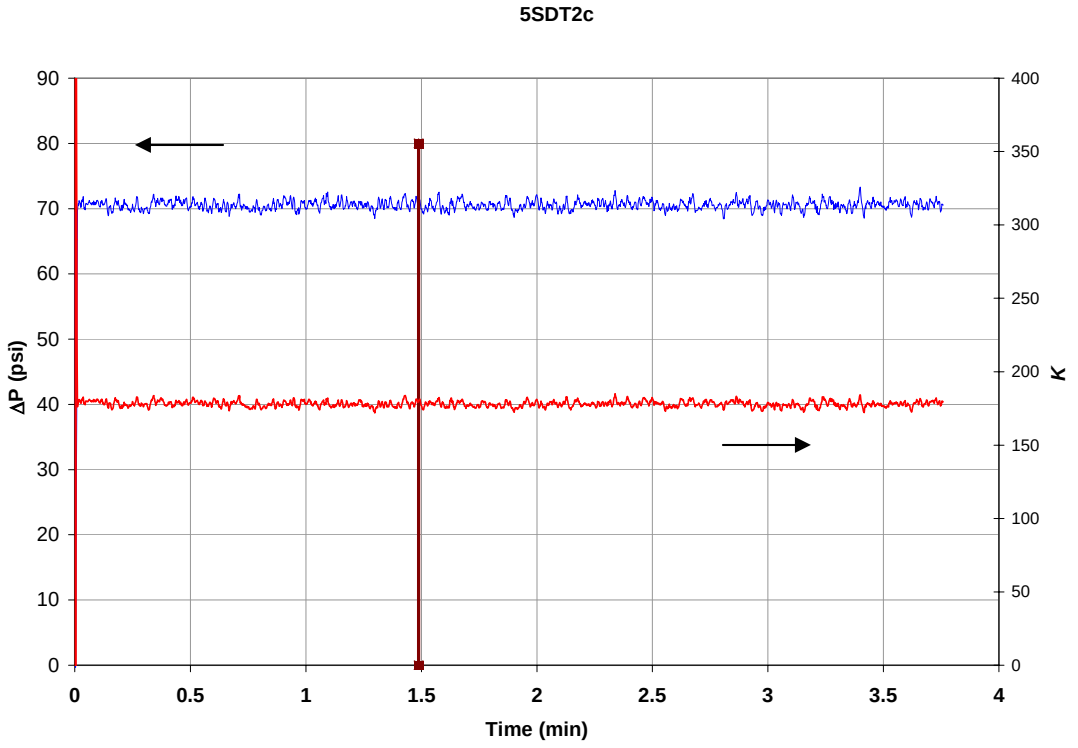
5SDT2c
ΔP (psi)
K
Time (min)
0
10
20
30
40
50
60
70
80
90
0
50
100
150
200
250
300
350
400
0
0.5
1
1.5
2
2.5
3
3.5
4

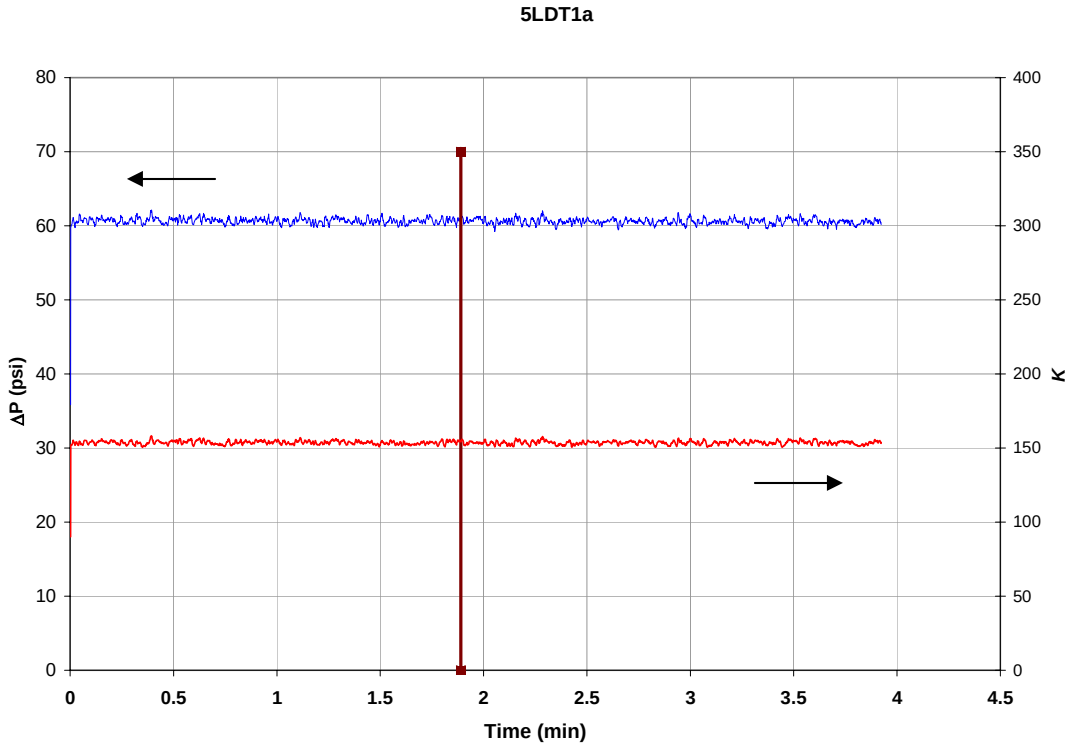
5LDT1a
ΔP (psi)
K
Time (min)
0
10
20
30
40
50
60
70
80
0
50
100
150
200
250
300
350
400
0
0.5
1
1.5
2
2.5
3
3.5
4
4.5

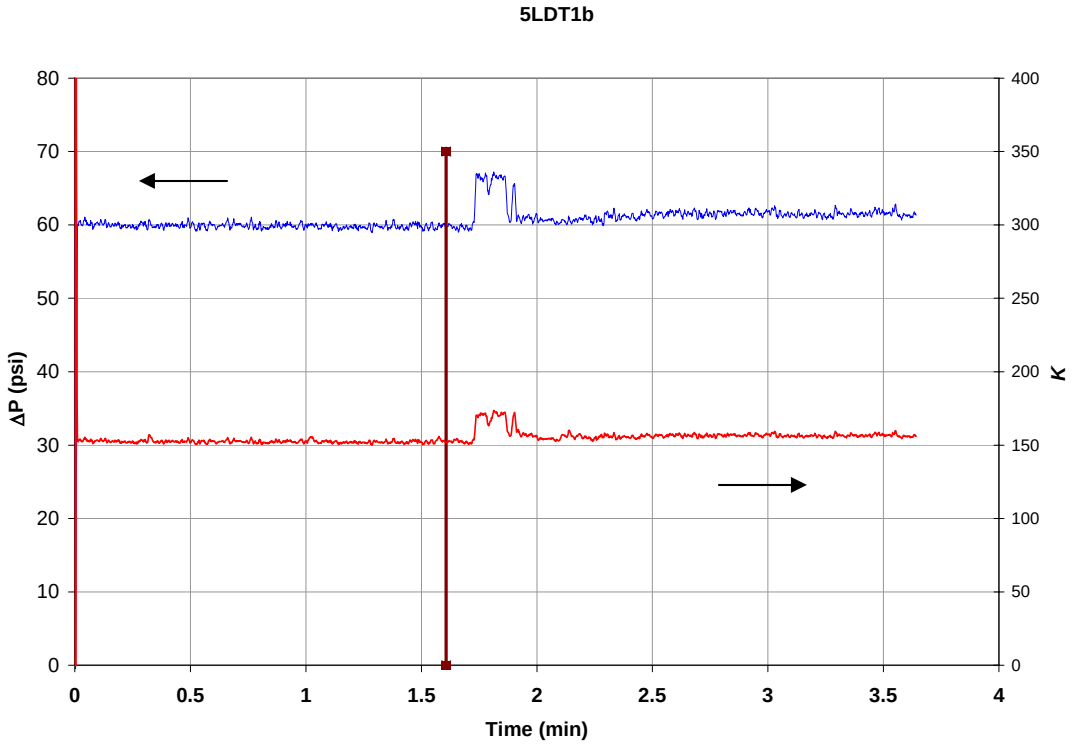
5LDT1b
80
70
60
50
40
30
20
10
0
400
350
300
250
200
150
100
50
0
ΔP (psi)
K
0
0.5
1
1.5
2
2.5
3
3.5
4
Time (min)

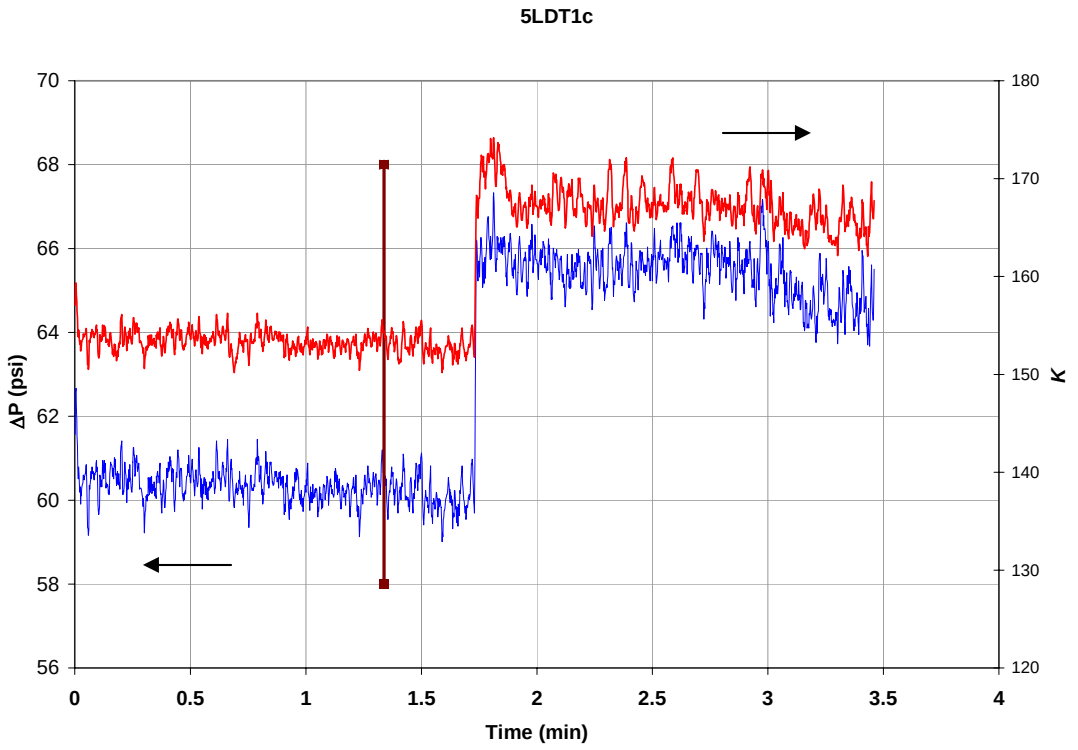
5LDT1c
70
68
66
64
62
60
58
56
180
170
160
150
140
130
120
ΔP (psi)
K
0
0.5
1
1.5
2
2.5
3
3.5
4
Time (min)

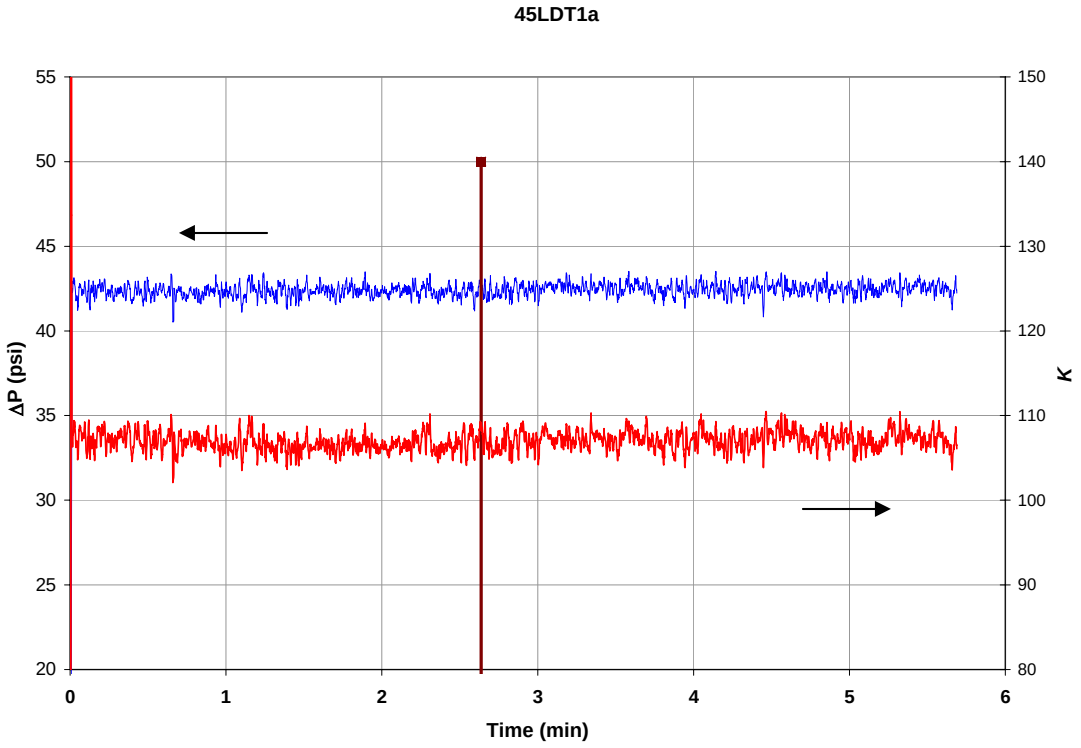
45LDT1a
55
50
45
40
35
30
25
20
ΔP (psi)
150
140
130
120
110
100
90
80
K
0
1
2
3
4
5
6
Time (min)

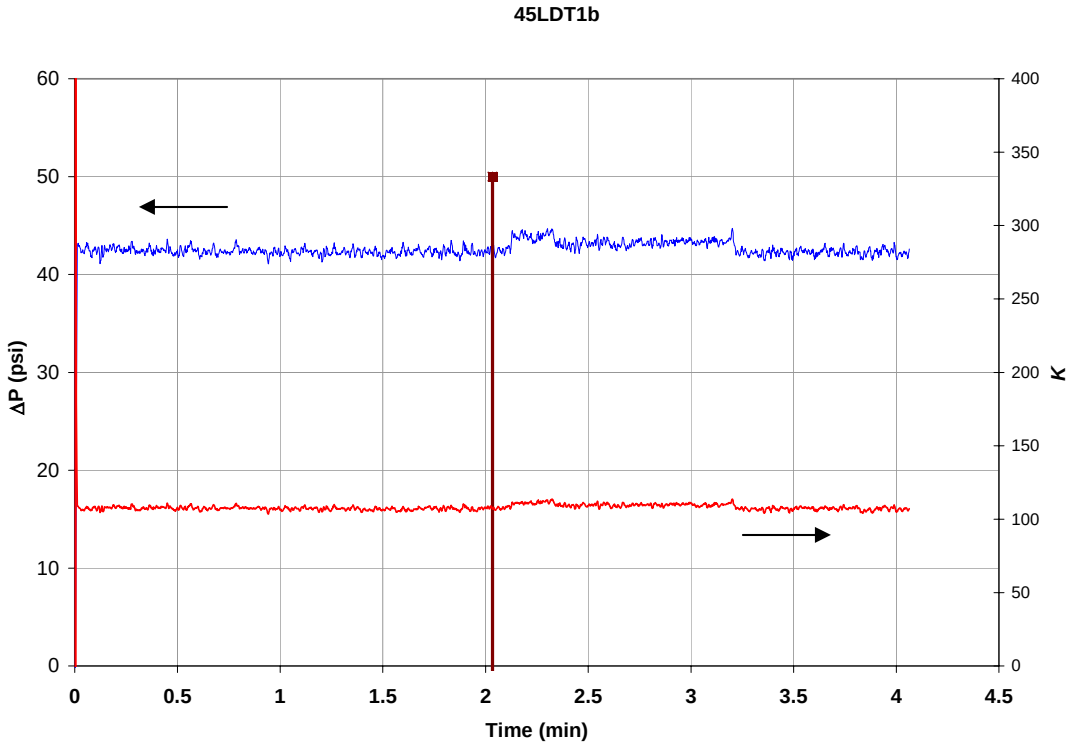
45LDT1b
60
50
40
30
20
10
0
ΔP (psi)
400
350
300
250
200
150
100
50
0
K
0
0.5
1
1.5
2
2.5
3
3.5
4
4.5
Time (min)

45LDT1c

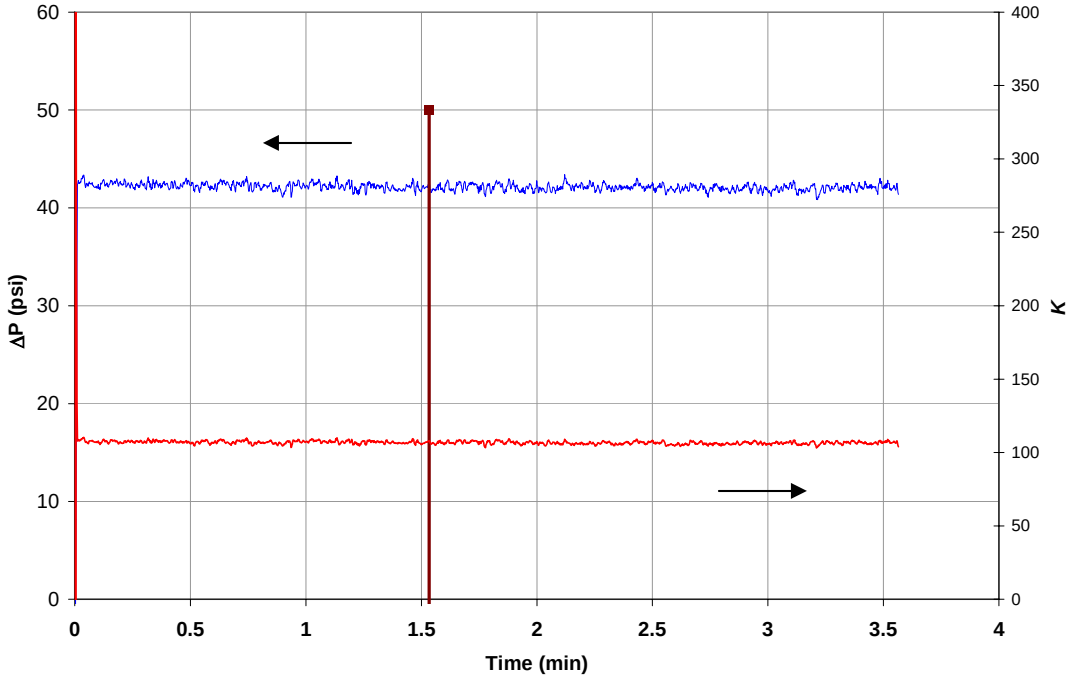

45LDT2a

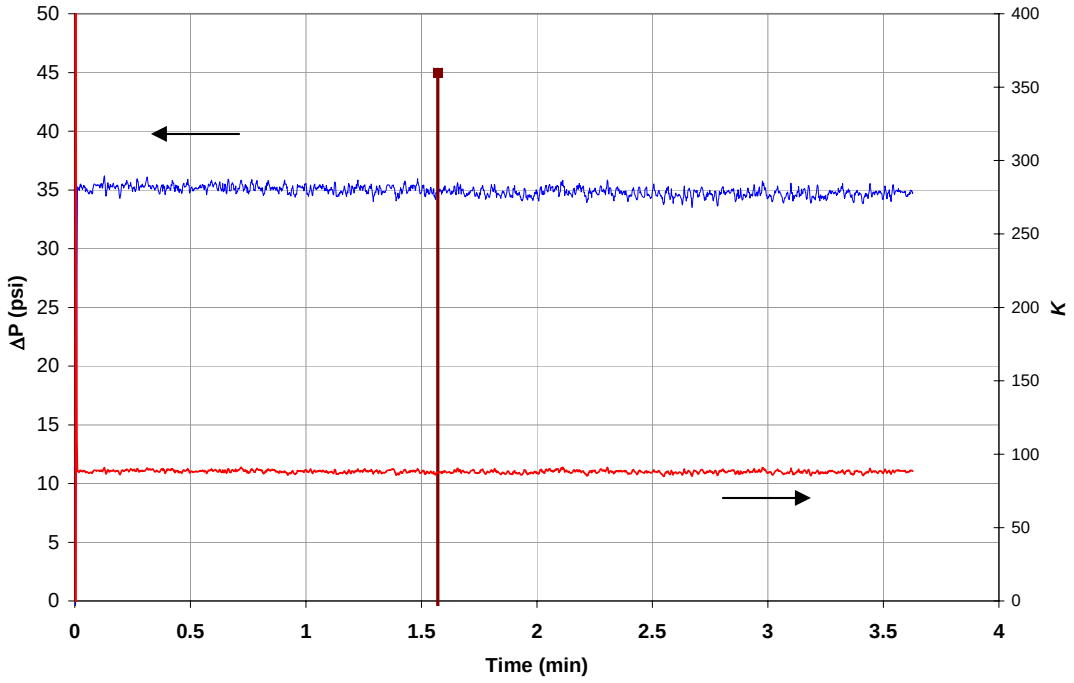

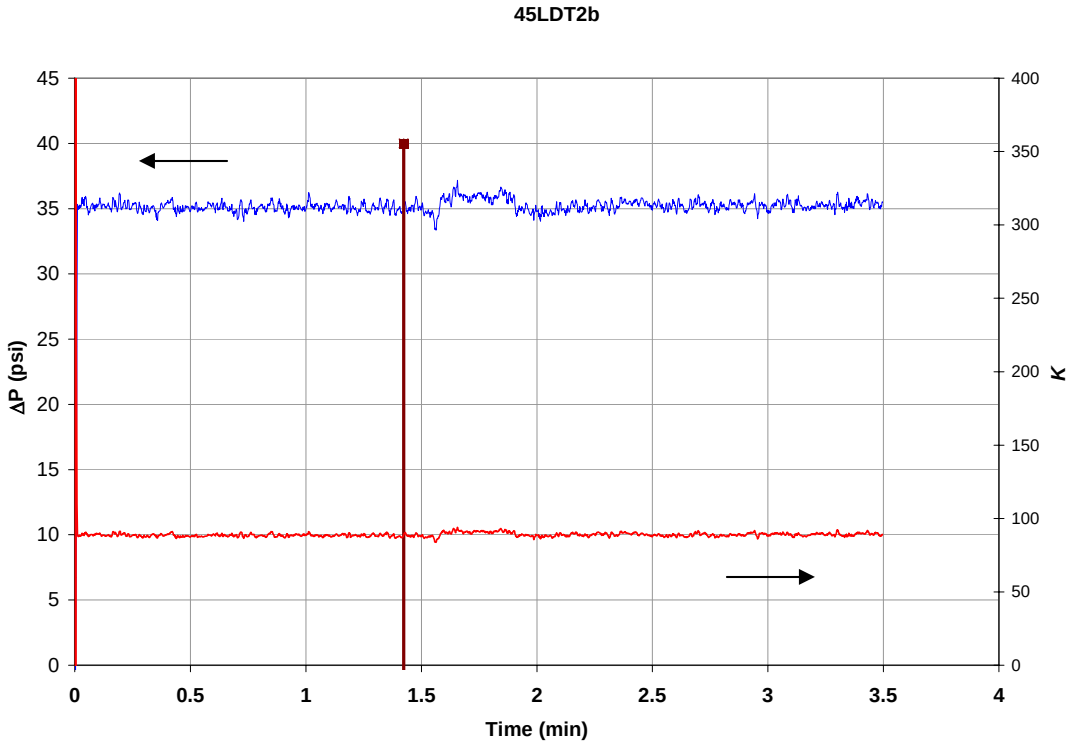
45LDT2b
ΔP (psi)
K
Time (min)
0
5
10
15
20
25
30
35
40
45
0
50
100
150
200
250
300
350
400
0
0.5
1
1.5
2
2.5
3
3.5
4

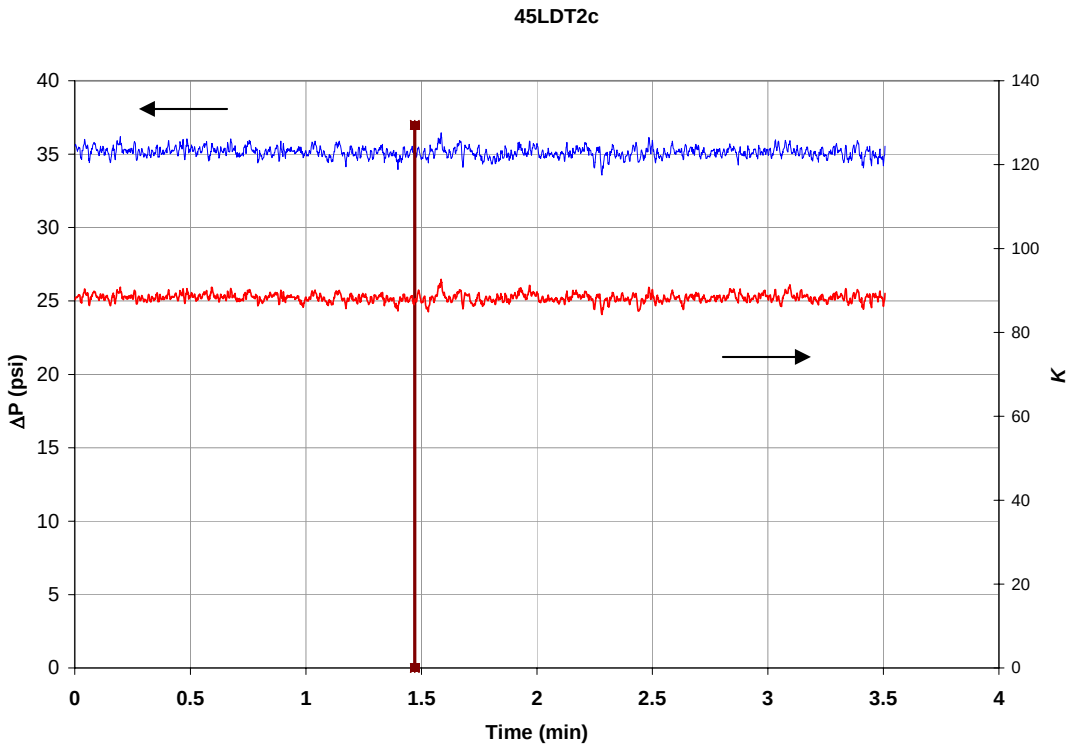
45LDT2c
ΔP (psi)
K
Time (min)
0
5
10
15
20
25
30
35
40
0
20
40
60
80
100
120
140
0
0.5
1
1.5
2
2.5
3
3.5
4

5LN2

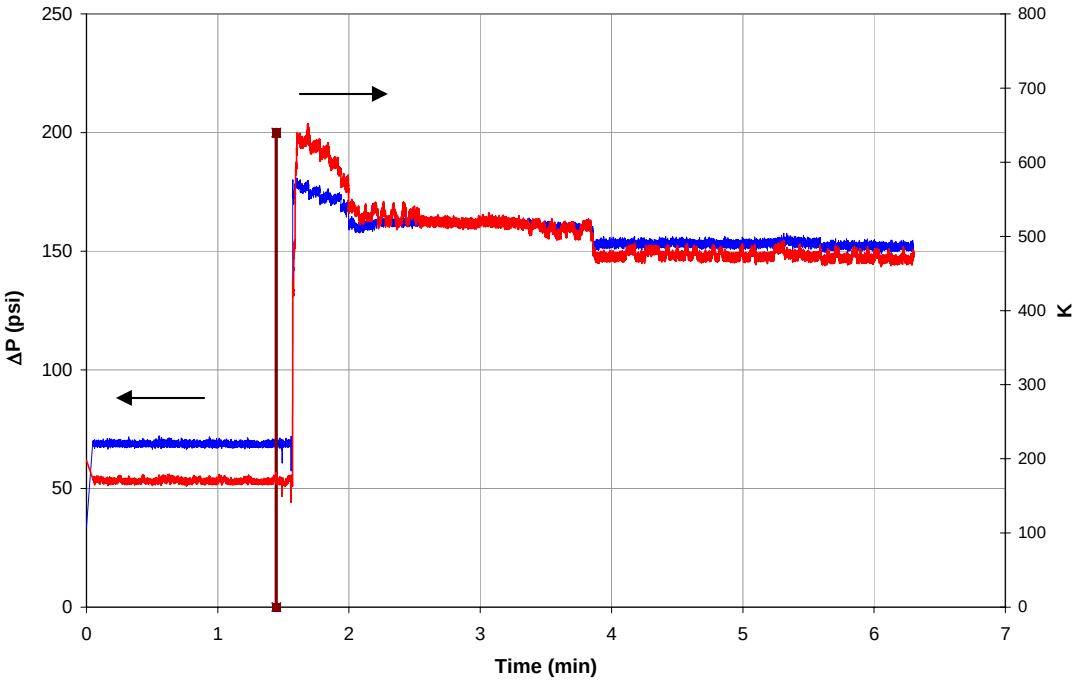
ΔP (psi)
K
Time (min)
0
50
100
150
200
250
0
100
200
300
400
500
600
700
800
0
1
2
3
4
5
6
7

5LN3

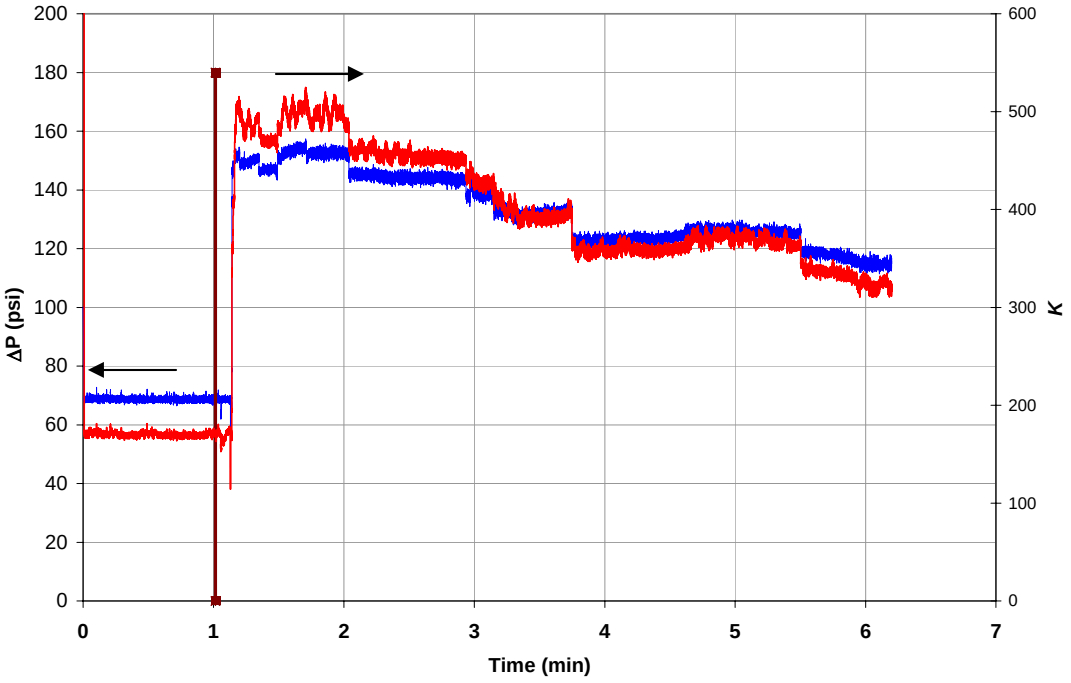
ΔP (psi)
K
Time (min)
0
20
40
60
80
100
120
140
160
180
200
0
100
200
300
400
500
600
0
1
2
3
4
5
6
7

5SN3

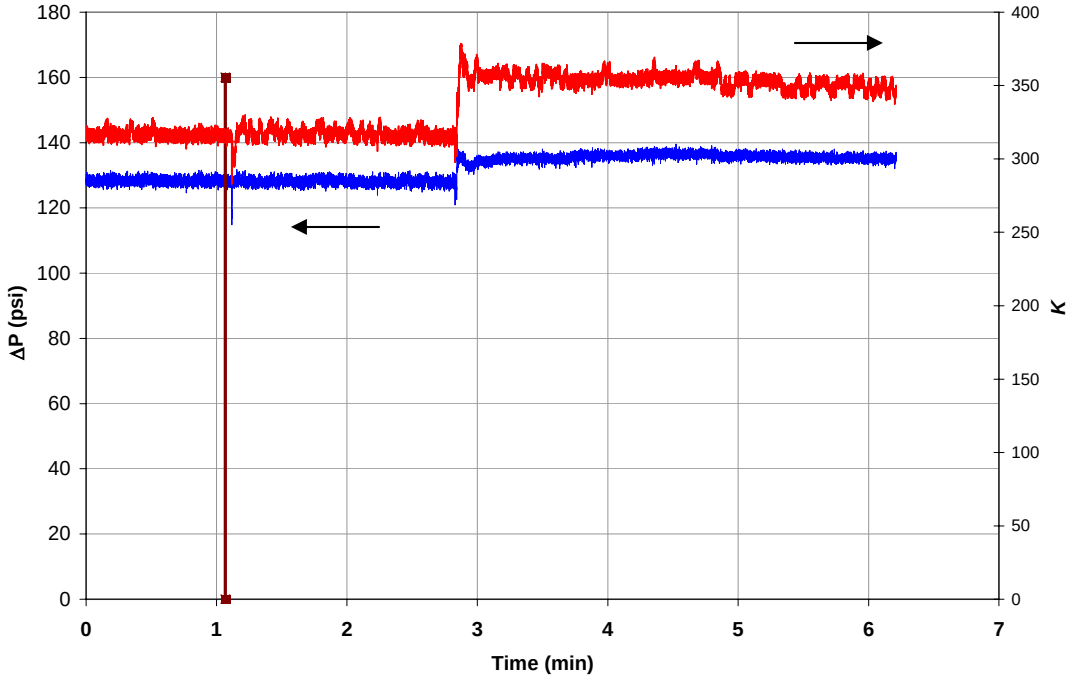
ΔP (psi)
K
Time (min)
0
20
40
60
80
100
120
140
160
180
0
50
100
150
200
250
300
350
400
0
1
2
3
4
5
6
7

5SN4

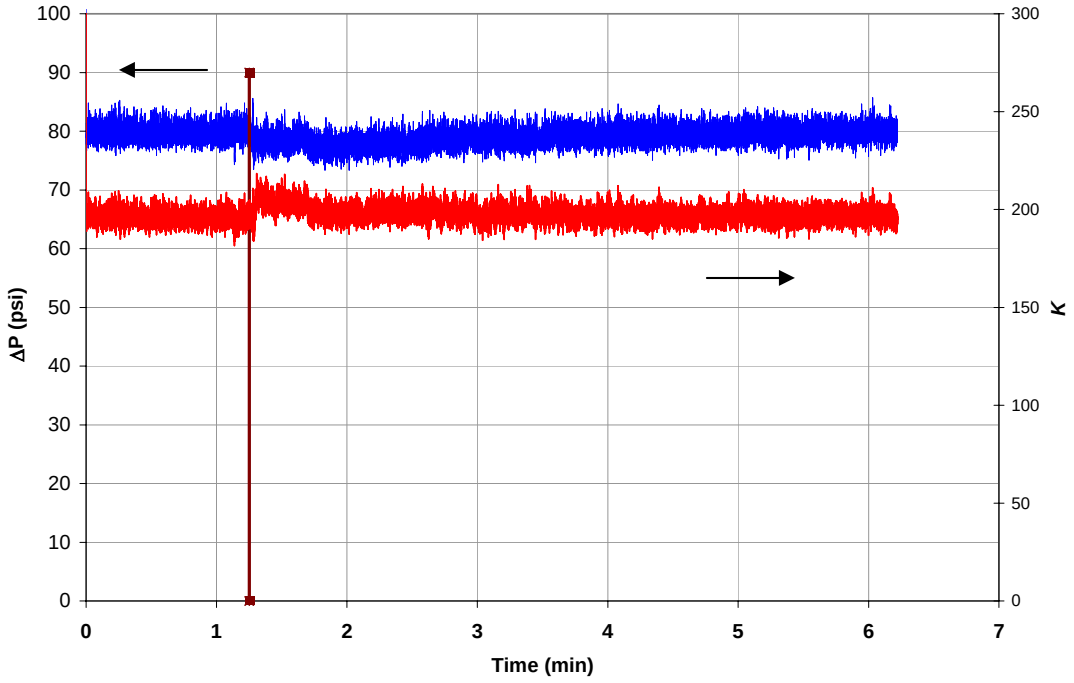
ΔP (psi)
K
Time (min)
0
10
20
30
40
50
60
70
80
90
100
0
50
100
150
200
250
300
0
1
2
3
4
5
6
7

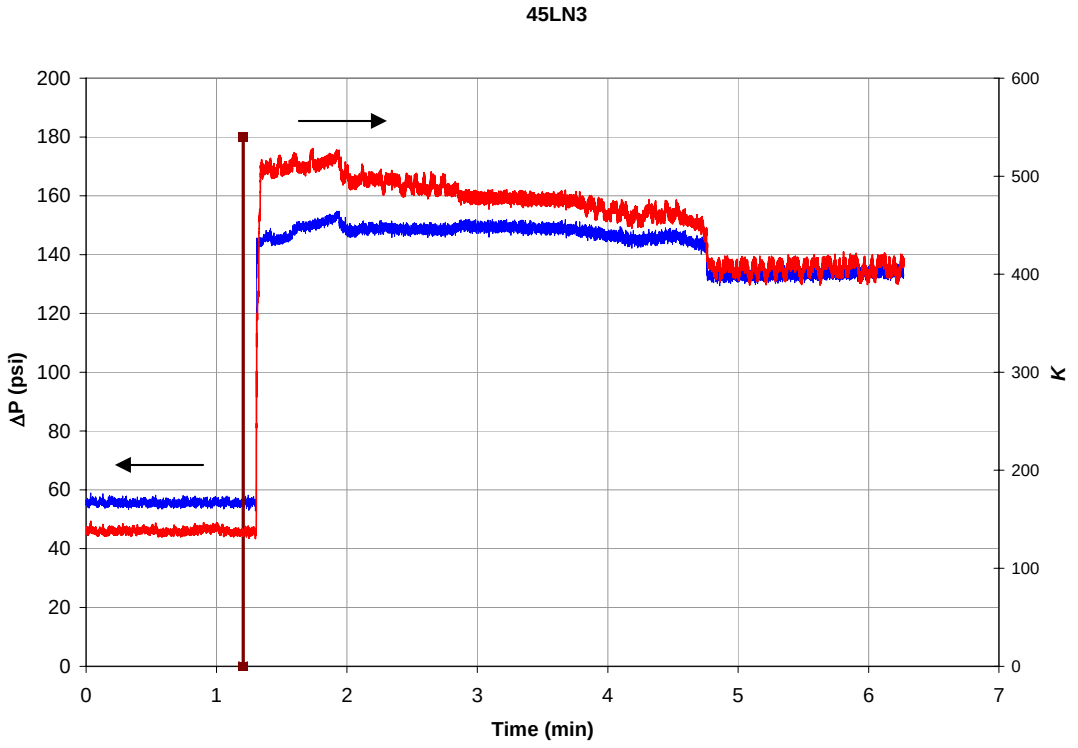
45LN3
ΔP (psi)
K
Time (min)
0
20
40
60
80
100
120
140
160
180
200
0
100
200
300
400
500
600
0
1
2
3
4
5
6
7

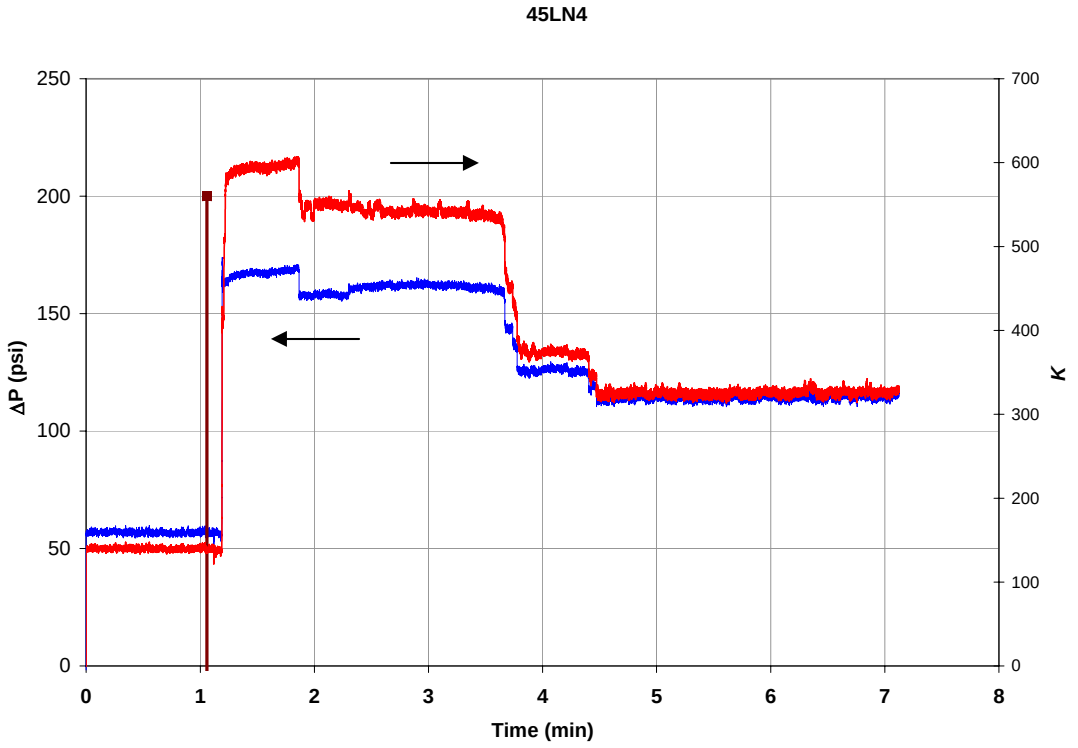
45LN4
ΔP (psi)
K
Time (min)
0
50
100
150
200
250
0
100
200
300
400
500
600
700
0
1
2
3
4
5
6
7
8

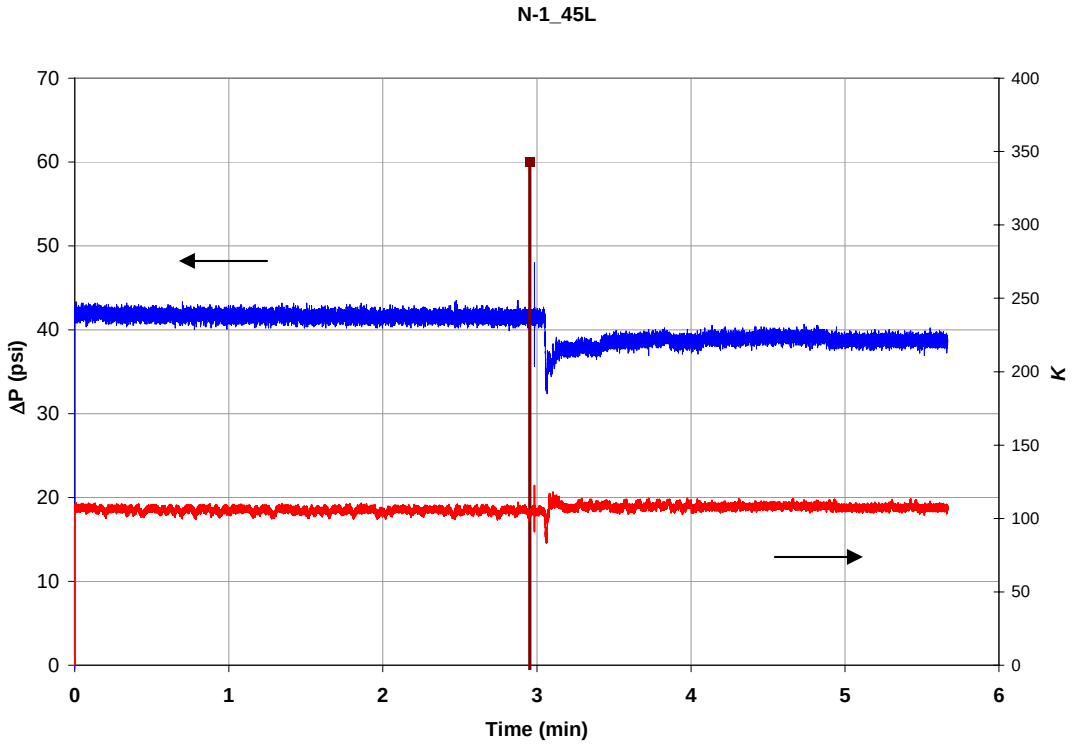
N-1_45L
ΔP (psi)
K
Time (min)
0
10
20
30
40
50
60
70
0
50
100
150
200
250
300
350
400
0
1
2
3
4
5
6

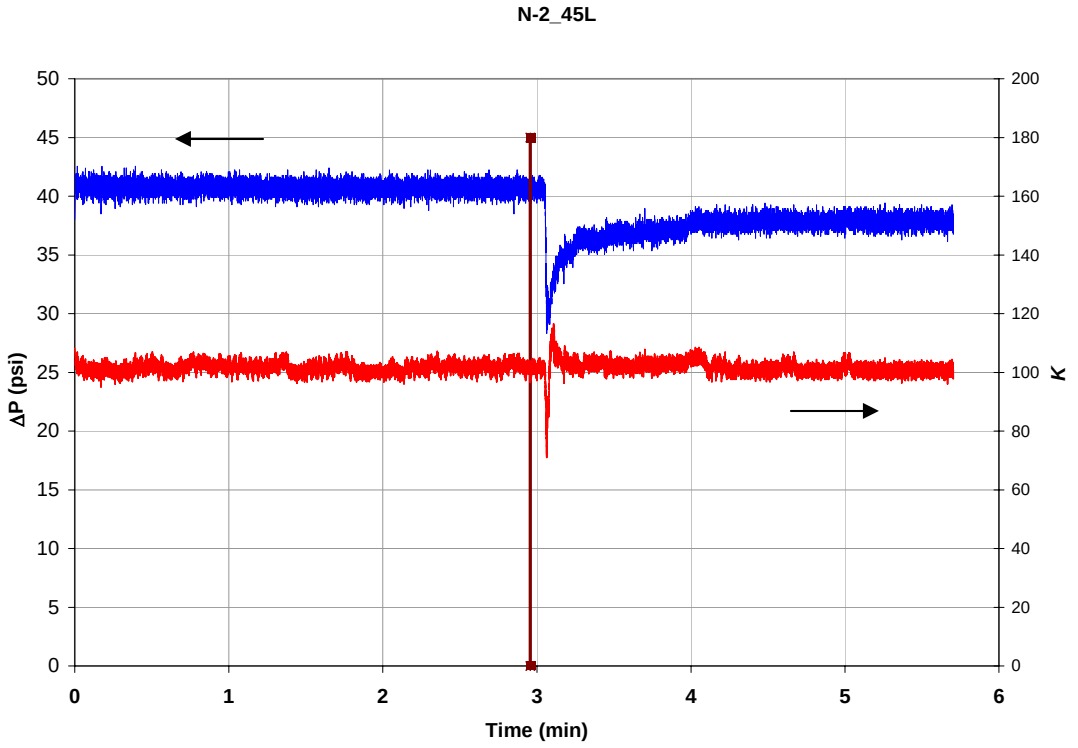
N-2_45L
ΔP (psi)
K
Time (min)
0
5
10
15
20
25
30
35
40
45
50
0
20
40
60
80
100
120
140
160
180
200
0
1
2
3
4
5
6

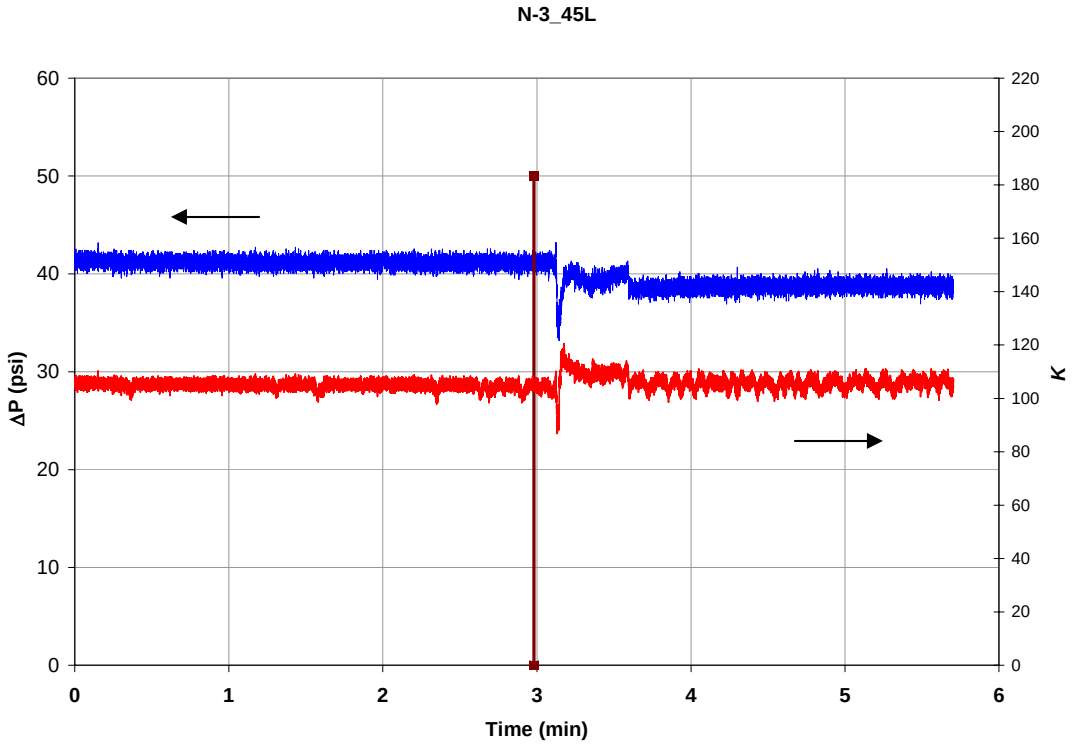
N-3_45L
ΔP (psi)
K
Time (min)
0
10
20
30
40
50
60
0
20
40
60
80
100
120
140
160
180
200
220
0
1
2
3
4
5
6

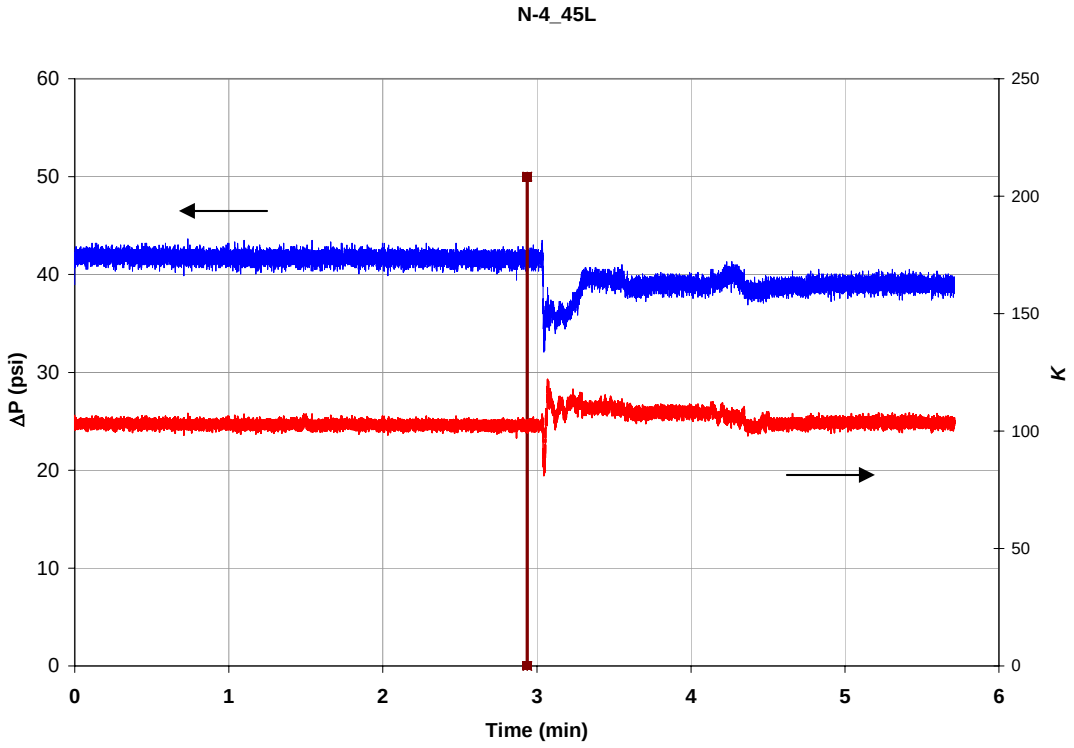
N-4_45L
ΔP (psi)
K
Time (min)
0
10
20
30
40
50
60
0
50
100
150
200
250
0
1
2
3
4
5
6

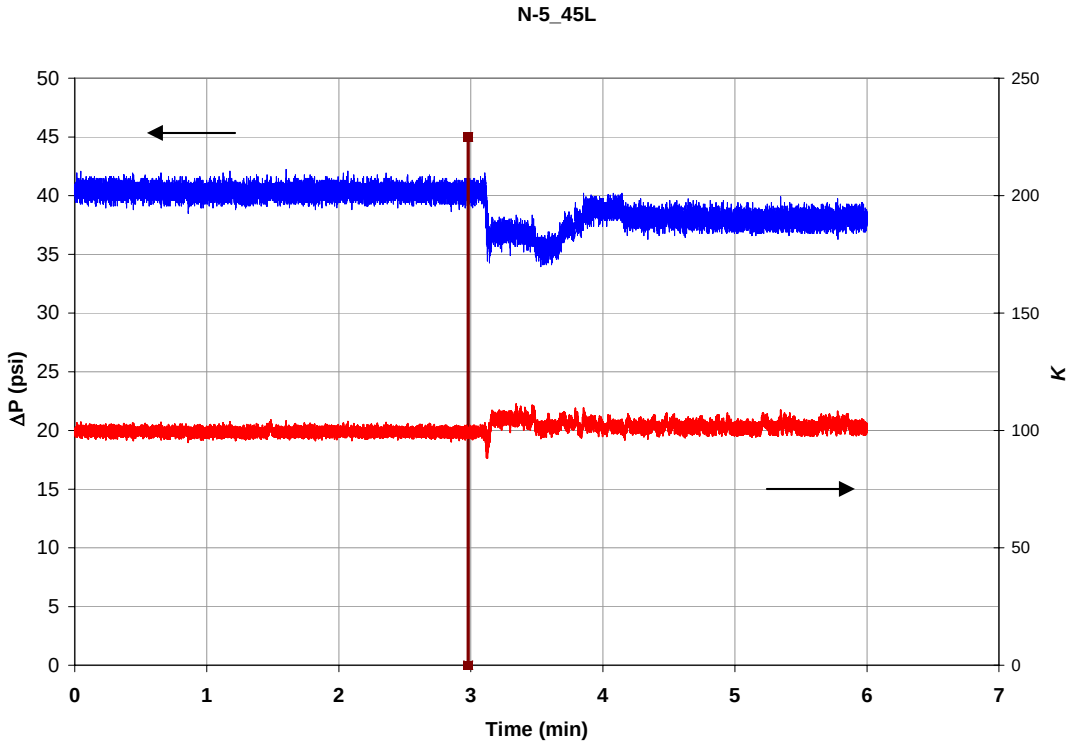
N-5_45L
ΔP (psi)
K
Time (min)
0
5
10
15
20
25
30
35
40
45
50
0
50
100
150
200
250
0
1
2
3
4
5
6
7

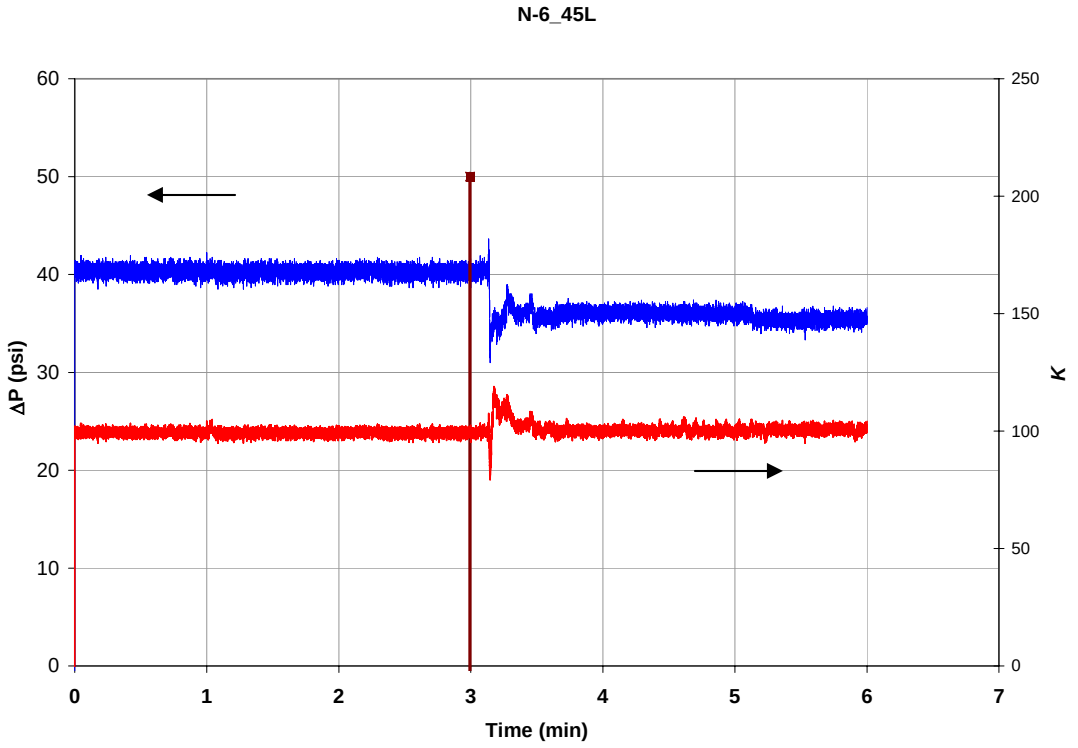
N-6_45L
ΔP (psi)
K
Time (min)
0
10
20
30
40
50
60
0
50
100
150
200
250
0
1
2
3
4
5
6
7

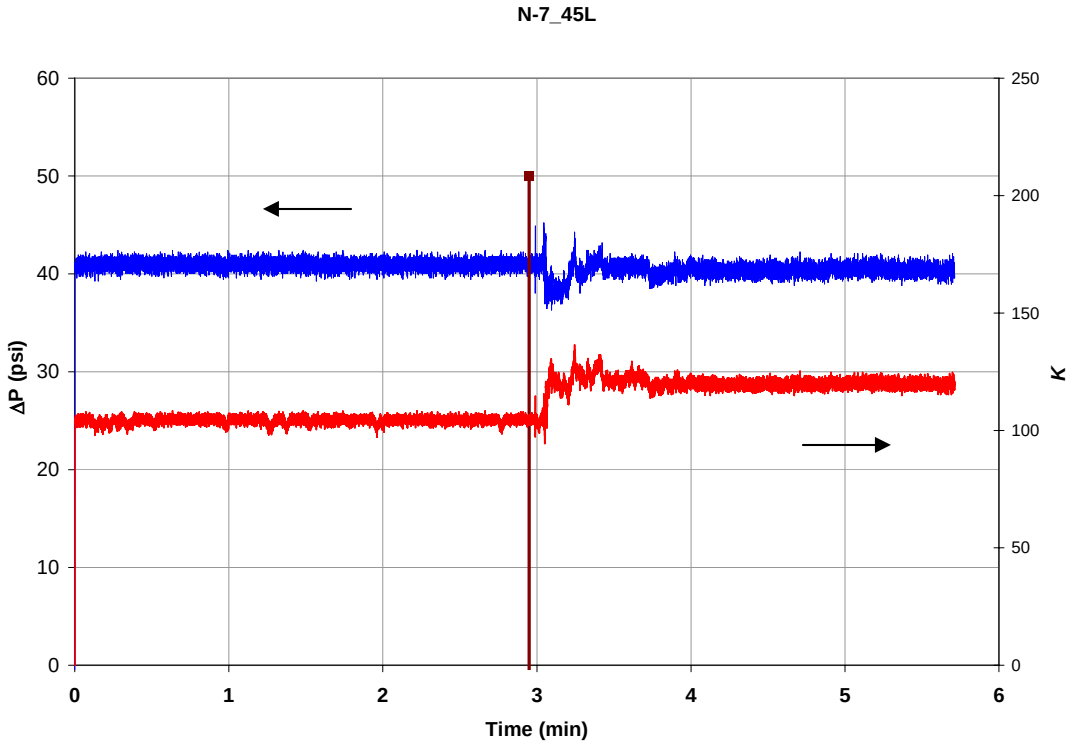
N-7_45L
ΔP (psi)
K
Time (min)
0
10
20
30
40
50
60
0
50
100
150
200
250
0
1
2
3
4
5
6

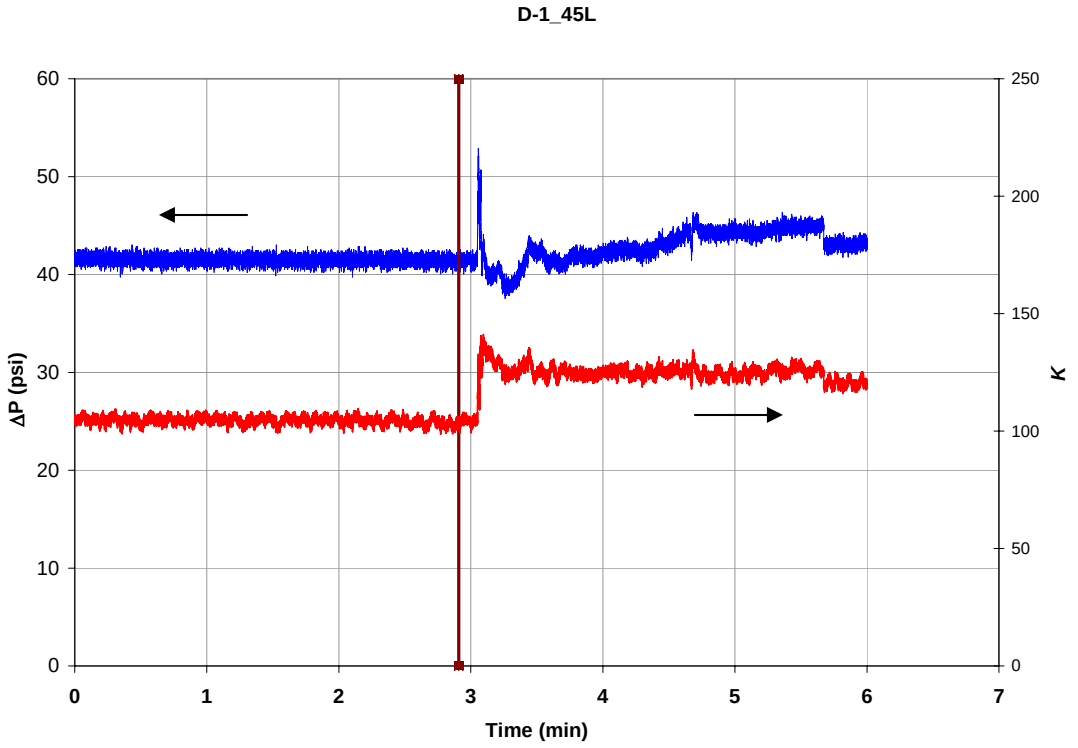
D-1_45L
ΔP (psi)
K
Time (min)
0
10
20
30
40
50
60
0
50
100
150
200
250
0
1
2
3
4
5
6
7

D-1-2_45L

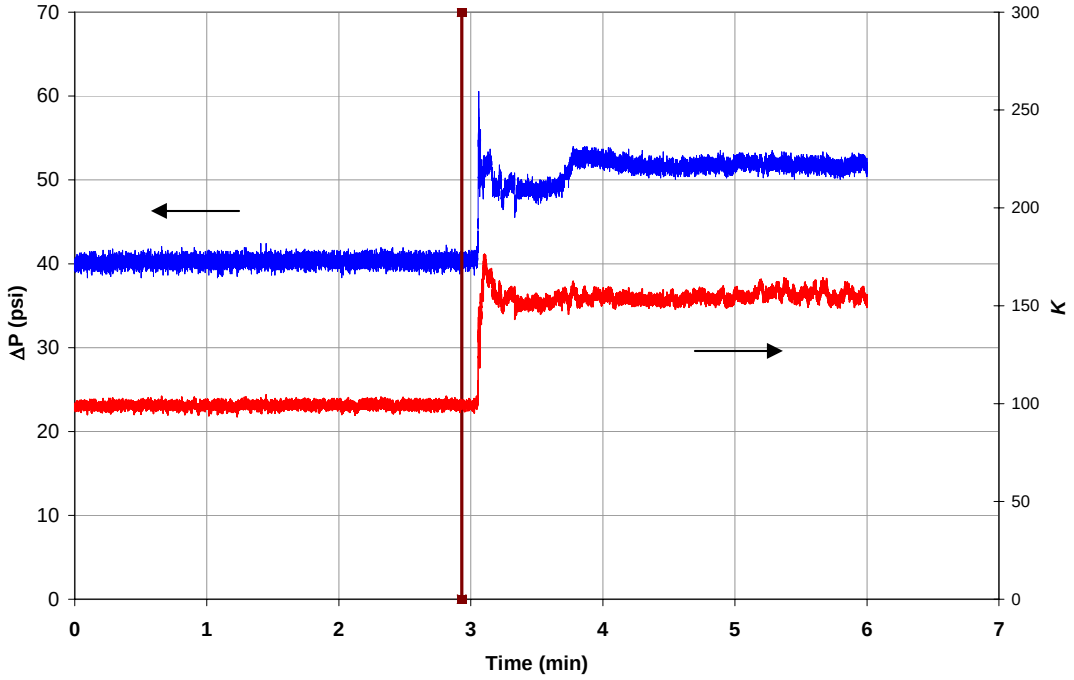

D-2_45L

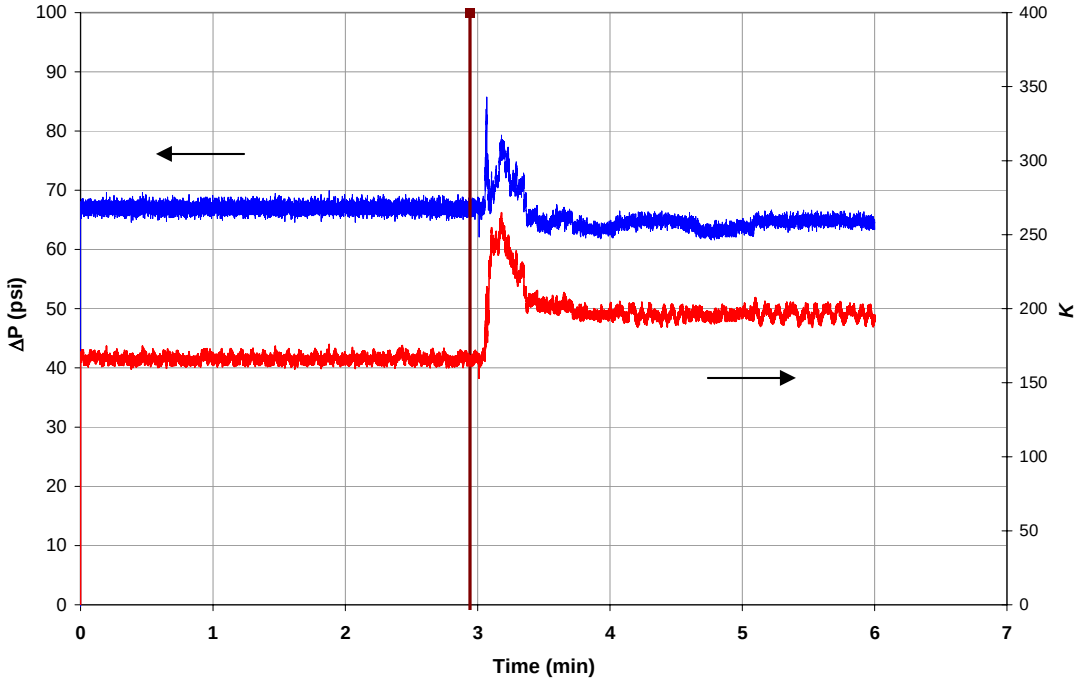

D-3_5L

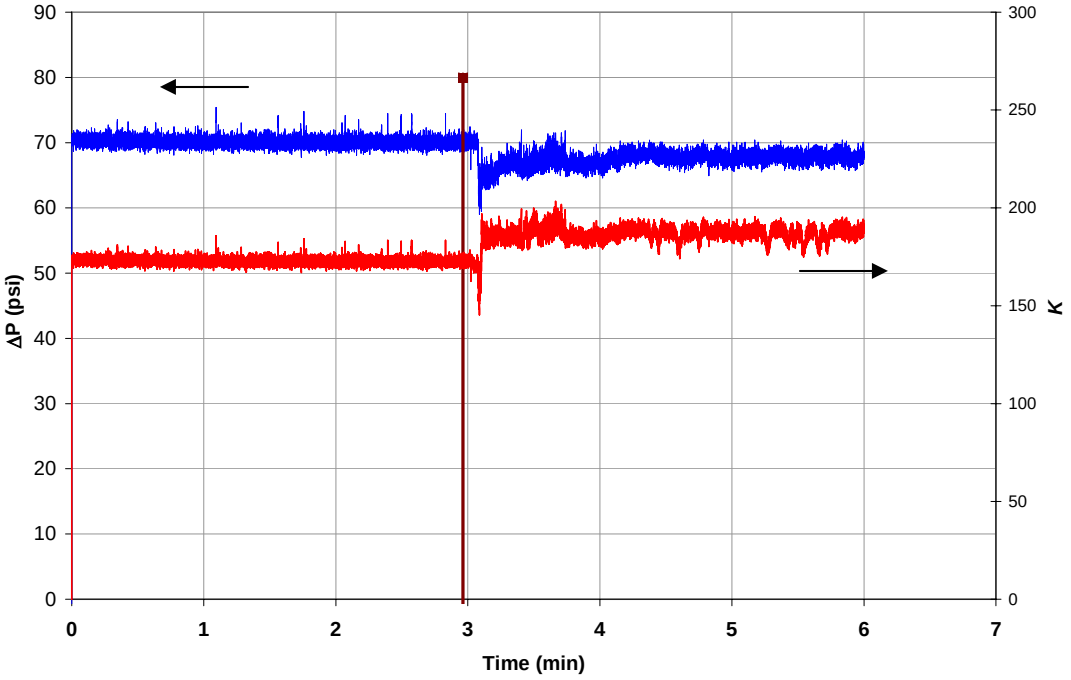
ΔP (psi)
K
Time (min)
0
10
20
30
40
50
60
70
80
90
0
50
100
150
200
250
300
0
1
2
3
4
5
6
7

D-16_45L

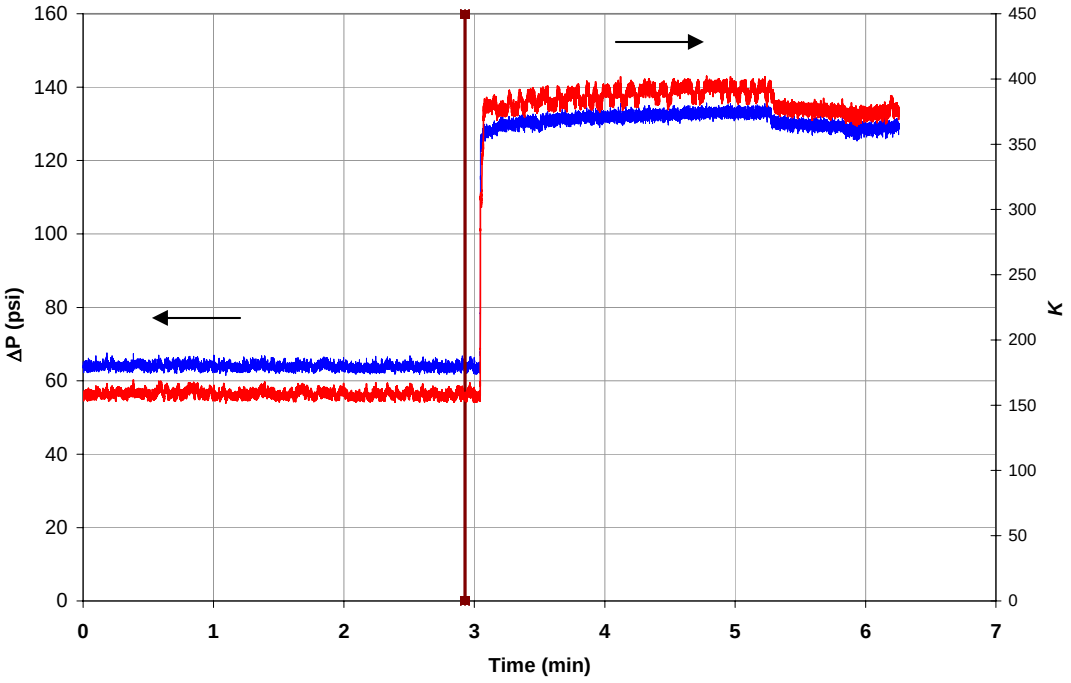
ΔP (psi)
K
Time (min)
0
20
40
60
80
100
120
140
160
0
50
100
150
200
250
300
350
400
450
0
1
2
3
4
5
6
7

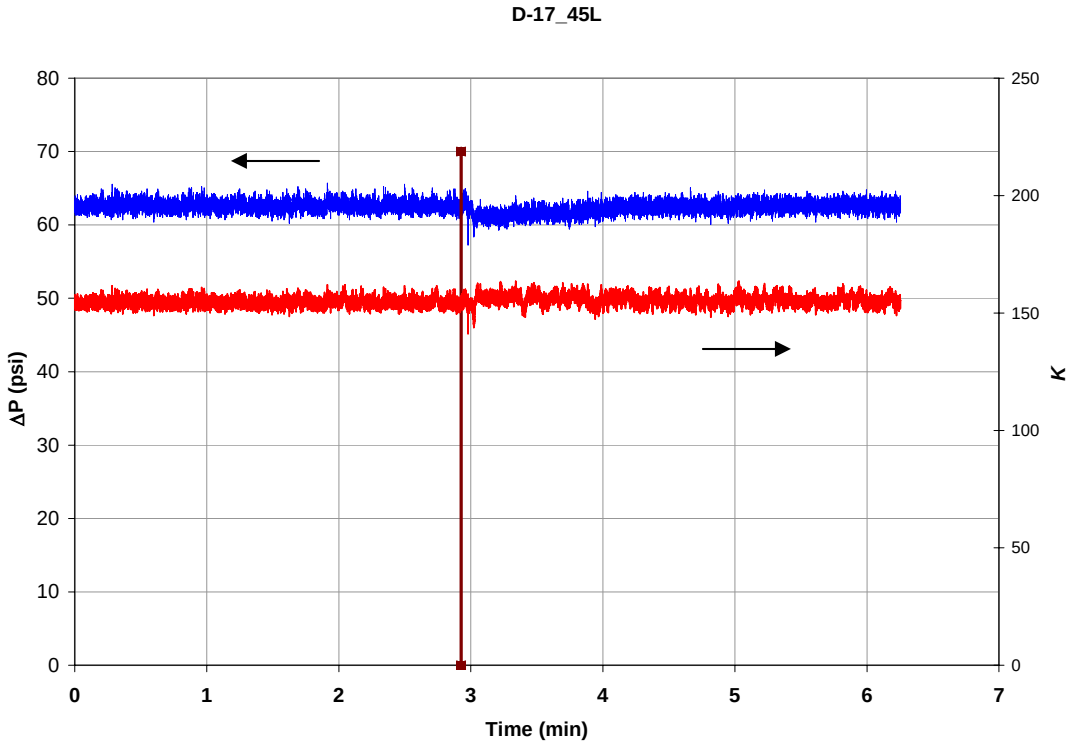
D-17_45L
80
70
60
50
40
30
20
10
0
250
200
150
100
50
0
ΔP (psi)
K
0
1
2
3
4
5
6
7
Time (min)

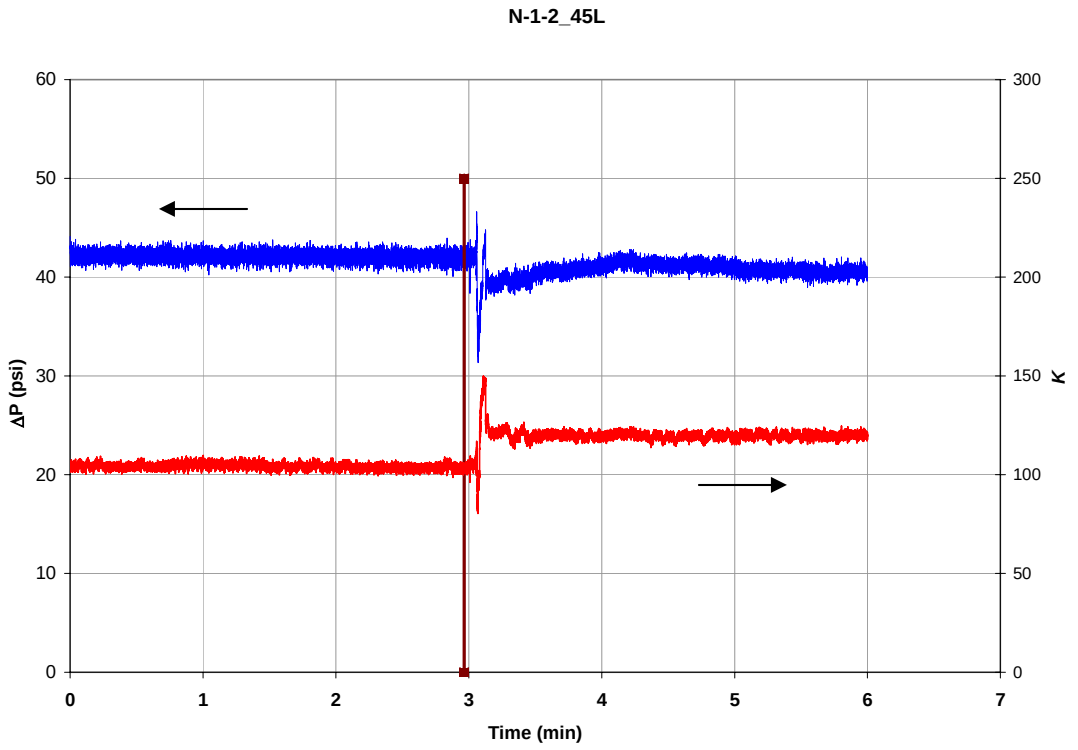
N-1-2_45L
60
50
40
30
20
10
0
300
250
200
150
100
50
0
ΔP (psi)
K
0
1
2
3
4
5
6
7
Time (min)

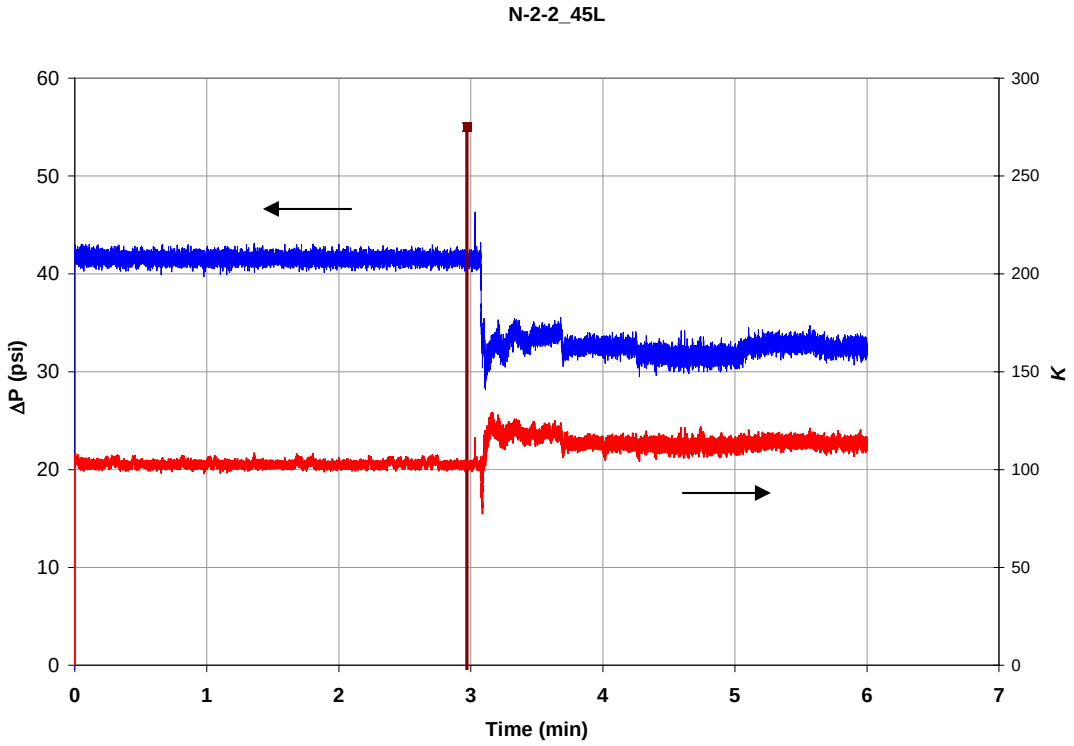
N-2-2_45L
ΔP (psi)
K
Time (min)
0
10
20
30
40
50
60
0
50
100
150
200
250
300
0
1
2
3
4
5
6
7

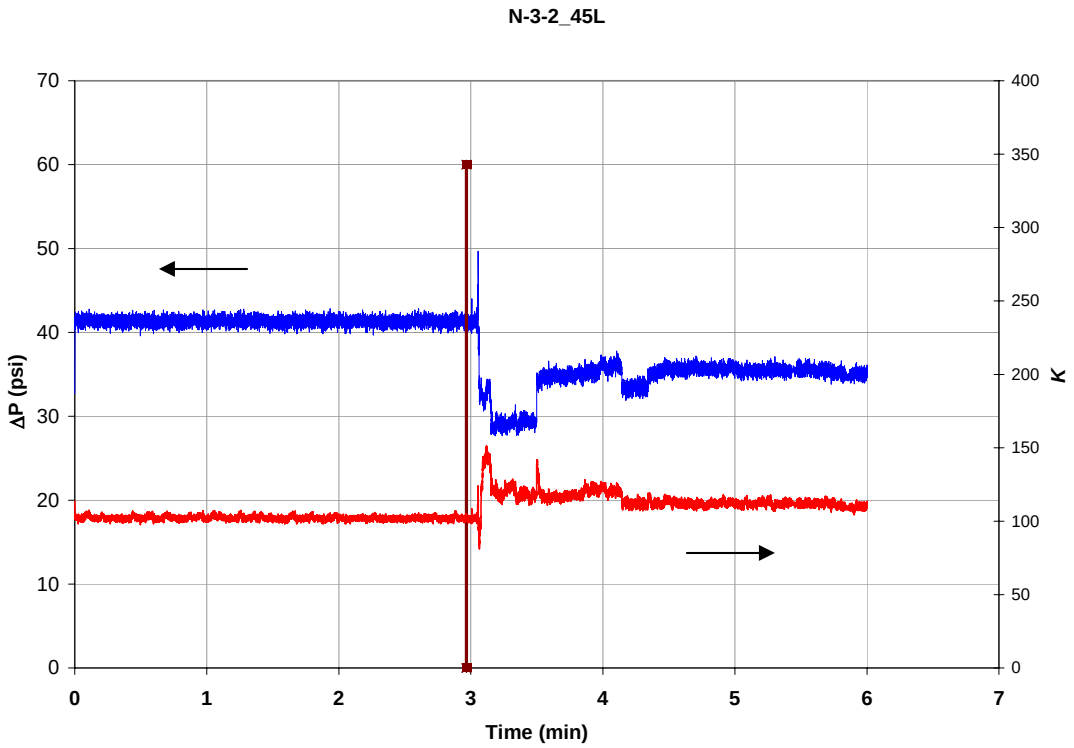
N-3-2_45L
ΔP (psi)
K
Time (min)
0
10
20
30
40
50
60
70
0
50
100
150
200
250
300
350
400
0
1
2
3
4
5
6
7

N-4-2_45L

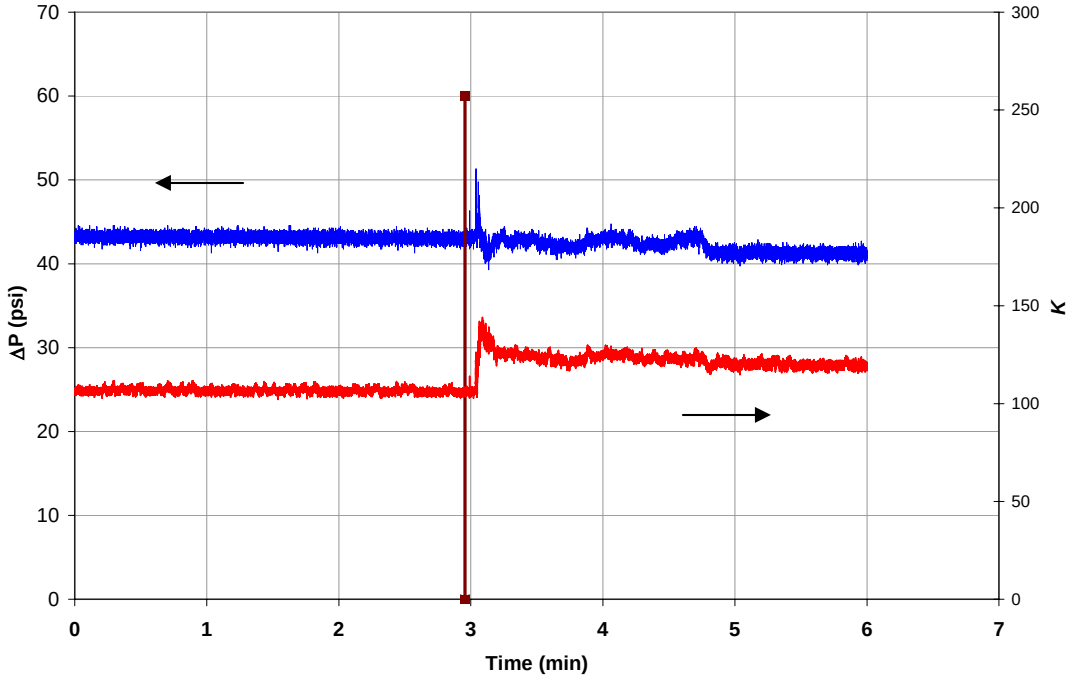

N-5-2_45L

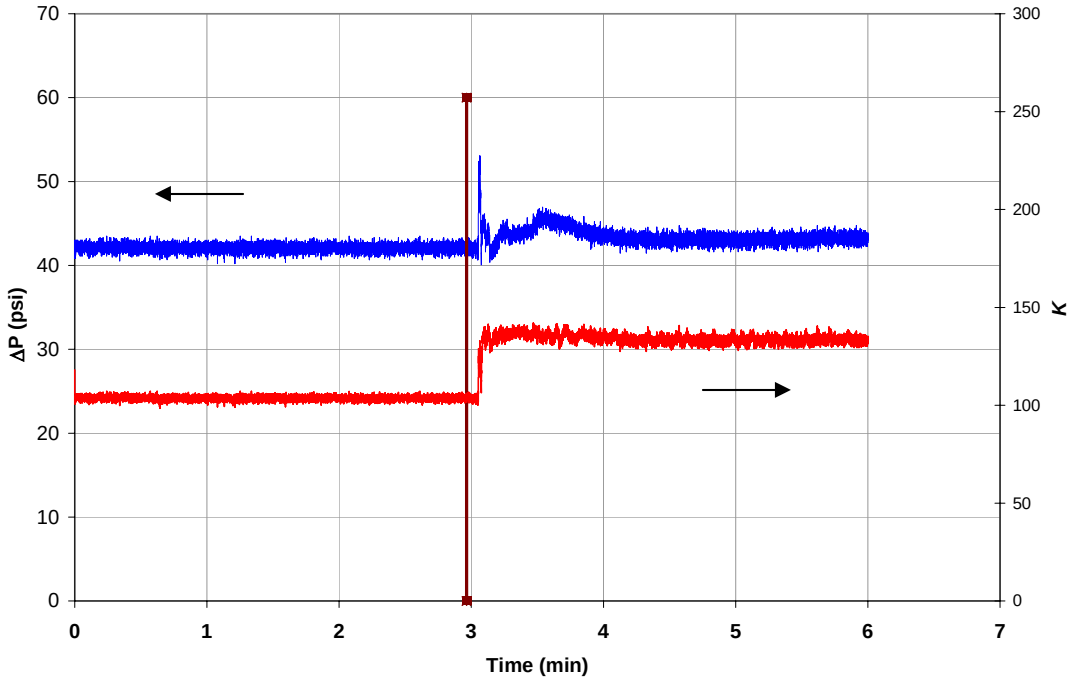

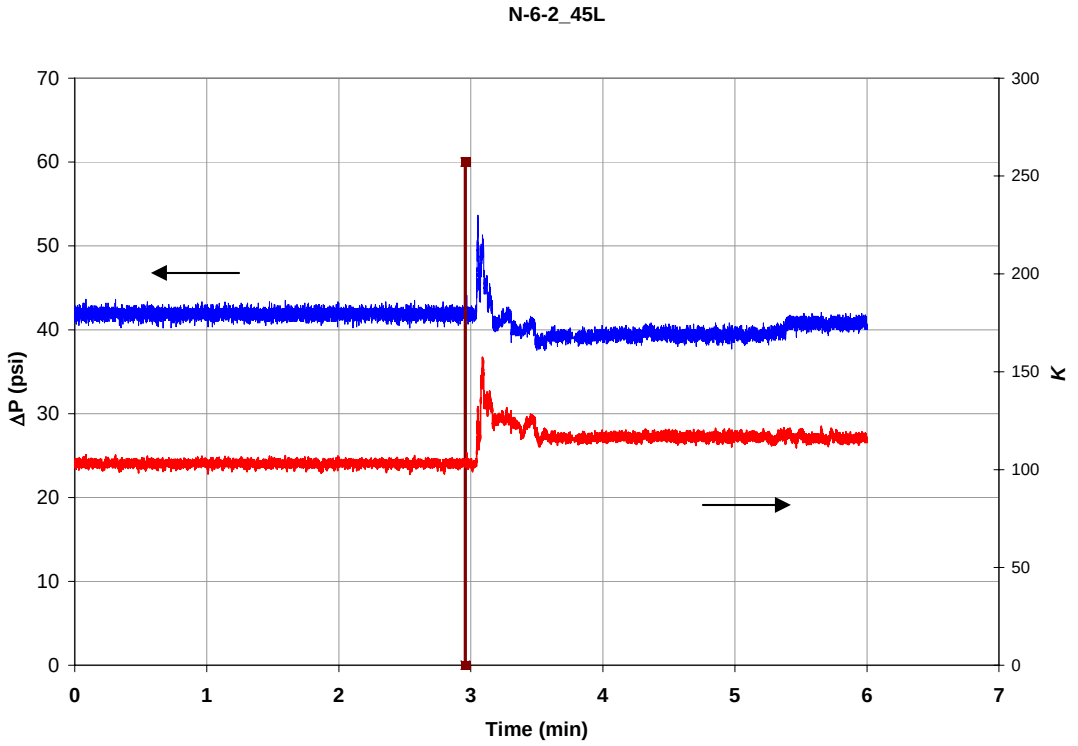
N-6-2_45L
ΔP (psi)
K
Time (min)
0
10
20
30
40
50
60
70
0
50
100
150
200
250
300
0
1
2
3
4
5
6
7

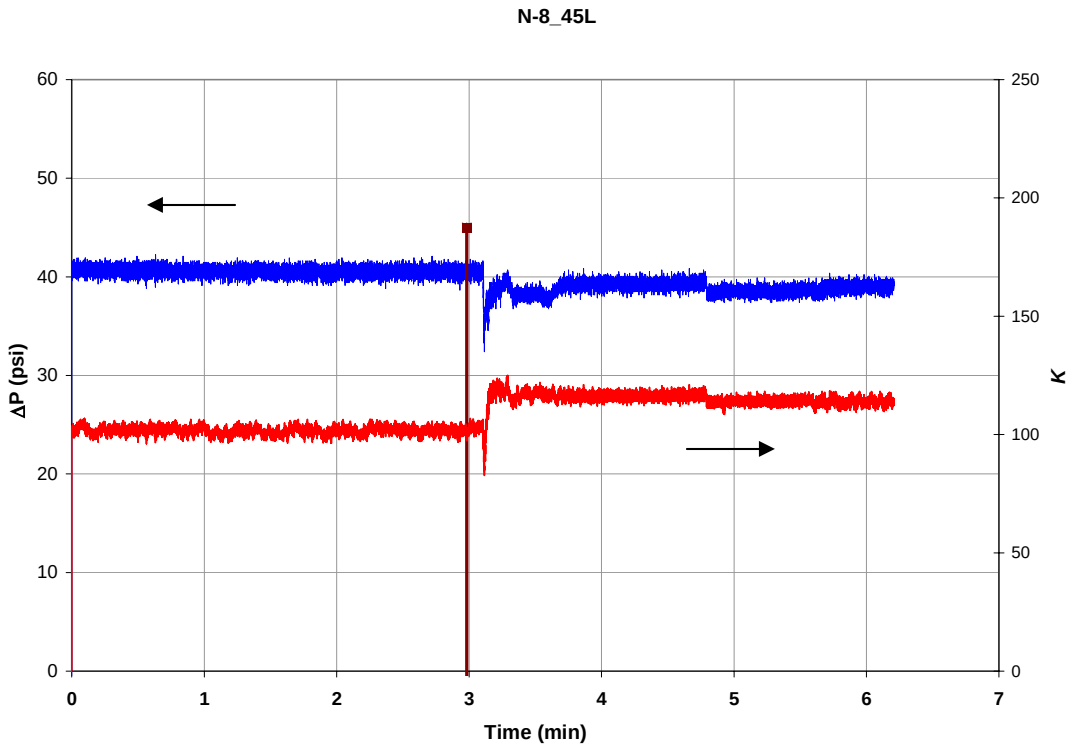
N-8_45L
ΔP (psi)
K
Time (min)
0
10
20
30
40
50
60
0
50
100
150
200
250
0
1
2
3
4
5
6
7

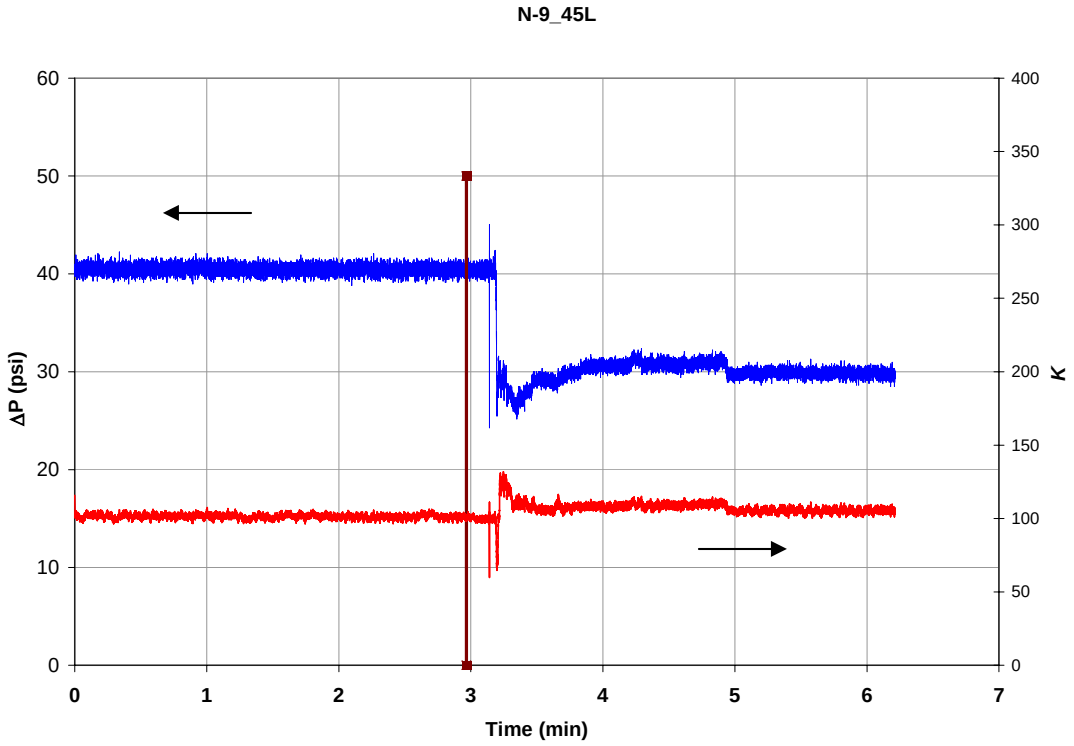
N-9_45L
ΔP (psi)
K
Time (min)
0
10
20
30
40
50
60
0
50
100
150
200
250
300
350
400
0
1
2
3
4
5
6
7

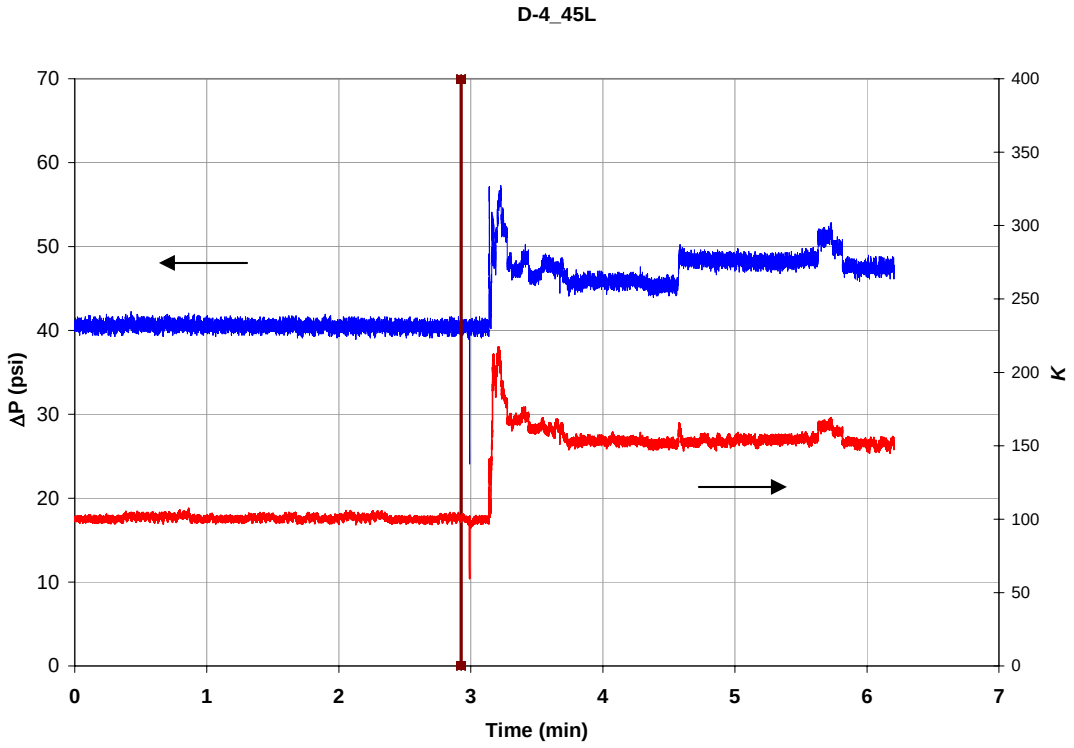
D-4_45L
ΔP (psi)
K
Time (min)
0
10
20
30
40
50
60
70
0
50
100
150
200
250
300
350
400
0
1
2
3
4
5
6
7

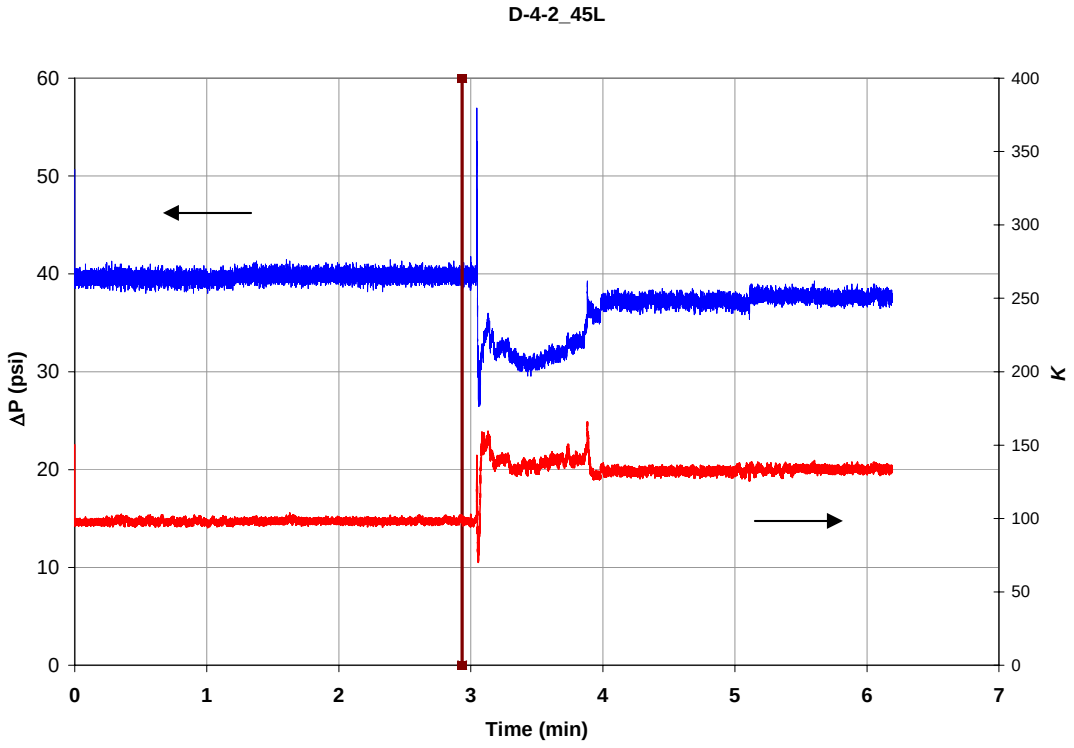
D-4-2_45L
ΔP (psi)
K
Time (min)
0
10
20
30
40
50
60
0
50
100
150
200
250
300
350
400
0
1
2
3
4
5
6
7

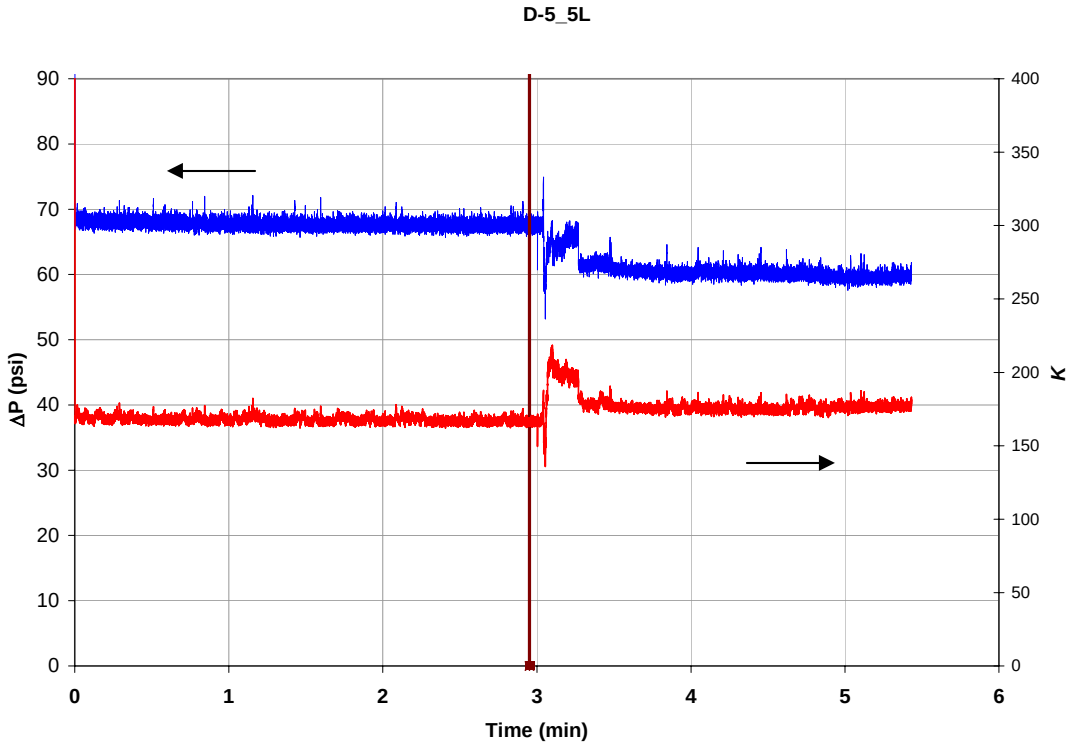
D-5_5L
ΔP (psi)
K
Time (min)
0
10
20
30
40
50
60
70
80
90
0
50
100
150
200
250
300
350
400
0
1
2
3
4
5
6

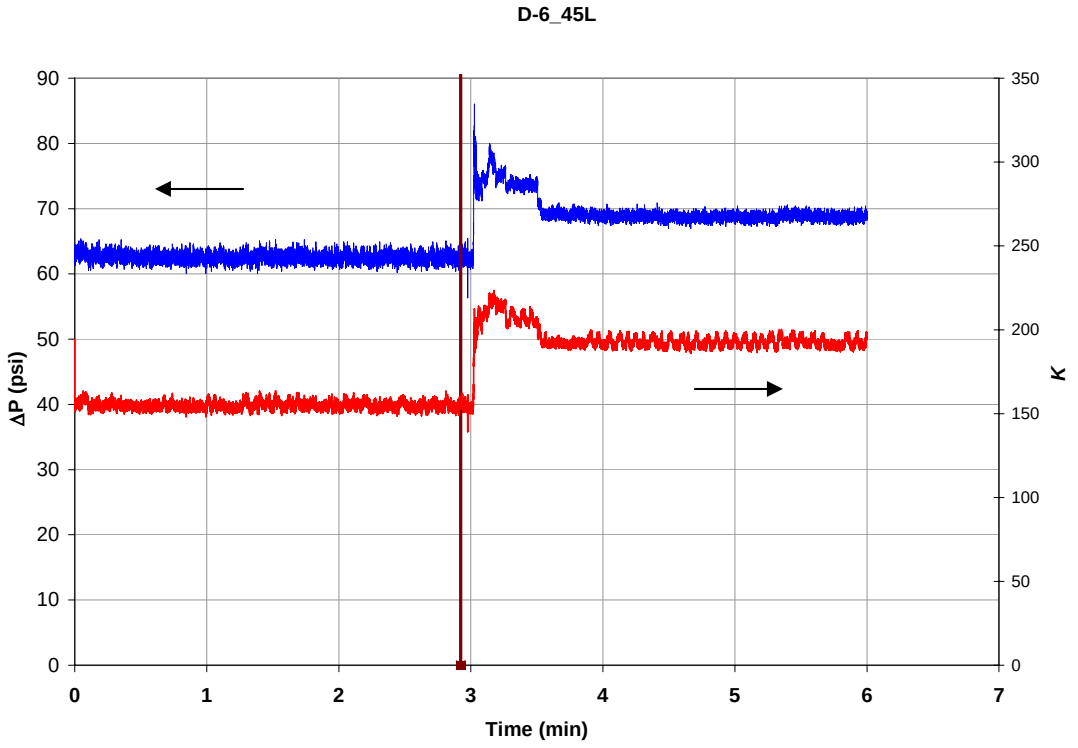
D-6_45L
ΔP (psi)
K
Time (min)
0
10
20
30
40
50
60
70
80
90
0
50
100
150
200
250
300
350
0
1
2
3
4
5
6
7

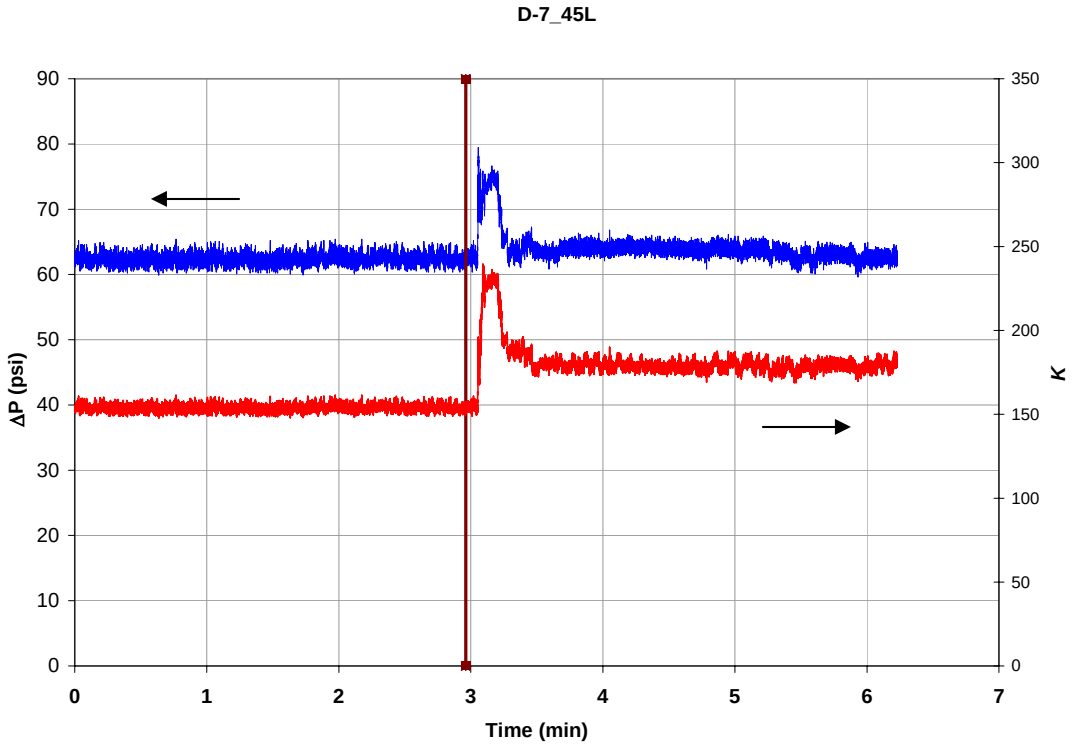
D-7_45L
ΔP (psi)
K
Time (min)
0
10
20
30
40
50
60
70
80
90
0
50
100
150
200
250
300
350
0
1
2
3
4
5
6
7

D-8_45L

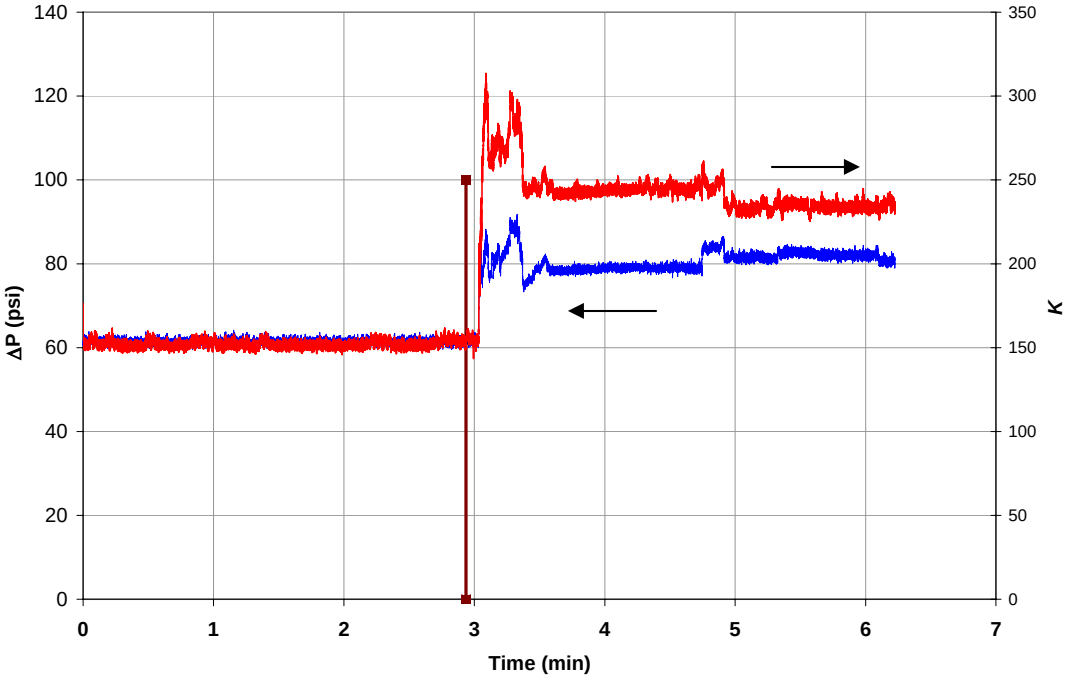
140
120
100
80
60
40
20
0
350
300
250
200
150
100
50
0
ΔP (psi)
K
0
1
2
3
4
5
6
7
Time (min)

D-9_45L

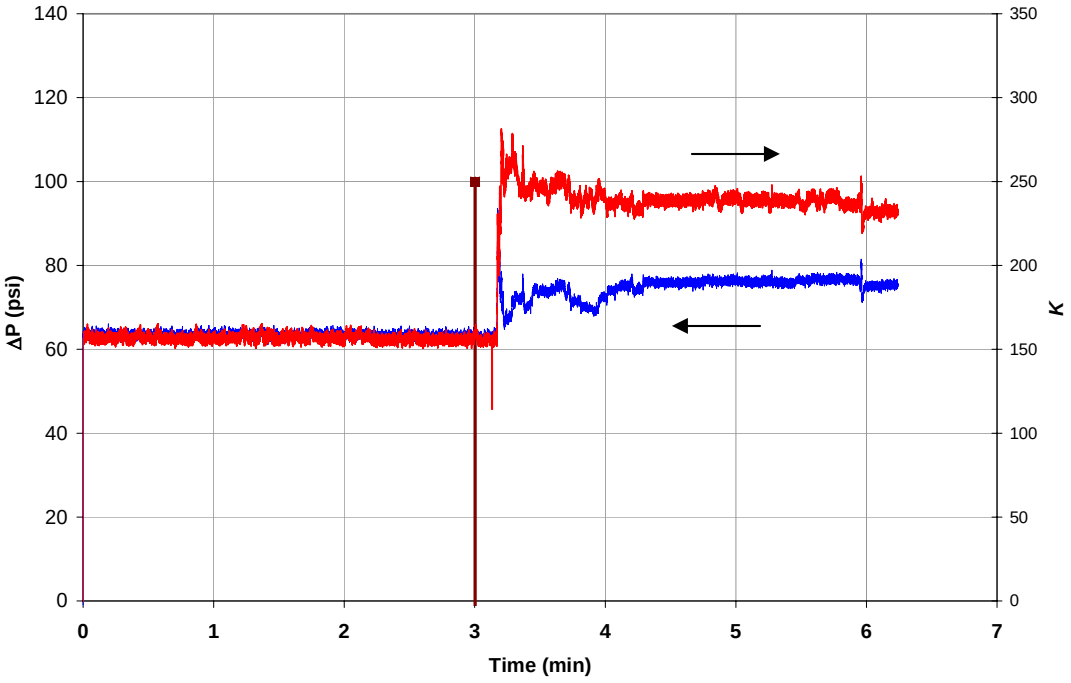
140
120
100
80
60
40
20
0
350
300
250
200
150
100
50
0
ΔP (psi)
K
0
1
2
3
4
5
6
7
Time (min)

D-10_45L

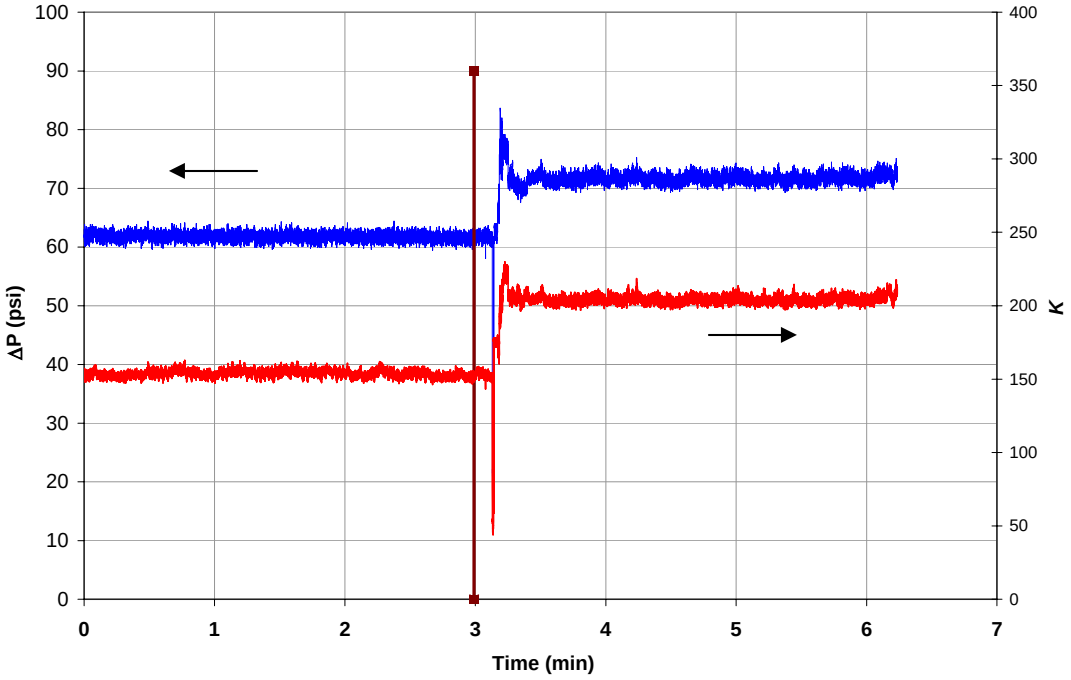

D-10-2_45L

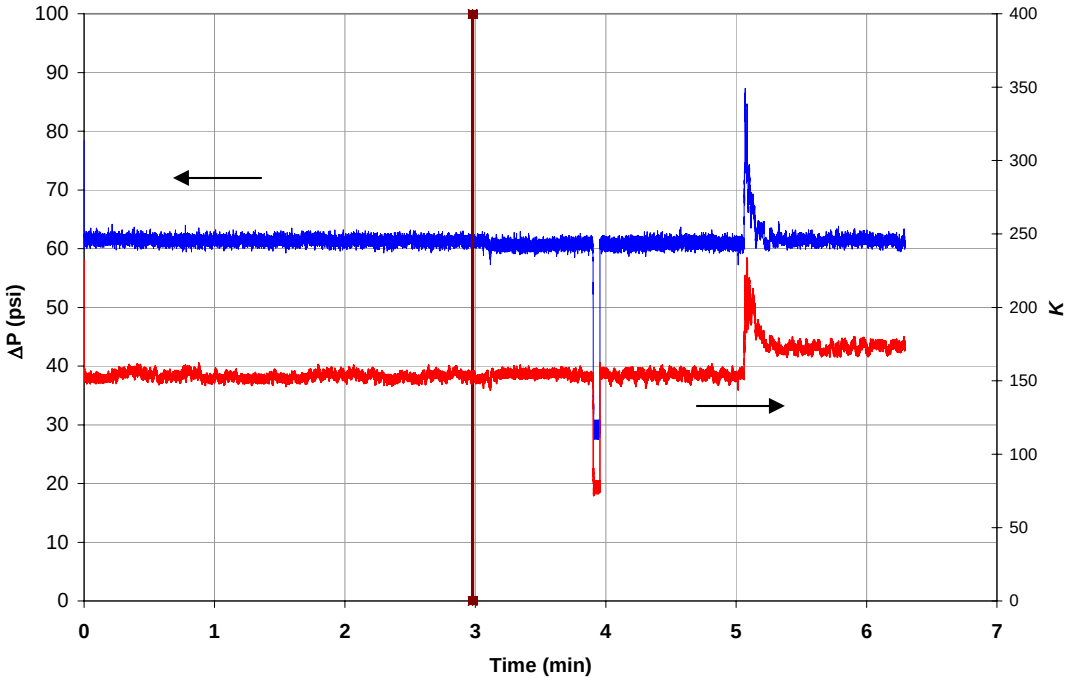

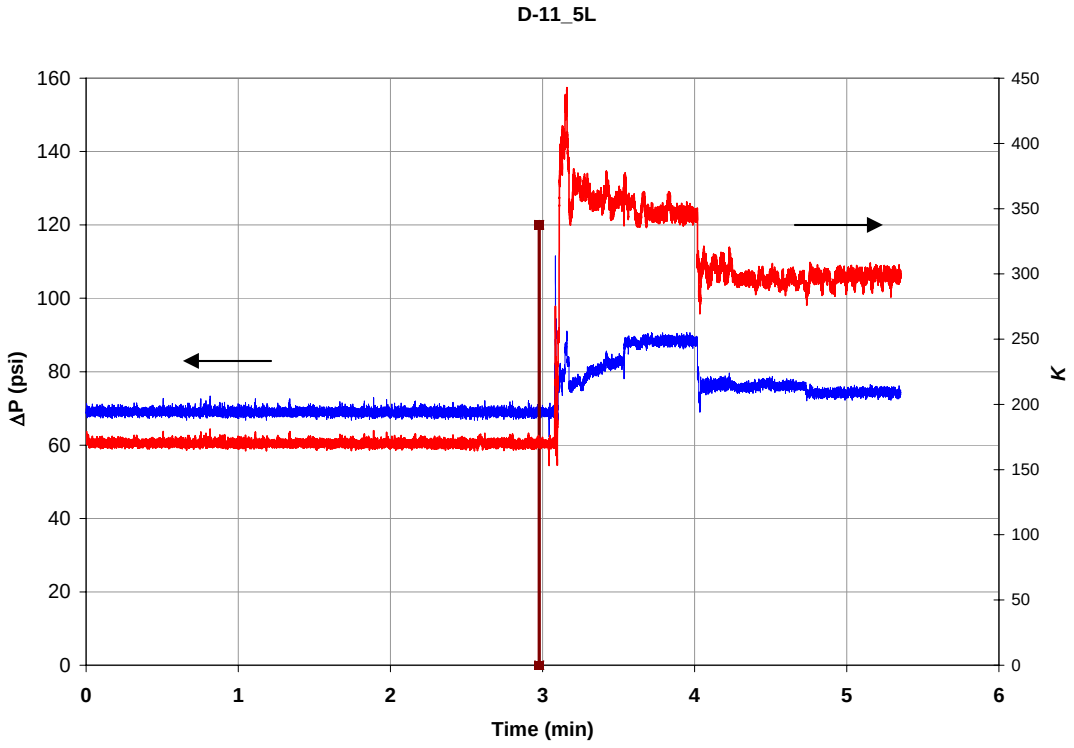
D-11_5L
160
140
120
100
80
60
40
20
0
ΔP (psi)
450
400
350
300
250
200
150
100
50
0
K
0
1
2
3
4
5
6
Time (min)

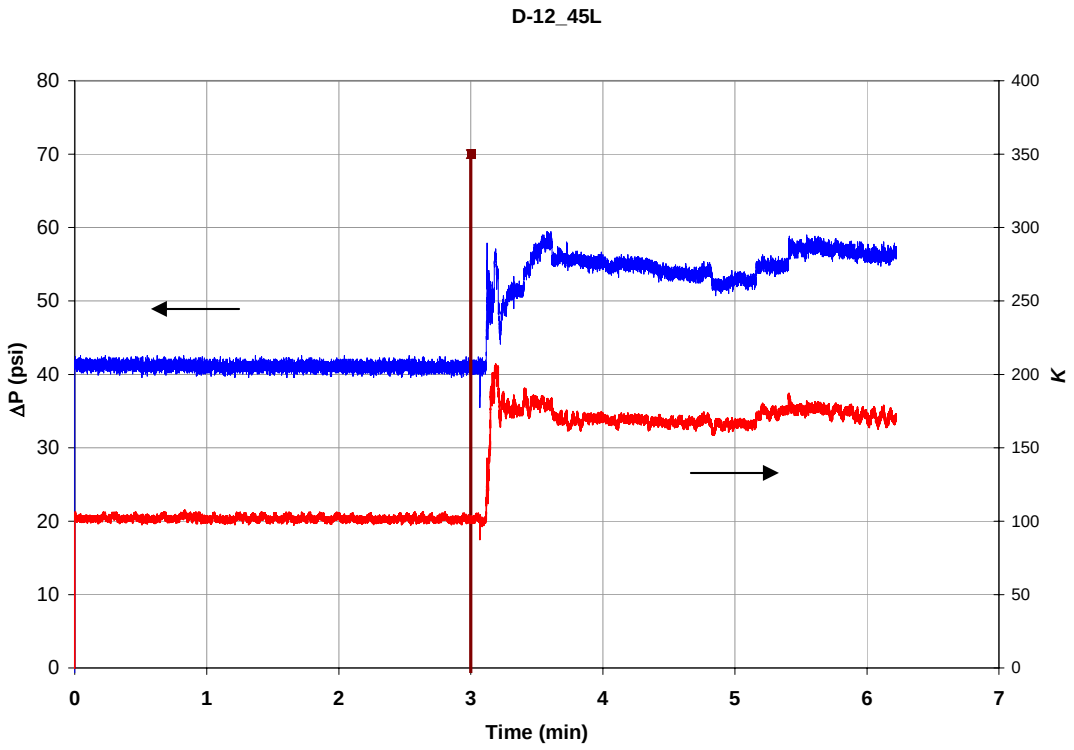
D-12_45L
80
70
60
50
40
30
20
10
0
ΔP (psi)
400
350
300
250
200
150
100
50
0
K
0
1
2
3
4
5
6
7
Time (min)

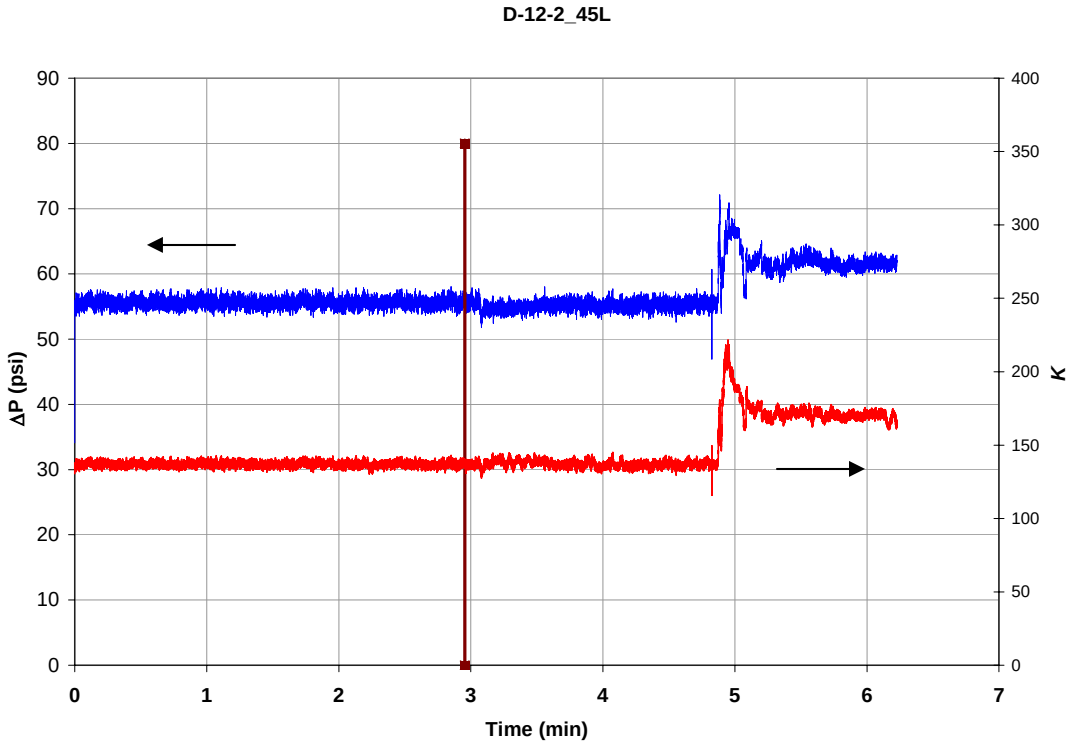
D-12-2_45L
ΔP (psi)
K
Time (min)
0
10
20
30
40
50
60
70
80
90
0
50
100
150
200
250
300
350
400
0
1
2
3
4
5
6
7

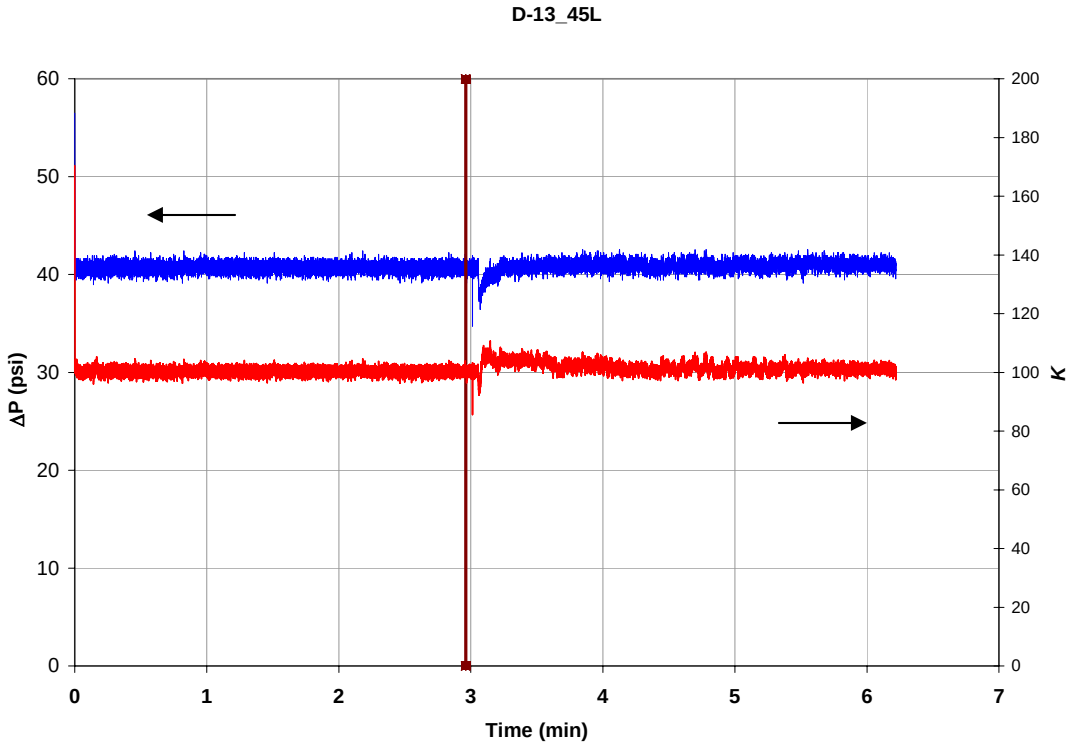
D-13_45L
ΔP (psi)
K
Time (min)
0
10
20
30
40
50
60
0
20
40
60
80
100
120
140
160
180
200
0
1
2
3
4
5
6
7

D-14_45L

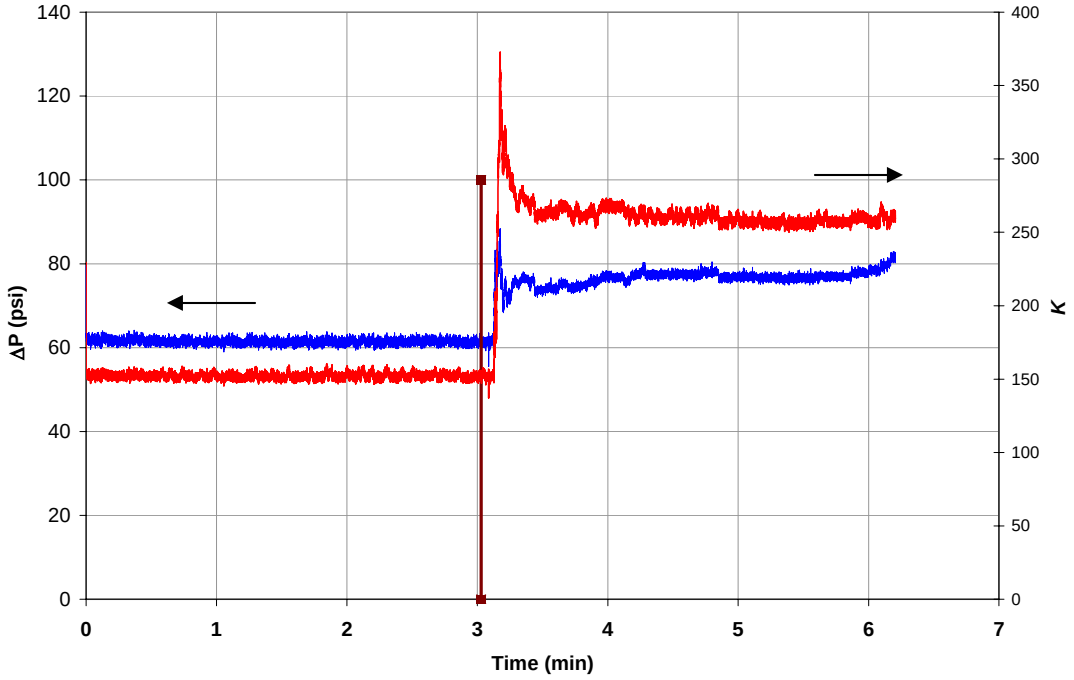

D-15_5L

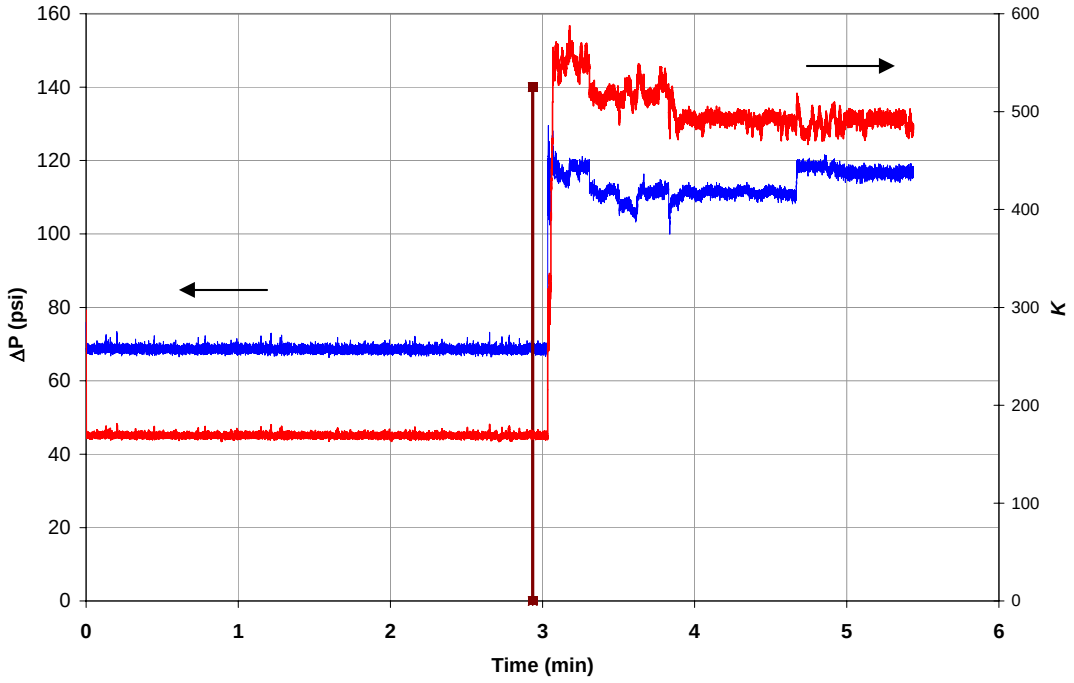

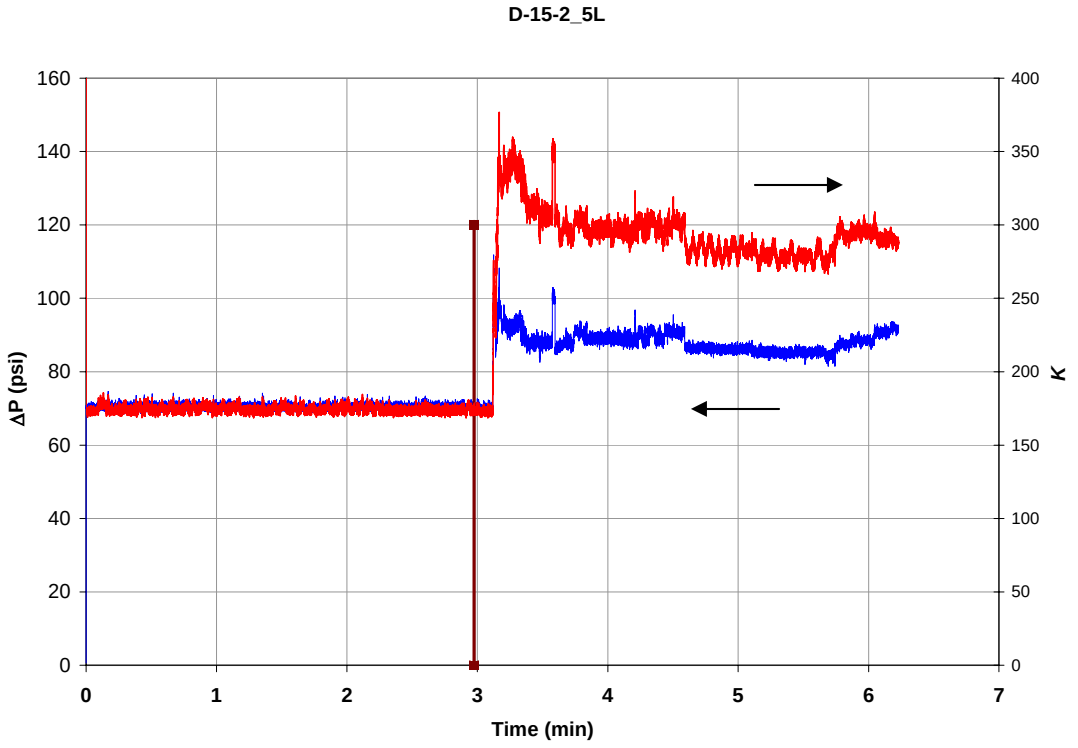
D-15-2_5L
ΔP (psi)
K
Time (min)
0
20
40
60
80
100
120
140
160
0
50
100
150
200
250
300
350
400
0
1
2
3
4
5
6
7

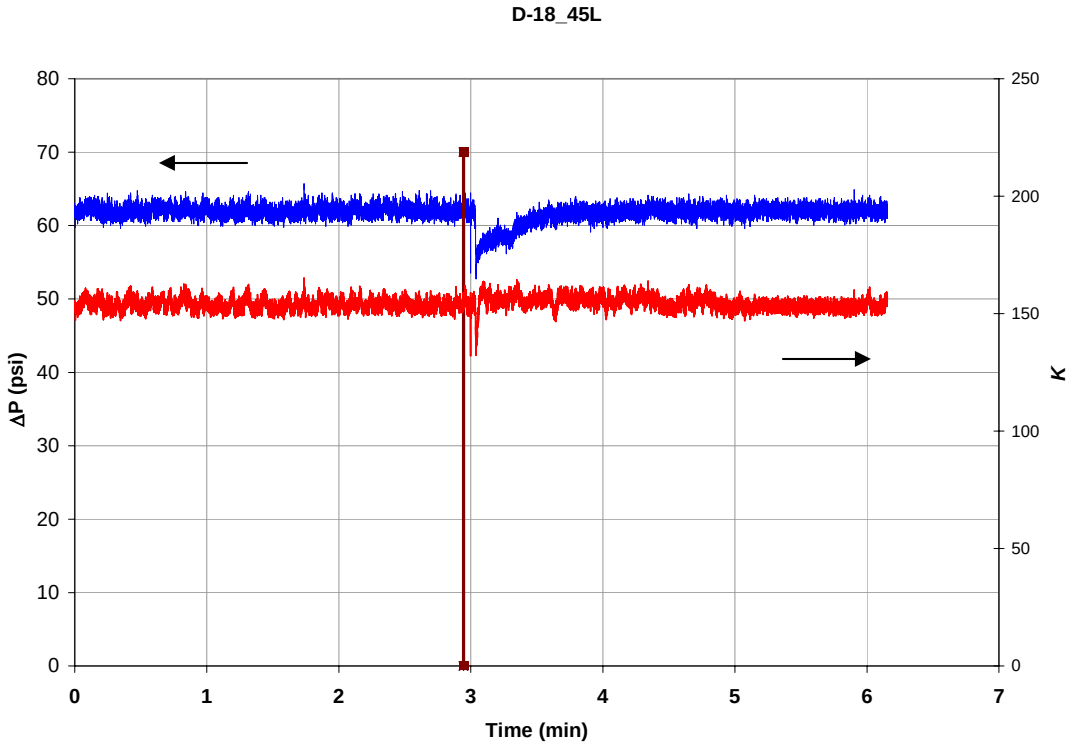
D-18_45L
ΔP (psi)
K
Time (min)
0
10
20
30
40
50
60
70
80
0
50
100
150
200
250
0
1
2
3
4
5
6
7

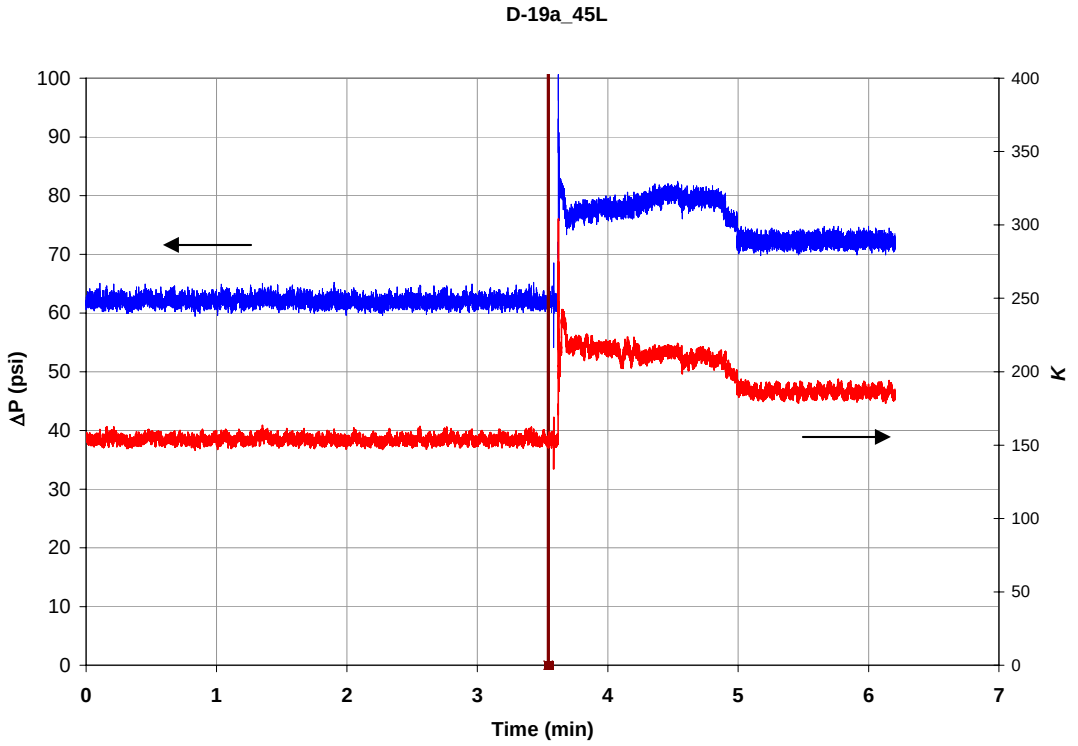
D-19a_45L
ΔP (psi)
K
Time (min)
0
10
20
30
40
50
60
70
80
90
100
0
50
100
150
200
250
300
350
400
0
1
2
3
4
5
6
7

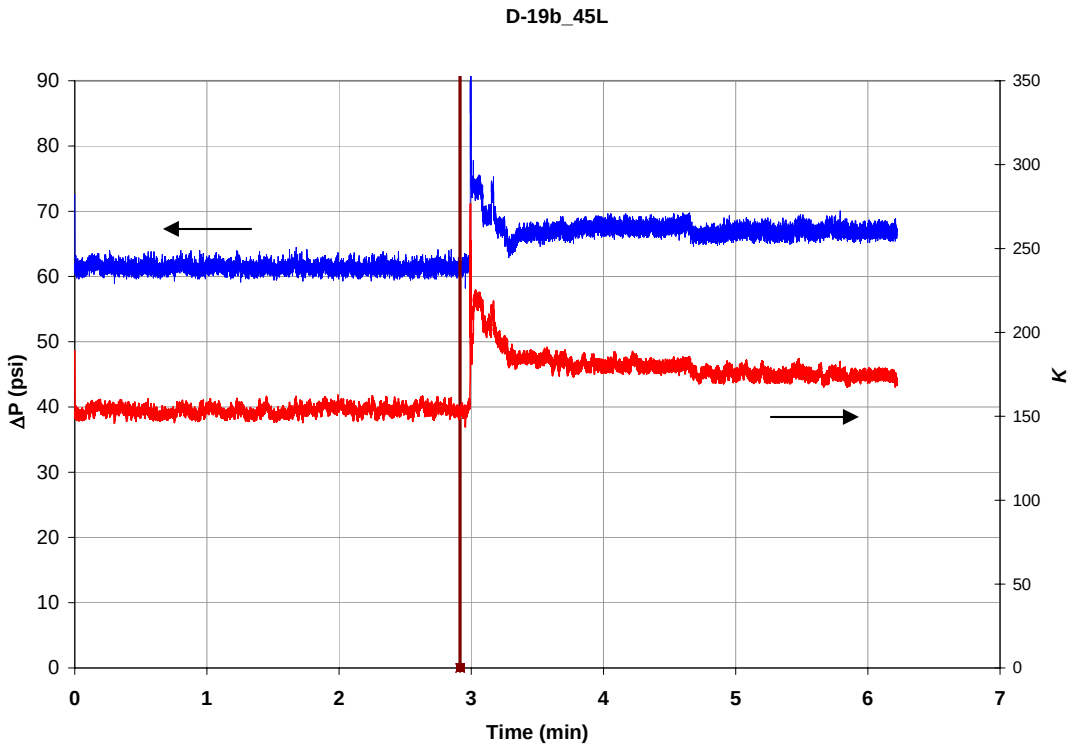
D-19b_45L
ΔP (psi)
K
Time (min)
0
10
20
30
40
50
60
70
80
90
0
50
100
150
200
250
300
350
0
1
2
3
4
5
6
7

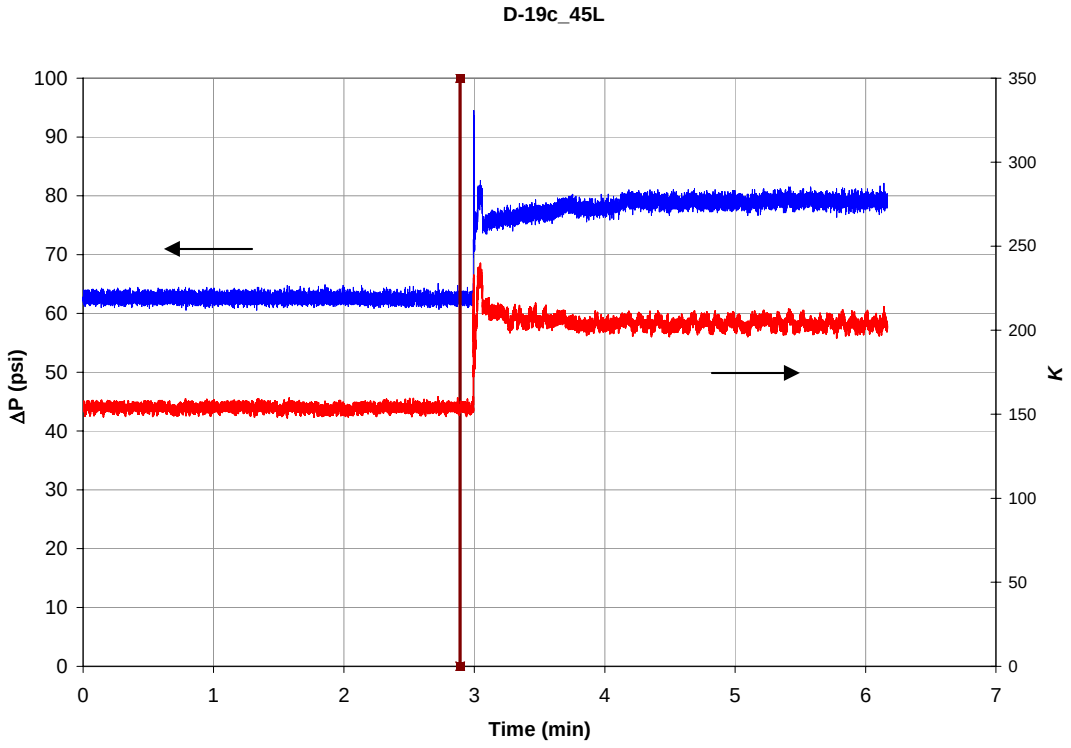
D-19c_45L
ΔP (psi)
K
Time (min)
0
10
20
30
40
50
60
70
80
90
100
0
50
100
150
200
250
300
350
0
1
2
3
4
5
6
7